DEVELOPMENT OF MATHEMATICAL MODEL FOR PNEUMATIC TIRE-SOIL INTERACTION

Leslie L. Karafiath

Grumman Aerospace Corporation

Prepared for:

Army Tank-Automotive Command

July 1974

Unclassified
Security Classification

AD: 783725

DOCUMENT CONTROL DATA - R & D

(Security classification of title, body of abstract and indexing annotation must be entered when the overall report is classified)

1 ORIGINATING ACTIVITY (Corporate author)
Grumman Aerospace Corporation
Research Department
Bethpage, New York 11714

2a REPORT SECURITY CLASSIFICATION
Unclassified

2b GROUP

3 REPORT TITLE
Development of Mathematical Model for Pneumatic Tire-Soil Interaction

4 DESCRIPTIVE NOTES (Type of report and inclusive dates)
Final Report

5 AUTHOR(S) (First name, middle initial, last name)
Leslie L. Karafiath

6 REPORT DATE	7a. TOTAL NO OF PAGES	7b. NO OF REFS
July 1974	212	20

8a. CONTRACT OR GRANT NO	9a. ORIGINATOR'S REPORT NUMBER(S)
Contract DAAE07-73-C-0115	
b. PROJECT NO 1T161102B52A	RE-479
c.	9b OTHER REPORT NO(S) (Any other numbers that may be assigned this report) TACOM Tech Report No. 11900(LL147)

10 DISTRIBUTION STATEMENT
Approved for public release;
Distribution Unlimited

11 SUPPLEMENTARY NOTES	12 SPONSORING MILITARY ACTIVITY
	U.S.Army Tank Automotive Command Mobility Systems Laboratory Warren, Michigan 48090

13 ABSTRACT

The role of tire deformation in tire-soil interaction is discussed, and a mathematical model is described that incorporates the qualitative relationships obtained from experimental data describing tire deformation as a function of the relative stiffness of the tire to the soil. The mathematical model assumes that the centerline geometry of tires consists of straight lines and logarithmic spirals and that there is a certain limit to the normal pressure that may develop beneath a tire. This limiting normal pressure is a tire property and is dependent on tire inflation pressure. Soil is modeled by its Coulomb strength parameters. Plastic equilibrium conditions in soil determine the interface stresses where the normal stress is less than the limiting normal pressure. Values of free parameters in the model that determine tire centerline geometry were analyzed. Tire performance predictions were compared with experimental data for a large number of combination of the free parameters, and relationships were established for the estimation of these parameters from tire deformation measurements on a rigid surface. Relationships between slip and mobilized interface shear stresses were established. On the basis of the tire-soil model a computer program was developed that computes the pull and torque coefficients and the sinkage for a given load and tire from the following inputs. slip, inflation pressure, tire deflection on rigid surface, tire dimensions and soil cohesion, friction angle, and unit weight. Alternatively, cone penetration data may be used with purely frictional or purely cohesive soils. Predictions by the tire-soil model are validated for available experimental data.

DD FORM 1 NOV 68 1473 REPLACES DD FORM 1473, 1 JAN 64, WHICH IS OBSOLETE FOR ARMY USE.

Unclassified
Security Classification

14 KEY WORDS	LINK A		LINK B		LINK C	
	ROLE	WT	ROLE	WT	ROLE	WT
Mathamatical Modeling						

RE-479

DEVELOPMENT OF MATHEMATICAL MODEL FOR PNEUMATIC TIRE-SOIL INTERACTION

Final Report No. 11900(LL147)

by

Leslie L. Karafiath

Prepared Under Contract DAAE07-73-C-0115

for

United States Army Tank-Automotive Command
Mobility Systems Laboratory
Warren, Michigan

by

Research Department
Grumman Aerospace Corporation
Bethpage, New York 11714

July 1974

Approved by: Charles E. Mack, Jr.
Director of Research

FOREWORD

Simulating the interaction of terrain, vehicle, and man is essential to improving land mobility technology — a goal of the U.S. Army Tank-Automotive Command (TACOM) and the U.S. Army Corps of Engineers Waterways Experiment Station (WES). Under TACOM contract, Grumman has been actively supporting this effort and has just completed the development of a mathematical model for pneumatic tires-soil interaction — an essential element in the terrain-vehicle-man system — which is the subject of this report.

For Grumman, participation in this program began in 1971, when the TACOM-WES first generation terrain-vehicle-man simulation called the "AMC '71 Vehicle Mobility Model" was completed. This model made it clear that one sub-model needing improvement was the simulation of a wheeled vehicle moving in soft soil, and, therefore, TACOM contracted with Grumman to develop a computerized model of rigid wheel-soil interaction on the basis of the plasticity theory for soil. The drawbar pull, torque requirements, slip, and sinkage for rigid wheel calculation by the model was validated in an experimental program.

A follow-on program, the results of which are presented in this report, began in 1972. Here the interaction concept is applied to pneumatic tires, and a mathematical model is developed for computing tire performance parameters from tire inputs (diameter, width, inflation pressure, and deflection) and from soil inputs (cohesion, friction angle, and bulk density). This mathematical model is the first step toward the development of a tire performance sub-model in the AMC Vehicle Mobility Model that can predict the speed of wheeled vehicles in soft soil, accurately assess torque and fuel consumption requirements in specific missions, and be suitable for eventual application in a vehicle dynamic model.

ABSTRACT

The role of tire deformation in tire-soil interaction is discussed, and a mathematical model is described that incorporates the qualitative relationships obtained from experimental data describing tire deformation as a function of the relative stiffness of the tire to the soil. The mathematical model assumes that the centerline geometry of tires consists of straight lines and logarithmic spirals and that there is a certain limit to the normal pressure that may develop beneath a tire. This limiting normal pressure is a tire property and is dependent on tire inflation pressure. Soil is modeled by its Coulomb strength parameters. Plastic equilibrium conditions in soil determine the interface stresses where the normal stress is less than the limiting normal pressure.

Values of free parameters in the model that determine tire centerline geometry were analyzed. Tire performance predictions were compared with experimental data for a large number of combination of the free parameters, and relationships were established for the estimation of these parameters from tire deformation measurements on a rigid surface. Relationships between slip and mobilized interface shear stresses were established. On the basis of the tire-soil model a computer program was developed that computes the pull and torque coefficients and the sinkage for a given load and tire from the following inputs: slip, inflation pressure, tire deflection on rigid surface, tire dimensions and soil cohesion, friction angle, and unit weight. Alternatively, cone penetration data may be used with purely frictional or purely cohesive soils. Predictions by the tire-soil model are validated for available experimental data.

ACKNOWLEDGMENTS

The work reported here was performed for the Mobility Systems Laboratory of the U.S. Army Tank-Automotive Command (TACOM), Warren, Michigan, under the general supervision of Mr. Robert T. Otto, Chief of the Surface Mobility Division, and Mr. Howard Dugoff, Supervisor, Research and Analysis Branch. Technical monitor was Mr. Zoltan J. Janosi, Supervisor, Vehicle Locomotion Function. Their help and valuable suggestions in carrying out this work are gratefully acknowledged.

Tire performance test data used for the development and validation of the mathematical model, motion pictures of tire tests on wooden peg soil model, and soil material for triaxial tests was obtained from the U.S. Army Engineer Waterways Experiment Station (WES). The author thanks Messrs. C. J. Nuttal, Jr., G. W. Turnage, and K. J. Melzer for the helpful cooperation in supplying the above material as well as for their valuable and constructive comments.

Tire performance tests conducted at the National Tillage Machinery Laboratory, Auburn, Alabama, were also used for model validation. The helpful cooperation of Dr. J. M. Taylor in providing the test data and soil material for triaxial testing is gratefully acknowledged.

In the development of the tire-soil model use was made of computer techniques, developed in an independent research program, that allow running of large programs on minicomputers. Acknowledgment is due to Mr. R. McGill, head of the Grumman Research Department's Computer Sciences Group, who made the necessary provisions in the program for its accommodation on the minicomputer. Without the use of the minicomputer the large scale analysis of

the effect of various parameters in the model would not have been economically feasible.

The laboratory triaxial tests were performed under the direction of Dr. E. A. Nowatzki. Mr. G. Homfeld assisted in the performance of experiments.

TABLE OF CONTENTS

LIST OF ILLUSTRATIONS

LIST OF SYMBOLS

A	singular point
B,b	width of tire
c	cohesion (lb/sq ft)
CGR	cone index gradient
CI	cone index
D	diameter (ft)
DB	drawbar pull (lb)
D_r	relative density
H	number of i lines in slip line field
h	height of tire cross section
i,j	nodal point designations
j	slip
j_o	constant in Eq. (5)
K	number of j lines in slip line field, constant in Eq. (5)
L	length of passive zone of slip line field
LD	load (lb)
L_o	design load (lb)
N_c	clay numeric
N_s	sand numeric
p_i	inflation pressure (psi)
p_l	limit pressure (psi)
q	normal stress
R	radius of undeflected tire (ft)
r	radius of deflected tire (ft)
SN	sinkage
TQ	torque
x,z	geometric coordinates

	central angle (measured from vertical)
′,	angles defining start and end of deflection
d	central angle at end of forward field
d′	central angle at end of rear field
e	entry angle
r	rear angle
sp	angle of tangent of log spiral with normal to the radius
	coefficient in Eq. (1)
	unit weight of soil (lb/cu ft)
	angle of inclination of resultant stress to normal, angle of shear mobilization, deflection in Waterways Experiment Station terminology
	deflection coefficient in Eq. (2)
	angle between x axis and major principal stress
	$\pi - 2\theta/d$
	$\pi/4 - \phi/2$
	tolerance limit
	$(\sigma_1 + \sigma_3)/2 + \gamma$
σ_n	normal stress
$\sigma_{1,3}$	principal stresses
	shear stress/shear strength
τ_{max}	maximum available shear strength
τ_{mob}	mobilized shear strength
	angle of internal friction
	c cot ϕ

I. SCOPE OF WORK

The scope of work as described in the RFP work statement for this contract was the application of plasticity theory for soils to the problem of pneumatic tire-soil interaction and the development of a mathematical tire-soil model for the purpose of tire performance predictions. Within this general scope emphasis was placed on the following items:

- Application of plasticity theory methods to the calculation of stresses at a deformed tire-soil interface
- Formulation of a mathematical tire-soil model for the description of tire-soil interaction
- Development of a computer program for tire performance calculations based on the mathematical model
- Verification of the model by comparisons of predicted tire performance with available experimental data.

II. IDEAL FORMULATION OF TIRE-SOIL INTERACTION

Theoretically rigorous simulation of physical phenomena is illusory since the characterization of the physical properties of materials and the description of the natural laws that govern their behavior are themselves idealizations. Rigorous solutions exist only for hypothetical materials and conditions. Thus, in principle, the physical phenomenon of tire-soil interaction cannot be treated in a theoretically rigorous manner. An ideal formulation would be one that would yield a rigorous solution for the hypothetical case that both tire and soil behave as their material characterization postulates. For such a hypothetical condition it would be possible to write a symbolic formulation for the problem on the basis of the equations of motions and the boundary conditions at the interface. A general solution of this problem, however, would present a formidable task and may be regarded only as the ultimate goal. Solutions of special cases that are considered attainable with present state of the art methods involve the following assumptions:

- The tire travels in a straight line at a constant, low velocity
- A "steady state" exists in the soil
- The tire load is constant — that is, there is no interaction between tire and suspension system
- The terrain is even.

To formulate the tire-soil interaction for these conditions, a tire model is needed for the calculation of tire deformation under a system of applied stresses. Finite element models of tires

that have been developed for other purposes would generally require extensive further development if they were to be applied to the problem of tire-soil interaction. While it would be desirable to have such a model for the study of tire deformation under various conditions occurring in tire-soil interaction situations, finite element models generally require large computer capacity and proportionate time for the computation of deformations under a single set of conditions. Since in a predictive tire-soil model such computations would be needed repeatedly because of the iterative nature of the prediction technique, the use of finite element tire models was deemed undesirable. Theoretical considerations as well as studies of tire-soil interaction experiments indicated that for the purpose of performance prediction a refined finite element tire model was not necessary, and that a simple tire model responsive to changes in soil stiffness could be successfully used. The experimental information available on the geometry of tires in various soil conditions and the development of the approximate tire model are described in subsequent sections.

III. EXPERIMENTAL INFORMATION ON TIRE-SOIL INTERACTION

Of the numerous tire tests that have been performed by various researchers over the years, the most valuable for the development of a tire model are those where interface stresses and tire deformations of tires moving in soils were directly measured. The experimental data on the deflection of tires moving in soft soils and the distribution of interface stresses obtained in various WES research projects (Refs. 1 through 6) are the most instructive available information on the role of tire deflection in tire-soil interaction and served as a basis for the development of the tire-soil model presented in Section VII.

Interface stress and tire deflection measurements performed by others and available in the literature (Refs. 7 through 10) were also studied and used in the development of the tire-soil model.

Direct measurements of tire deflection and interface stresses are expensive and time consuming, and, therefore, only few were performed. On the other hand, performance tests, without direct geometry and stress measurements, have been performed for a wide variety of conditions. Since tire geometry changes with the slip rate, those tests where performance was measured over a range of slip offered the experimental information necessary for the development and validation of the tire-soil model. At our request, WES furnished data on such tests (Ref. 11) on various types of tires. A summary of tests performed at WES in Yuma sand is given in Table 1 and of those performed in Buckshot clay in Table 2. Results of these tests are shown graphically in conjunction with the evaluation of predictions by the tire-soil model. More detailed information on the performance of these tests is contained in WES Technical Report No. 3-666 (Ref. 12).

TABLE 1. TIRE PERFORMANCE TESTS PERFORMED AT WES IN YUMA SAND

No.	WES Designation	Tire Size	Infl. Press. (psi)	Deflection (%)	Nominal Load (lb)	Cone Index Gradient (psi)
	164-777A	9.00-14	16.5	15	440	8.9
2	164-813A	6.00-16	5.0	35	240	16.4
3	164-816A	6.00-16	7.0	25	240	13.5
4	164-818A	6.00-16	10.0	25	450	15.6
5	164-822A	4.00-7	13.0	25	210	13.0
6	164-826A	4.00-7	26.0	25	340	12.1
7	164-830A	4.00-7	17.0	35	220	19.6
8	164-832A	4.00-7	21.9	35	440	19.9
9	165-3A	9.00-14	14.0	25	840	13.8
10	165-4A	9.00-14	5.0	25	220	11.2
11	165-6A	9.00-14	9.0	25	440	12.4
12	165-7A	9.00-14	6.0	25	210	22.5
13	165-8A	9.00-14	11.8	25	620	3.5
14	165-10A	9.00-14	10.0	35	870	12.4
15	165-11A	9.00-14	3.7	35	225	13.0
16	165-12A	9.00-14	7.5	35	670	16.2
17	165-15A	4.00-20	11.4	25	225	14.4
18	165-16A	4.00-20	24.7	25	450	13.0
19	165-19A	4.00-20	18.2	25	330	16.1
20	165-20A	4.00-20	15.0	35	440	16.4
21	165-21A	4.00-20	6.7	35	230	25.6
22	165-22A	4.00-20	11.0	35	340	25.6
23	165-23A	4.00-20	6.7	35	240	3.2
24	165-24A	9.00-14	16.0	25	850	15.0
25	165-27A	9.00-14	9.5	25	460	11.8
26	165-37A	6.00-16	7.00	25	220	15.0
27	165-13A	9.00-14	8.50	35	650	3.7

TABLE 2. TIRE TESTS PERFORMED AT WES IN BUCKSHOT CLAY

No.	WES Designation	Tire Size	Infl. Press. (psi)	Deflection (%)	Nominal Load (lb)	Cone Index (psi)
CL-1	418-C	9.00-14	36.7	15	870	52
CL-2	409-C	9.00-14	7.50	35	650	22
CL-3	321-C	6.00-16	8.50	15	250	20
CL-4	338-C	6.00-16	16.20	25	700	22
CL-5	345-C	6.00-16	21.0	25	880	37
CL-6	374-C	4.00-7	26.0	25	335	42
CL-7	377-C	4.00-7	22.0	35	450	38
CL-8	637-C	16 x 15-6	3.9	35	450	16
CL-9	665-C	31 x 15-13	5.6	15	450	20
CL-10	667-C	31 x 15-13	6.0	25	880	28
CL-11	663-C	31 x 15-13	7.25	25	1 70	22

The WES tests were performed in either the purely frictional Yuma sand or in the purely cohesive Buckshot clay. In order to have some information on tire performance in frictional-cohesive soils, results of tire tests performed in two clayey soils at the National Tillage Machinery Laboratory, Auburn, Alabama, were obtained (Table 3). These tests were performed for comparative studies rather than performance prediction, and, therefore, evaluation of soil strength had to be done in retrospect from the available data on soil properties.

TABLE 3. TIRE TESTS PERFORMED AT THE NATIONAL TILLAGE MACHINERY LABORATORY

No.	NTL No.	Soil	Tire Size	Infl. Press. (psi)	Nominal Load (lb)
A1	1970	Decatur Silty Loam	11 x 38	12	2185
A2	1971	Silty Loam			
A3	2047	Vaiden Clay			
A4	2048				
A5	2049				
A6	2050				

IV. GENERAL APPROACH TO THE DEVELOPMENT OF TIRE-SOIL MODEL

In view of the paucity of specific deflection and stress measurements and the wide variety of tire performance tests, the following approach to the development of tire-soil model was pursued.

- Establish qualitative relationships between tire deflections and soil properties and between interface stresses and inflation pressure
- Modify the validated rigid wheel-soil model (Ref. 13) so as to allow for the influence of tire deflection and inflation pressure. In the model allow for a sufficient number of free parameters so that existing deflection and stress measurements may be matched
- Analyze the effect of free parameters and other assumptions on tire performance, modify assumptions, and establish values for free parameters on the basis of comparisons with tire performance tests
- Establish methods to determine model parameters for prediction purposes.

V. TIRE DEFLECTION IN SOFT SOILS

The tire deflection measurements carried out at WES under various loading and soil conditions and reported in Refs. 1 through 6 have conclusively shown that deflection of the cross section of tires as well as that of their centerline in the plane of motion is dependent on both the stiffness of the tire and the stiffness of the soil. The deflection of the cross section of the tire influences tire performance primarily by enlarging the width of the contact area. This width change is within a narrow range, its lower limit being the width of the unloaded tire and its upper limit the width of the tire loaded on a rigid surface. These limiting widths are generally available or can be easily measured; the width of a tire loaded in soft soil may be estimated from these limits with sufficient accuracy. Since the proposed tire-soil model is a two dimensional one, effects of transverse deflection are considered only by changes in width.

The deflection of the centerline of the tire in the plane of motion determines the average inclination of the contact area to the horizontal and thereby influences tire performance profoundly.

The inclination of the contact area acts as if the tire were to climb a slope. For a rigid wheel the average inclination of the contact area is the angle bisecting the entry and exit angles and may easily be in the range of 10 to 20 degrees. On the other hand, a very flexible tire may flatten out appreciably so that the contact area becomes almost horizontal. The inclination of the contact area affects the pull coefficient directly, approximately by the value of the tangent of the angle of the inclination.

The above considerations show the importance of centerline geometry in a tire-soil model. The experiments performed at WES show the variation of centerline geometry with slip, soil strength, and inflation pressure. From these experiments the following qualitative conclusions were drawn.

The centerline geometry of a tire is affected by slip, inflation pressure, and soil strength. The combined effect of tire and soil stiffness may be graphically represented as shown in Fig. 1. Tire deformation is negligible, and the tire behaves as a rigid wheel if the tire stiffness is great relative to that of the ground. In the other extreme, tire deformation is comparable to that on a rigid surface if the stiffness of the soil relative to that of the tire is great.

Another finding related to the geometry of centerline is that the resultant of normal stresses at the tire soil interface passes through the centerline of the wheel axle (Ref. 4).

These qualitative relations defining the effect of tire and soil stiffness on centerline geometry were the basis for the development of the tire-soil model.

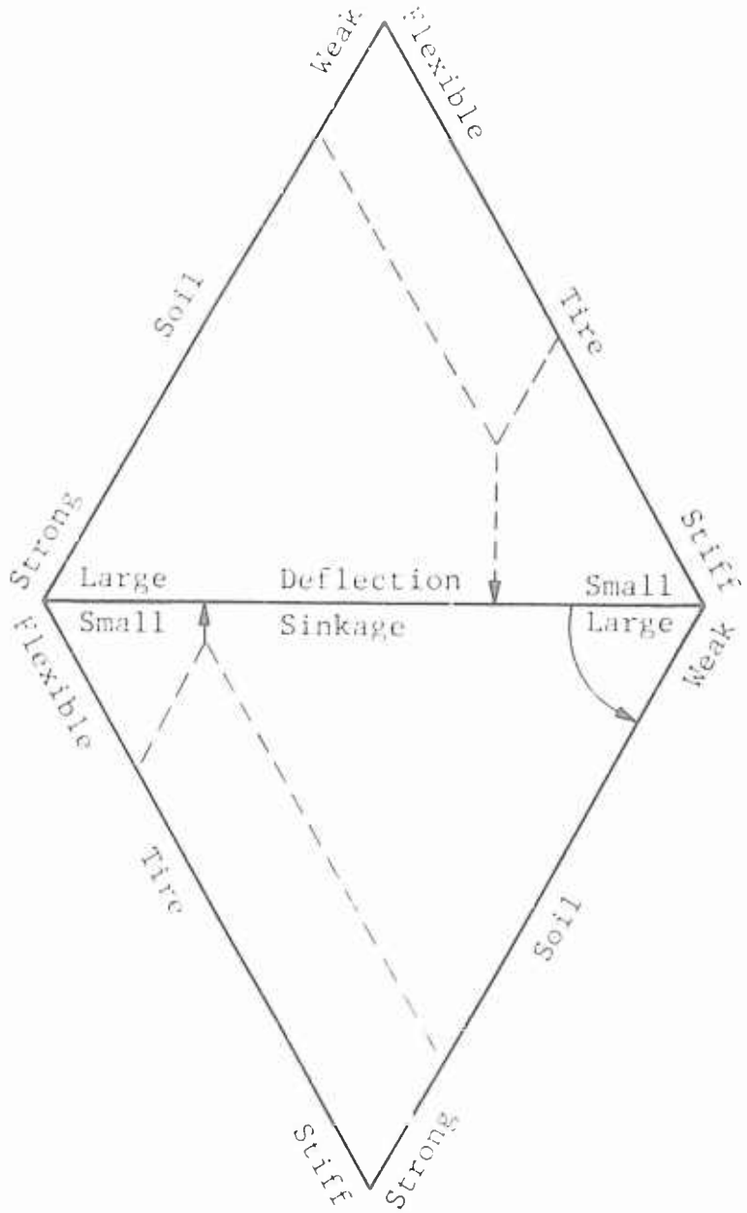

Fig. 1 Schematic Representation of Tire-Soil Behavior (Based on WES Experiments)

VI. STRESSES BENEATH A TIRE MOVING IN SOFT SOIL

Tire deflection affects tire-soil interaction not only by its effect on the geometry of the contact area, but also by relieving the stresses that would develop in the soil if the interface were undeformable. Stress measurements at the tire-soil interface confirm this latter effect and give an indication of the magnitude of stress relief.

Tire-soil interface stress measurements at WES were first made on unyielding surfaces with sensor placement in the unyielding surface (Ref. 5). Results of these measurements are of interest for tire-soil interaction studies because stresses measured on an unyielding surface represent the upper limit of stresses that would develop in a soil that yields relatively little under tire load. The general pattern of stress distribution observed in these tests showed a center portion in the contact area with fairly uniform stress distribution and stress concentrations, called "edge stresses," at the perimeter of the contact area. These edge stresses are related to the sidewall stiffness of the tire, while the magnitude of the average center portion stresses is related to the inflation pressure of the tire.

Measurements of interface stresses in soils were also made by VandenBerg and Gill (Ref. 8). These measurements, using smooth tires, indicate a stress distribution pattern similar to that observed on unyielding surfaces. The magnitude of the uniform pressure in the center portion depends on the inflation pressure and is generally somewhat higher.

Freitag et al. (Ref. 4) investigated the distribution of normal stresses in the contact area of both towed and powered tires

inflated to various pressures. Tests, carried out in both sand and clay, indicated that the maximum normal stress in each case exceeded only slightly the inflation pressure.

Krick (Refs. 9 and 10) measured both normal and shear stresses on the interface of both rigid wheels and tires in a sandy loam. Normal stresses measured at a deformable tire interface clearly showed the effect of pressure relief when compared with those obtained with rigid wheels.

VII. CONCEPT OF TIRE-SOIL MODEL

The deformation and stress measurements discussed briefly in Section VI indicate the complexity of the tire-soil interaction problem. The shape of the tire and geometry of the contact area depend not only on the properties of the tire, but also on the properties of soil and on the loads applied. The stresses measured in the contact area are far from uniform; stress concentrations occur at the edges of the contact area. Obviously, all these variations cannot be considered in any workable tire-soil model, and simplifications are required. An appropriately simplified model often yields sufficiently accurate results, as many computational methods in engineering demonstrate.

To decide what simplifications can be undertaken in a model without jeopardizing its accuracy and usefulness, it is expedient to consider the tire as a free body and to assess the effect of possible simplifications on the performance of the tire. The edge stresses in the contact area, as experiments indicate, are symmetrical both crosswise and lengthwise. This symmetry allows one to consider average stresses across the tire width without any significant loss of accuracy. Likewise, edge stresses may be smoothed lengthwise and the resulting torque, load, and drawbar pull still may be reasonably close to the actual values. Conversely, it is important to duplicate the deflected shape of the tire and its orientation to the ground surface as closely as possible. In the summation of the interface stresses for the computation of drawbar pull, the inclination of interface elements relative to the ground surface cannot be neglected. Depending on the inclination of the element, normal stresses on the interface yield a component (plus or minus) in the direction of the drawbar pull that may or may not be significant relative to the component of shear stresses.

The tire-soil model, conceived on the basis of these considerations, is shown in Fig. 2. The essential features of the model are as follows: The tire is assumed to have a constant width in both the undeformed and deformed states. The stresses across the tire width are assumed to be uniform so that the tire-soil interaction problem can be treated as two dimensional. Tire deformation is represented by the shape of the tire in the center plane in the direction of travel. Tire shape is assumed to be the same in all parallel planes. The centerline geometry is assumed to consist of two curvilinear segments separated by a linear or flat section. It is assumed that the tire starts to deform ahead of the entry angle $_c$ and reaches its original form past the exit angle $_r$, as shown in Fig. 2. The curvilinear segments are logarithmic spirals with the radii decreasing according to the following relationship

$$r = R\, e^{(- _o)} \qquad (1)$$

where

R = radius of unloaded tire

r = deflected radius

= constant

= central angle

$_o$ = initial central angle

The effect of tire deflection on soil reaction is represented in the proposed tire-soil model in two ways: Soil failure conditions as determined by plasticity theory govern the interface normal stresses in a front and rear failure zone. Deflection of the centerline affects the magnitude of these stresses; this effect is taken into account by using the deflected geometry as boundary

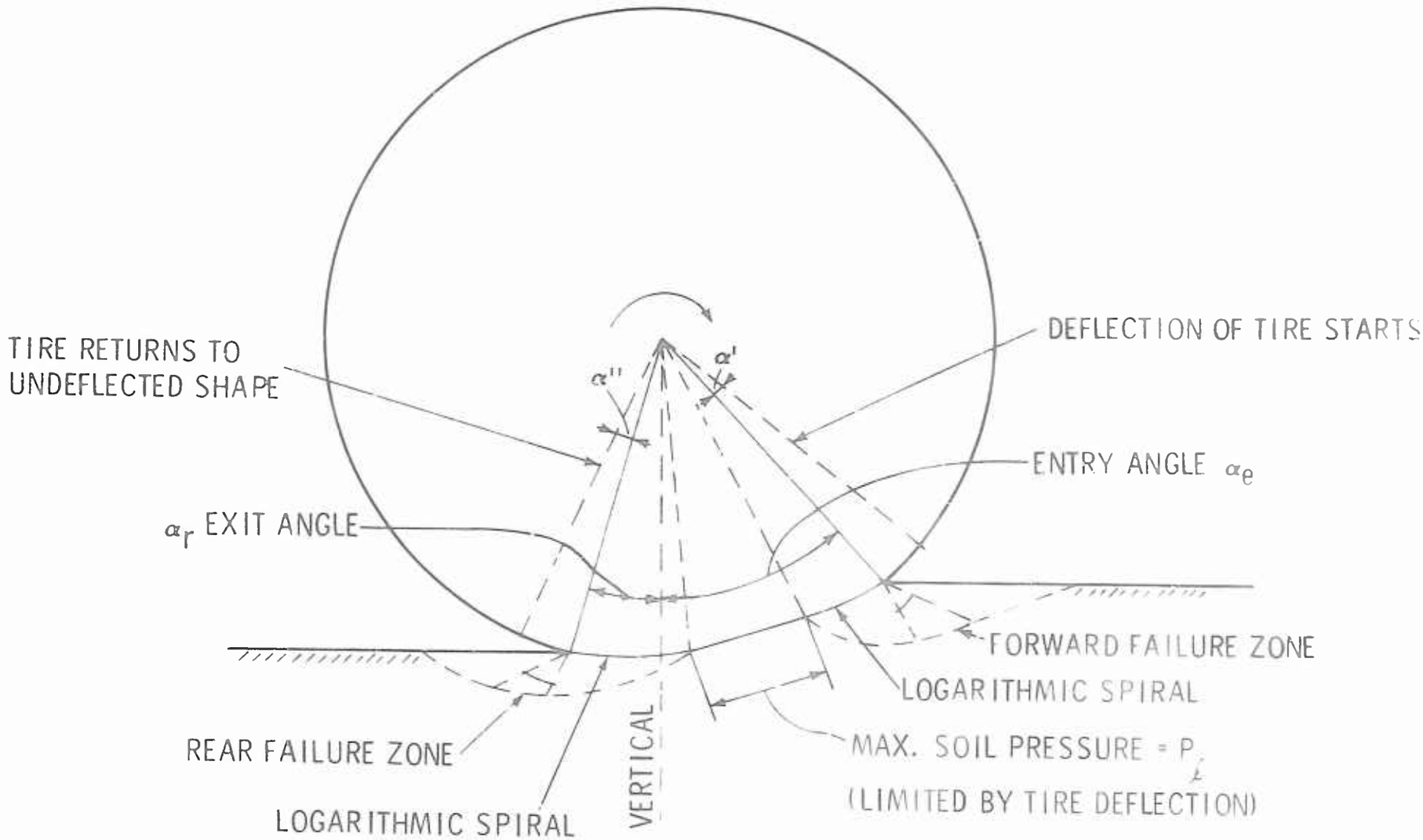

Fig. 2 Tire-Soil Model

condition in the numerical computation. Furthermore, in the model it is assumed that tire deflection limits the normal stresses that may arise at the interface. This idea was originally proposed by Bekker and Janosi for a towed tire model (Ref. 14). The magnitude of this limiting pressure depends on the inflation pressure and tire stiffness. In the proposed tire-soil model the limiting pressure is considered as a free parameter whose value is to be established by a parametric analysis of experimental results. The role of shear stresses generated by the applied torque is implicit in the model in that the geometry of the slip line fields and the associated interface normal stresses depend on them. The normal stress of the inner end of the rear failure zone equals the limiting pressure p_1. If the rise of the normal stresses in this zone is moderate or slow because of the applied shear stresses, the failure zone extends further toward the front zone, and the zone of uniform normal stresses where the soil is not in failure condition is reduced or entirely eliminated. In such cases the tire-soil model becomes similar to the rigid wheel-soil model.

The key feature of the proposed tire-soil model is the determination of the constant in Eq. (1). This constant determines the curvature of the logarithmic spiral and is a measure of tire deflection. As discussed in Section V, tire deflection in soft soils depends on the relative stiffness of the tire to that of the soil. Tire stiffness depends on the inflation pressure, while soil stiffness is directly related to the strength of the soil. The coefficient in Eq. (1) should reflect the combination effect of tire and soil stiffness. In the mathematical formulation of the model this is accomplished in the following way: The arc length of the interface of the forward failure zone depends on both the limiting pressure and the soil strength. In strong soils the rise

of the normal stresses is steep, and the limiting pressure is reached over a short arc length; whereas in a weak soil a longer arc length is needed to reach the same limiting pressure. If soil conditions are the same, the arc length depends on the limiting pressure; low limiting pressure will result in small arc length, while high limiting pressure will result in long arc length. Thus the arc length of the forward failure zone is governed, at least qualitatively, by the same interrelationship that governs tire deflection according to the experiments illustrated schematically in Fig. 1. In order to introduce this interrelationship into the mathematical formulation of the proposed tire-soil model, a deflection coefficient, ϵ, is introduced that defines the shortening of the tire radius by deflection at a specified central angle, (α_ϵ), as follows:

$$r = \epsilon R \quad . \tag{2}$$

The coefficient ϵ is calculated for any given ϵ value from Eq. (1). By this method of calculation, depends on the arc length of the front failure zone and reflects, at least qualitatively, the desired interrelationship between tire deflection and soil stiffness. In the development stage the angle α_ϵ to which Eq. (2) refers was considered as a free parameter. The analysis of tire performance experiments showed that good simulation can be achieved if $\alpha_\epsilon = 0.5\ \alpha_d$ is assumed.

VIII. DEVELOPMENT OF MATHEMATICAL TIRE-SOIL MODEL

The concept of the tire-soil model described in Section VII takes into account, at least qualitatively, the interaction effects between tire and soil evidenced in various experiments. In the mathematical model it was necessary to express the interrelationships quantitatively and check the validity of these relationships against experimental data. The first step in this direction was to write a computer program for the model and check whether the model was capable of duplicating experimentally determined centerline geometrics and stress distributions. In this matching procedure, the as yet undefined free parameters were selected by trial and error. While the assessment of whether an acceptable duplication of the experimental data was achieved was somewhat subjective, this trial and error exercise was also useful in obtaining a feel for the effect of the variables on the tire geometry and stresses. In many cases it was found that close duplication could be achieved by various combinations of the free parameters, pointing to the possibility of reducing the number of free parameters in the mathematical model. The basic elements in the computer program used in this development, such as the subroutine for the calculation of slip line fields, were essentially the same as in the final program for the performance prediction presented in Appendix B, but many of the iteration procedures were operated with manual interaction.

Although the computer program in the above development stage with its capability to duplicate experimental data was valuable in itself for the analysis of tire-soil interaction, for the purpose of tire performance prediction it was necessary to establish its general validity and develop relationships among the free and input parameters and methods to determine the input parameters from available

information on tire and soil for the prediction of performance. Since experimental information on tire-soil interaction that covered a wide range of conditions and a number of tire types was limited to tire performance data, a method was devised to utilize these data for these purposes. The computer program at this stage established a multivariate relationship between tire performance and a number of free and input parameters. The problem was to find values for these parameters so that the experimentally determined performance data be matched for all conditions tested. The available experimental data listed in Tables 1 and 2 represented 38 different conditions; each of the 38 tests contained load, pull, torque, and sinkage data at several values of slip. The computer time required to compute the performance parameters for the possible combinations of free and input parameters for each slip rate in the 38 tests on the PDP-10 computer was economically prohibitive, and recourse was made to the use of minicomputers for this purpose. In an independent research project of the Research Department methods were developed to run relatively large programs on minicomputers by storing segments of the program on disks and bring selected portions into the core when needed (Ref. 15). As a result of this operation and the lower computation speed available with minicomputers the running time is about two to six times longer than on the PDP-10 or similar computers, but the cost of computation is minimal. The program was easily adapted to the research department's NOVA 800 minicomputer; the main program and the subroutine constituted two segments that the core was capable of accommodating. The longer running time was of no disadvantage inasmuch as loops for the desired variations of parameters were incorporated into the program, and the extended program was run overnight without any supervision. This way performance calculations

were made for over 15,000 combinations of the parameters without incurring costs other than minimal depreciation and maintenance.

Even though the use of the minicomputer made an extensive analysis of the program feasible, it was desirable to reduce the number of combinations of the various parameters as much as possible. To this end it was decided to allow variation of certain parameters only if no combination of the other parameters yielded satisfactory results. This restriction of the variation of the parameters involved the following assumptions:

- The α' and α'' angles (Fig. 2) were assumed to be equal
- The curvature of the logarithmic spiral section was assumed to be the same in the front and rear section
- It was assumed that the soil strength parameters φ and c were uniquely determined by the cone index or its gradient in the experiments listed in Tables 1 and 2. The following relationships between strength and cone index parameters were established:

Yuma sand:

$$D_r(\%) = 71.1 \log (CGR) + 11.33 \qquad (3)$$

$$\varphi = \arctan\left(1/(1.64 - 0.68\, D_r)\right)$$

Buckshot clay:

$$C(\text{psi}) = CI/12.5 \qquad (4)$$

$$\varphi(^\circ) = CI/4$$

Since the establishment of these relationships is closely related to the general problem of the determination of strength properties of soils for mobility purposes, it is discussed in detail under that heading in Appendix A.

The effect of model parameters on performance simulation was analyzed by a systematic variation of the following parameters:

- Deflection coefficient
- Limiting pressure p_l
- Angle
- Angle
- Initial values of $_r$ and $_d$

In these performance simulation analyses the main objective was to simulate the pull coefficient-slip relationship. Simulation of sinkage was considered only as a secondary objective, partly because sinkage measurements are somewhat uncertain (sinkage was not directly measured in the tests but derived by an experimental formula from the vertical movement of the hub). Comparison of computed and measured sinkage was, however, very useful in deciding whether discrepancies in pull coefficients occurred because of bad centerline geometry simulation or for other reasons. Generally speaking, good simulation of the pull coefficient was not possible without fairly good sinkage approximation. Computed and measured torque coefficients generally agreed well when the pull coefficient simulation was good; reasons for exceptions are discussed in Section X.

The performance simulation analyses resulted in the establishment of initial values of $_r = 10°$ and $_d = 5°$.

In strong cohesive soils, θ_d loses its meaning when the strength of the soil is such that there is no failure condition in the front field and only a rear plastic failure zone develops the angle of separation of the front field. In such a case, good simulation results if the entry angle is assumed as one and a half times the rear angle.

For the value of the angle θ_ϵ the relationship $\theta_\epsilon = \theta_d/2$ was found to result in good simulation.

The values established above for these angles are not necessarily the best ones, but were found to yield acceptable performance simulation in the cases analyzed.

In the concept of the tire-soil model, the angle of the developed interface friction, δ, is the independent variable that enters into the computation of slip line field. The angle δ is related to slip by the following:

$$\tan \delta = \tan \delta_{max}\left(1 - e^{-(j+j_o)/K}\right) \qquad (5)$$

This equation is the same type as proposed by Janosi and Hanamoto for the relationship between mobilized shear stress and slip for tracked vehicles (Ref. 16). The slip-shear parameters in Eq. (5) were not known beforehand and had to be assumed so that a slip value corresponding to the δ value could be determined and the computed pull coefficients compared with the measured ones.

With the values of the various θ angles established by the analysis for model development, a systematic analysis of each of the 33 tire performance tests was made to determine the values of the parameters ϵ, p_1, j_o, and K that yielded good simulation. Figures 3 through 8 are examples of good simulation of pull coefficients obtained in this systematic analysis. The excellent agreement

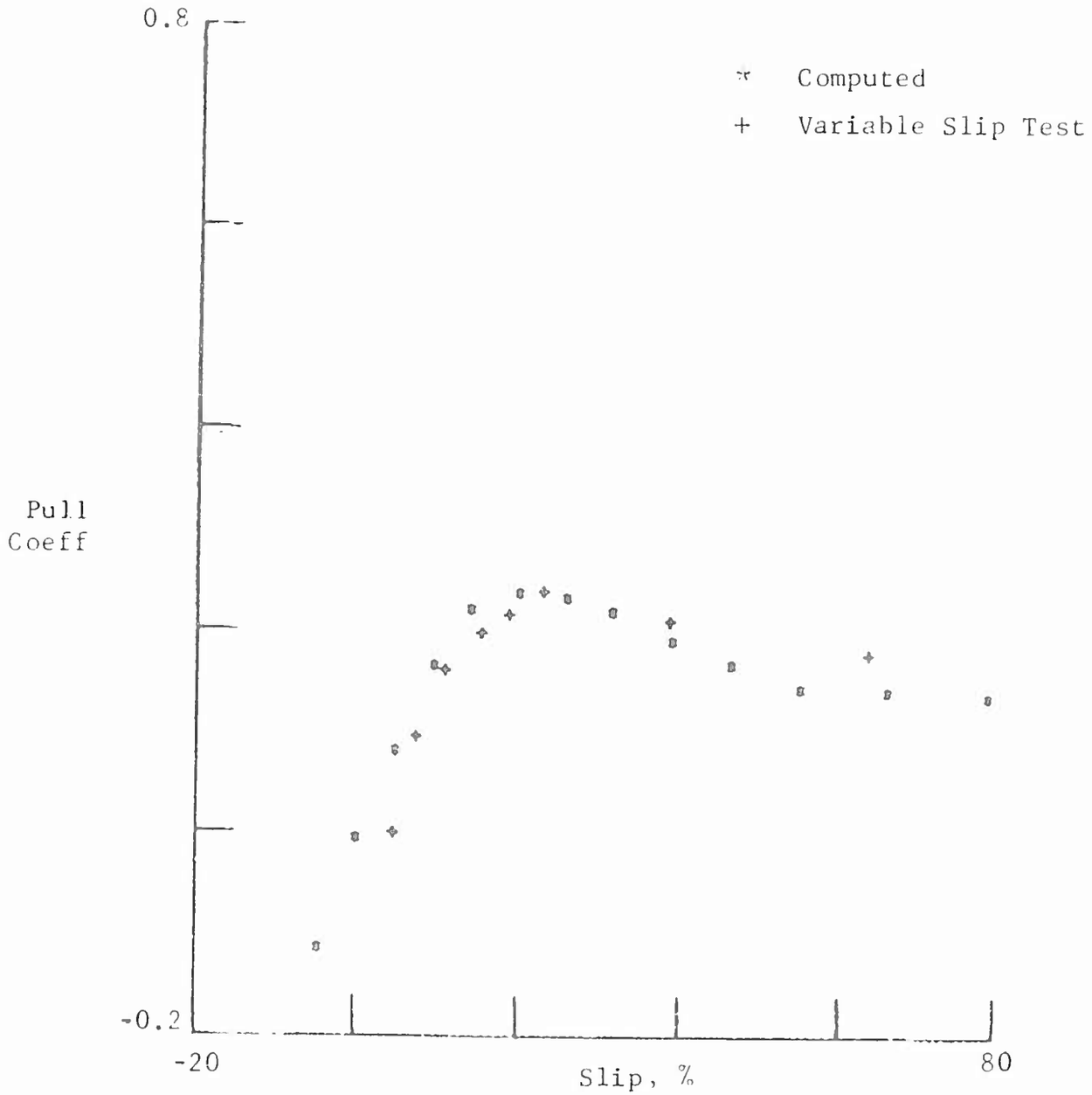

Tire: 9.00-14 Load: 450 lbs Infl. Pressure := 16.4 psi
Defl: 15% ϵ = 0.97 P_ℓ = 16.5 psi
Cone Index Gradient: 8.9 Friction Angle: 42.4°
Slip Parameters: j_o = 0.47 K = 0.184

Fig. 3 Simulation of Pull Performance with Freely Selected Parameters, Test No. 1

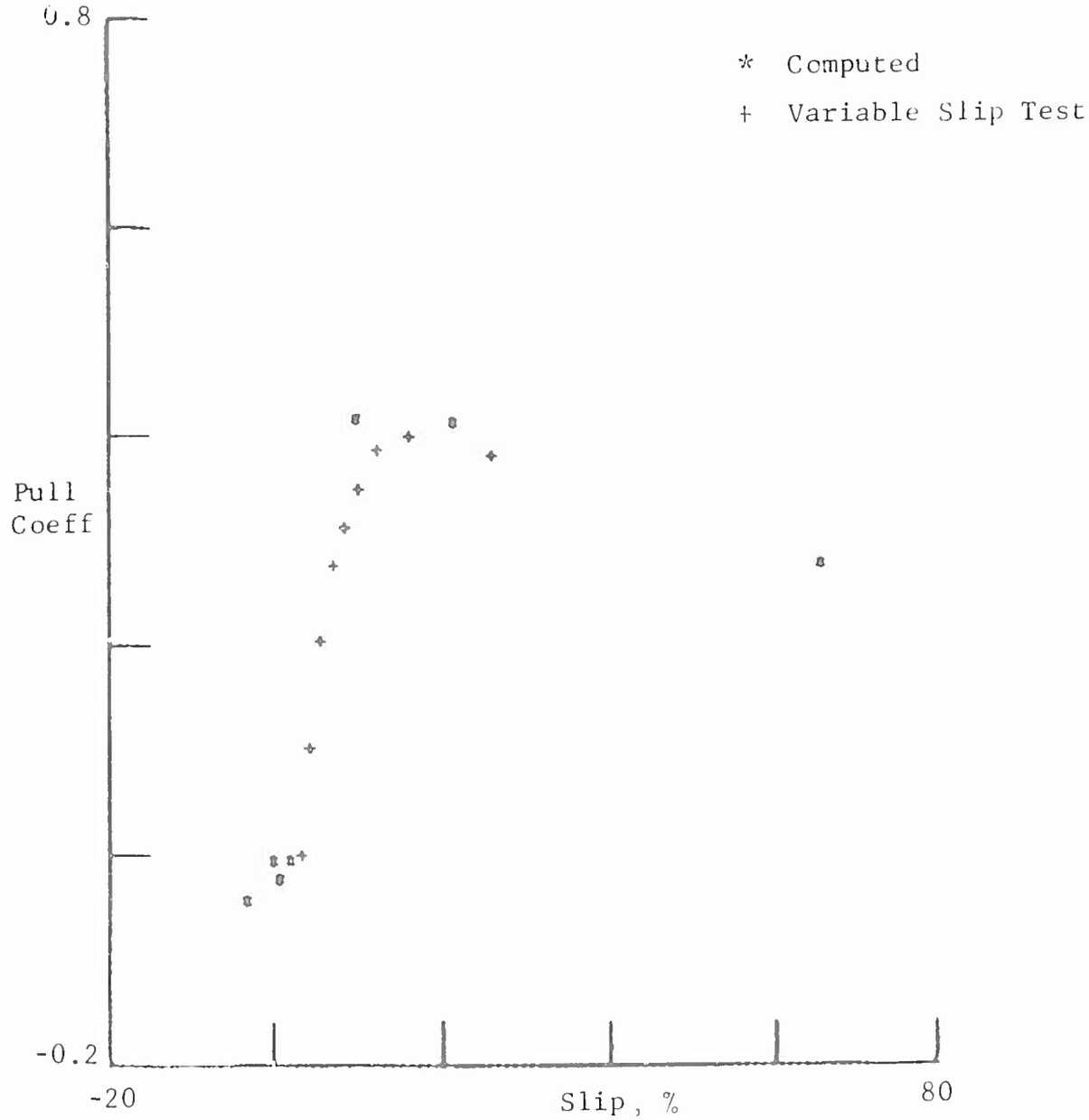

Tire: 6.00-16 Load: 455 lbs Infl. Pressure: 10.3 psi
Defl: 25% ϵ = 0.88 P_i = 10 psi
Cone Index Gradient: 15.6 Friction Angle: 45.4°
Slip Parameters: j_o = 0.03 K = 0.07

Fig. 4 Simulation of Pull Performance with Freely Selected Parameters, Test No. 4

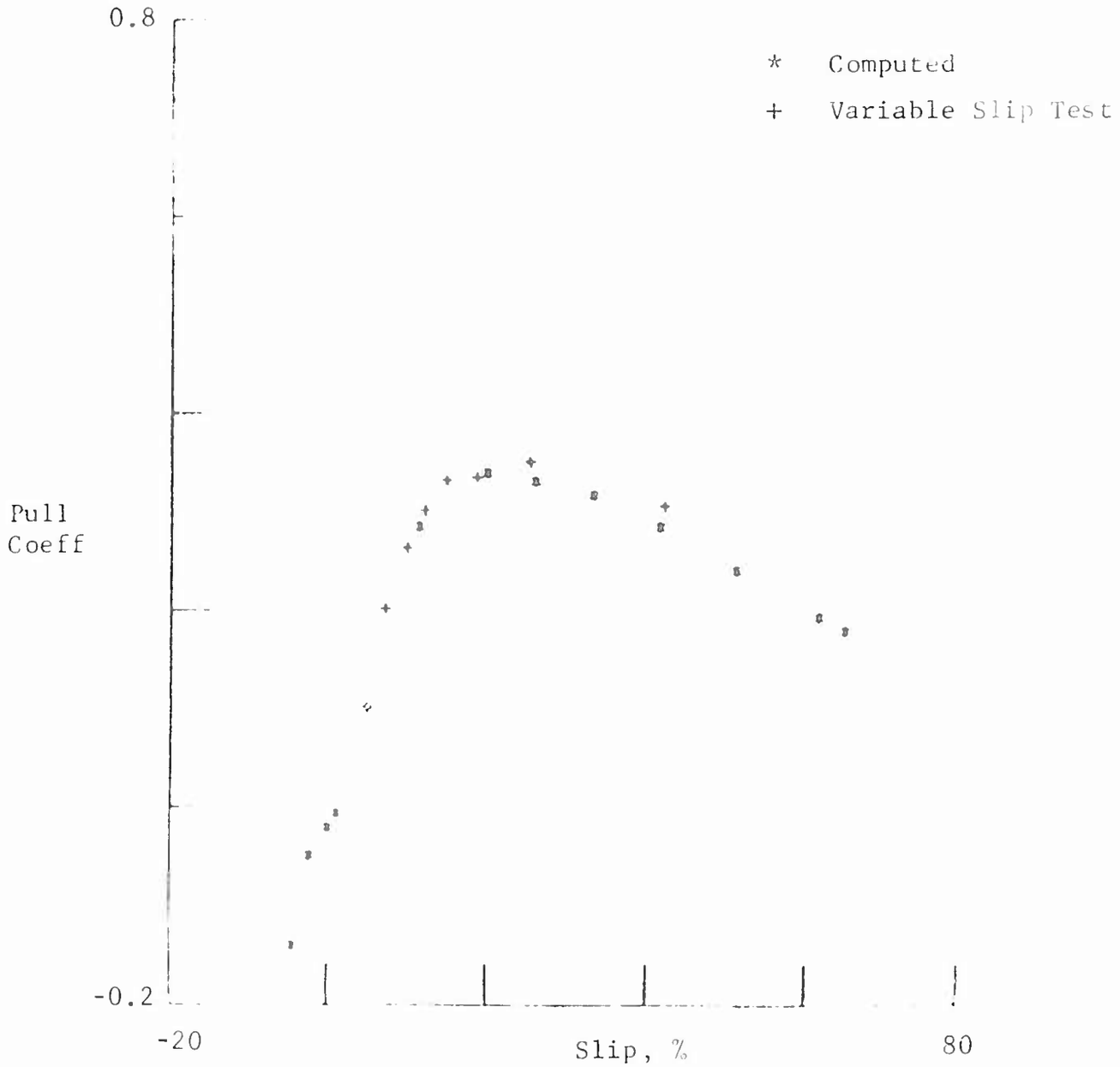

Tire: 9.00-14 Load: 890 lbs Infl. Pressure: 16.4 psi
Defl: 25% ϵ = 0.88 P_g = 16.0 psi
Cone Index Gradient: 13.8 Friction Angle: 44.7°
Slip Parameters: j_o = 0.03 K = 0.12

Fig. 5 Simulation of Pull Performance with Freely Selected Parameters, Test No. 9

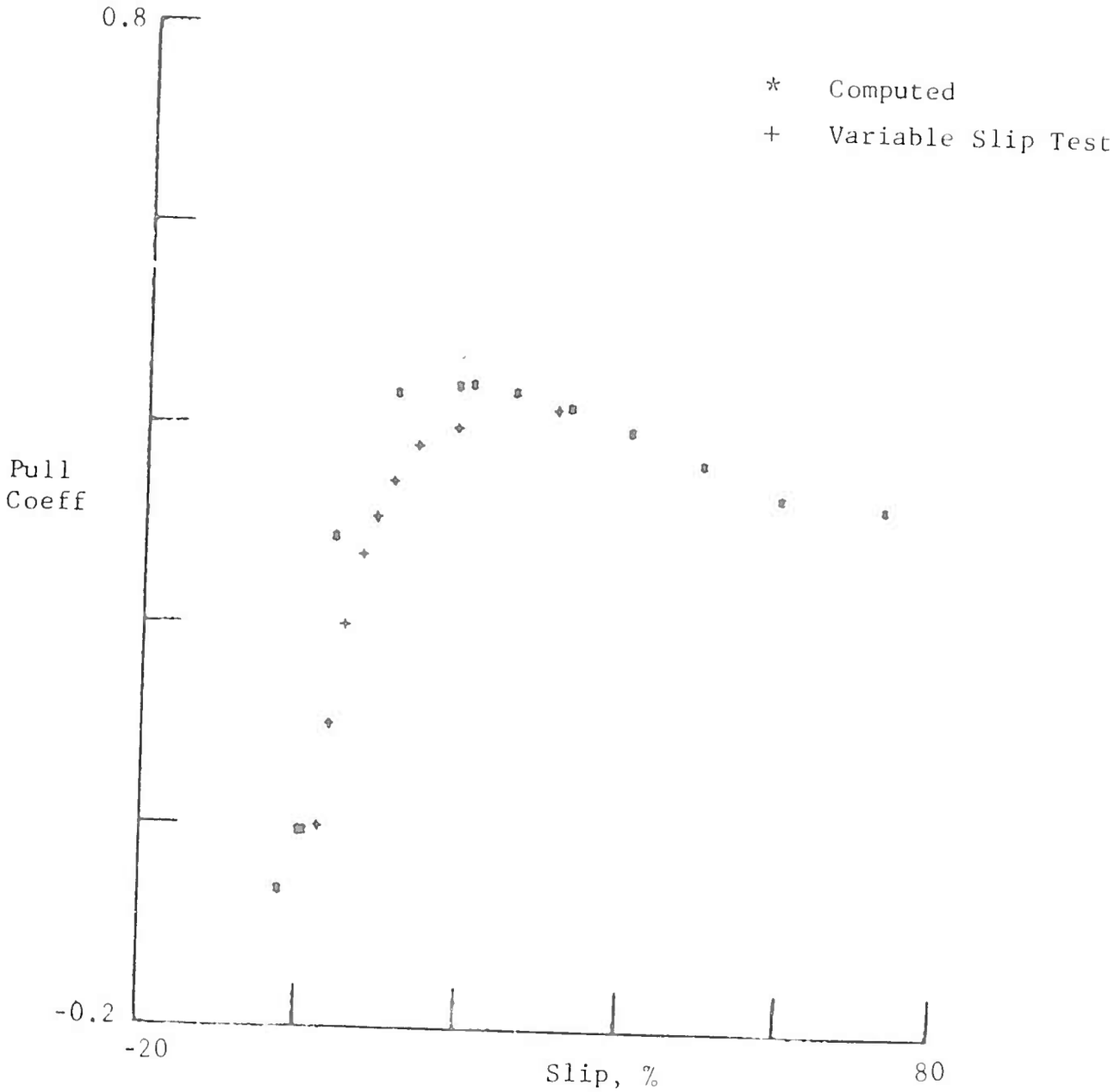

Tire: 9.00-14 Load: 430 lbs Infl. Pressure: 7.50 psi
Defl: 25% ϵ = 0.85 P_l = 9 psi
Cone Index Gradient: 12.40 Friction Angle: 44.7°
Slip Parameters: j_o = 0.024 K = 0.09

Fig. 6 Simulation of Pull Performance with Freely Selected Parameters, Test No. 11

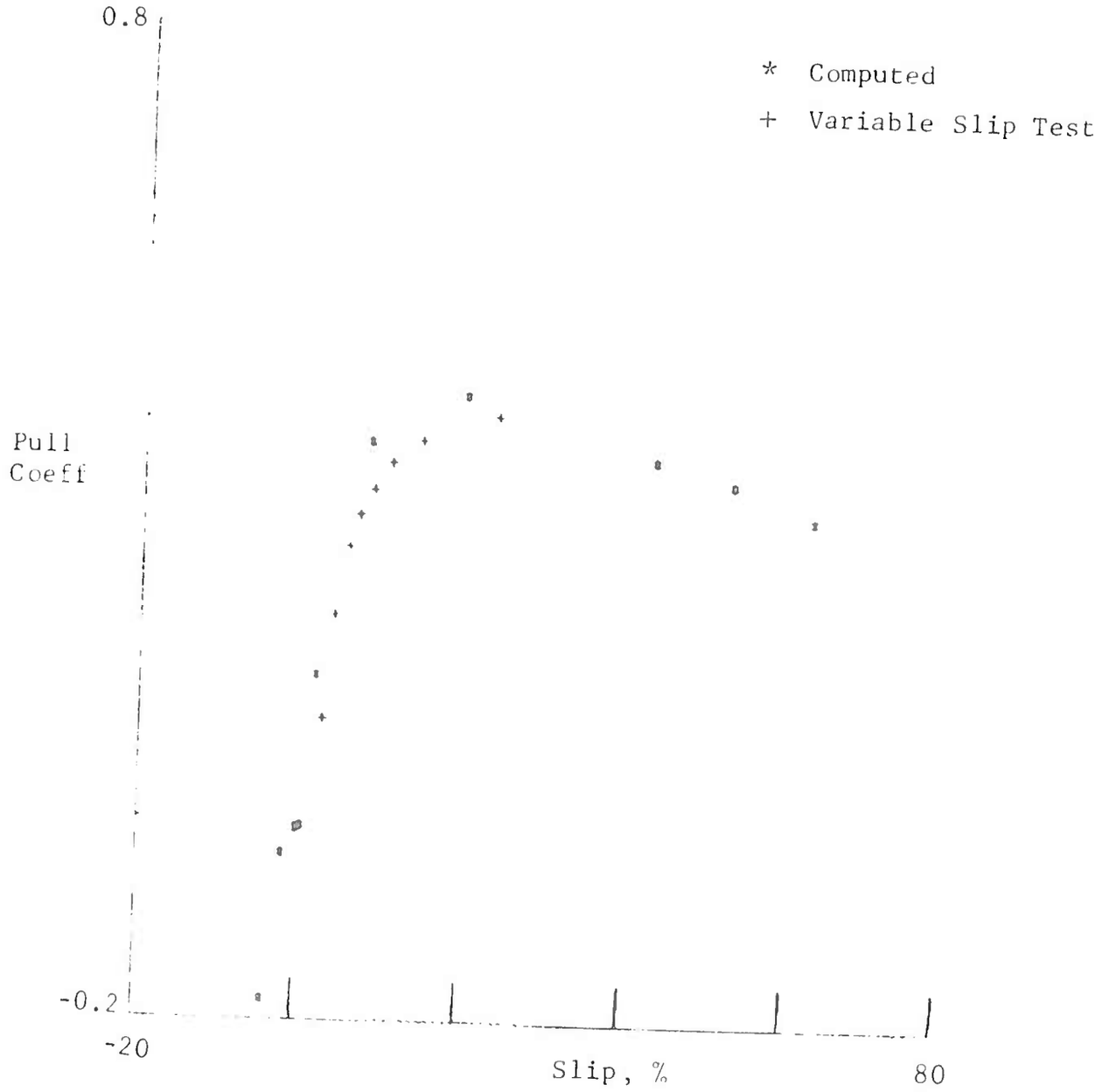

Tire: 4.00-20 Load: 340 lbs Infl. Pressure: 11 psi
Defl: 35% ϵ = 0.92 P_ℓ = 10 psi
Cone Index Gradient: 25.6 Friction Angle: 46.2°
Slip Parameters: j_o = 0.03 K = 0.18

Fig. 7 Simulation of Pull Performance with Freely Selected Parameters, Test No. 22

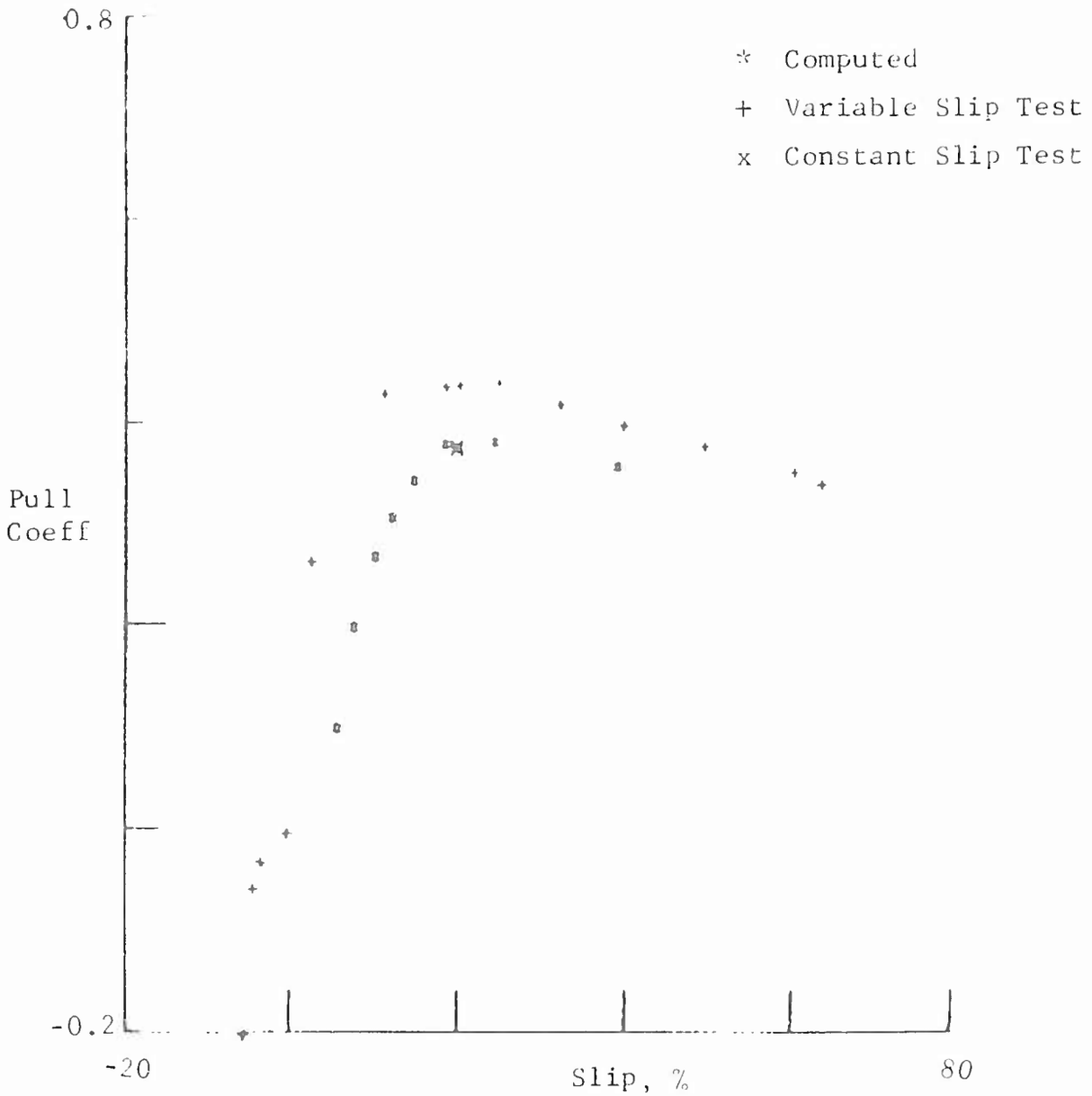

Tire: 9.00-14 Load: 455 lbs Infl. Pressure: 7.5 psi
Defl: 25% ϵ = 0.87 P_ℓ = 8.5 psi
Cone Index Gradient: 11.8 Friction Angle = 43.8°
Slip Parameters: j_o = 0.04 K = 0.11

Fig. 8 Simulation of Pull Performance with Freely Selected Parameters, Test No. 25

between experimental and calculated values was indicative of the capability of the model to simulate tire-soil interaction and in most cases was within the probable limits of accuracy of the experiments. Obviously, there was no need for further refinement of the model, but relationships between parameter ϵ, p_1, j_o, and K and measurable tire and soil properties still had to be developed for prediction purposes. An extensive study of the freely selected parameters that yielded good simulation was made, and the following rules for the estimation of these parameters were developed.

Estimation of the Deflection Coefficient ϵ

The deflection coefficient ϵ is closely related to the design deflection coefficient $2\delta/d$ used by WES and can be determined by a deflection measurement on a rigid surface. Table 4 contains the relationships for the estimation of coefficient ϵ for the various sizes of tires in terms of $\kappa = 1 - 2\delta/d$.

TABLE 4. ESTIMATION OF THE DEFLECTION COEFFICIENT ϵ FOR VARIOUS SIZE TIRES

Tire Size	Relationship for Estimation, ϵ =
9.00-14	$1.24\kappa - 0.195$
6.00-16	$1.62\kappa - 0.59$
4.00-7	$1.14\kappa - 0.115$
4.00-20.0	$0.91\kappa + 0.085$
31 x 15-13	$0.98\kappa + 0.065$

The relationships listed in Table 4 for the estimation of ϵ are shown in Fig. 9. It can be seen that they are very similar to each other and allow an approximate estimate of ϵ for tire sizes other than those listed in Table 4. If no other information is available, the relationship $\epsilon = \kappa$ shown by a heavy dashed line in Fig. 9 can serve as a first approximation.

Estimation of the Limiting Pressure, p_l

It was found that the limiting pressure p_l may be estimated on the basis of inflation pressure for all tire sizes by the following relationship:

$$p_l(\text{psi}) = 0.64 \times p_i + 4 \qquad (6)$$

The p_l values determined by the above relationship are higher than p_i up to about 11 psi and lower than p_i above 11 psi. (The p_l values should not be interpreted as the average pressure in a rigid surface.) The p_l value is a model parameter that refers to the limiting pressure that yields acceptable tire-soil interaction simulation with the proposed tire-soil model. It may be interesting to note, however, that some tires at high values of inflation pressure exhibit average pressures lower than the inflation pressure (Ref. 17).

Estimation of the Slip-Shear Parameters j_o and K

The equation for the relationship between mobilized shear strength and slip proposed by Janosi and Hanamoto (Ref. 16) was based on the analogy of tracks and direct shear tests from which the parameter K in the proposed equation could be evaluated. In applying the same concept to wheels it was necessary to include the

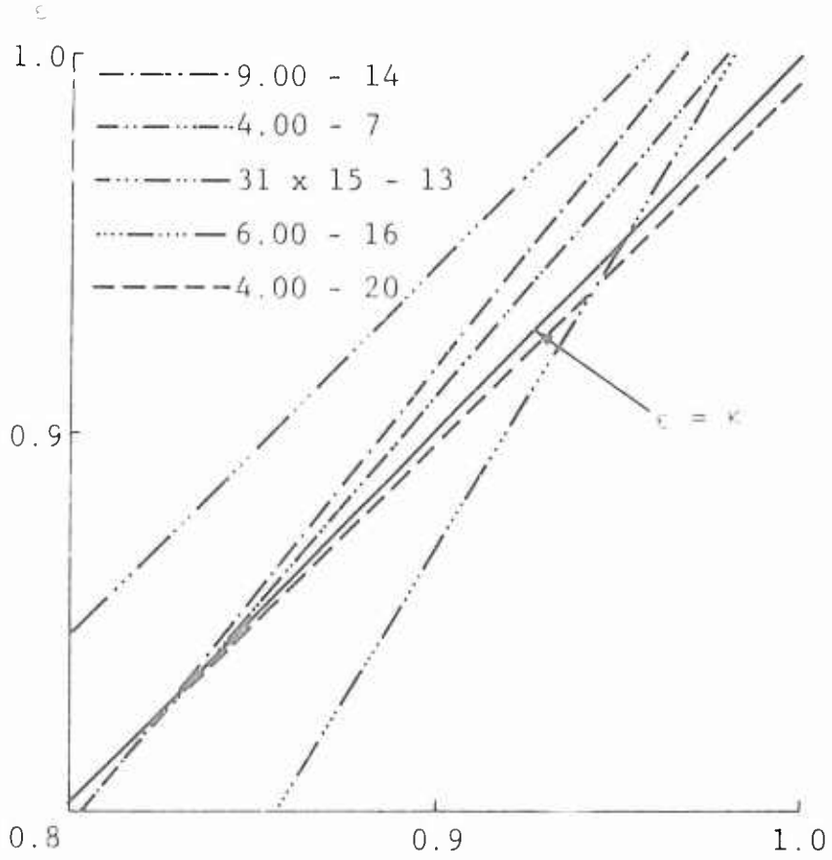

$$\kappa = 1 - \frac{2\delta}{d}$$

Fig. 9 Relationship Between the Deflection Parameters ε and κ

initial value j_o in the slip term since experiments showed a negative slip at the towed point where the developed shear stress is zero. In the case of wheels and tires the analogy with the direct shear test is not evident since it is difficult to define and measure the differential displacement between points on the wheel surface and soil. Theoretical modeling of the slip-shear phenomenon in both shear strength tests and tire-soil interaction would be necessary to develop a theoretical basis for the estimation of these parameters. In view of the lack of such theory extensive studies were made to determine whether there is a correlation between soil strength properties and the slip-shear parameters that were found to yield good simulation of the experimental pull coefficient-slip curves. These studies showed no close correlation between slip-shear and strength parameters.

Further studies indicated that the relation of tire dimensions to load has some effect on the slip-shear parameters. A correlation was found to exist between the dimensionless numerics developed at WES and the slip-shear parameters. The following relationships were tentatively established:

Yuma sand:

$$j_o = 0.046 - 0.0006\, N_s$$

$$K = e^{-0.58 \times \log 2N_s} \tag{7}$$

where

$$N_s = \frac{CGR.(b.d)^{3/2}}{W} \cdot \frac{b}{h}$$

Buckshot clay:

$$j_o = -0.065 + 0.49/N_c$$
$$K = -0.06 + 0.66/N_c \qquad (8)$$

where

$$N_c = \frac{Cl.b.d}{W} \cdot \left(\frac{\delta}{h}\right)^{1/2} < 7.5$$

These equations are purely empirical and are not intended to represent causative relationships.

IX. PREDICTION OF TIRE PERFORMANCE BY THE PROPOSED TIRE-SOIL MODEL

In Section VIII, relationships were established that allow the prediction of tire performance from input parameters that are generally available or can be obtained by conventional testing techniques. To evaluate the accuracy of performance predictions using these relationships, performance calculations were made using the computer program described in Appendix B for all cases for which experimental data were available. It should be emphasized that the comparison of experimental and predicted performance shown graphically in the subsequent figures represents results that can be obtained from data generally available for mobility evaluation.

Figures 10 through 36 show predicted and measured pull coefficients as a function of slip for tests 1 through 27 performed in Yuma sand. Figures 37 through 47 show the same for tests C1-1 through C1-11 performed in Buckshot clay.

Figures 48 through 50 show typical tire centerline geometries and outlines of slip line fields as obtained in the computer program for the various slip rates in tests 1, 5, and 18, respectively. Figure 51 shows the same in the case of a strong cohesive soil when there is only one rearward failure zone (test C1-1).

Figures 52 through 56 show comparisons of predicted and measured torque coefficients in some typical cases. Note that the torque coefficient is not very well defined for the centerline geometry of the tire-soil model and questions arise as to which value of the continuously changing tire radius should be used in the denominator of the formula for the torque coefficient. To

avoid this ambiguity the nominal tire radius was used in the computation of the torque coefficient from both the measured and computed torque.

Figures 57 and 58 show comparisons of measured and predicted sinkages in some typical cases.

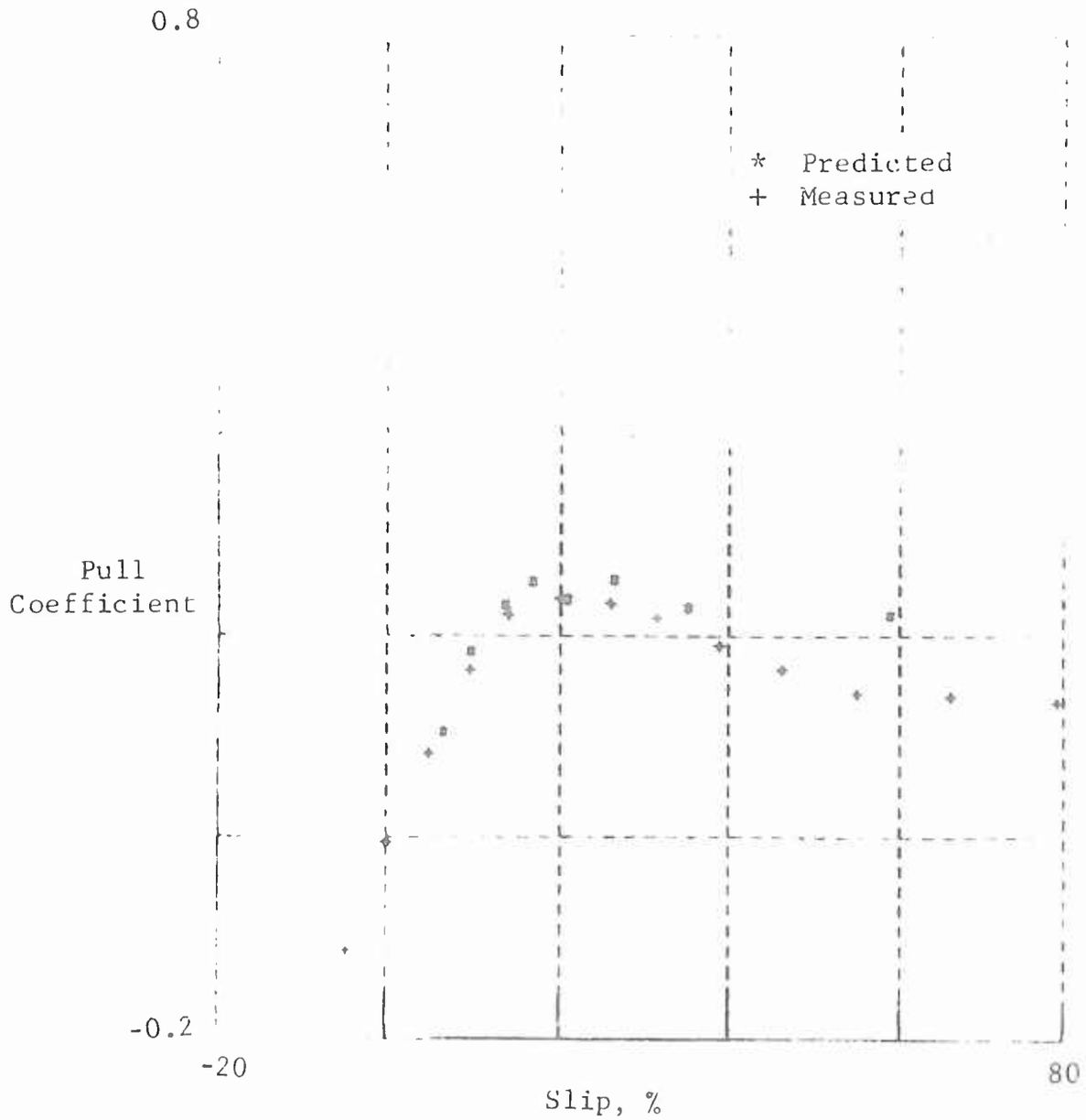

Fig. 10 Pull Coefficient Versus Slip - Test 1
Yuma Sand, CGR = 8.9
Tire: 9.00-14, Load: 440 lb

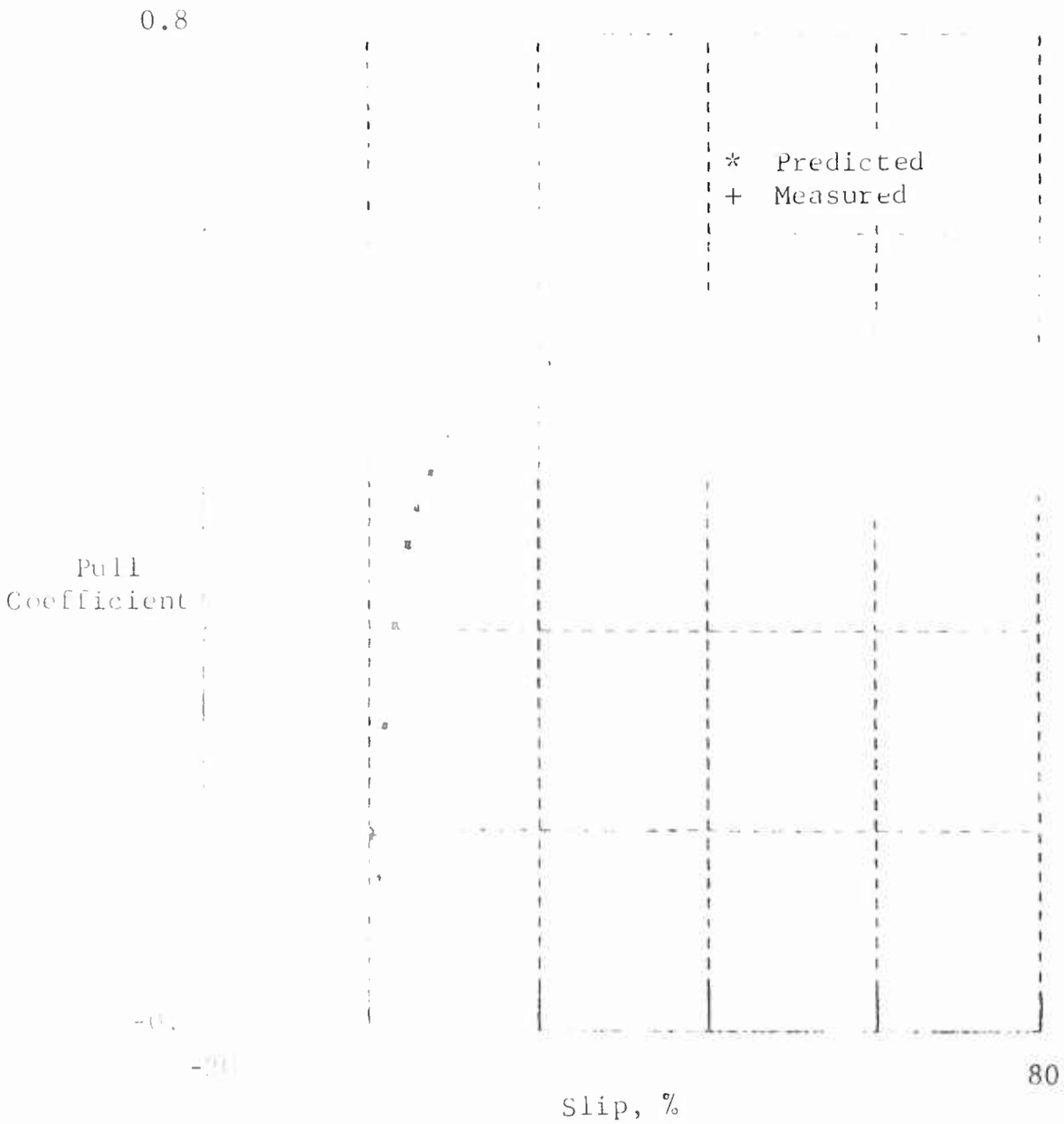

Fig. 11 Pull Coefficient Versus Slip - Test 2
Yuma Sand, CGR = 16.4
Tire: 6.00-16, Load: 240 lb

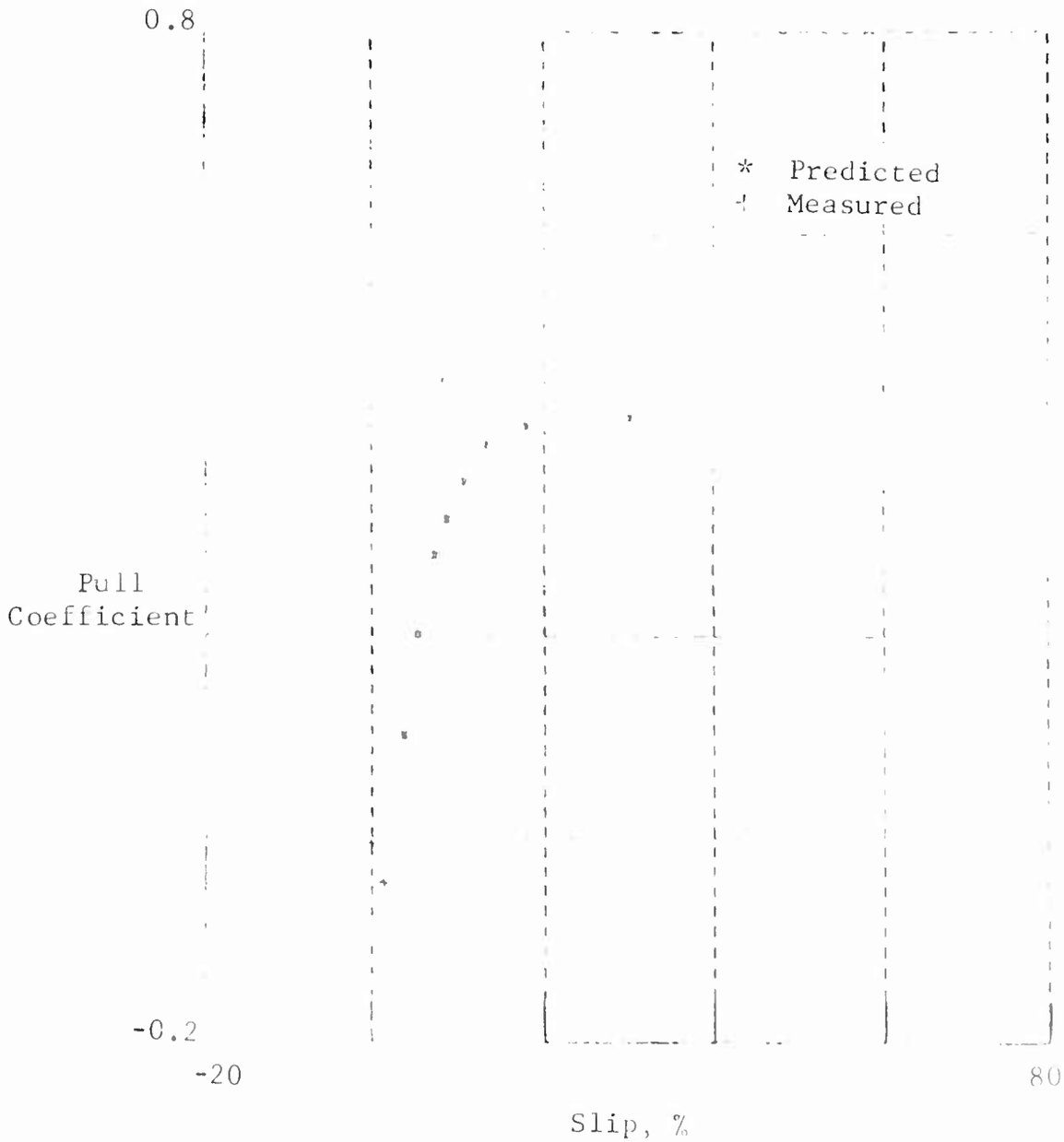

Fig. 12 Pull Coefficient Versus Slip - Test 3
Yuma Sand, CGR = 13.5
Tire: 6.00-16, Load: 240 lb

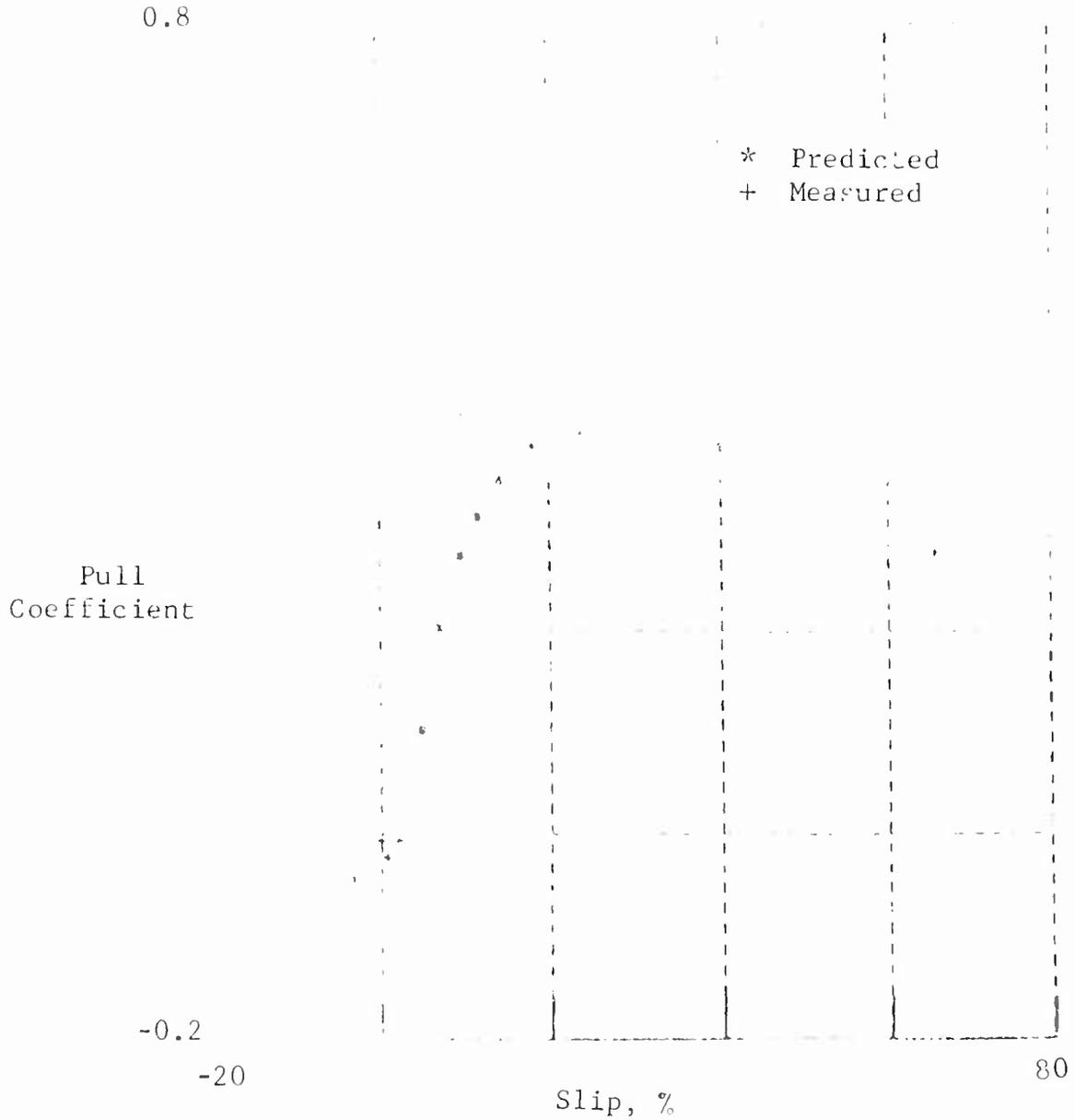

Fig. 13 Pull Coefficient Versus Slip - Test 4
Yuma Sand, CGR = 15.6
Tire: 6.00-16, Load: 450 lb

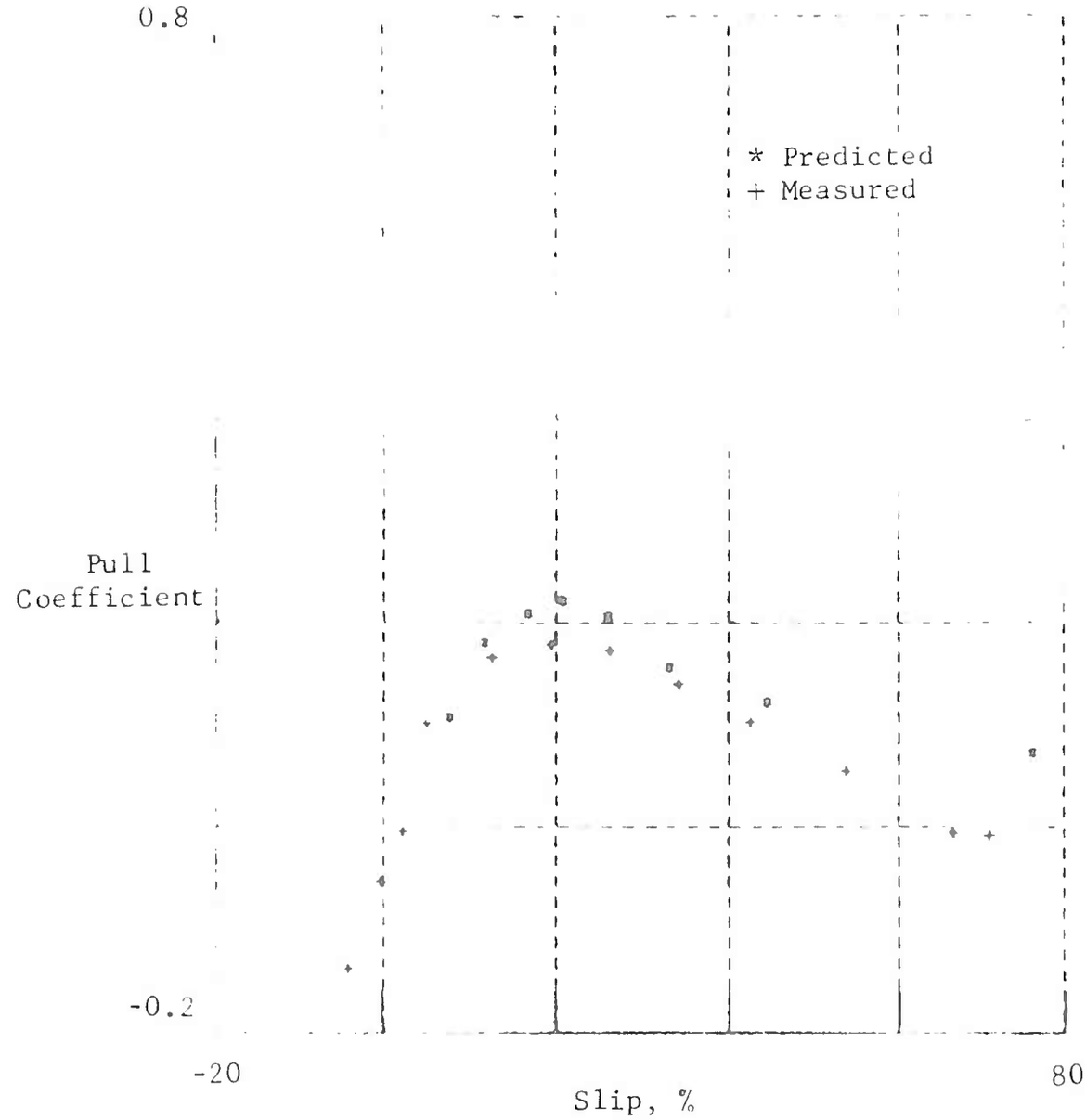

Fig. 14 Pull Coefficient Versus Slip - Test 5
Yuma Sand, CGR = 13.0
Tire: 4.00-7, Load: 210 lb

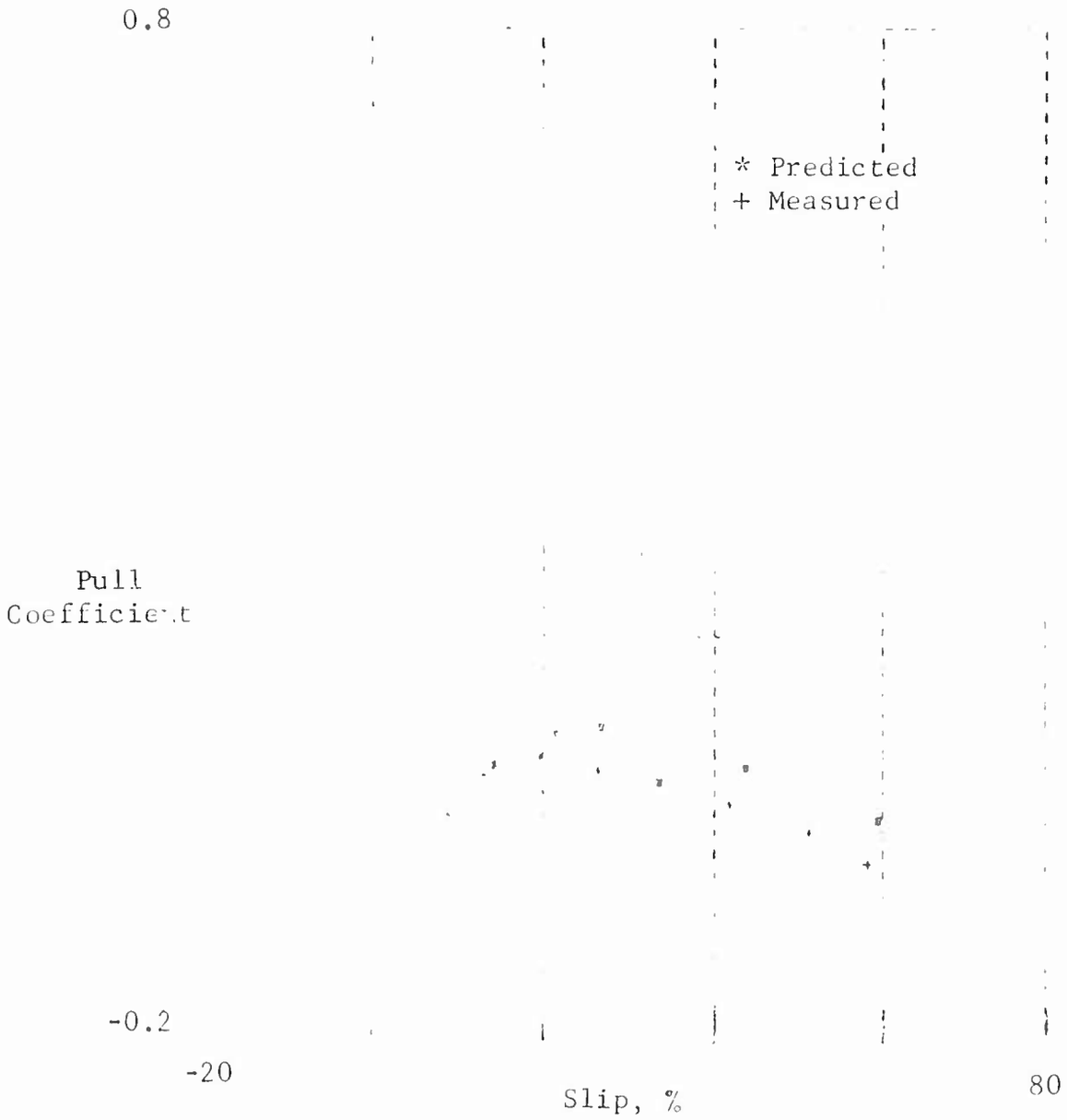

Fig. 15 Pull Coefficient Versus Slip - Test 6
Yuma Sand, CGR = 12.1
Tire: 4.00-7, Load: 340 lb

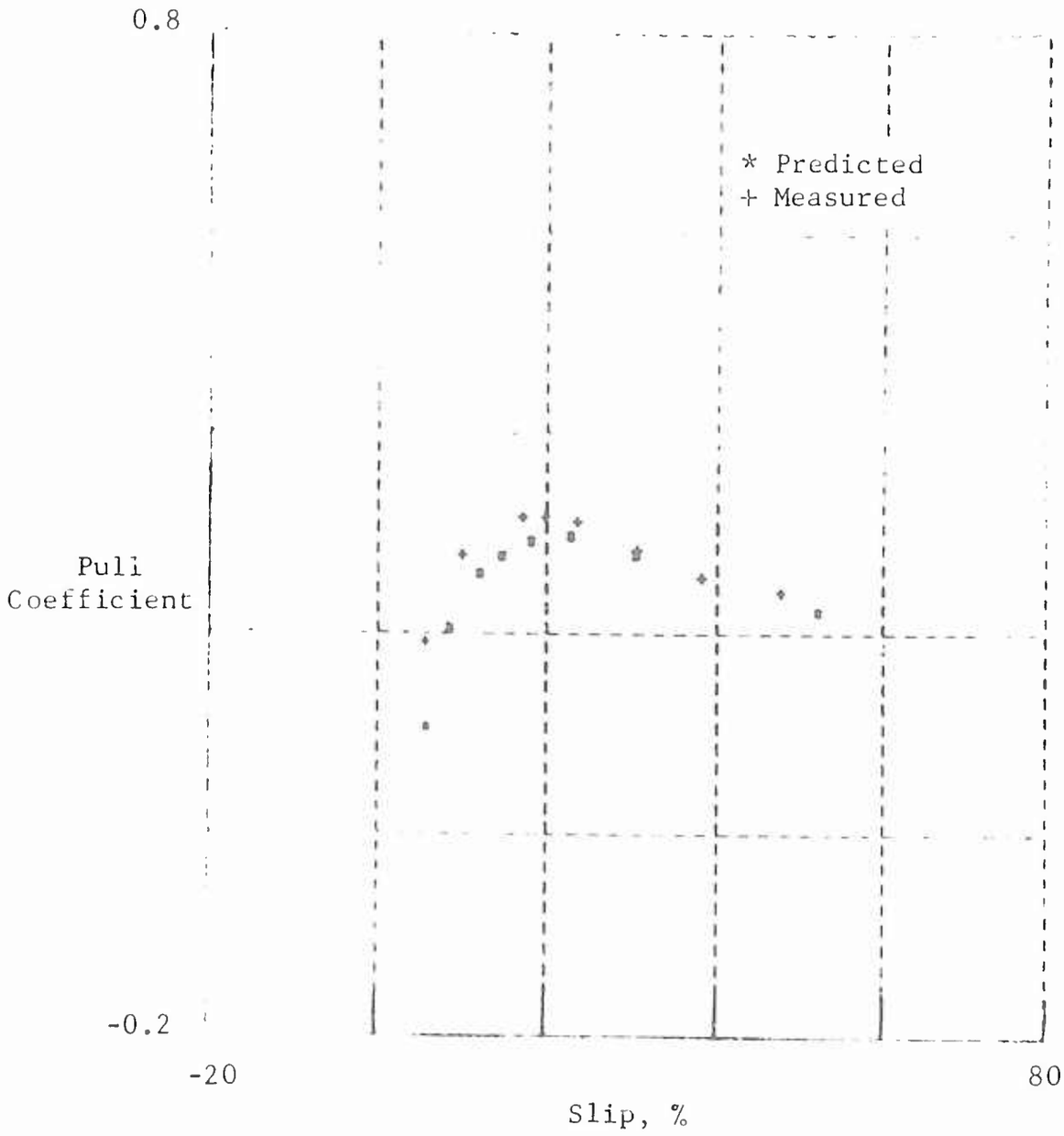

Fig. 16 Puil Coefficient Versus Slip - Test 7
Yuma Sand, CGR = 19.6
Tire: 4.00-7, Load: 220 lb

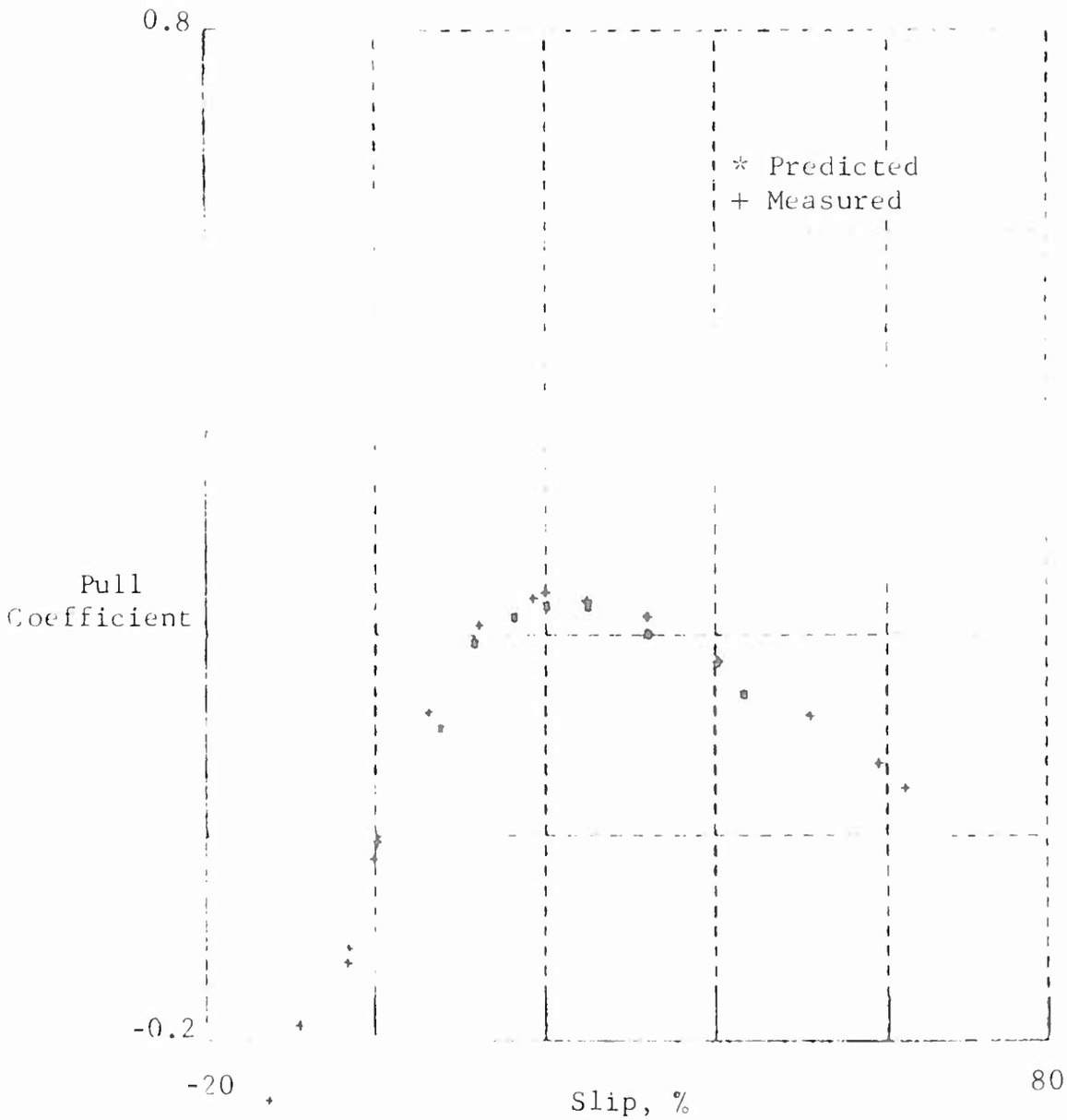

Fig. 17 Pull Coefficient Versus Slip - Test 8
Yuma Sand, CGR = 19.9
Tire: 4.00-7, Load: 440 lb

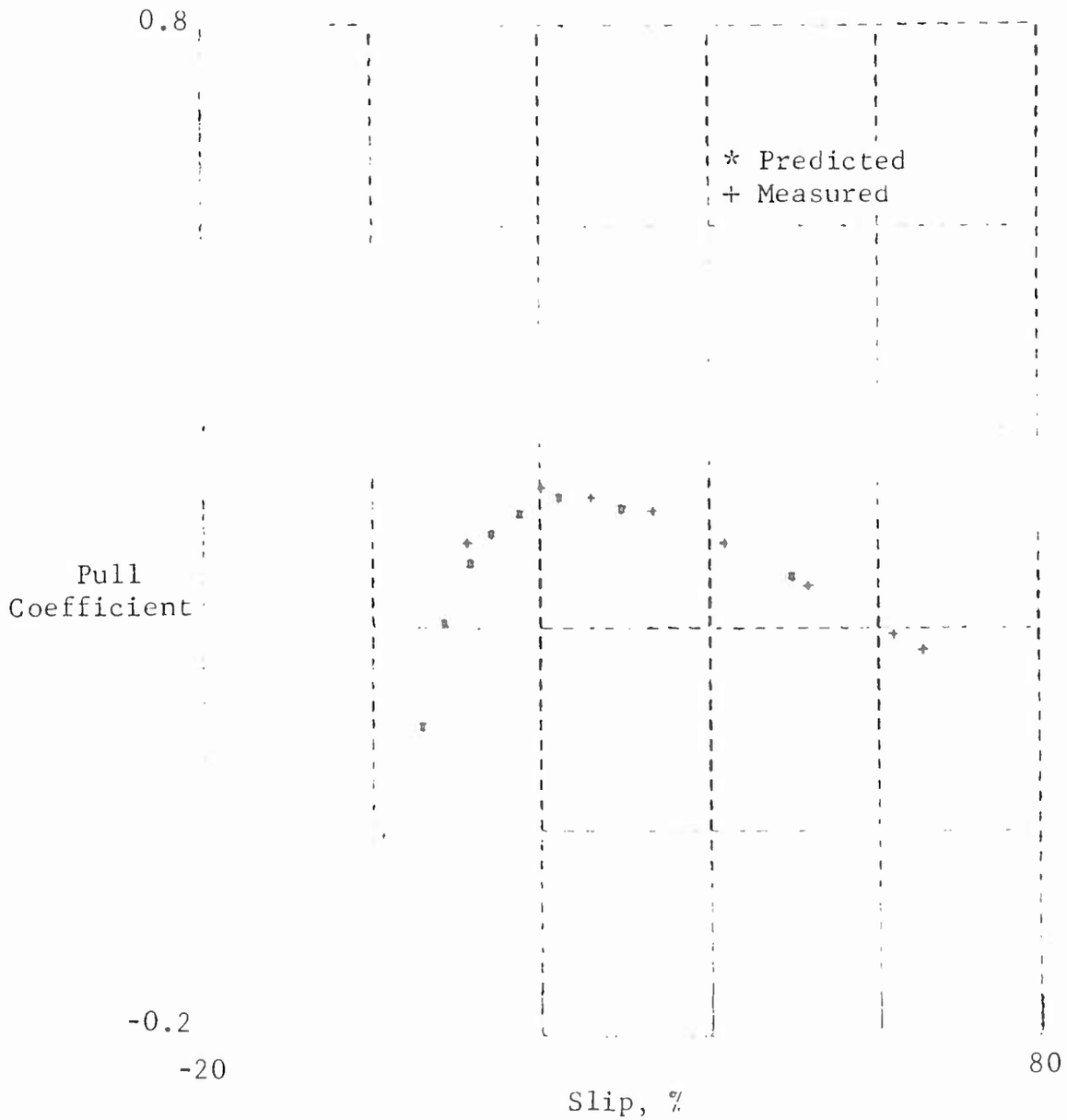

Fig. 18 Pull Coefficient Versus Slip - Test 9
Yuma Sand, CGR = 13.8
Tire: 9.00-14, Load: 840 lb

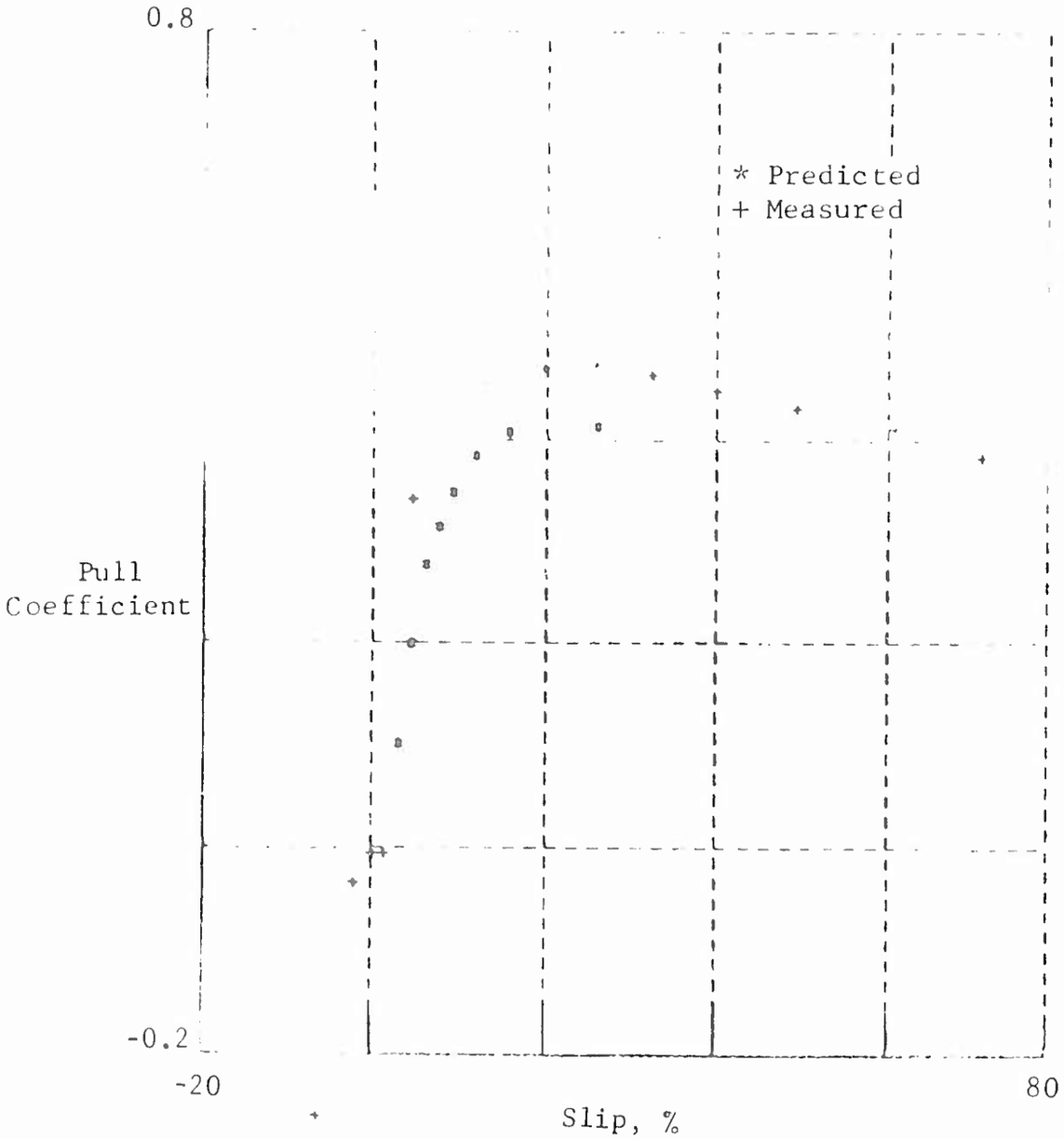

Fig. 19 Pull Coefficient Versus Slip - Test 10
Yuma Sand, CGR = 11.2
Tire: 9.00-14, Load: 220 lb

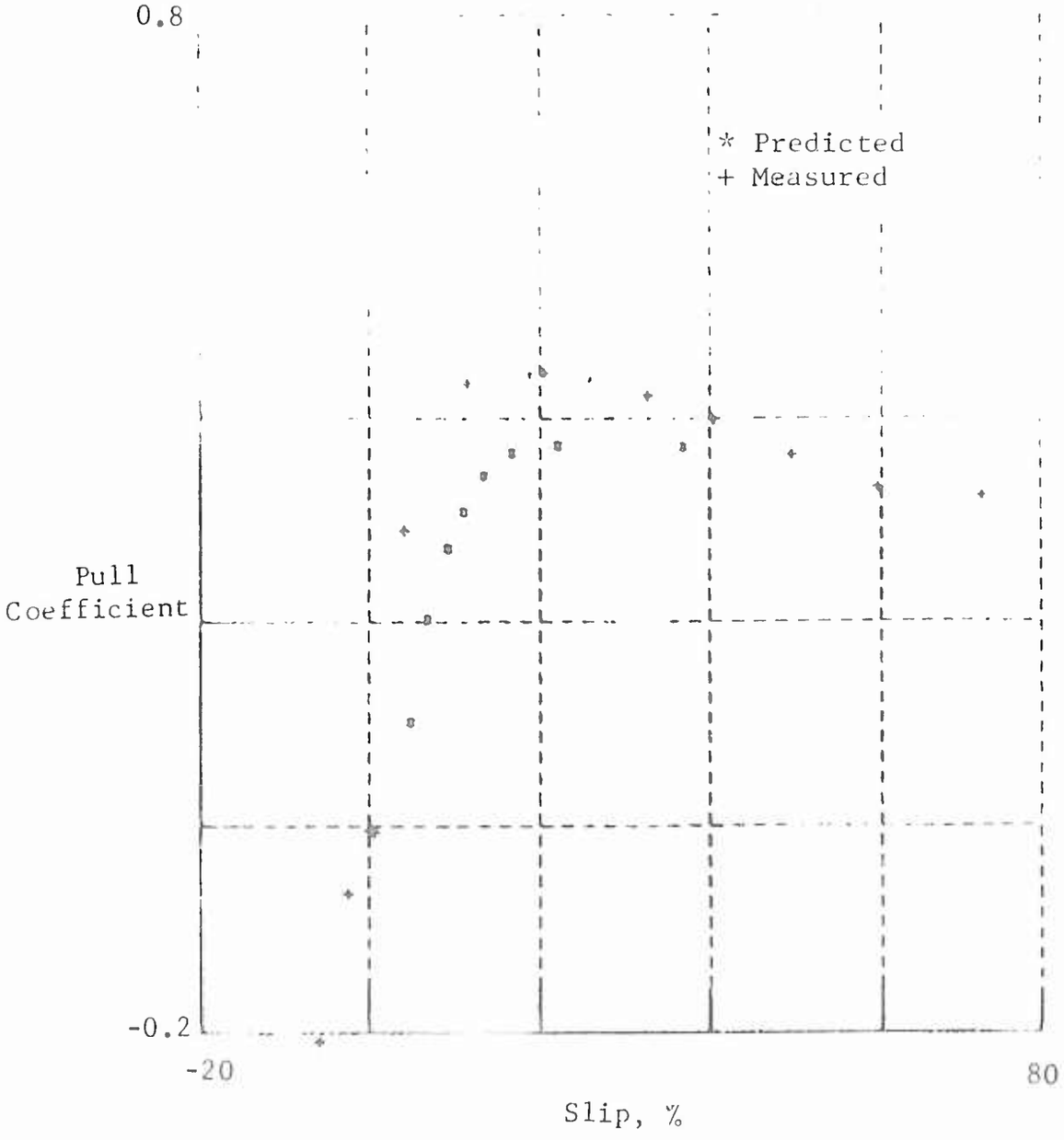

Fig. 20 Pull Coefficient Versus Slip - Test 11
Yuma Sand, CGR = 12.4
Tire: 9.00-14, Load: 440 lb

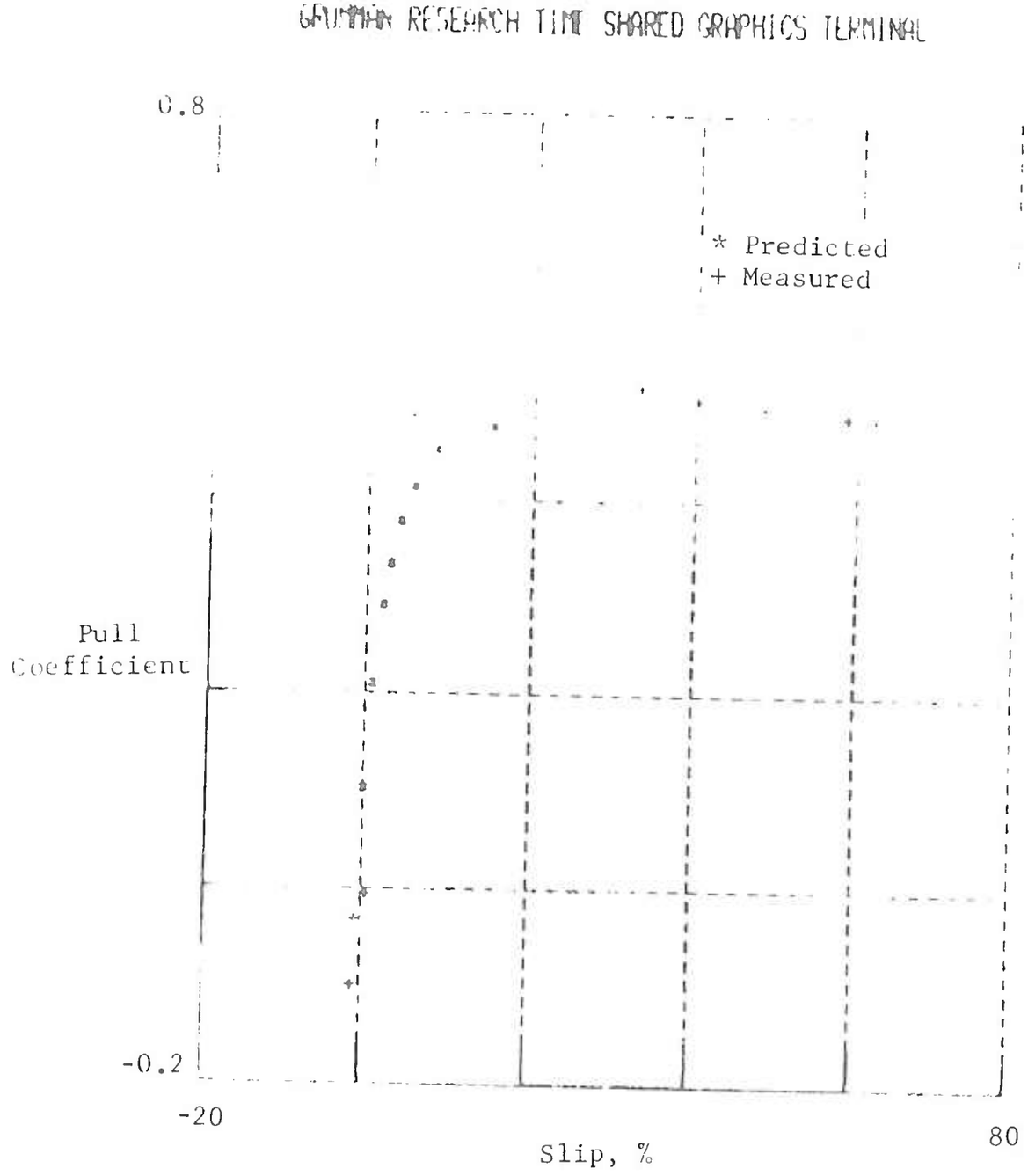

Fig. 21 Pull Coefficient Versus Slip - Test 12
Yuma Sand, CGR = 22.5
Tire: 9.00-14, Load: 210 lb

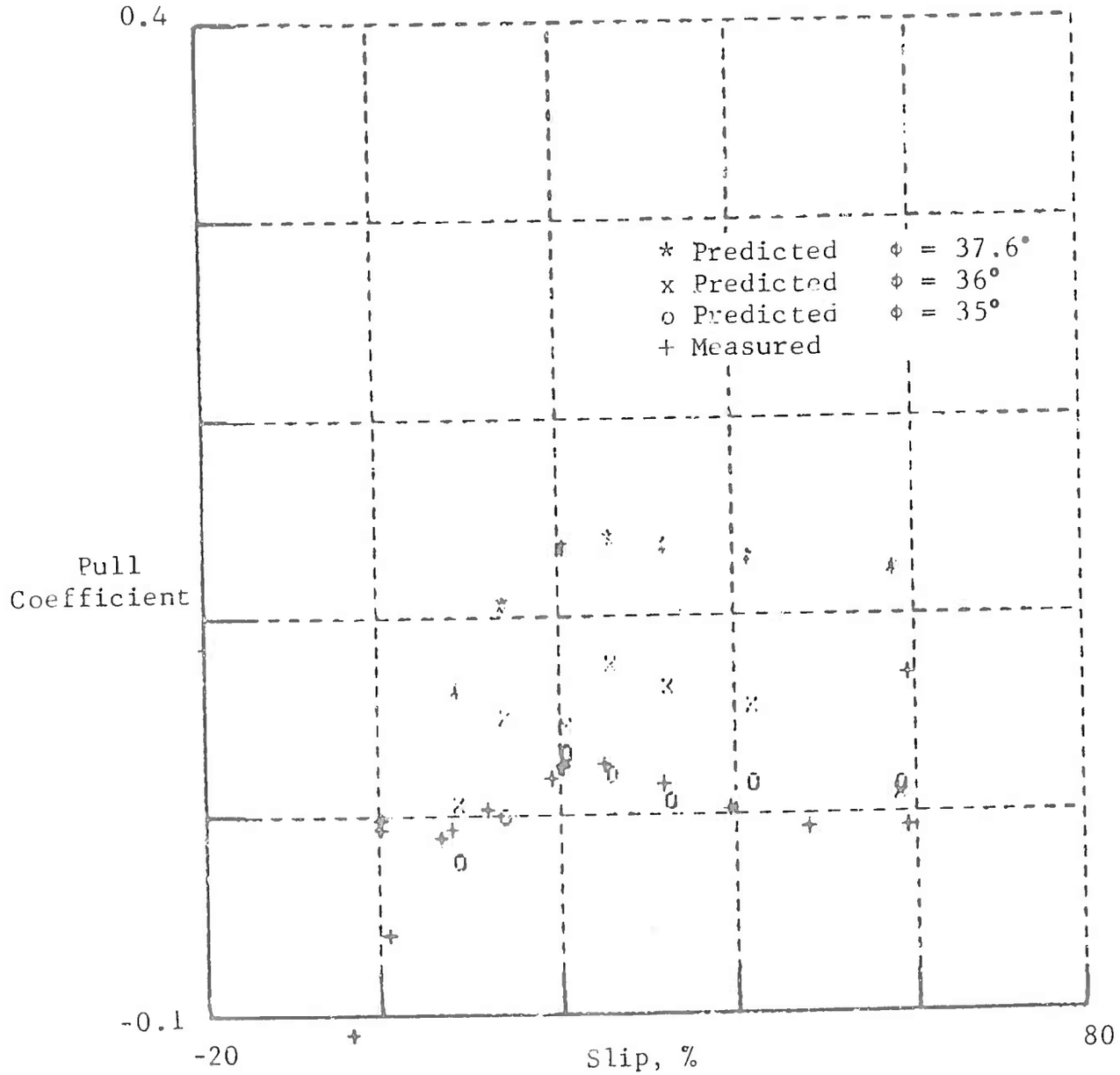

Fig. 22 Pull Coefficient Versus Slip - Test 13
Yuma Sand, CGR = 3.5
Tire: 9.00-14, Load: 620 lb

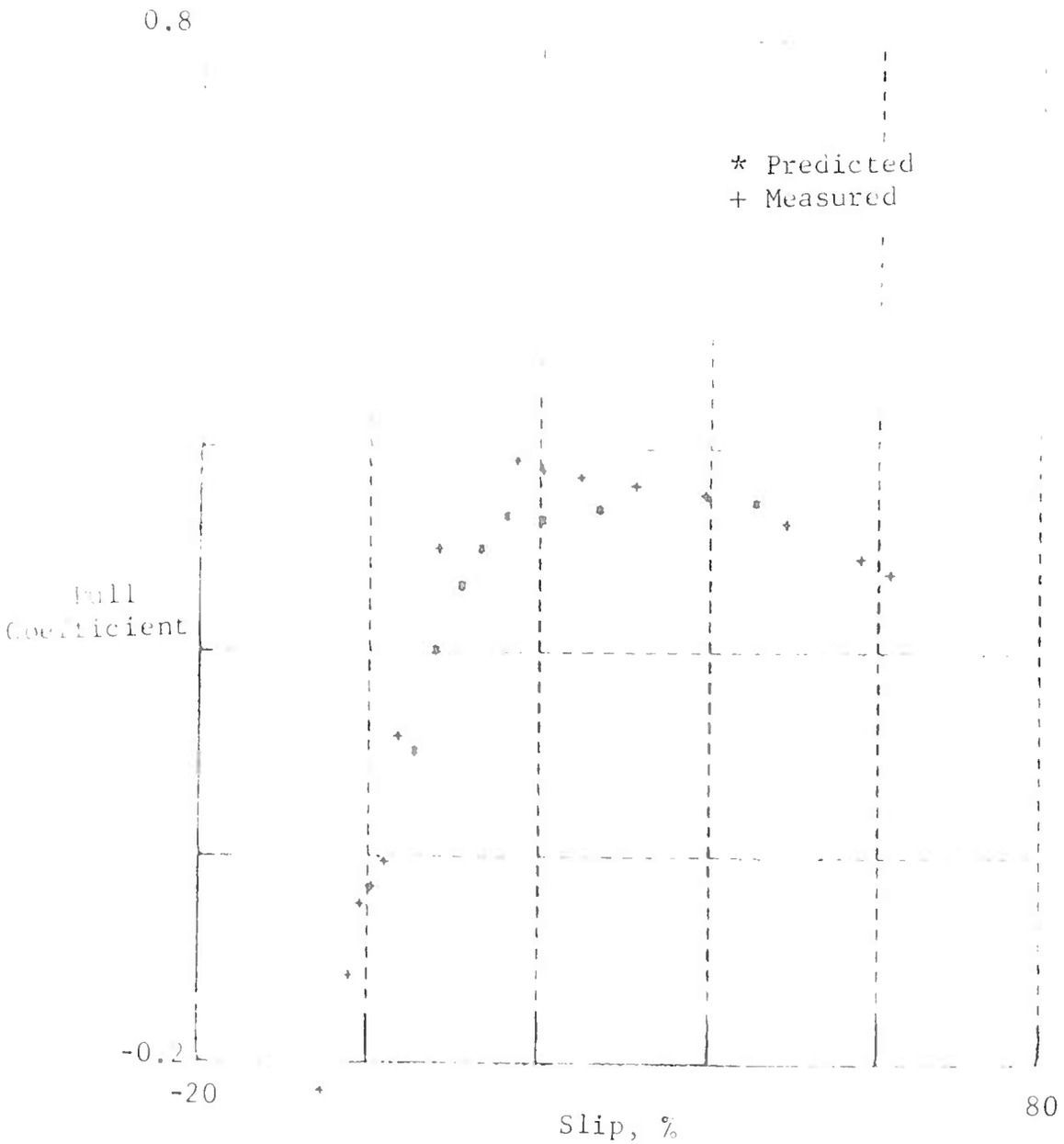

Fig. 23 Pull Coefficient Versus Slip - Test 14
Yuma Sand, CGR = 12.4
Tire: 9.00-14, Load: 870 lb

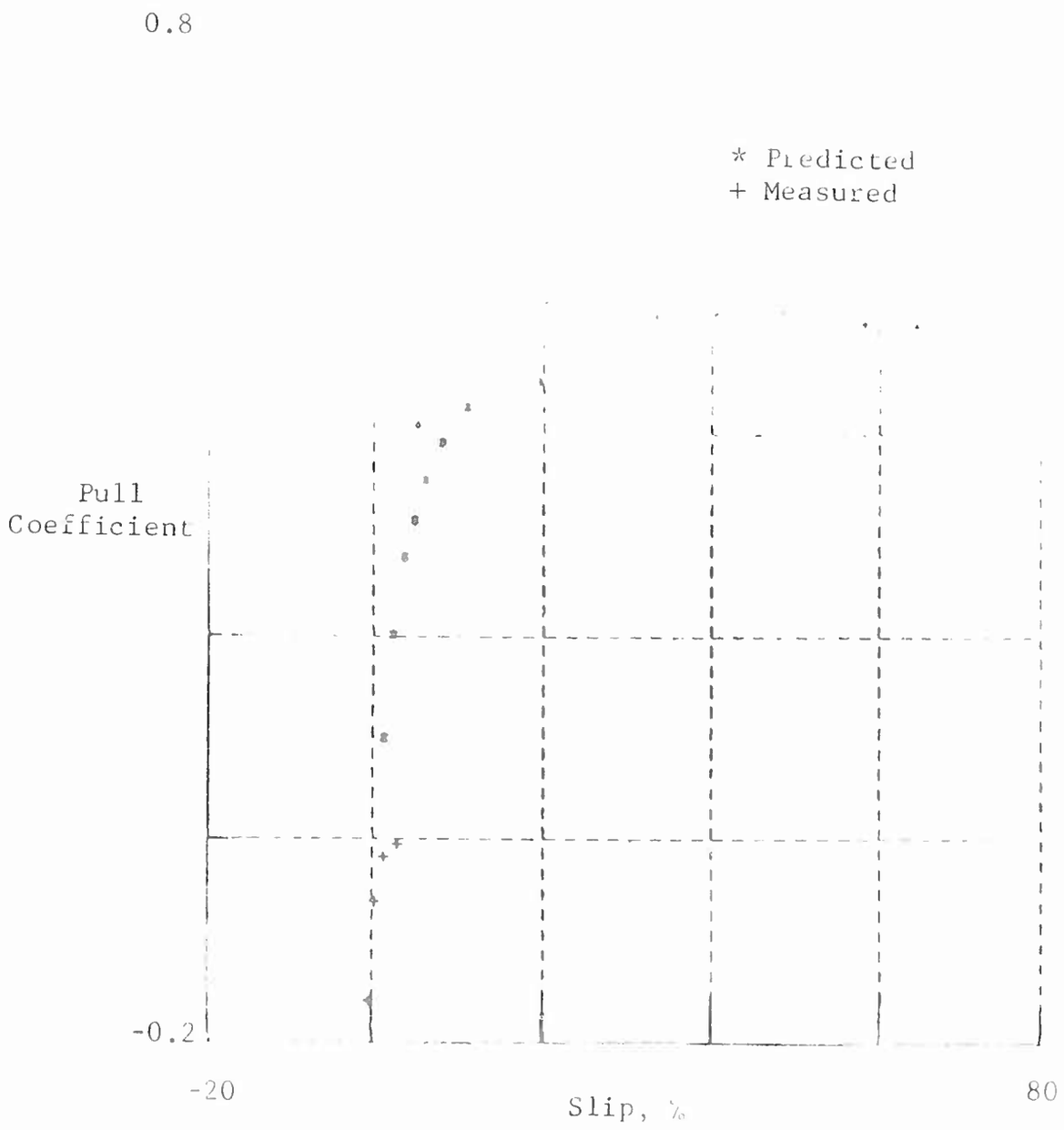

Fig. 24 Pull Coefficient Versus Slip - Test 15
Yuma Sand, CGR = 13.0
Tire: 9.00-14, Load: 225 lb

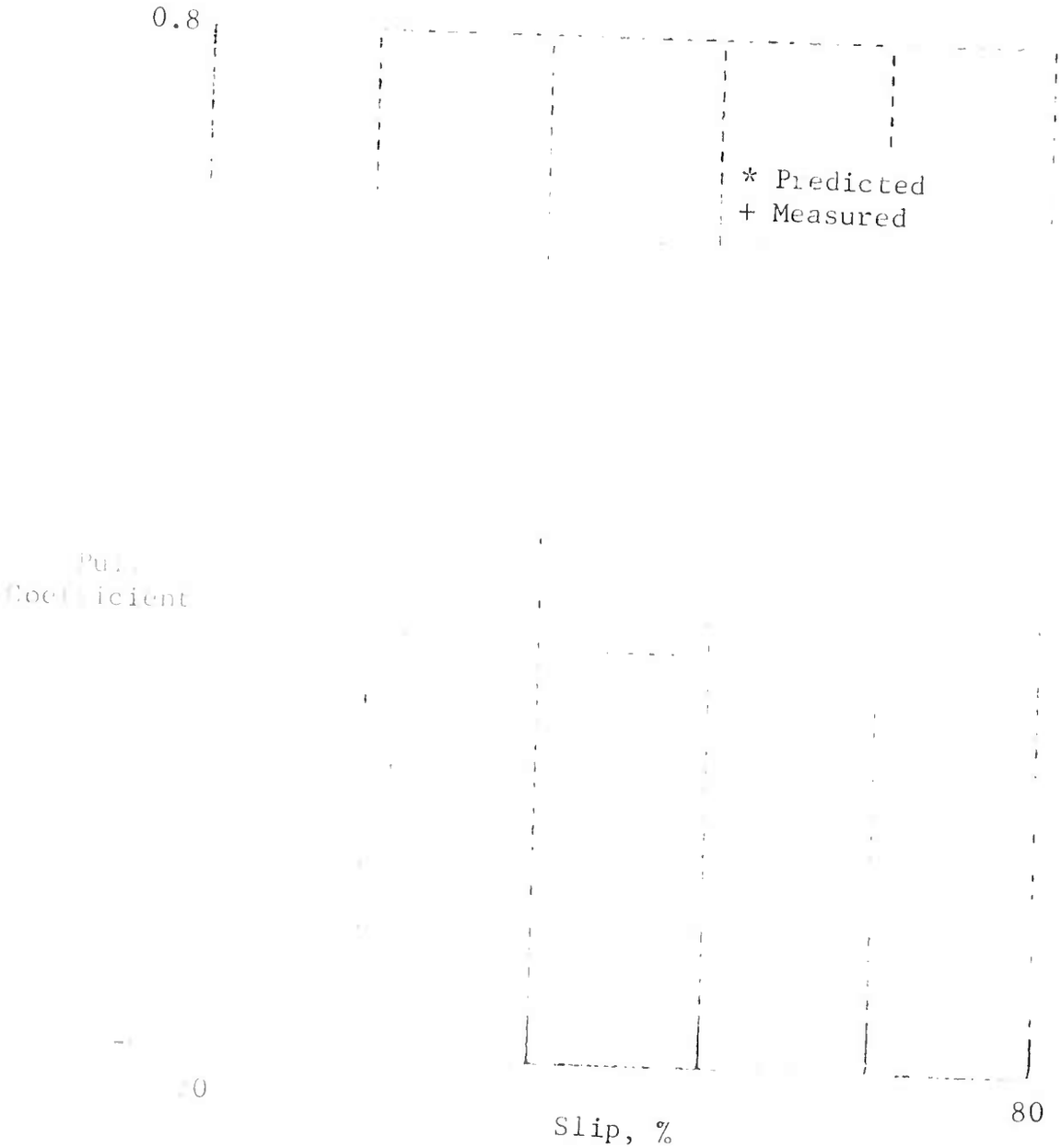

Fig. 25 Pull Coefficient Versus Slip - Test 16
Yuma Sand, CGR = 24.2
Tire: 9.00-14, Load: 670 lb

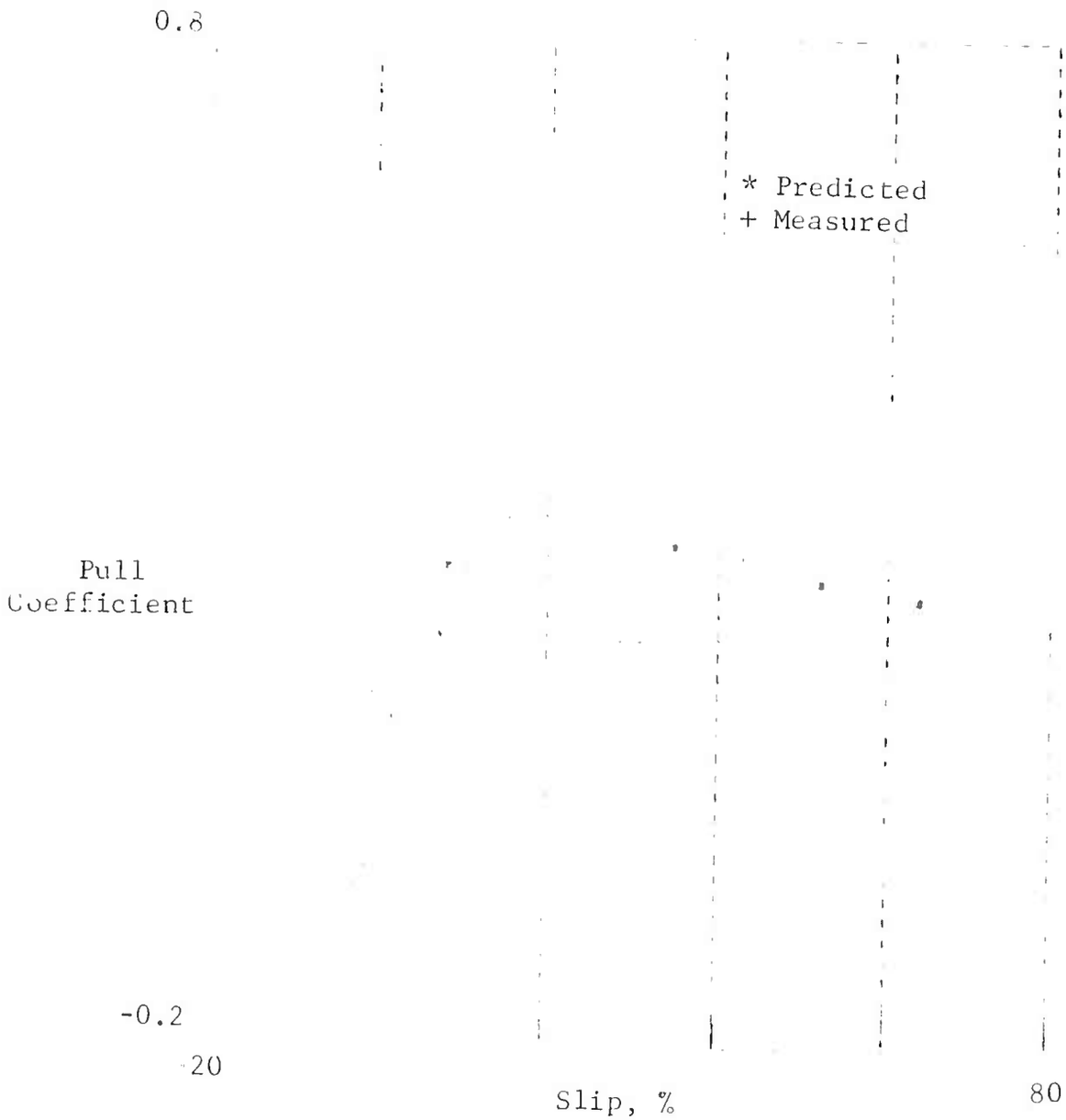

Fig. 26 Pull Coefficient Versus Slip - Test 17
Yuma Sand, CGR = 14.4
Tire: 4.00-20, Load: 225 lb

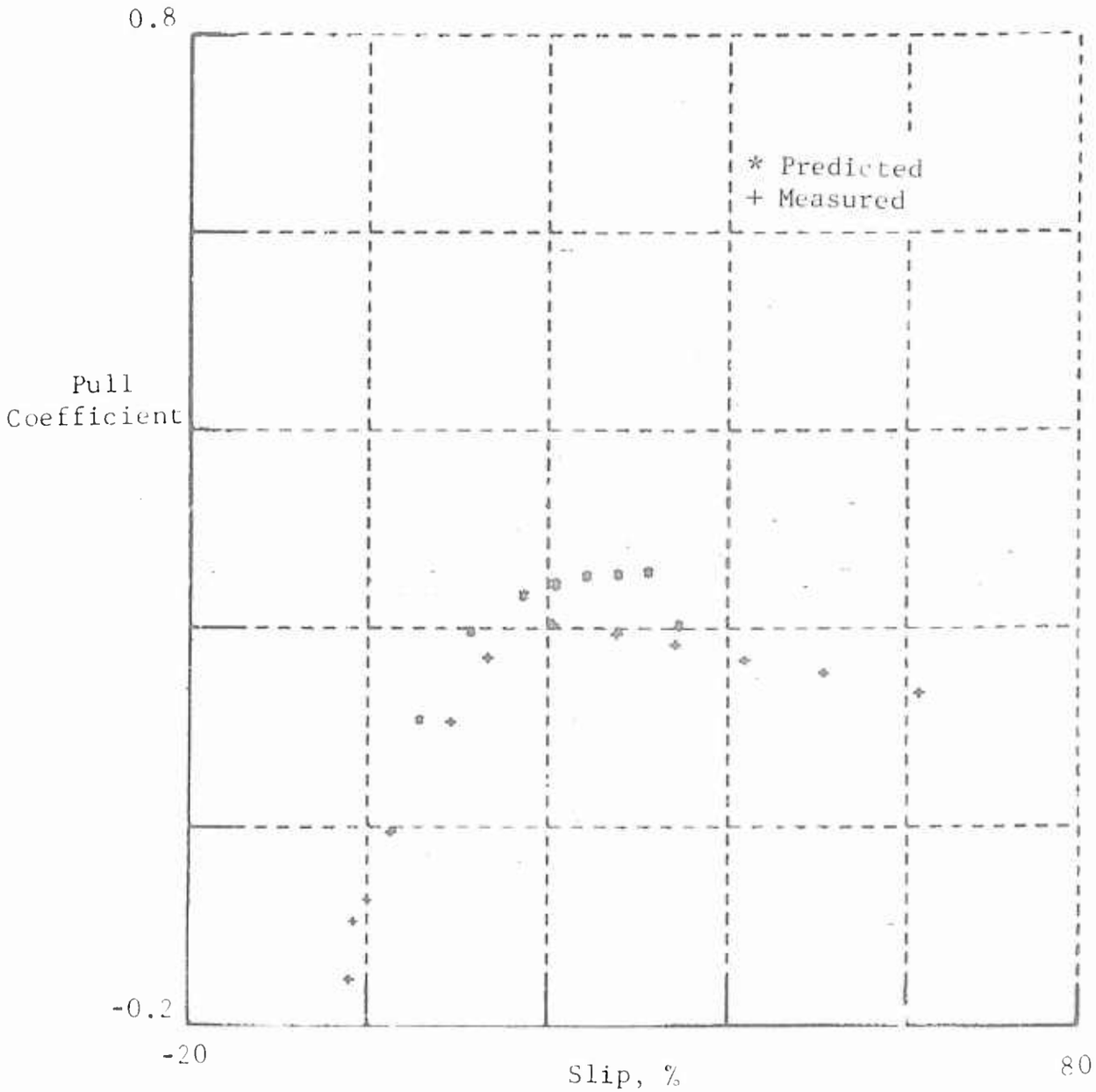

Fig. 27 Pull Coefficient Versus Slip - Test 18
Yuma Sand, CGR = 12.0
Tire: 4.00-20, Load: 450 lb

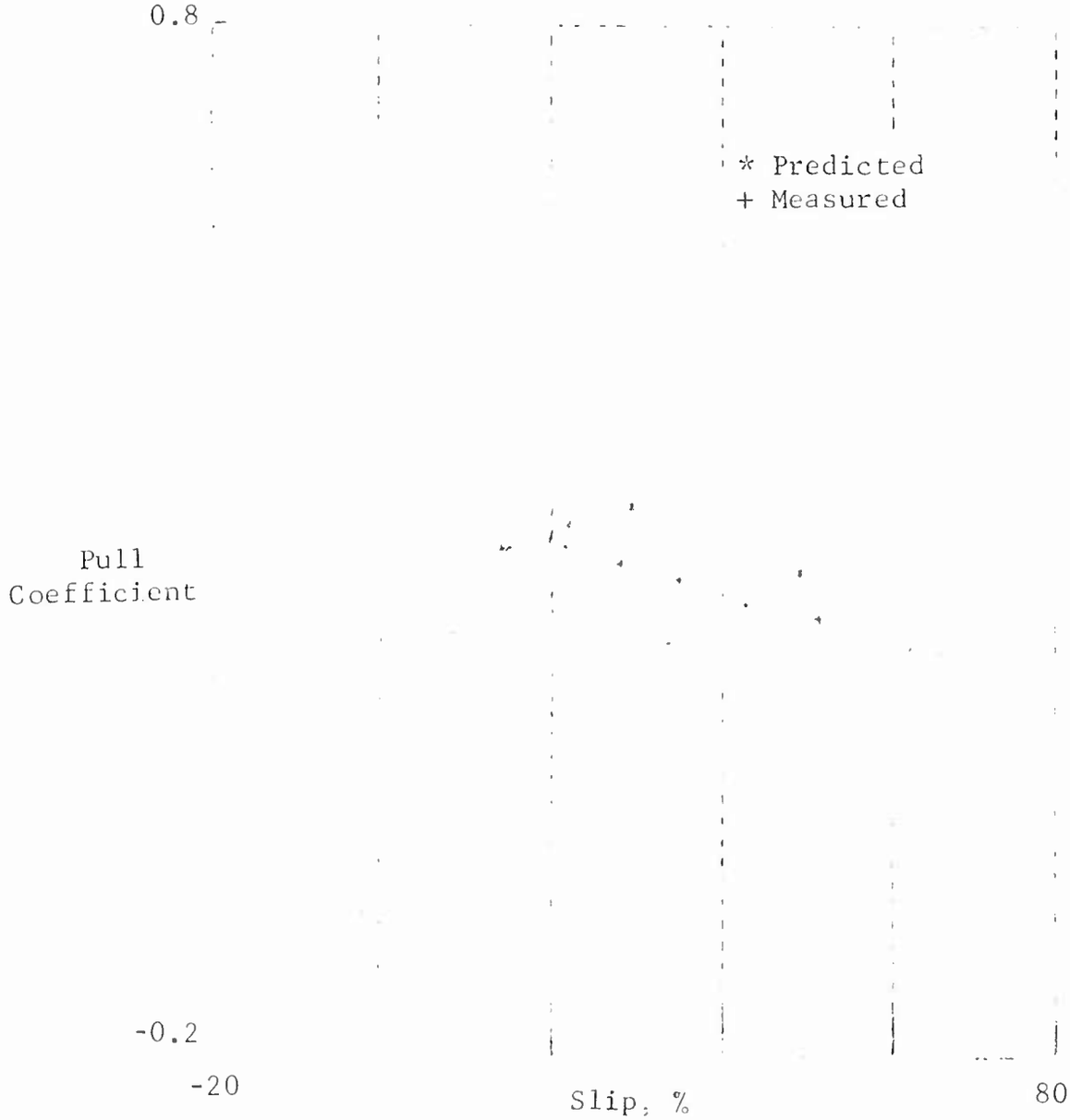

Fig. 28 Pull Coefficient Versus Slip - Test 19
Yuma Sand, CGR = 16.1
Tire: 4.00-20, Load: 330 lb

Fig. 29 Pull Coefficient Versus Slip - Test 20
Yuma Sand, CGR = 16.4
Tire: 4.00-20, Load: 440 lb

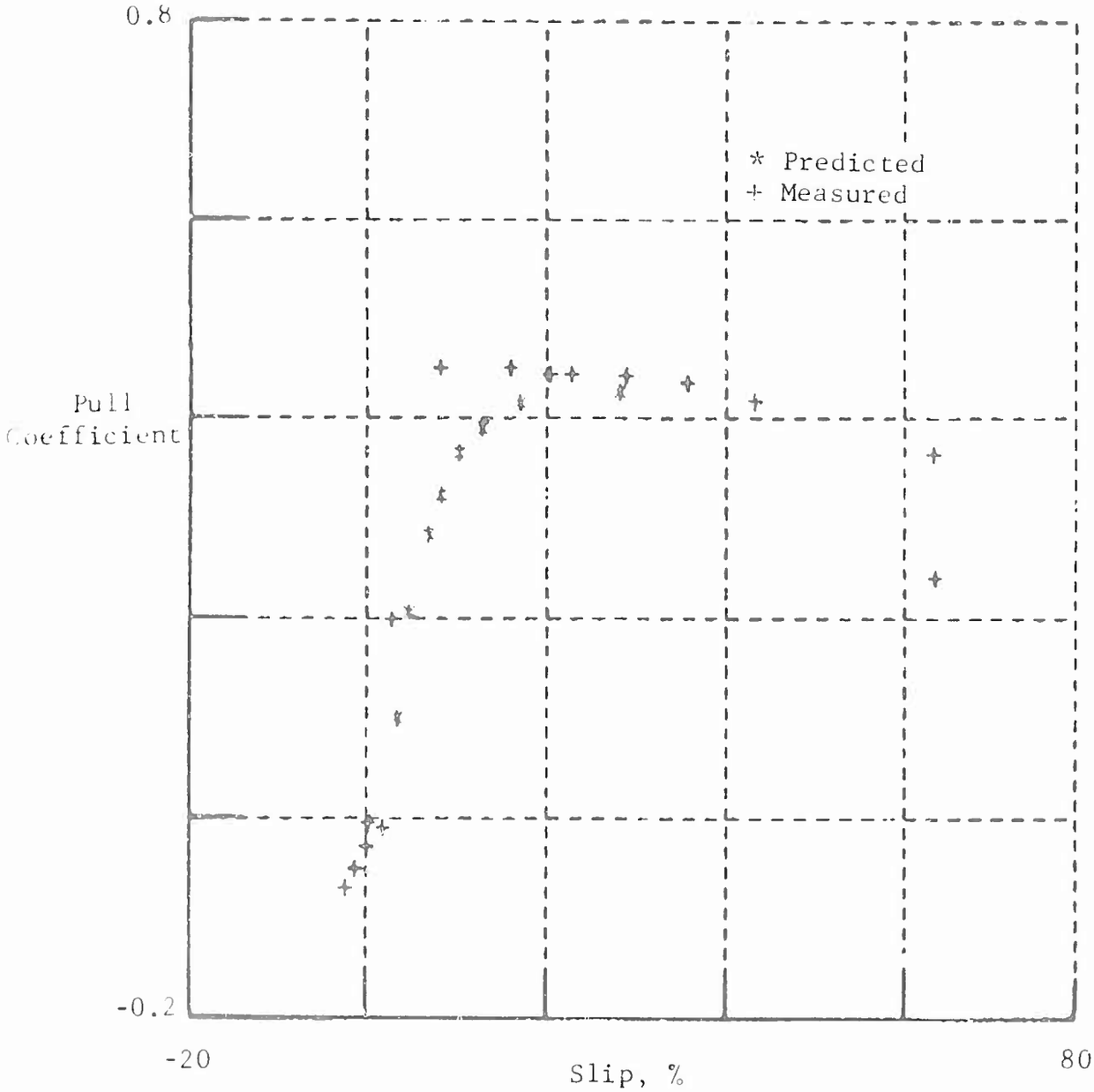

Fig. 30 Pull Coefficient Versus Slip - Test 21
Yuma Sand, CGR = 25.6
Tire: 4.00-20, Load: 230 lb

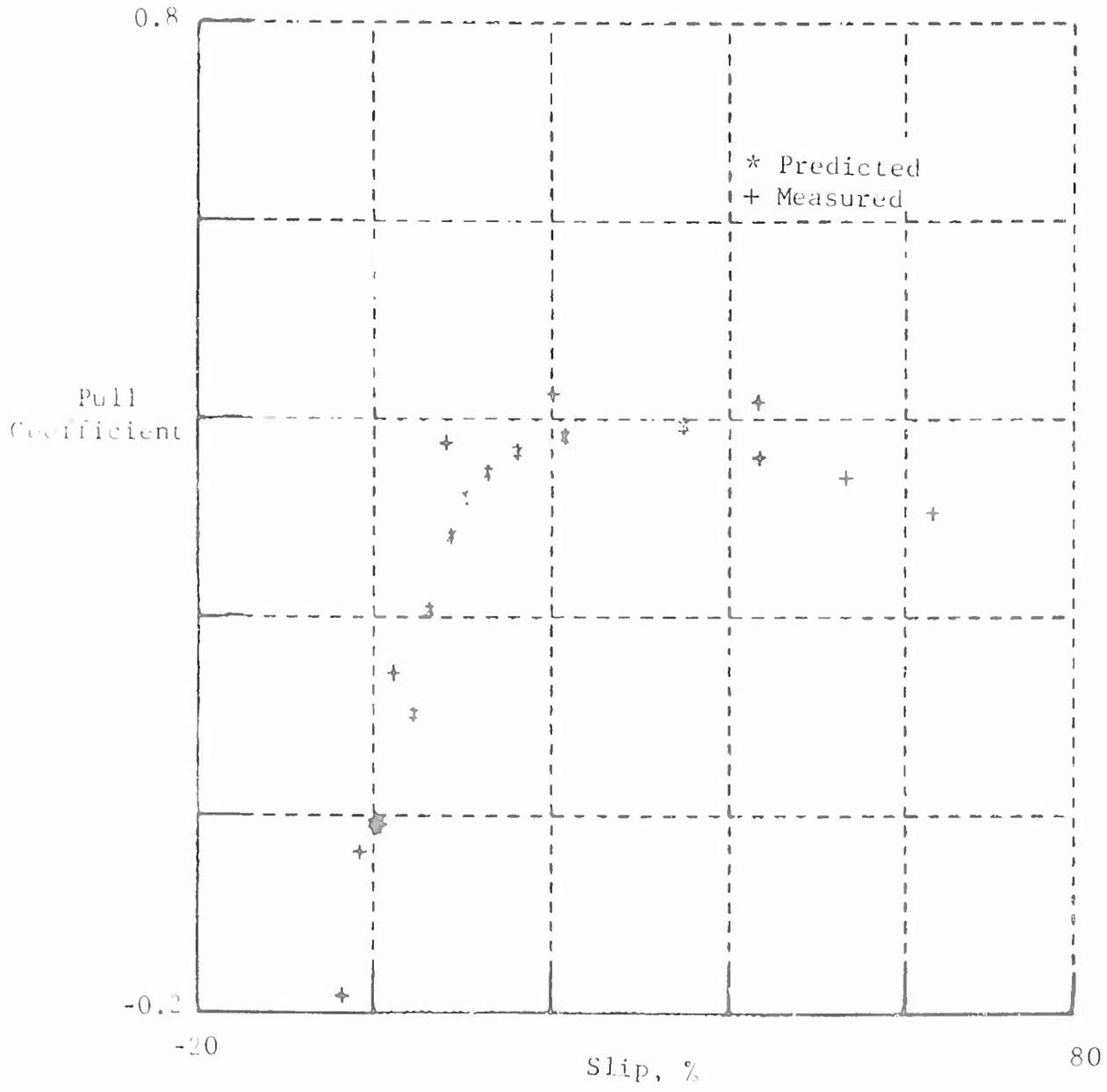

Fig. 31 Pull Coefficient Versus Slip - Test 22
Yuma Sand, CGR = 25.6
Tire: 4.00-20, Load: 340 lb

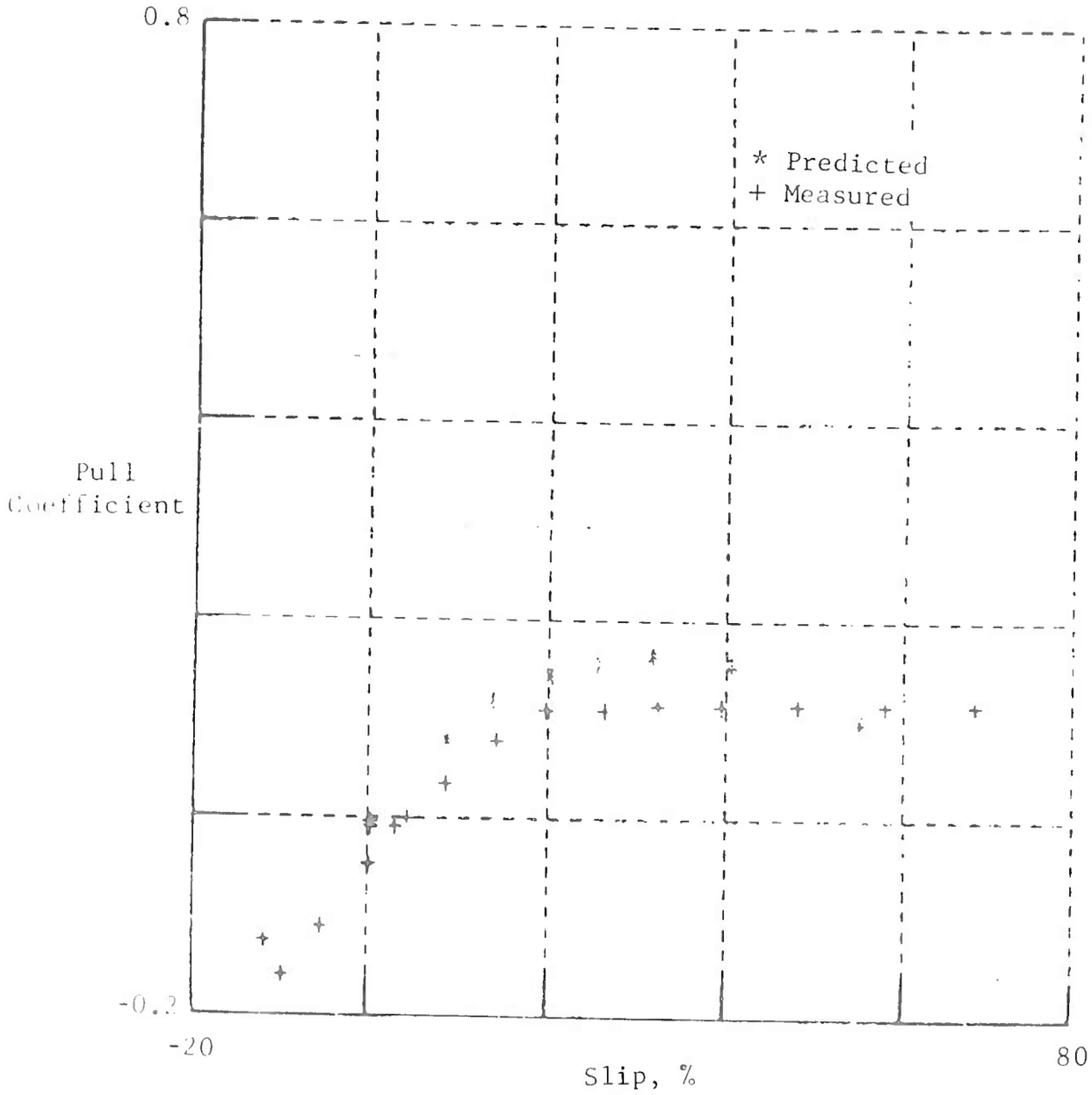

Fig. 32 Pull Coefficient Versus Slip - Test 23
Yuma Sand, CGR = 3.2
Tire: 4.00-20, Load: 240 lb

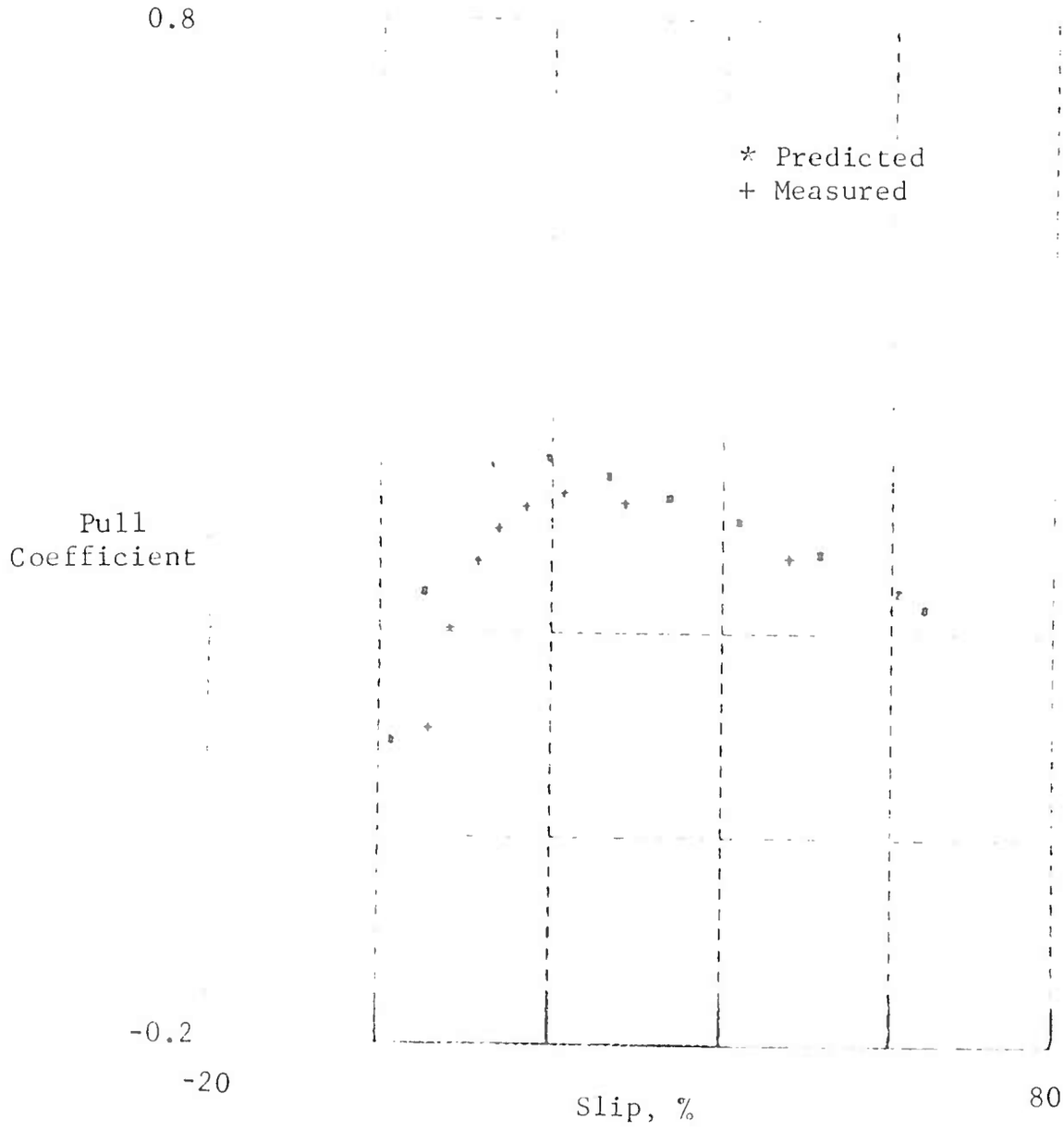

Fig. 33 Pull Coefficient Versus Slip - Test 24
Yuma Sand, CGR = 15.0
Tire: 9.00-14, Load: 850 lb

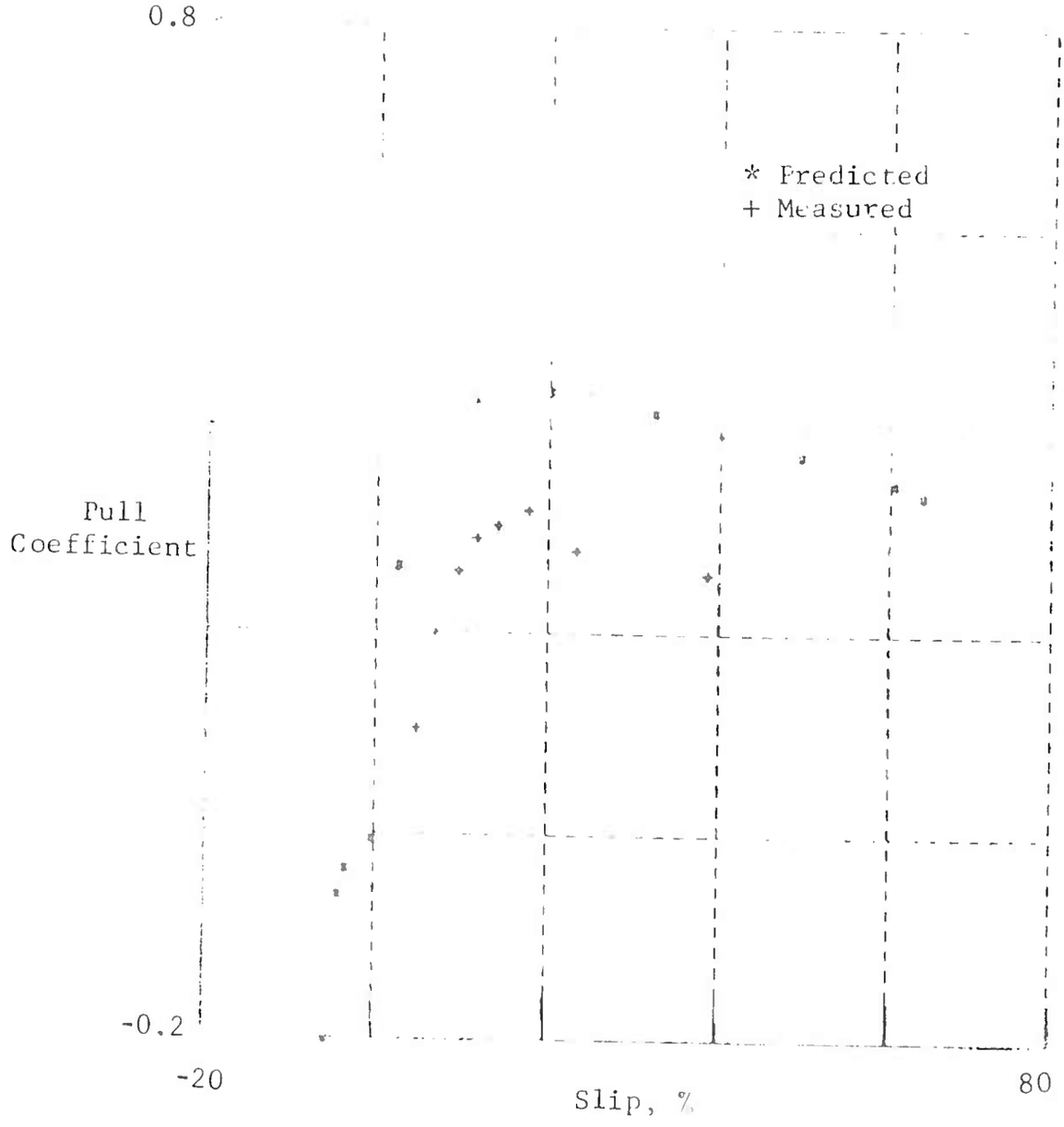

Fig. 34 Pull Coefficient Versus Slip - Test 25
Yuma Sand, CGR = 11.8
Tire: 9.00-14, Load: 460 lb

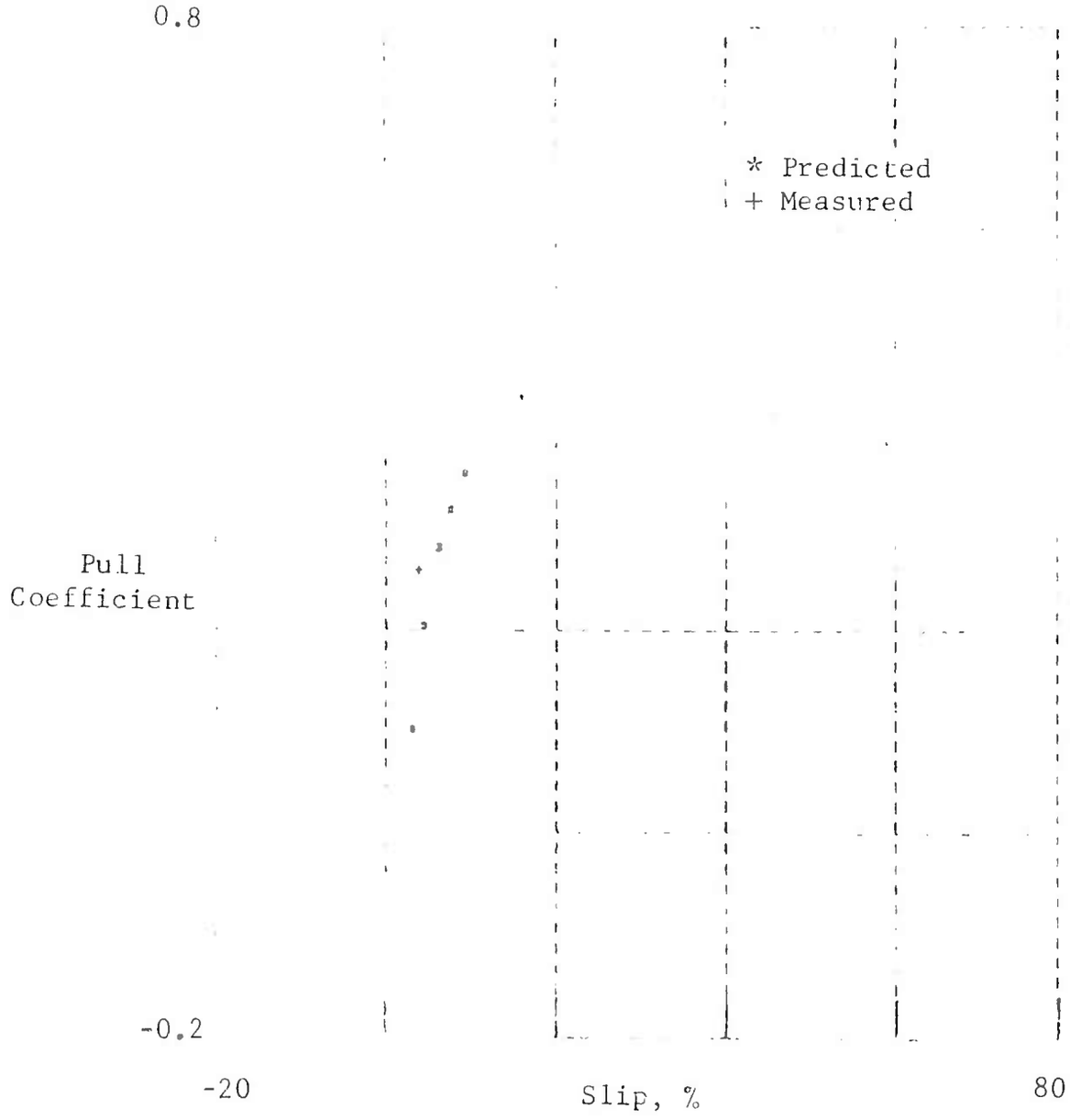

Fig. 35 Pull Coefficient Versus Slip - Test 26
Yuma Sand, CGR = 15.0
Tire: 6.00-16, Load: 220 lb

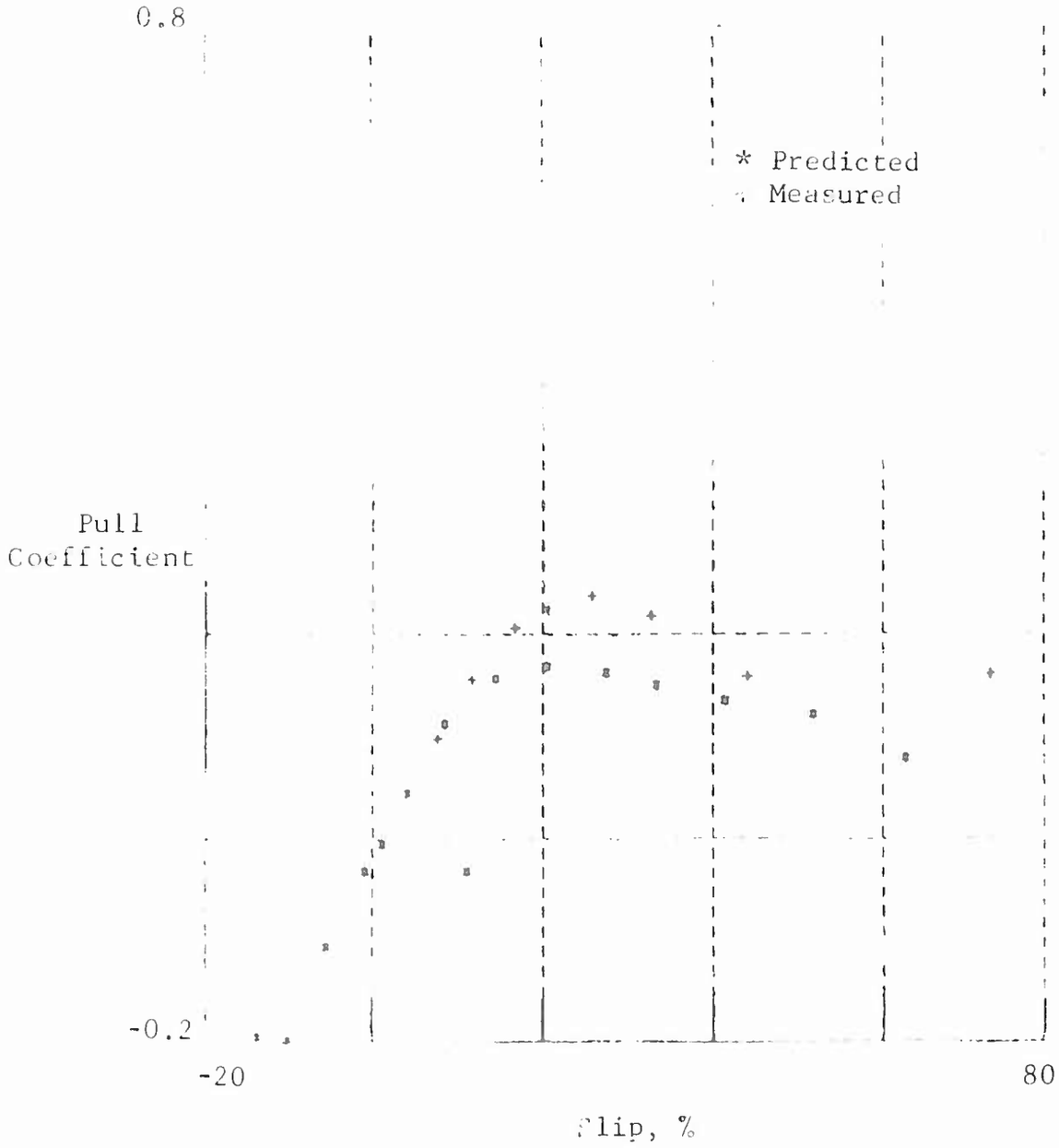

Fig. 36 Pull Coefficient Versus Slip - Test 27
Yuma Sand, CGR = 3.7
Tire: 9.00-14, Load: 650 lb

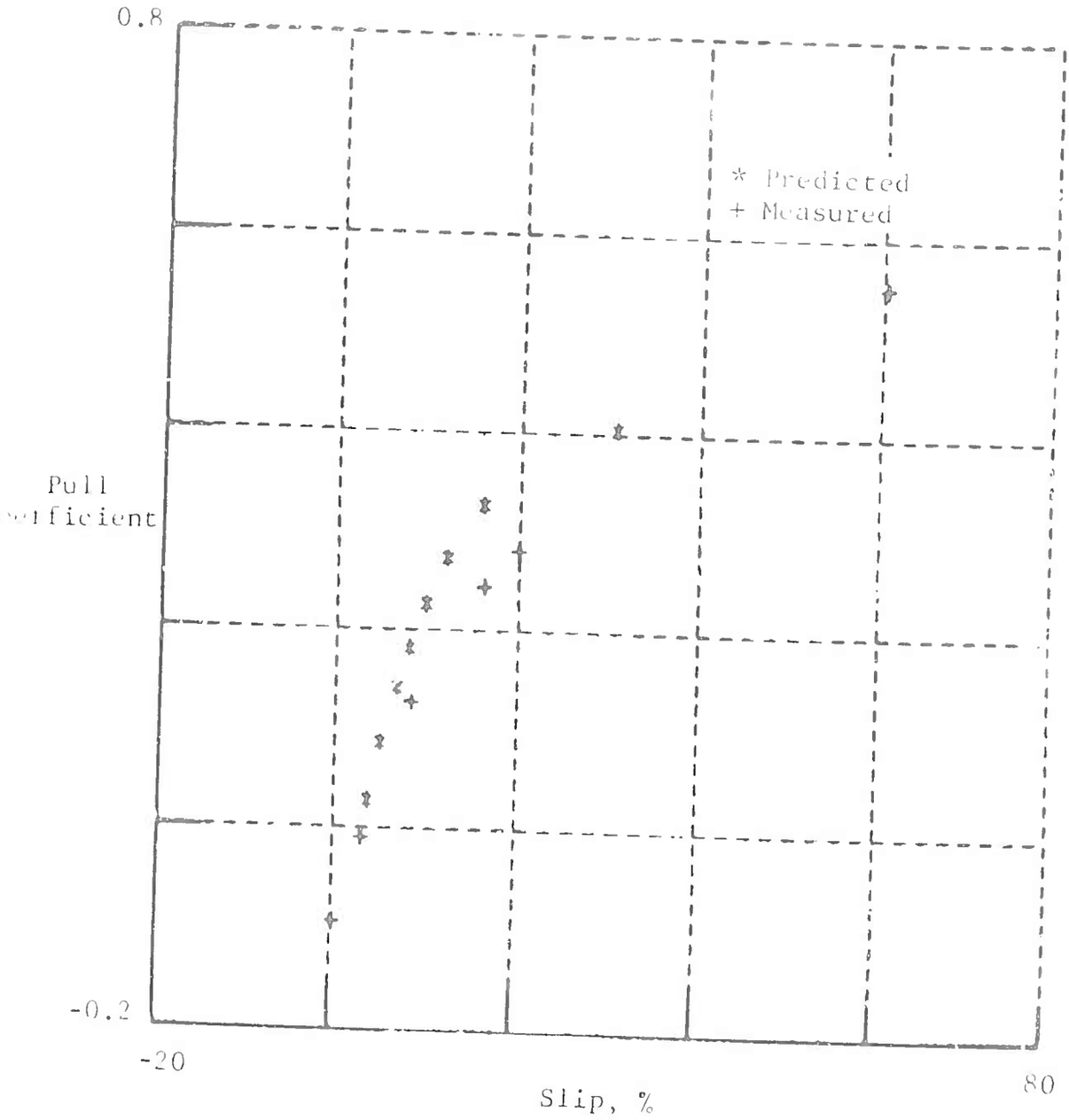

Fig. 37 Pull Coefficient Versus Slip - Test CL-1
Buckshot Clay, CI = 52
Tire: 9.00-14, Load: 870 lb

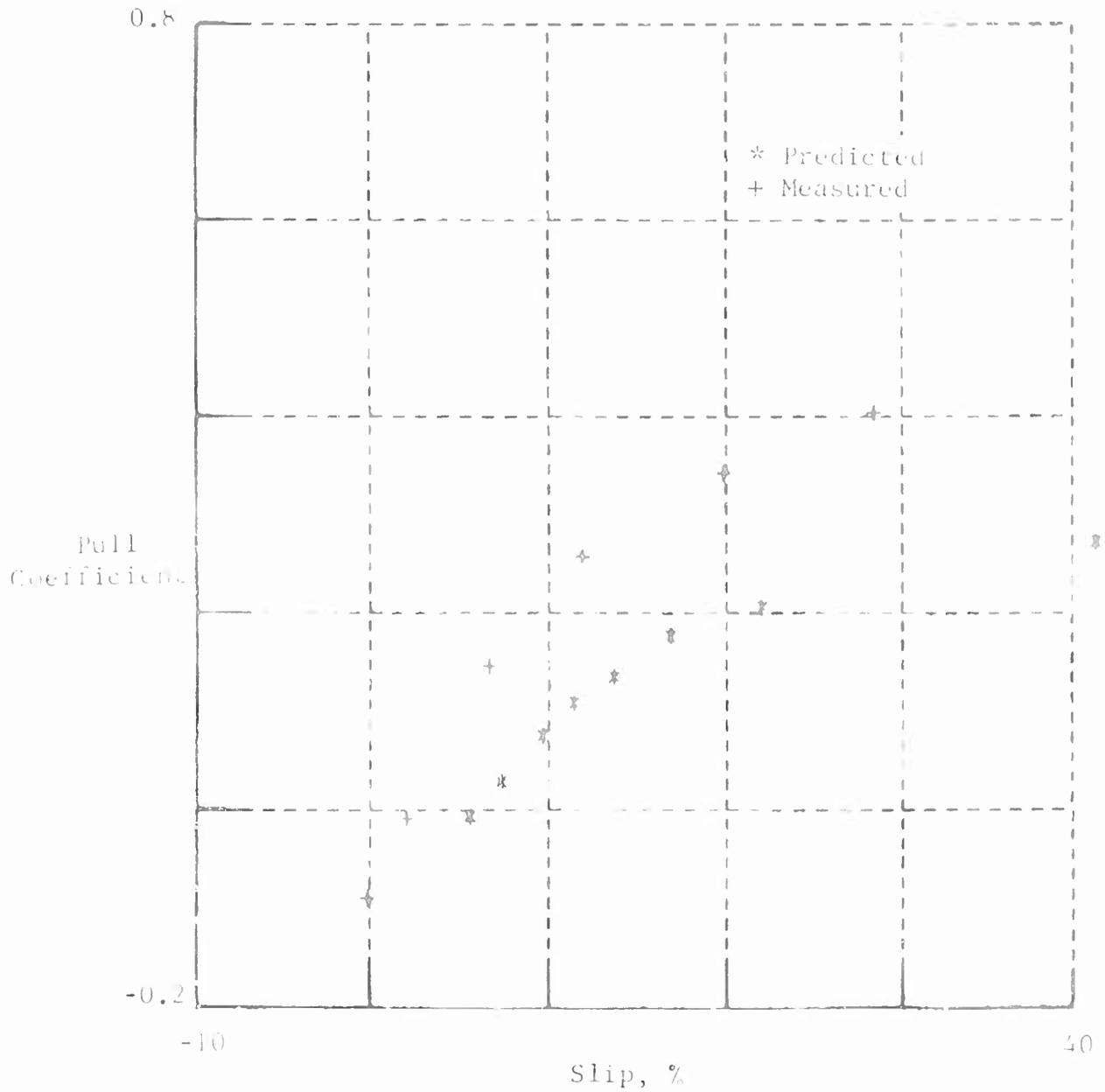

Fig. 38 Pull Coefficient Versus Slip - Test CL-2
Buckshot Clay, CI = 22
Tire: 9.00-14, Load: 650 lb

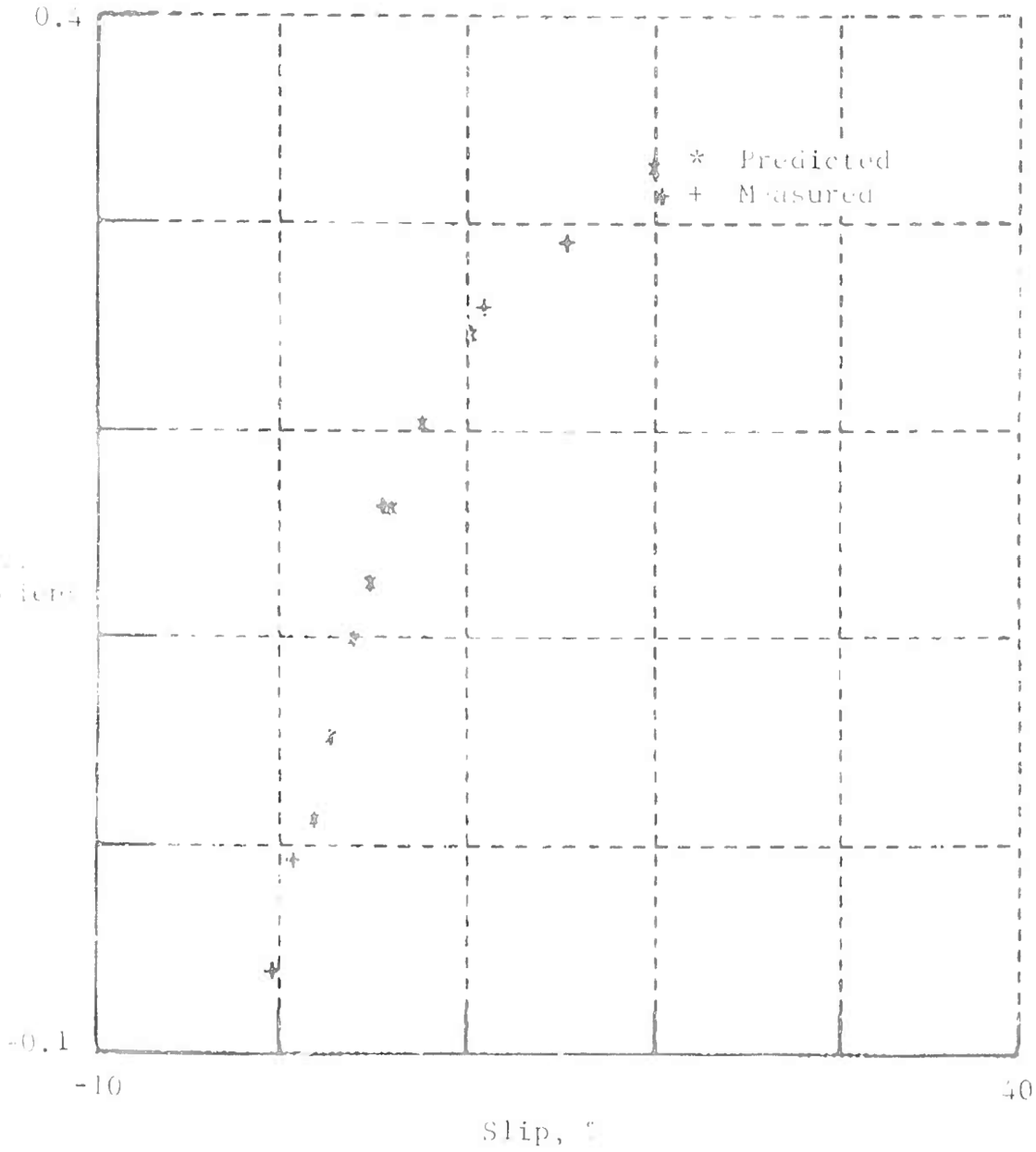

Fig. 39 Pull Coefficient Versus Slip - Test CL-3
Buckshot Clay, CI = 20
Tire: 6.00-16, Load: 250 lb

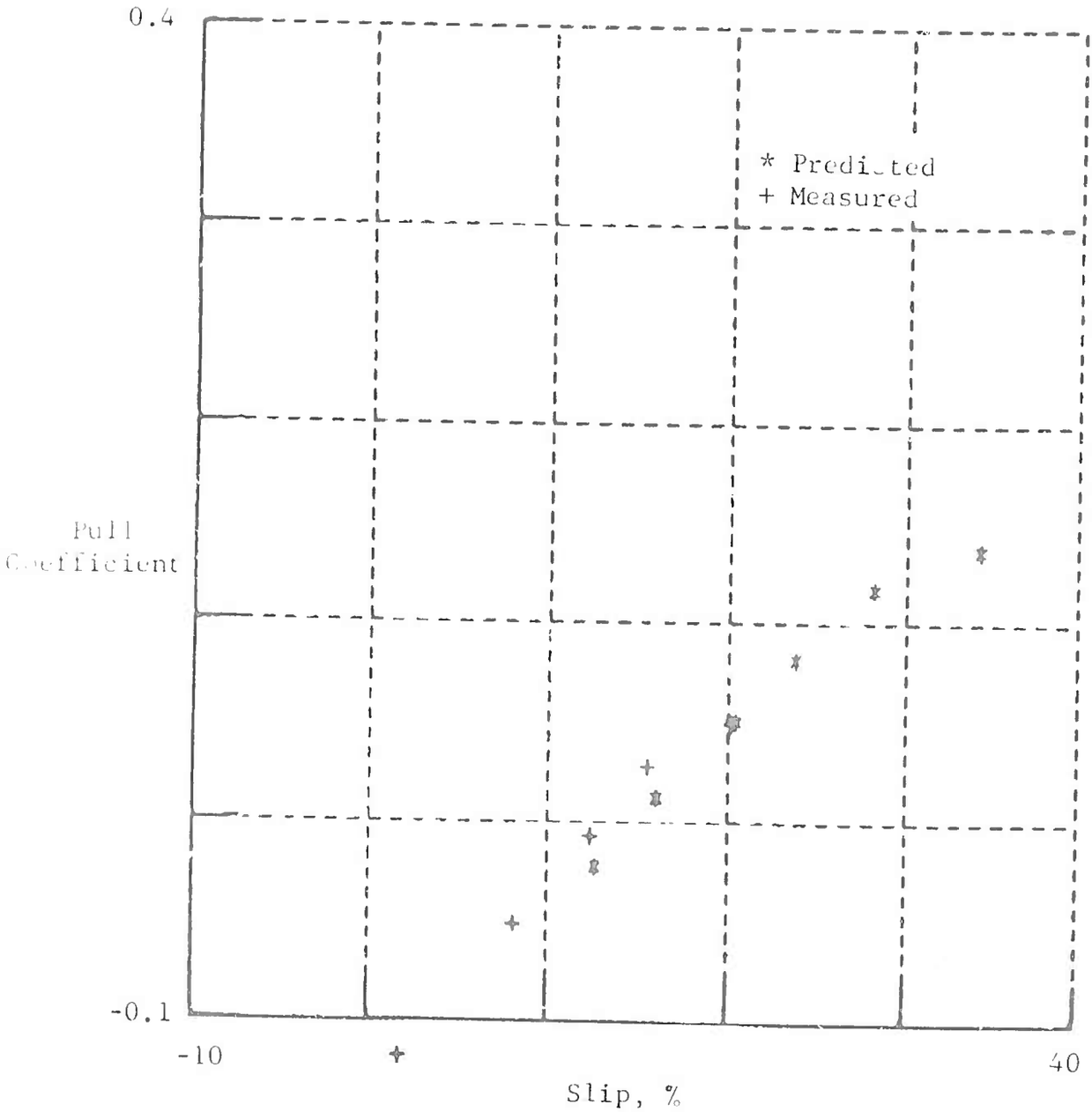

Fig. 40 Pull Coefficient Versus Slip - Test CL-4
Buckshot Clay, CI = 22
Tire: 6.00-16, Load: 700 lb

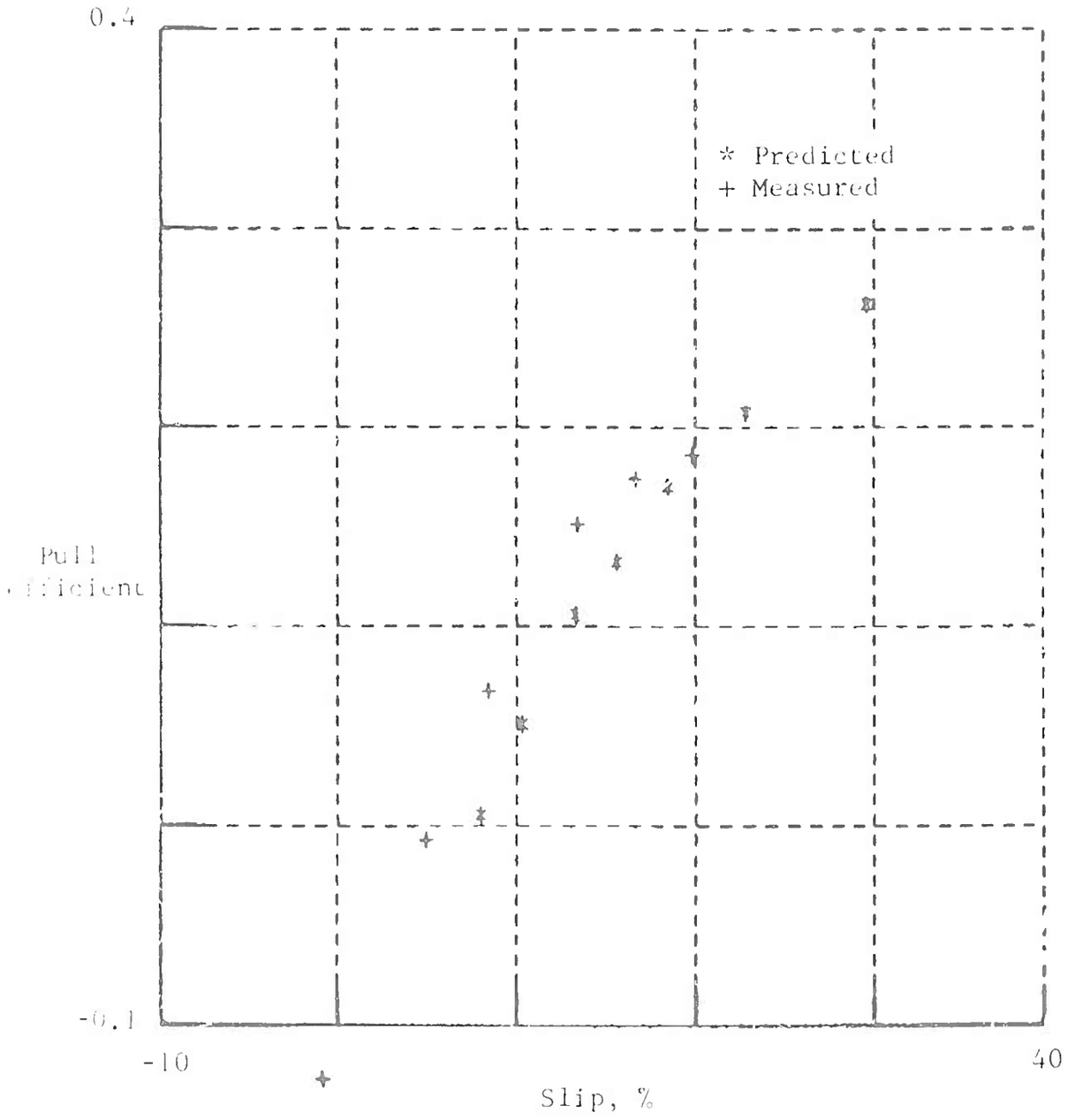

Fig. 41 Pull Coefficient Versus Slip - Test CL-5
Buckshot Clay, CI = 37
Tire: 6.00-16, Load: 880 lb

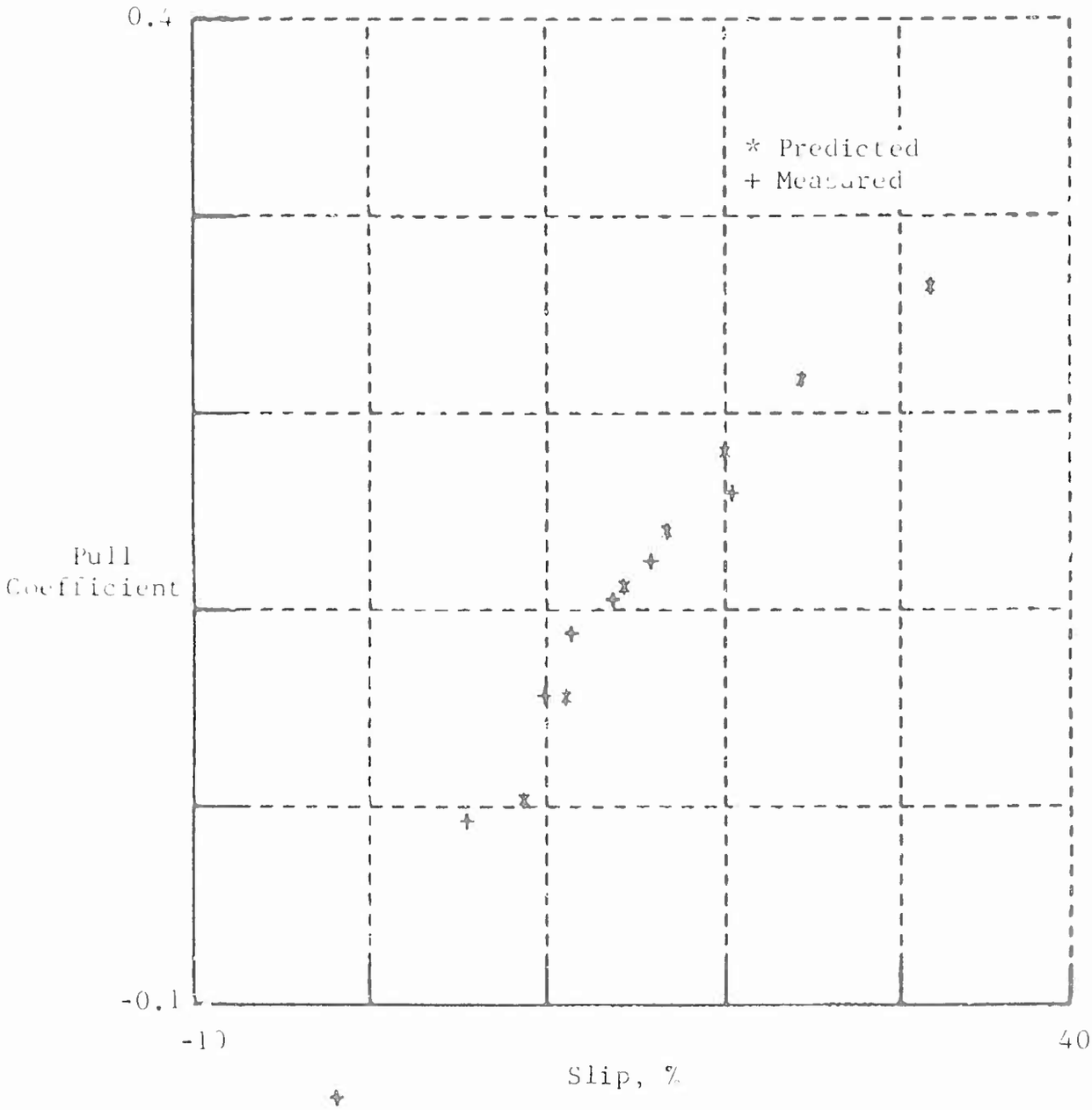

Fig. 42 Pull Coefficient Versus Slip - Test CL-6
Buckshot Clay, CI = 42
Tire: 4.00-7, Load: 335 lb

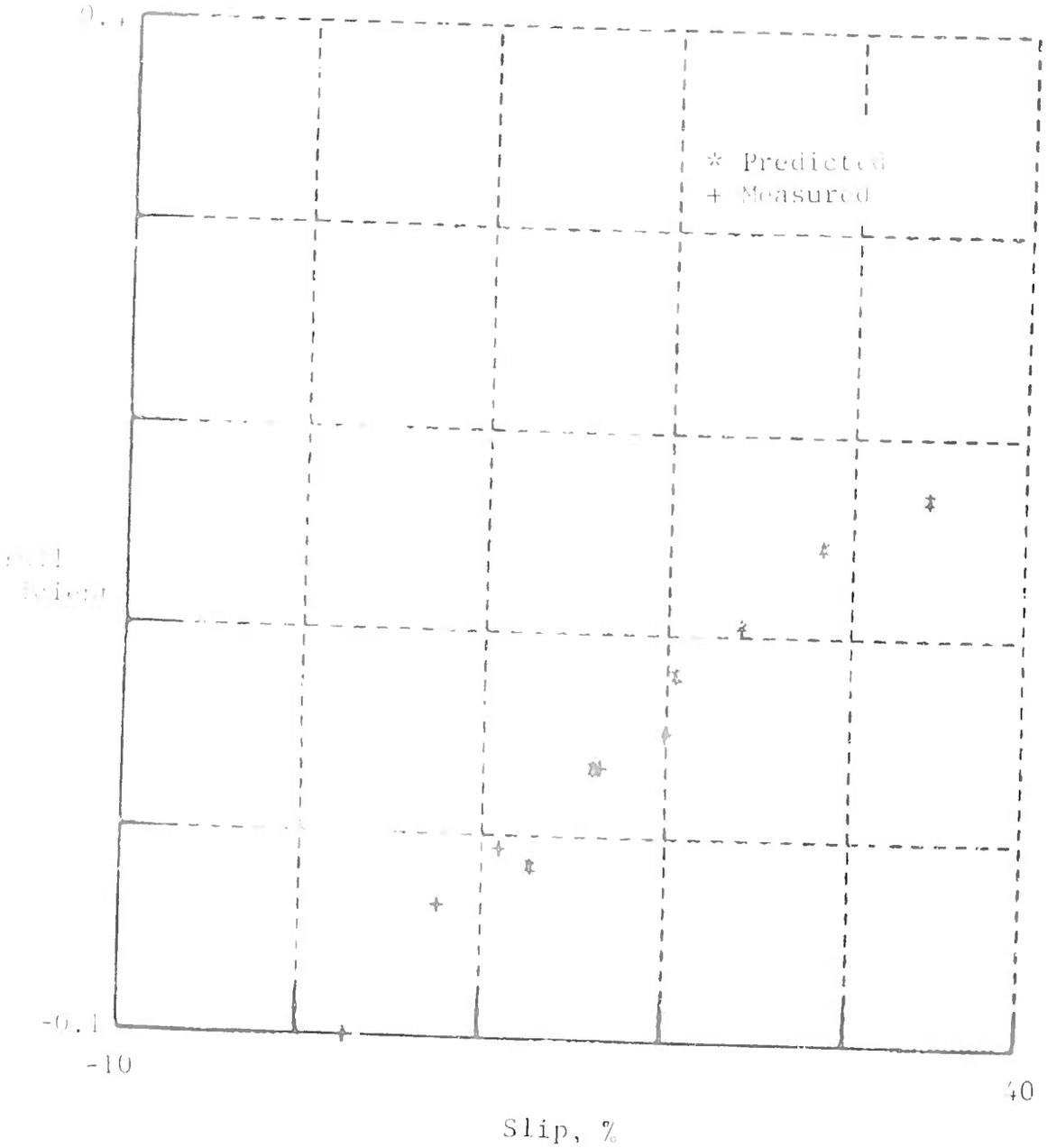

Fig. 43 Pull Coefficient Versus Slip - Test CL-7
Buckshot Clay, CI = 38
Tire: 4.00-7, Load: 450 lb

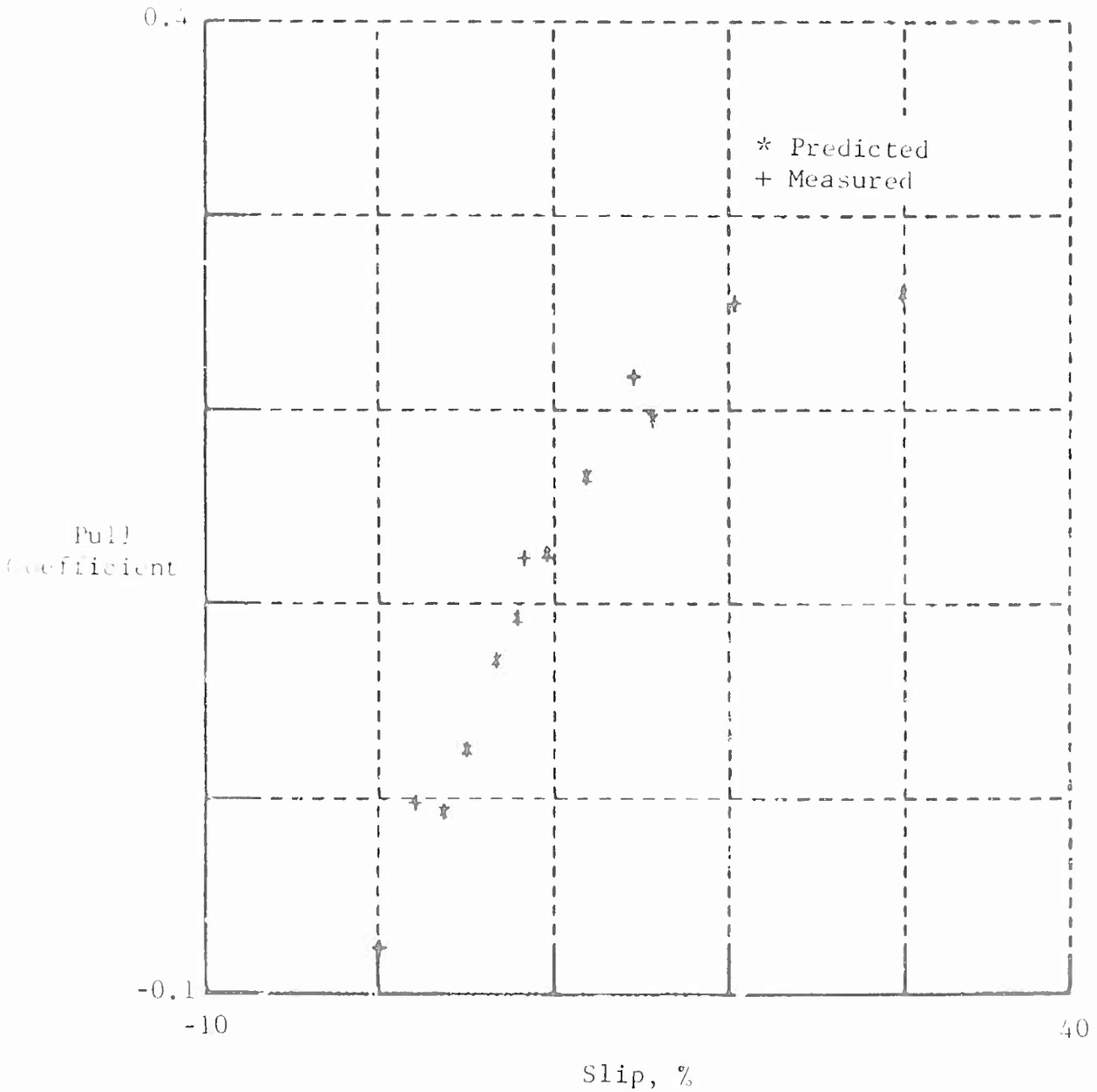

Fig. 44 Pull Coefficient Versus Slip - Test CL-8
Bucksnot Clay, CI = 16
Tire: 16 x 15-[illegible], Load: 450 lb

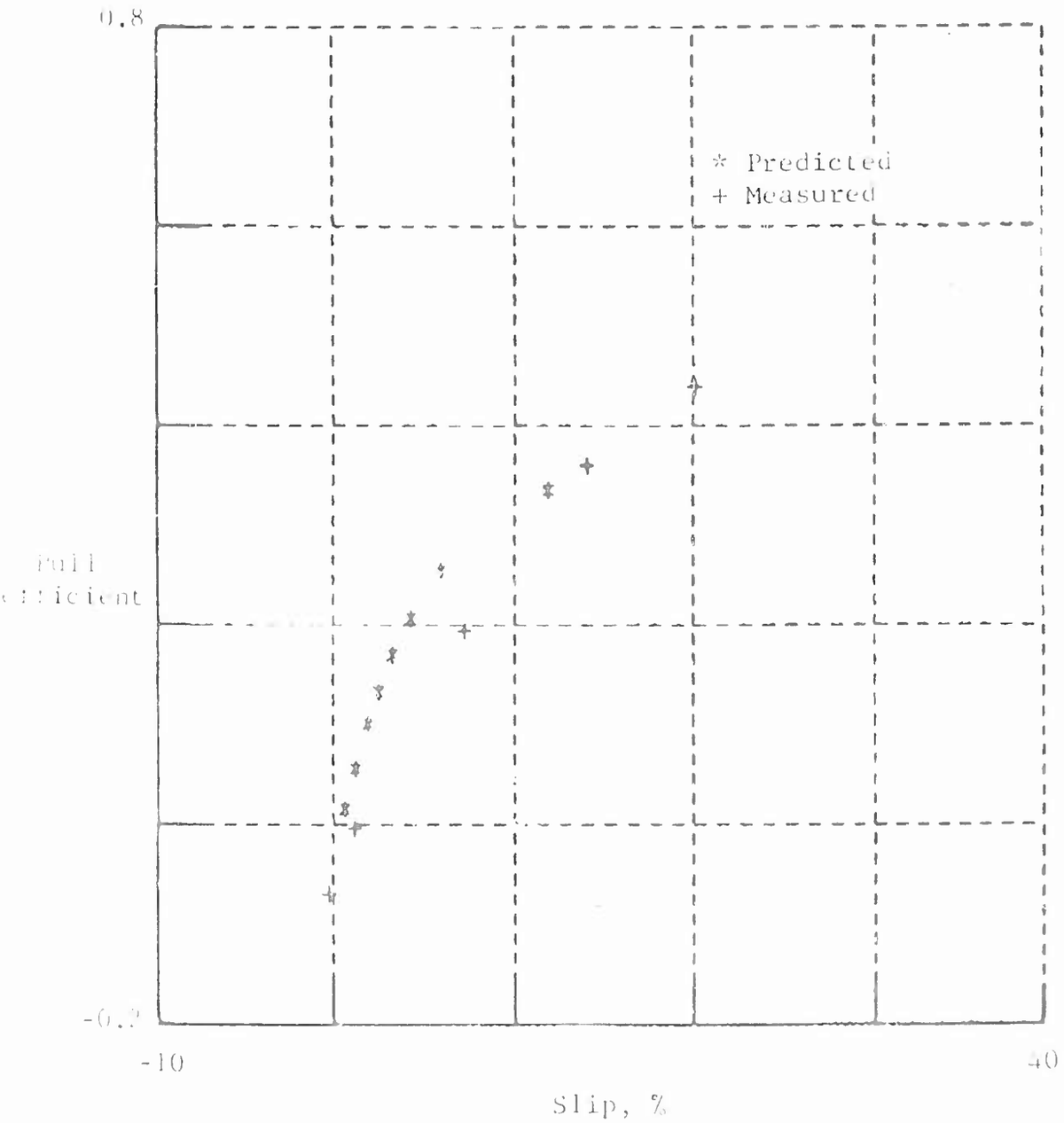

Fig. 40 Pull Coefficient Versus Slip - Test CL-9
Buckshot Clay, CI = 29
Tire: 31 x 15-13, Load: 450 lb

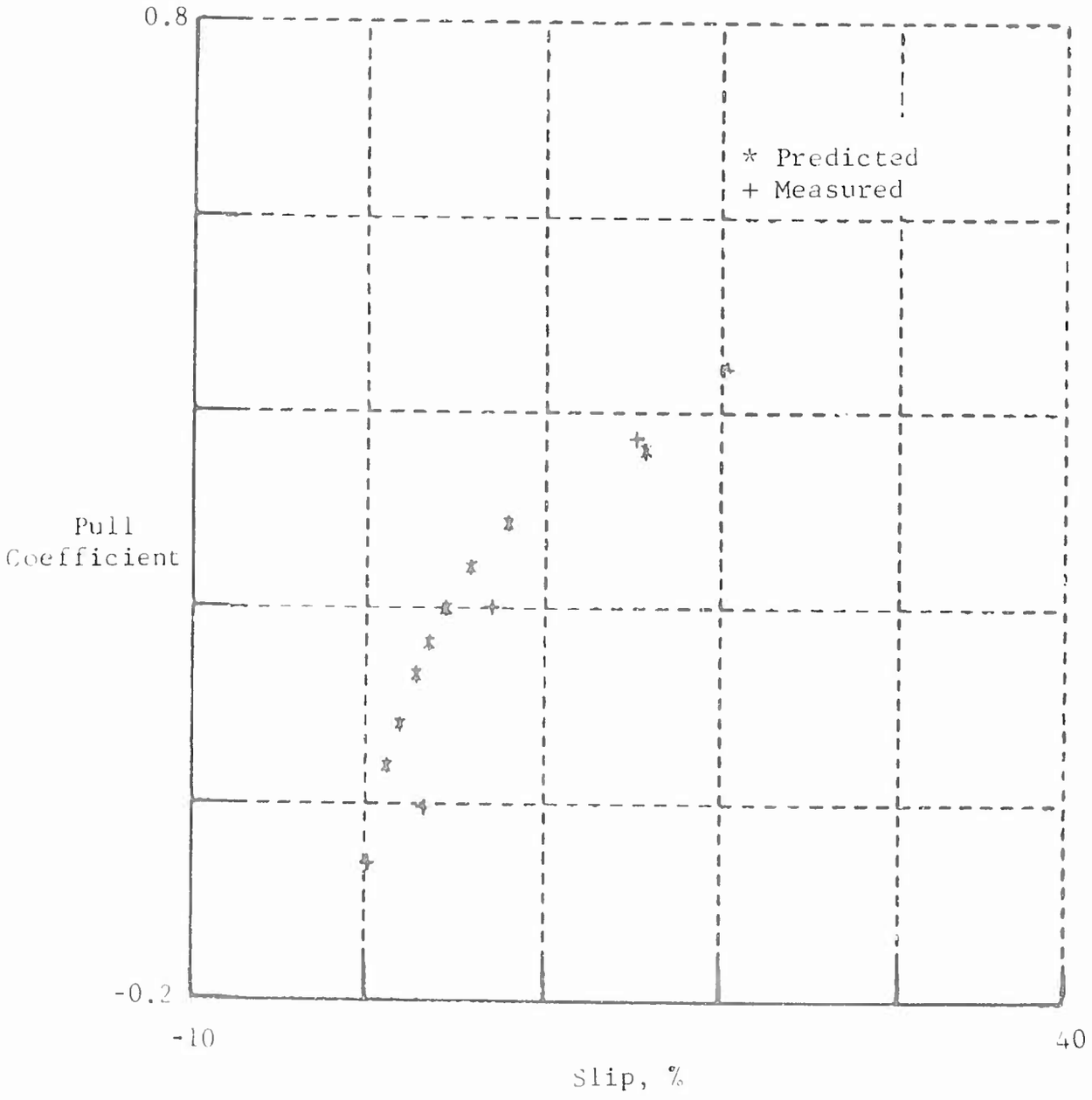

Fig. 46 Pull Coefficient Versus Slip - Test CL-10
Buckshot Clay, CI = 28
Tire: 31 x 15-13, Load: 880 lb

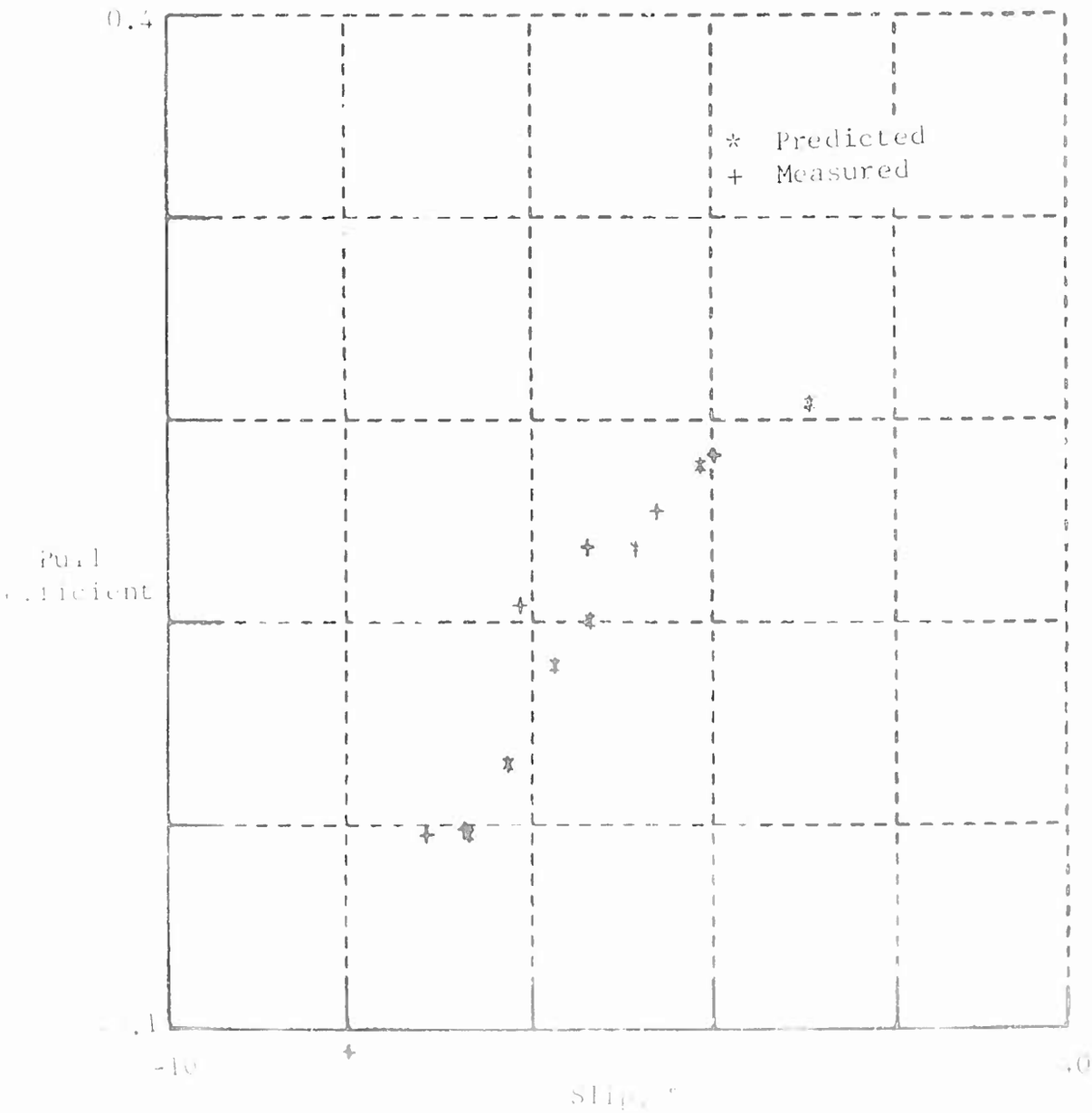

Fig. 47 Pull Coefficient Versus Slip - Test CL-11
Buckshot Clay, CI = 22
Tire: 31 x 15-13, Load: 1170 lb

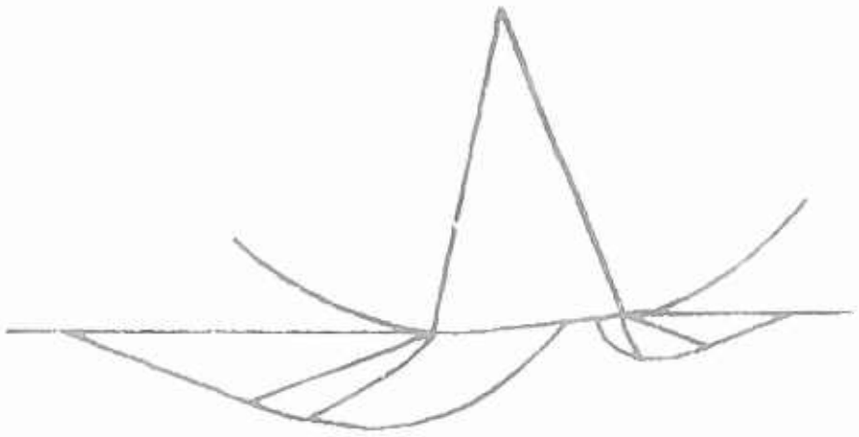

a) Slip = 10%

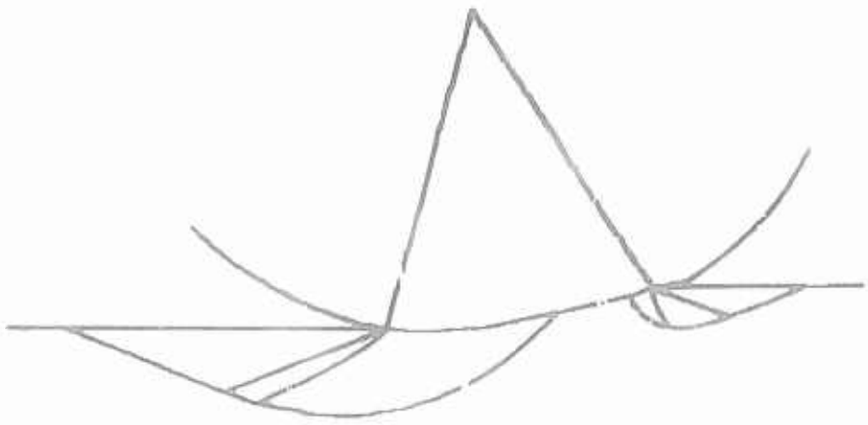

b) Slip = 25%

Fig. 48 Geometry of the Centerline of Tire and Slip Line Fields for Test 1

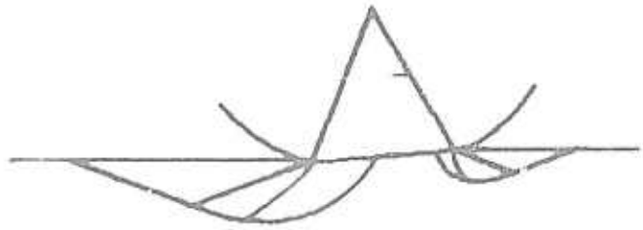

a) Slip = 10%

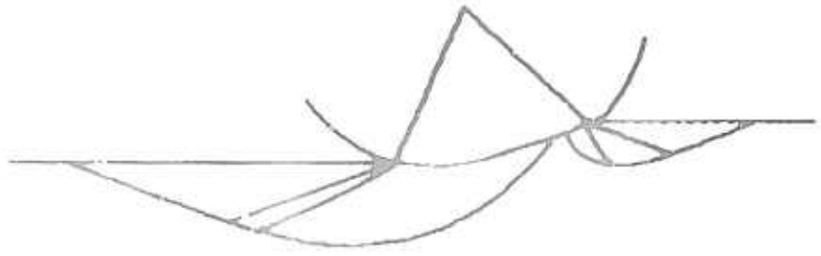

b) Slip = 40%

Fig. 49 Geometry of the Centerline of Tire and Slip Line Fields for Test 5

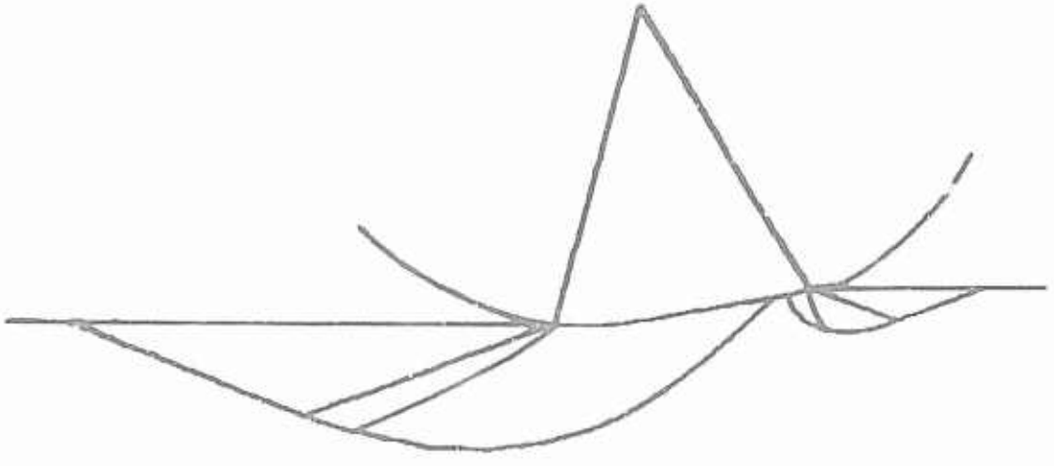

a) Slip = 25%

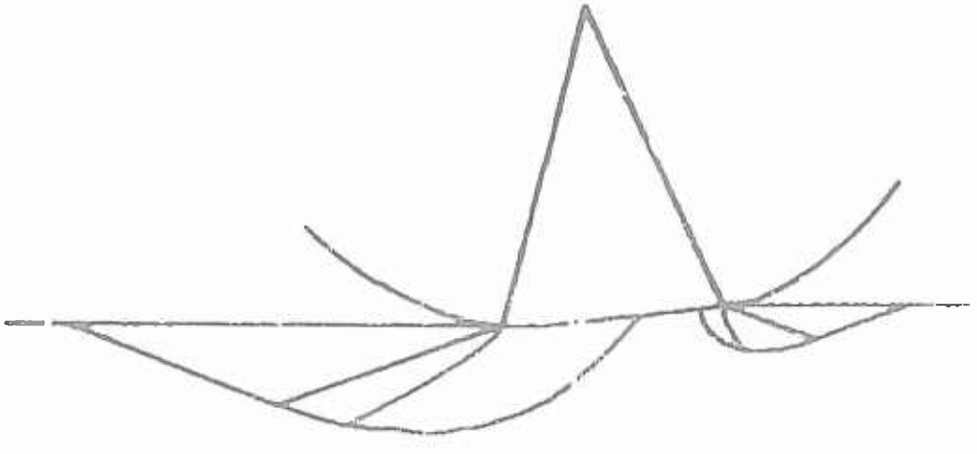

b) Slip = 10%

Fig. 50 Geometry of the Centerline of Tire and Slip Line Fields for Test 18

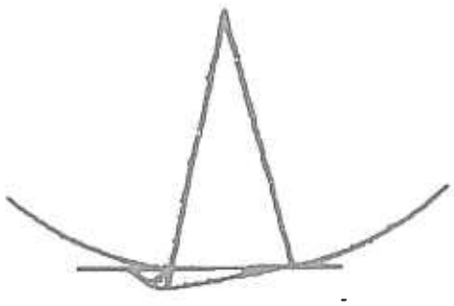

a) Slip = 20%

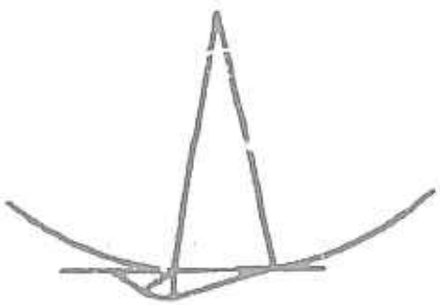

b) Slip = 10%

Fig. 51 Geometry of the Centerline of Tire and Slip Line Field in Strong Cohesive Soil, Test CL-1

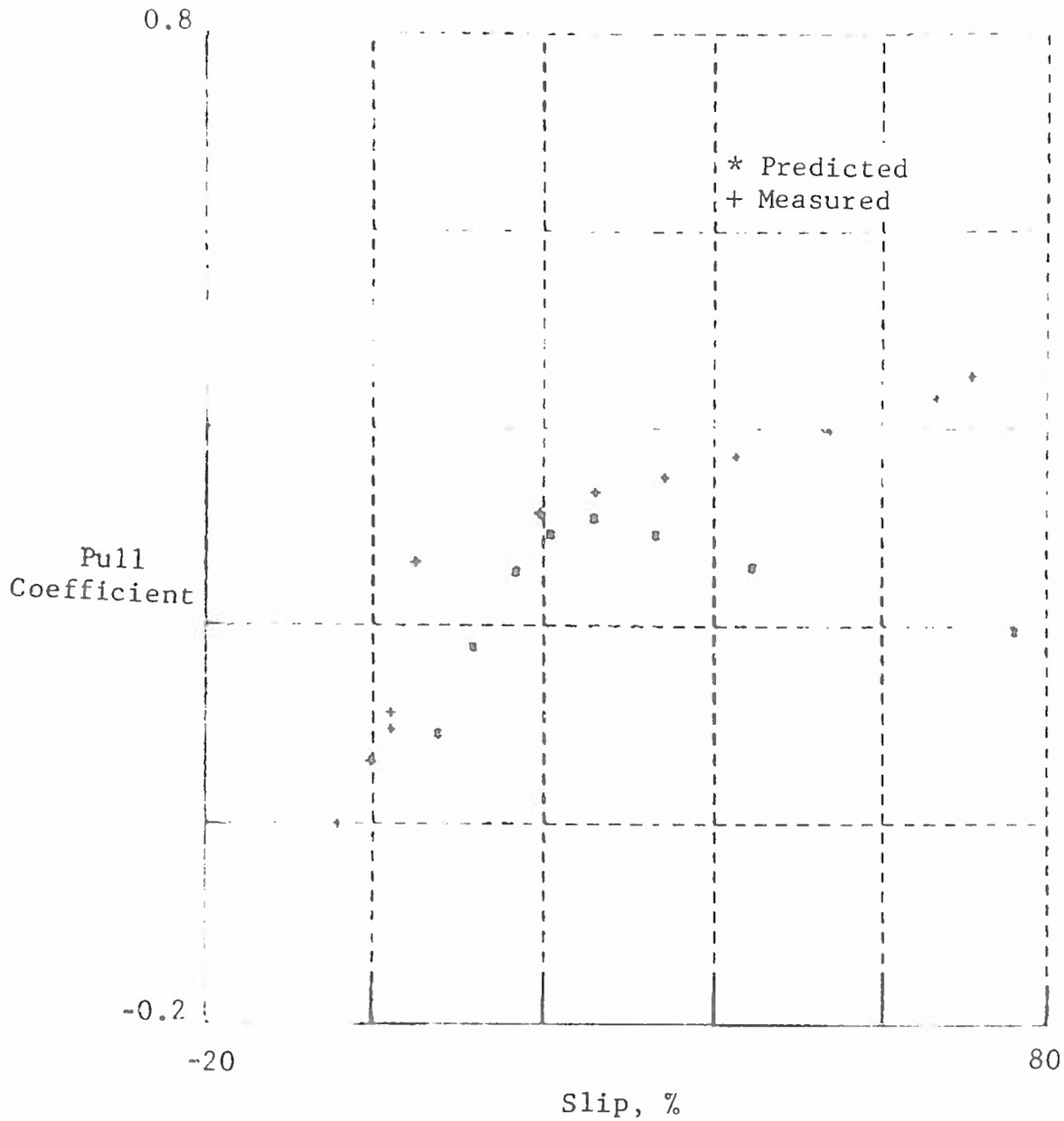

Fig. 52 Torque Coefficient Versus Slip - Test 5
Yuma Sand, CGR = 13.0
Tire: 4.00-7, Load: 210 lb

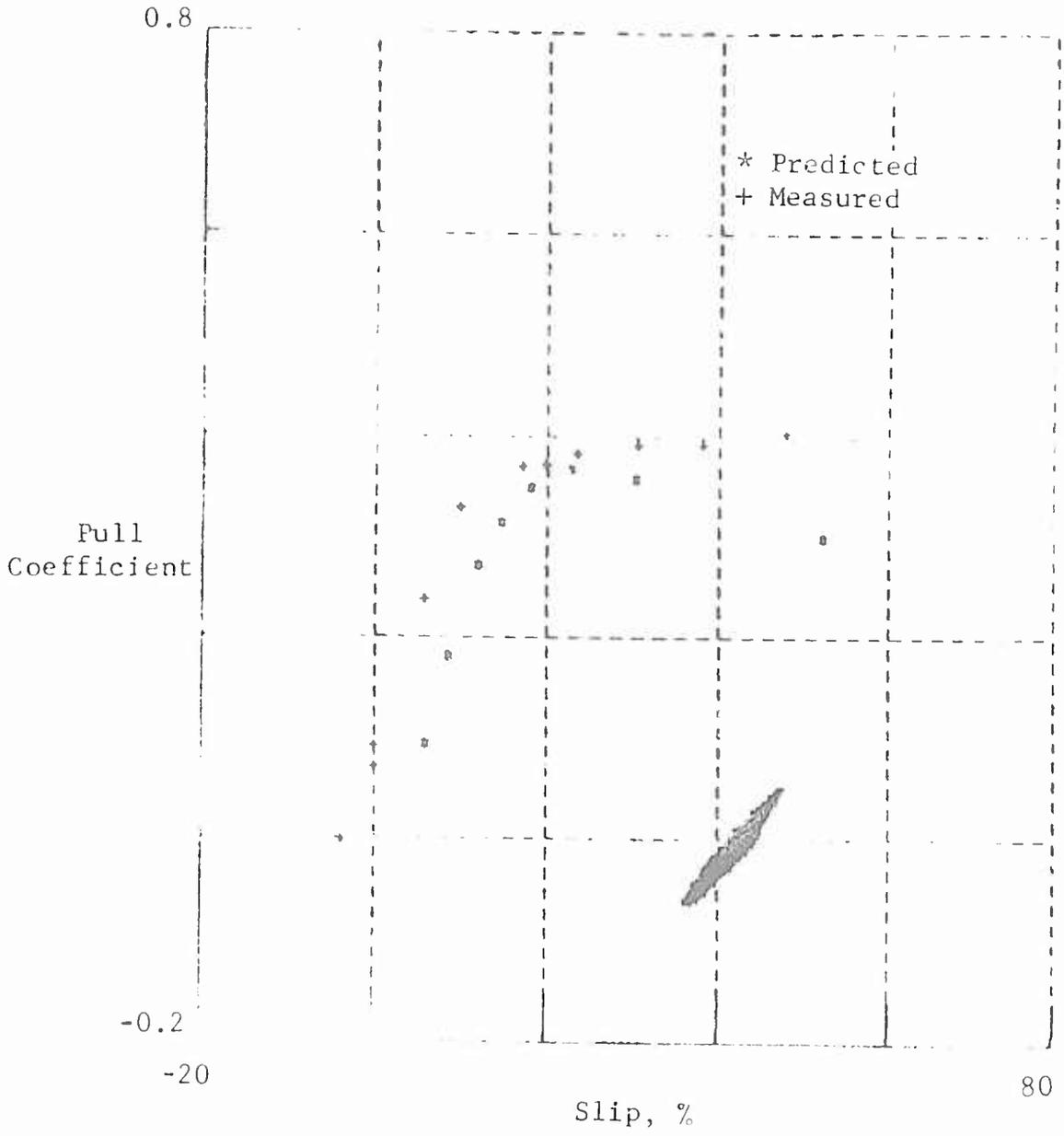

Fig. 53 Torque Coefficient Versus Slip - Test 7
Yuma Sand, CGR = 19.6
Tire: 4.00-7, Load: 220 lb

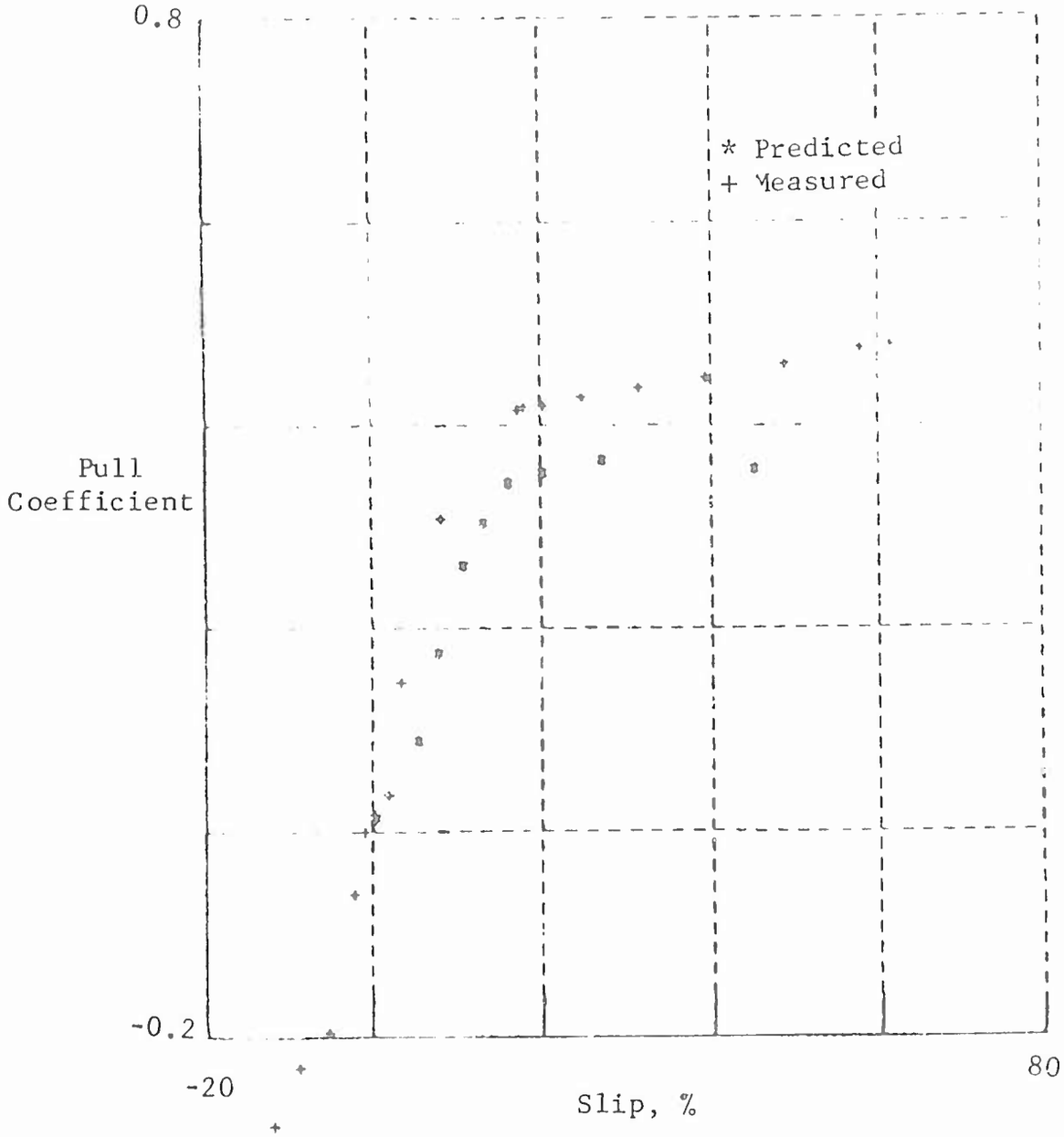

Fig. 54 Torque Coefficient Versus Slip - Test 14
Yuma Sand, CGR = 12.4
Tire: 9.00-14, Load: 870 lb

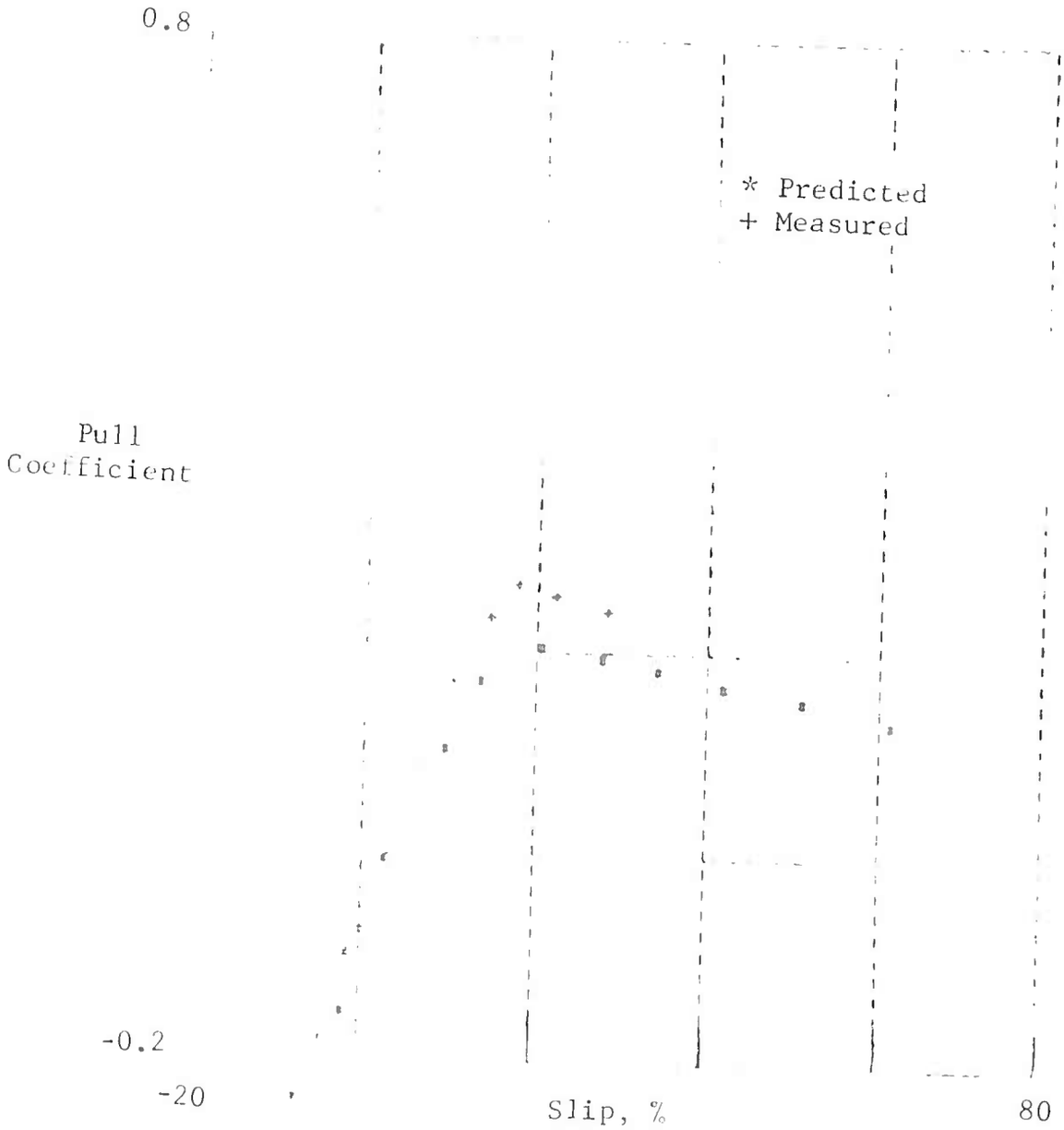

Fig. 55 Torque Coefficient Versus Slip - Test 18
Yuma Sand, CGR = 13.0
Tire: 4.00-30, Load: 450 lb

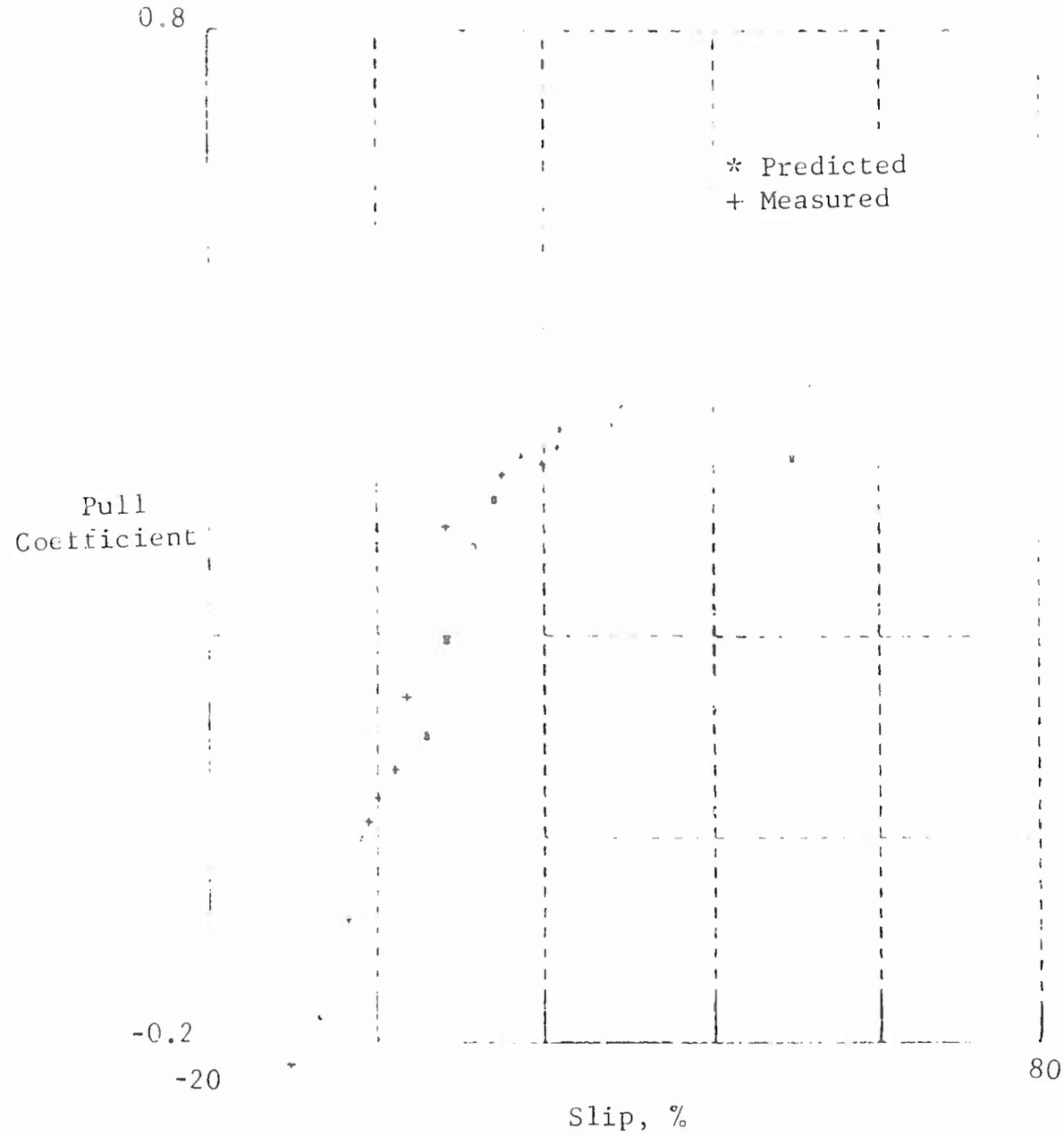

Fig. 56 Torque Coefficient Versus Slip - Test 19
Yuma Sand, CGR = 16.1
Tire: 7.00-20, Load: 330 lb

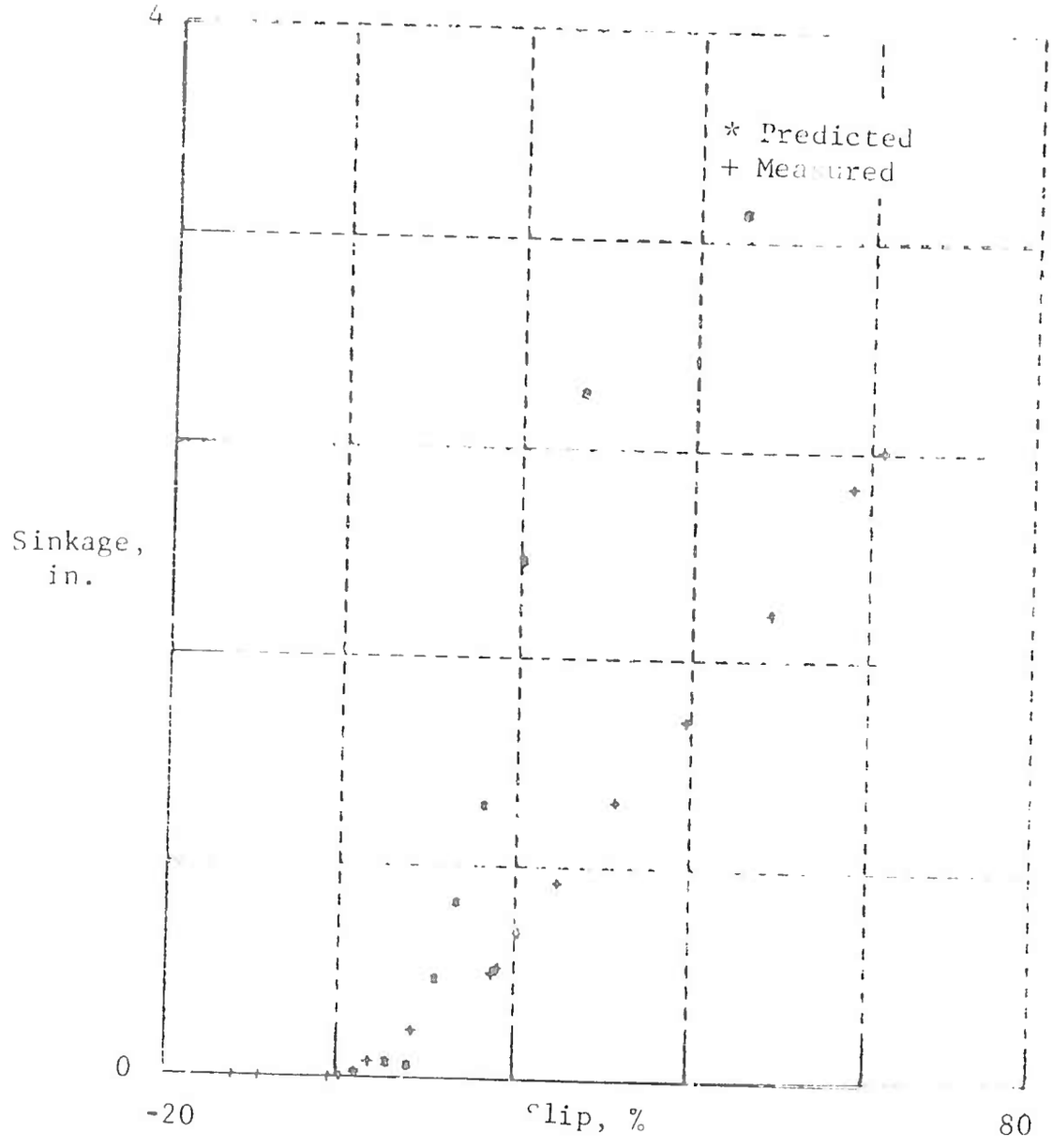

Fig. 57 Sinkage Versus Slip - Test 14
Yuma Sand, CGR = 12.4
Tire: 9.00-14, Load: 810 lb

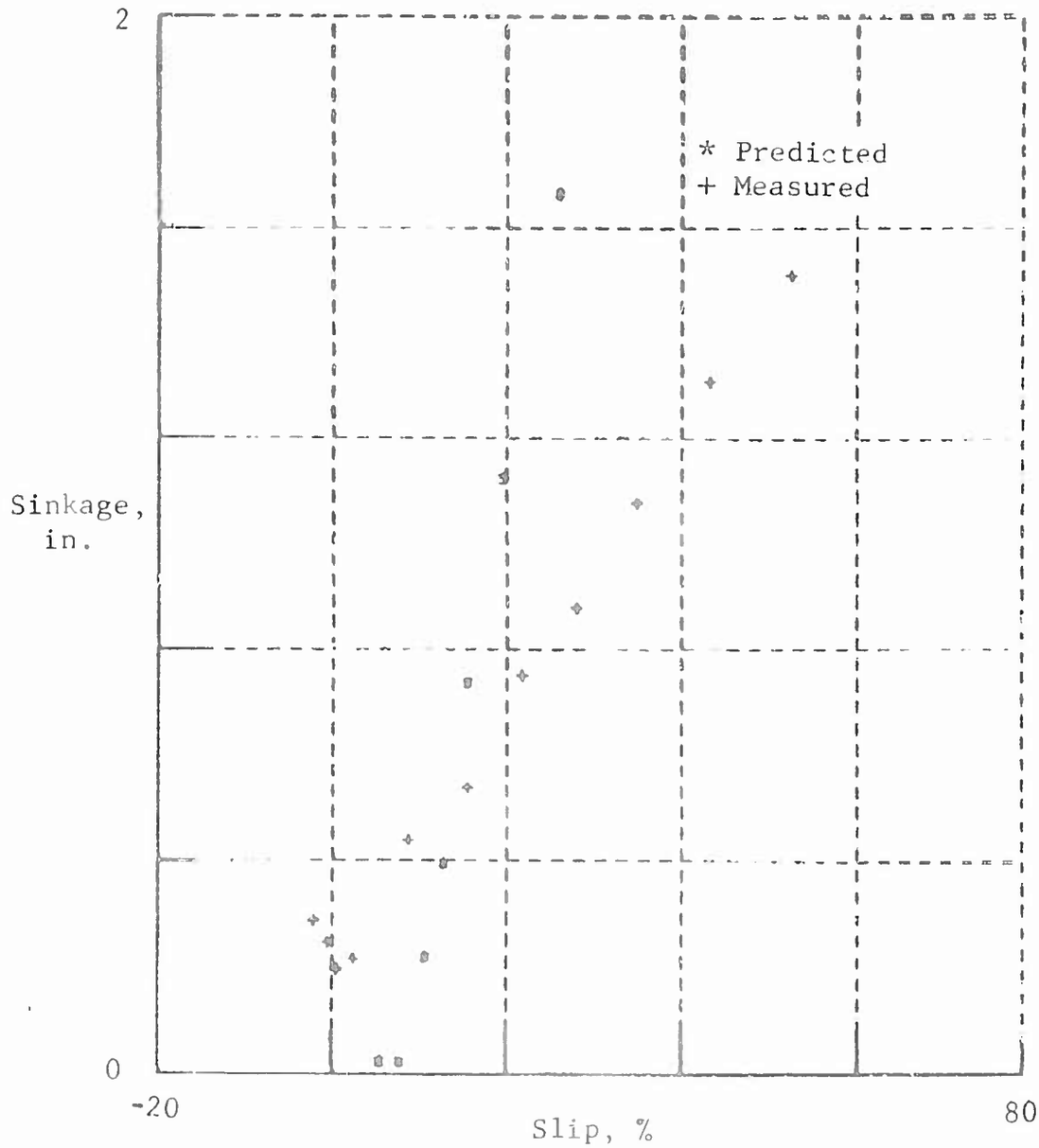

Fig. 58 Sinkage Versus Slip - Test 17
Yuma Sand, CGR = 14.4
Tire: 4.00-20, Load: 225 lb

X. EVALUATION OF PERFORMANCE PREDICTIONS

The comparison of computed and measured performance coefficients presented in Section IX shows a predictive capability of the tire-soil model that is truly remarkable in view of the many assumptions that were employed to make the model simple. It was expected that three dimensional effects and bow wave effects that may be appreciable under certain circumstances and were not accounted for in the model would have caused greater scatter in the predictions than actually occurred. These unaccounted-for effects were analyzed in detail. Results of the analyses are presented in Section XII.

In all computations a uniform angle of interface friction, δ, was assumed. This assumption resulted in inaccuracies of performance predictions for the rigid wheel (Ref. 13) whenever δ showed an appreciable variation over the contact area. The performance predictions by the tire-soil model do not appear to be affected by possible deviations from the assumed uniform distribution of δ. The most likely explanation for this is that the distribution of δ is probably close to a uniform one in the case of tires. The deformability of the tires and their ability to comply to the kinematic conditions at the interface are very likely to result in a uniform straining and associated interface friction over the contact area.

An interesting feature of the tire-soil model is that it shows the drop in the pull-coefficient with slip increasing past the optimum. The shape of the pull-coefficient versus slip curve in frictional soils is similar to that of the shear stress-displacement curve in direct shear stress tests experienced in dense soils. The decrease in pull-coefficient was often attributed to the decrease

in mobilized shear stress with slip. However, the mobilized shear-slip curve used with the present tire-soil model and represented by Eq. (5) does not show a peak but increases monotonically. Thus the decrease of the pull-coefficient at high slip rates cannot be attributed to this effect, but is the consequence of tire-soil interaction. When the shear stress at the interface approaches its maximum value, the normal stresses in the rear field that are controlled by soil failure conditions rapidly decrease. The tire-soil model responds to this decrease by an increase of the entry and rear angles and of the sinkage associated with these angles. The average inclination of the contact area increases as does the horizontal component of the normal stresses acting on this area. The net result is a decrease of the pull-coefficient even though the mobilization of the shear strength at the interface is close to its maximum.

The above finding is significant inasmuch as strain softening of the interface shear strength may be discounted as the cause of drawbar pull decrease at high slip rates. Strain softening is characteristic of the shear strength properties of dense granular materials where part of the shear strength is derived from the necessity that particles override each other. When the dense material loosens up shear may occur without much override, and the shear strength decreases. At the interface the mechanism of shear strength mobilization is different from that described above in that the failure surface is a solid one where shear may occur without particle overriding. Thus the monotonical increase of shear strength mobilization as intuitively suggested by Janosi and Hanamoto and represented by Eq. (5) is more representative of the mechanism of shear at the interface than other relationships that show a peak.

While the decrease in pull-coefficient was well reproduced by the model, the accompanying significant increase in the torque coefficient was not always reproduced. Figures 52 through 54 show an increase of the measured torque at high rates of slip while the predicted torque decreases. On the other hand, Fig. 55 shows a case where both the measured and predicted torque coefficient decrease at high slip rates. An analysis of the possible causes of this discrepancy was made and the following conclusions were reached.

The tire-soil model does not account for the internal friction caused by the deformation of carcass and friction in the bearings while the effect of these are included in the torque measurements. It is estimated that discrepancies on this account may amount to 2-3 percent in the value of the torque coefficient.

Some rotational inertia effects may have affected the torque measurements. Inaccuracies on this account are probably small.

The centerline geometries and radius variations assumed in the tire-soil model for these high slip rates were estimated. It was found that differences in torque prediction on account of misestimated radii are not likely to result in a difference of more than 2-3 percent in the predicted value of the torque coefficient.

The assumed smooth distribution of interface stresses in contrast to that observed in experiments that show peaks due to carcass stiffness may result in underestimated torque. The peaks occur close to the entry and exit angles where deflection is less and radius is greater than in the center (Fig. 59). Again, differences on this account are not likely to exceed 2-3 percent in the torque value.

Even if the sources of discrepancies act cumulatively, the over-all effect would not be more than 10 percent in the value

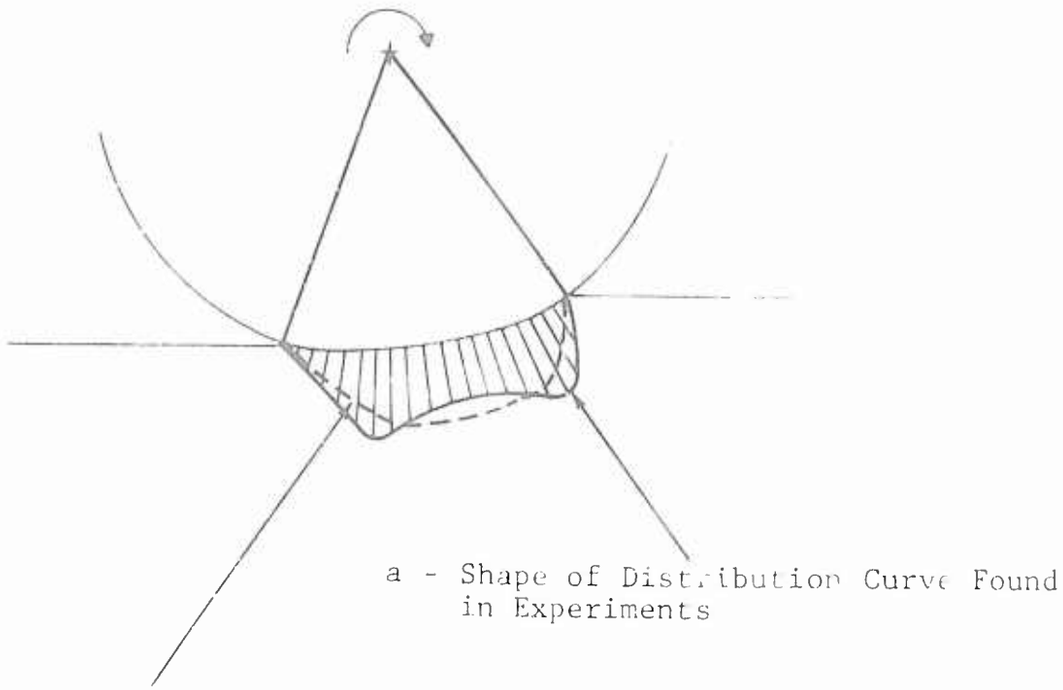

Fig. 59 Distribution of Interface Normal Stresses Beneath a Tire

of torque coefficient. Since at very high slips discrepancies occurred in the torque coefficient as high as 20 percent, there must be yet another source of these discrepancies. It was found that the most likely cause of discrepancies higher than 10 percent is that the assumption that the moment of interface normal stresses about the axle is zero does not hold true at high slip rates. This assumption was based on the experimental finding of Freitag et al. (Ref. 4). It appears that generalization of the validity of the conclusion drawn in Ref. 4 from a limited number of experiments (that the moment of normal stresses is zero) was not warranted. It appears that at high slip rates the center of tire axis shifts in such a way that normal interface stresses generate moments about the axis. Such a shift in the relative position of the axis to the interface was observed in the experiments where centerline geometry was measured (Fig. 60). Unfortunately, there were no simultaneous interface stress measurements in these experiments so that there is no way to check the validity of the assumption that the torque from normal stresses is zero.

The speculative conclusion that at high slip rates interface normal stresses may cause moments about the axis is indirectly supported by the dimensional analysis of tire-soil interaction (Ref. 18) and the comparatively poor torque performance prediction with the WES method. In the dimensional analysis it was found that the relation of the torque number to the sand number was not well defined (p. 117, Ref. 18) and torque performance predictions were found to separate for various tire shapes (p. 15, Ref. 18). Obviously, a shift in the relative position of the tire axis to the interface is a tire property that cannot possibly be characterized by a single deflection number obtained under vertical loading conditions on a rigid surface and, therefore, cannot be accounted for

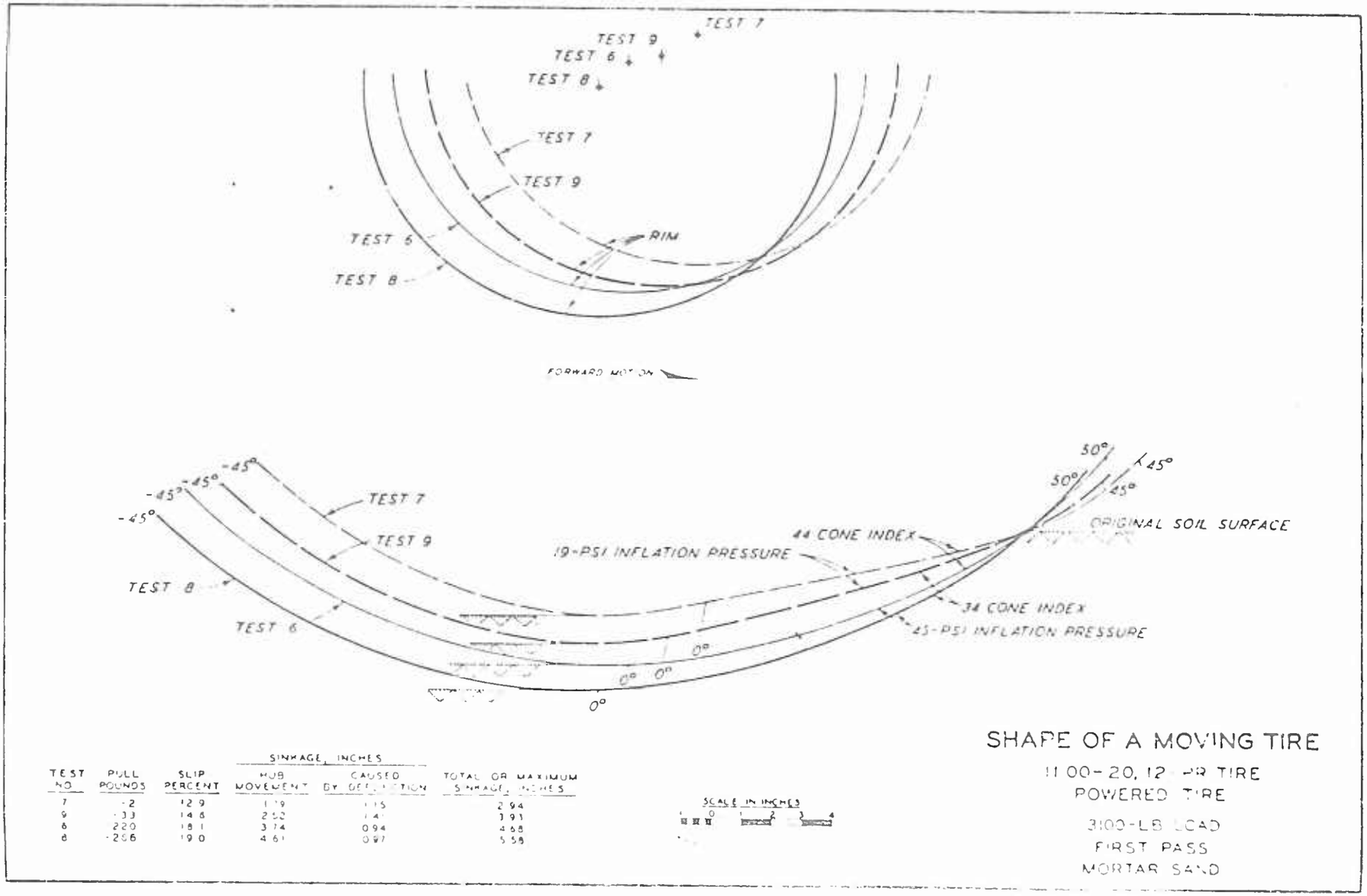

TEST NO.	PULL POUNDS	SLIP PERCENT	SINKAGE, INCHES: HUB MOVEMENT	SINKAGE, INCHES: CAUSED BY DEFLECTION	TOTAL OR MAXIMUM SINKAGE, INCHES
7	-2	12.9	1.19	1.15	2.94
9	-33	14.8	2.52	1.41	3.93
6	220	18.1	3.74	0.94	4.68
8	-256	19.0	4.61	0.97	5.58

Fig. 60 Shape of Relative Position of Tire Axis with Slip (from Ref. 3)

by dimensional analysis techniques using this tire characterization. A shift in the position of the axis would affect the torque coefficient but not the other performance characteristics and would explain the discrepancies of torque coefficient predictions by both the tire-soil model and WES techniques.

The performance prediction for test 13 was analyzed in detail since, in contrast to the other tests, performance prediction in this case was relatively poor (Fig. 22). A look at the pull performance prediction curve established by WES (Fig. 61) reveals that this curve is very steep at the sand numeric for test 13 (N_s = 5.06). This indicates that under these conditions a small variation in soil strength results in a large variation of the pull-coefficient.

An investigation was made to determine the effect of such small variations on the tire performance predicted by the model. Figure 22 shows pull-coefficients computed for ϕ = 37.6°, established by Eq. (3), and for ϕ = 36° and 35°. These two latter friction angles yield acceptable performance prediction and are within the limits of accuracy by which the friction angle can be determined from cone penetration measurements. Thus modification of the tire-soil model on account of test 13 was not deemed necessary.

The pull-coefficient prediction for test C1-1 was also analyzed in detail. These analyses indicated that it was not possible to duplicate the pull-coefficient of 0.56 observed in the test at 60 percent slip with any reasonable variation of the model parameters. An examination of the predicted sinkages in these analyses indicated that at 20 percent slip (where sinkage measurement was available) the predicted sinkage was less than the measured one

excluding the possibility that underestimation of the pull coefficient resulted from an overestimated sinkage. For small sinkages the contact area may be approximated by a plane inclined at an angle ϵ to the horizontal, and the following approximate relationships for the maximum value of the pull-coefficient may be developed (Fig. 62).

$$T_{max} = N \cdot \tan \varphi + c.A \tag{9}$$

$$H_{max} = (T_{max} - T') \cos \epsilon = T_{max} \cdot \cos \epsilon - W \tan \epsilon \tag{10}$$

$$A = N/p_{av} \tag{11}$$

$$\text{Pull-coefficient} = (H/W)_{max} = \left(\tan \varphi + \frac{c}{p_{av}}\right) \cos^2 \epsilon - \tan \epsilon \tag{12}$$

An examination of Eq. (12) shows that for the pull-coefficient to become as high as 0.56, either $\tan \varphi$ or c/p_{av} or both would have to have much higher values than assumed or calculated in the model. It is highly unlikely that the clay as prepared for the test at a high degree of saturation would exhibit a friction angle appreciably higher than 13°. In cohesive soils the value of c/p_{av} is not appreciably affected by the value of cohesion when the soil strength controls the interface stresses. In such a case p_{av} is approximately five times the cohesion resulting in a c/p_{av} value of about 0.2. The value of c/p_{av} could be significantly higher only if the limiting pressure, p_l, controlled the average pressure p_{av}. In order for this to be the case, the actual inflation pressure would have had to be much lower than the design pressure. Although it is conceivable that some leakage occurred during the test, it is unlikely that a significant drop in the inflation pressure would have gone unnoticed.

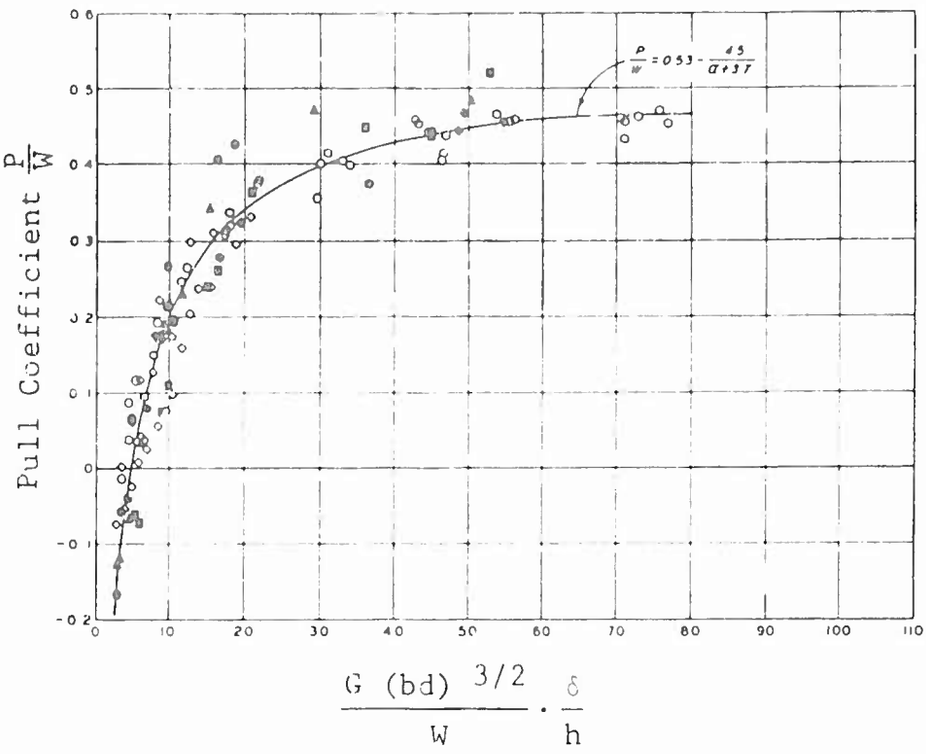

Fig. 61 Relationship Between Pull Coefficient and Sand Numeric (From Ref. 12)

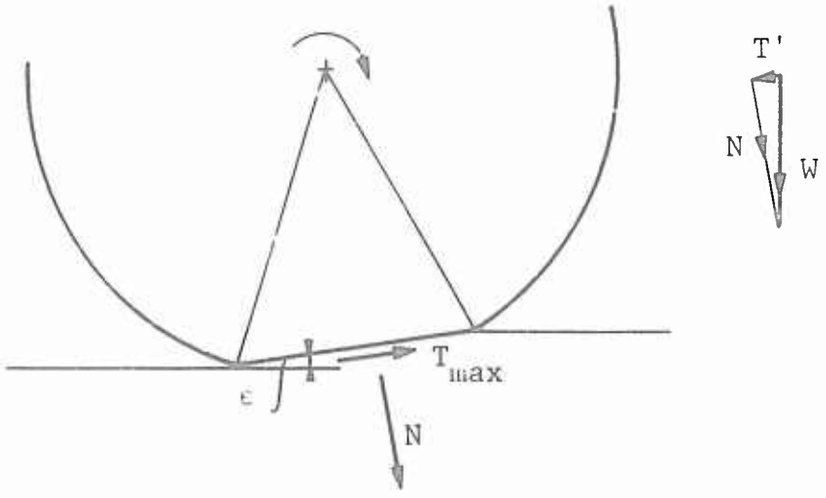

Fig. 62 Forces Acting on the Contact Area Approximated by a Plane

A factor that may increase the pull-coefficient and is not accounted for in the model is the effect of side wall adhesion. An estimate of the effect of this adhesion showed that it could not affect the pull-coefficient by more than 2-3 percent.

All the above considerations indicate that the underestimation of the pull-coefficient in this case cannot be attributed to an unsatisfactory simulation by the model or to inaccuracies in the estimates of the strength properties of soil. The most likely explanation for the discrepancy between observation and model simulation is that soil conditions were not uniform during the test and the strength of soil at the surface was higher than the strength averaged over a six-inch depth. In experiments with clays close to saturation it is very difficult to prevent evaporation from the surface; a relative humidity corresponding to the moisture equilibrium of the soil would have to be maintained during the preparation of the soil bed as well as during the test. In earlier experiments at WES a decrease in the moisture content of the uppermost layer in the soil bed was indeed observed (Ref. 19), and attention was called to the importance of surface strength in tire performance tests. Unfortunately, cone penetrometer tests are not very well suited to discriminate between surface soil strength and the average strength of a six-inch deep layer, and later investigations were confined to the detrimental effect of weak (wet) surface layers.

The strength of the surface layer affects the pull-coefficient in the following way: In Eq. (9) for the maximum traction, the strength parameters of the surface layer may be used. The failure conditions in the soil, however, are controlled by the lower strength of the soil below the surface layer so that the normal pressures and

p_{av} remain essentially unaffected by the higher strength of the surface layer. Thus in Eq. (12) both ϕ and c refer to the stronger surface layer while p_{av} corresponds to the lower strength of the underlying layer. The result is a significantly higher pull-coefficient than that obtainable under uniform soil conditions.

The potential effect of a strong surface layer on the pull-coefficient is subject to limitations imposed by the underlying layer. The strength of the upper layer to develop traction can only be utilized to the extent that the shear stresses at the interface between the upper and lower layer do not exceed the failure criteria for the lower layer. This will depend on the thickness of the upper layer and the relative strength of the upper layer to that of the lower one. These conditions may be analyzed by expanding the present tire-soil model so as to allow for a two-layer system or for soil strength changing gradually with depth. Such a model would be essentially the same as proposed previously for the analysis of slipperiness. Slipperiness is essentially the same phenomenon as discussed previously except that the strength ratios of the upper and lower layer are reversed.

XI. SIMULATION OF TIRE PERFORMANCE IN COHESIVE-FRICTIONAL SOILS

The comparisons of predicted tire performances with measured ones given in Section X show that the proposed tire-soil model yields very good predictions for a variety of tires and soil conditions. The experimental data available for these comparisons however, were restricted to two types of soil: the purely frictional Yuma sand or the purely cohesive Buckshot clay. From the viewpoint of the tire-soil model this restriction is not considered as a limitation to the use of the model in frictional-cohesive soils. On the contrary, the computation of interface stresses by plasticity theory takes into consideration the simultaneous effect of friction and cohesion and, therefore, it can be assumed that the tire-soil model simulates tire performance in cohesive-frictional soils as well as in the cases shown in Section X. Nevertheless, it seemed desirable to evaluate model performance under soil conditions other than tested at WES. The tire performance tests conducted at the National Tillage Machinery Laboratory in various types of agricultural soil appeared to be suitable for this purpose. However, these tests were performed for comparative tire performance studies where soil conditions were intended to duplicate conditions likely to be encountered in the field by agricultural tractors (for example, moisture content increasing with depth). Since at this time the tire-soil model has not yet been expanded to include layered or nonuniform soil conditions, the simulation of these agricultural tire performance tests by the model strictly applicable to homogeneous soils can only be considered as a crude approximation.

The tire performance tests selected for simulation were part of a larger program where the effect of lug angle on performance

was investigated. These tests are described in detail in Ref. 20. The selected tests are the ones performed with smooth tires that were tested in the large program for reference purposes.

In order to have performance evaluations comparable to that reported in the preceding sections, the digital data points received on a punched paper tape from the National Tillage Machinery Laboratory for various travel reduction rates had to be converted to slip rates. In this conversion in the absence of tire deflection data, the so-called loaded tire radius taken from the manufacturer's catalog was used in the computation of the slip rate. The slip rates shown in the various figures may be in a slight error on this account. For each test over 100, data points were obtained. Figure 63 shows data points for test A1 together with the best fitting second degree polynomial obtained by the appropriate computer library program and displayed on the visual display terminal. In the following comparisons of performance predictions with National Tillage Machinery Laboratory test results only the best fitting curves are shown to preserve clarity. The best fitting curves for tests A1 and A2 shown in Fig. 64 and those for tests A3 through A6 shown in Fig. 65 are almost identical, indicating the good reproducibility of these tests.

Results of the simulation of these tests by the tire-soil model are shown in Figs. 64 and 65 by crosses. The results of the tests performed in the Decatur silty loam were duplicated fairly closely using the strength properties determined by triaxial tests for the uppermost layer with the least moisture content. Simulation of the tests performed in the Vaiden clay is not as good as in the Decatur silty loam, although in the simulation shown, a cohesion value about 30 percent higher was used than that determined by

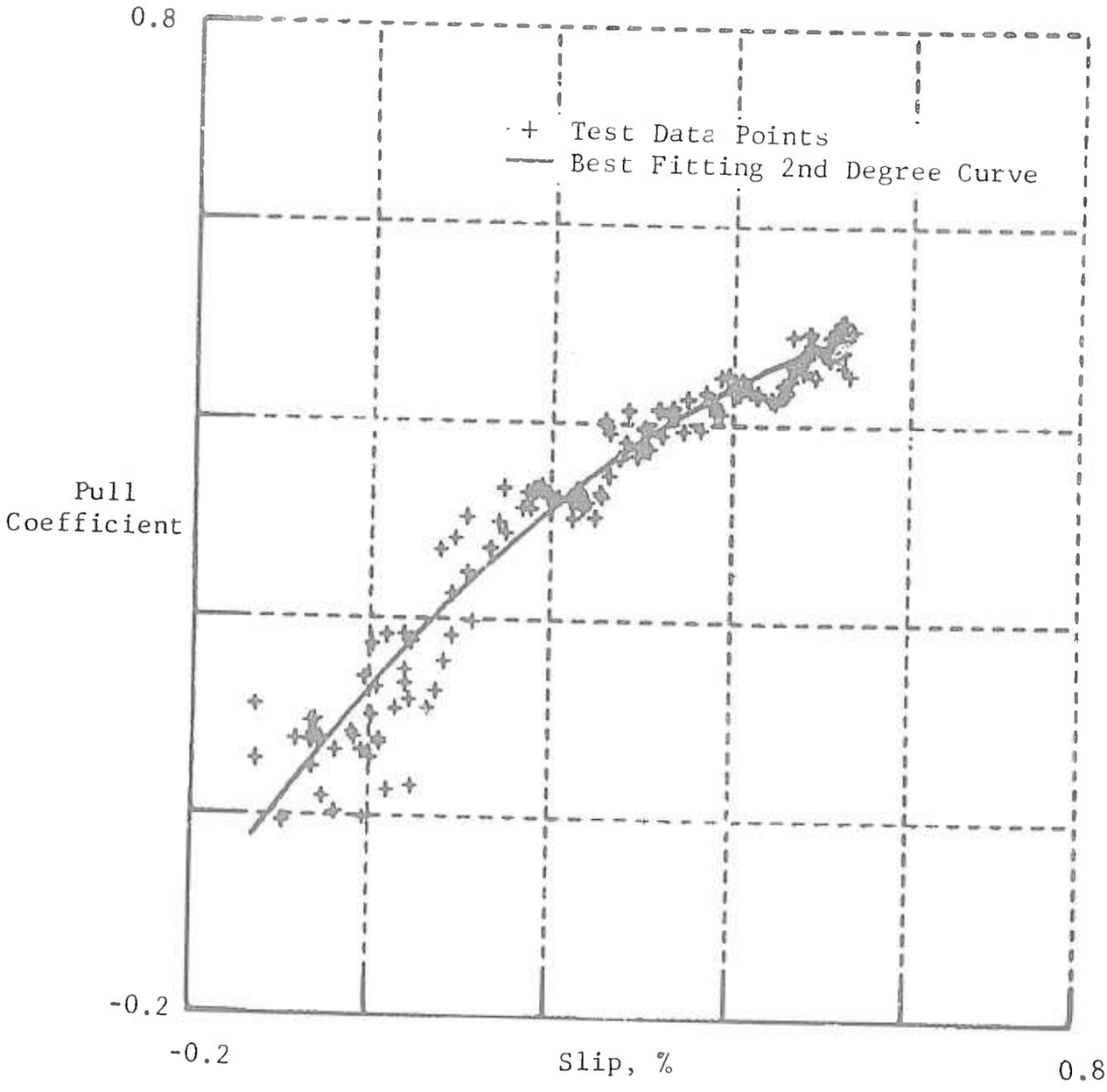

Fig. 63 Pull Performance Data Points and Best Fitting 2nd Degree Polynomial - Test A1, Decatur Silty Loam, Tire: 11 x 38, Infl. Pressure: 12 psi, Load: 2185 lb

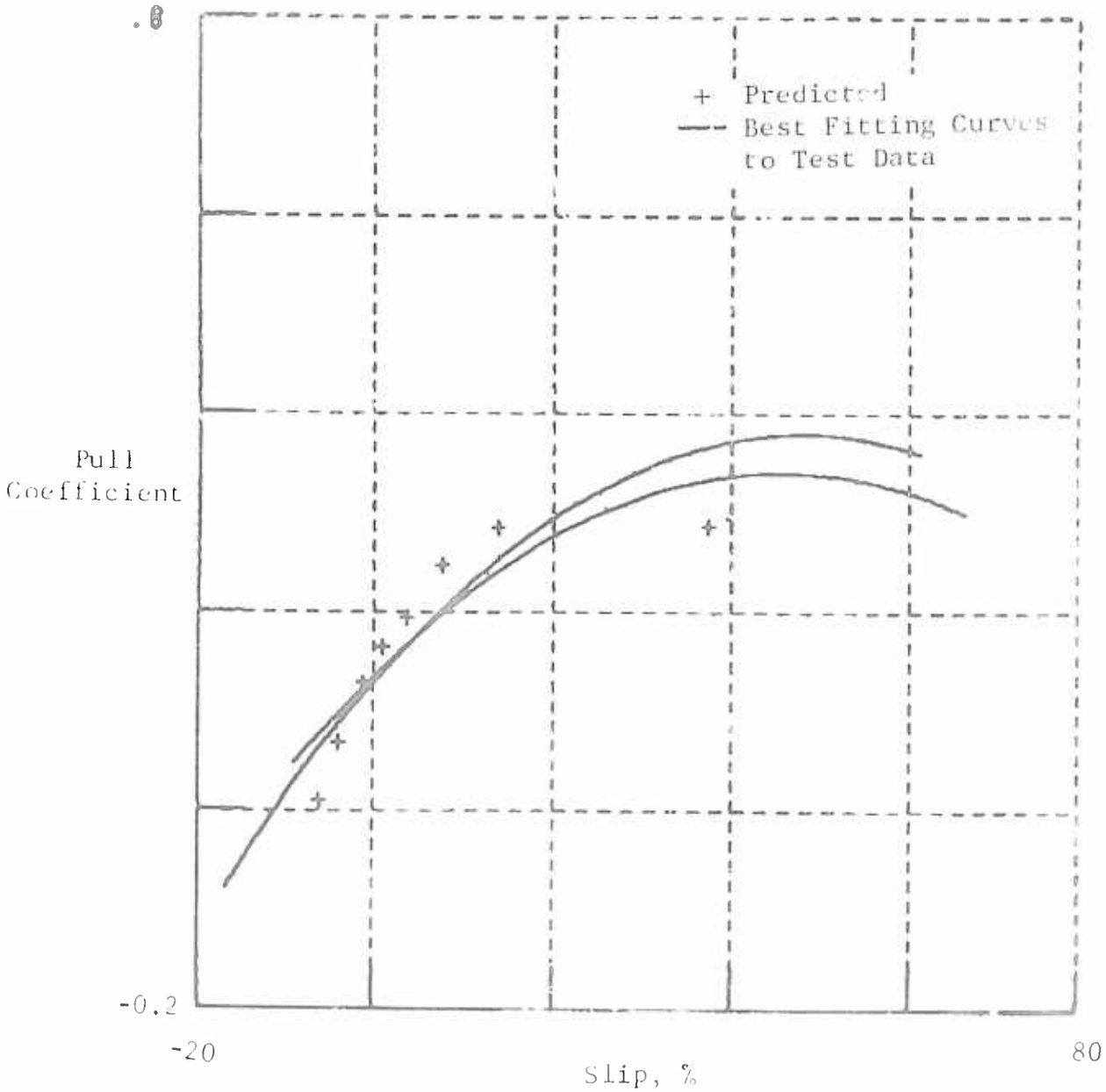

Fig. 64 Pull Coefficient Versus Slip - Tests A1 and A2, Decatur Silty Loam, Tire: 11 x 38, Load: 2185 lb

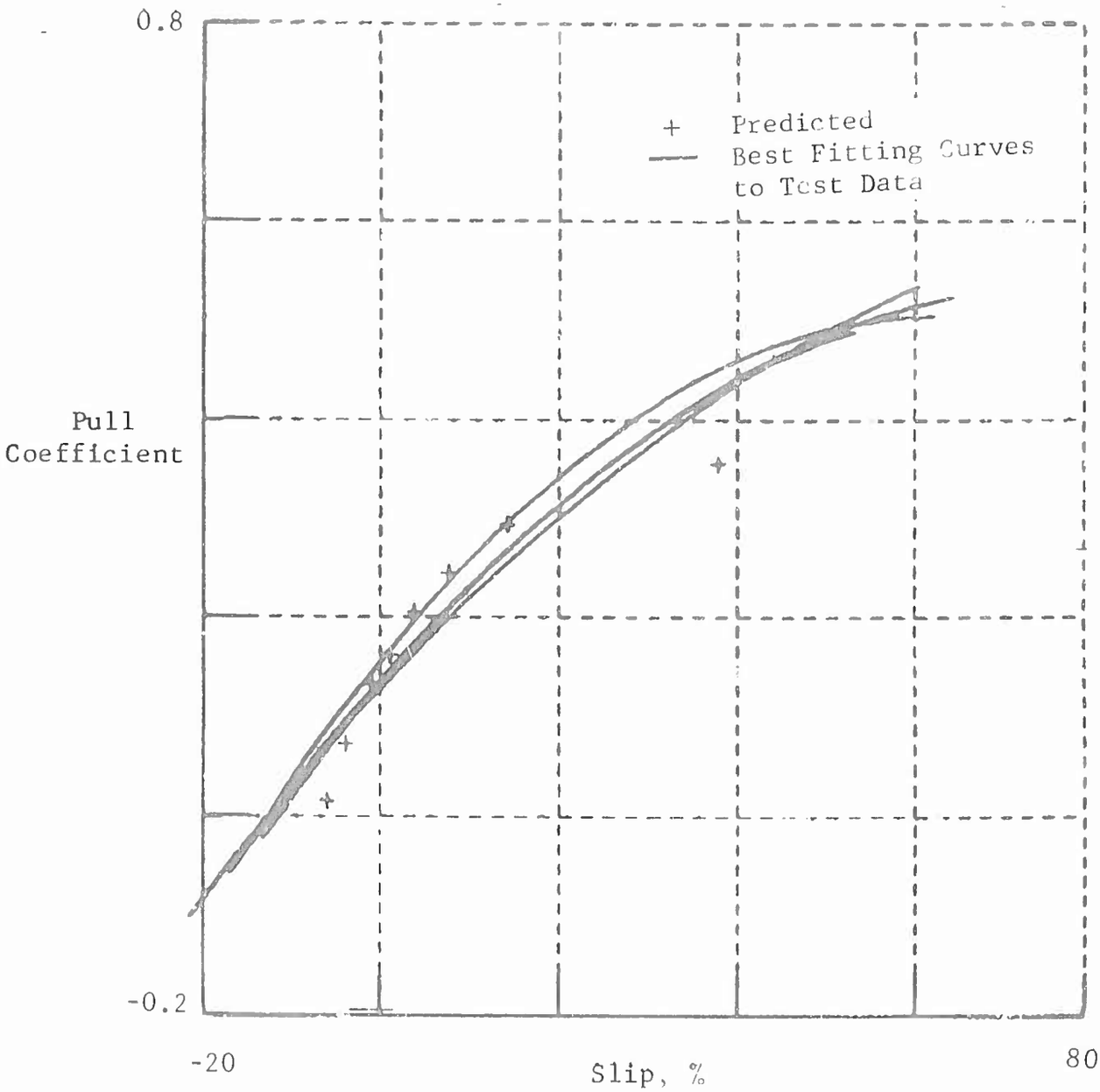

Fig. 65 Pull Coefficient Versus Slip - Tests A3 through A6, Voiden Clay, Tire: 11 x 38, Load: 2185 lb

triaxial tests for the uppermost layer of the Vaiden clay. In the simulation slip parameters were assumed by trial and error procedure.

It appears that in order to obtain good simulation, soil strength values equal or higher than that of the strongest uppermost layer would have to be used with the tire-soil model. One explanation for this is that the soil strength determination by triaxial tests was conducted at a lower rate than the loading rate applied to the soil in the tire test. Another possibility that at first glance may seem paradoxical is that in a layered system with strength properties decreasing with depth a higher pull-coefficient can be obtained than in a uniform soil that would exhibit the strength properties of the uppermost, strongest layer. There are indications that a weaker underlying layer would act in a similar way as a low inflation pressure: it would reduce the normal interface stresses while allowing interface shear stresses as high as the strength of the upper layer. The extension of the tire-soil model to layered soil system and nonuniform soil conditions would allow the analysis of such cases; until such a model is available no conclusive evaluation of the test results can be made.

XII. EVALUATION OF THE TIRE-SOIL MODEL AND SUGGESTED IMPROVEMENTS

The prediction of tire performance presented in the various figures of Section IX is very good and one could say much better than might be expected from a two dimensional model that cannot take into account three dimensional effects. Since three dimensional effects as well as bow waves certainly affected tire performance at least in some of the tests conducted, it was thought necessary to analyze these effects and determine why it was possible to achieve good prediction accuracy without the consideration of these effects. Following are the results of these analyses.

It was pointed out in the previous report on rigid wheel-soil interaction (Ref. 13) that lateral failure conditions constitute a limitation of the normal stresses that may arise at the interface. The interface stress measurements performed with rigid wheels conclusively indicated that the distribution of normal stresses across the interface is no longer uniform if lateral failure conditions prevail. The limitation on the normal stresses imposed by lateral failure conditions may be formulated and computed by plasticity theory; this development was outside the scope of the present program. However, for the purpose of this discussion an approximate formula was developed for the computation of normal stresses at the outside edge of the tire on the basis of lateral failure. In the case of cohesionless soils the maximum normal stress that can arise at the edge of the interface depends on the friction angle and on the depth of the point of the interface below the original surface. Typical edge stresses computed by this approximate formula are compared with normal stresses computed in the tire-soil model in Figs. 66 through 68. Centerline geometries for the same test are shown in Fig. 49. It can be seen that the smaller the

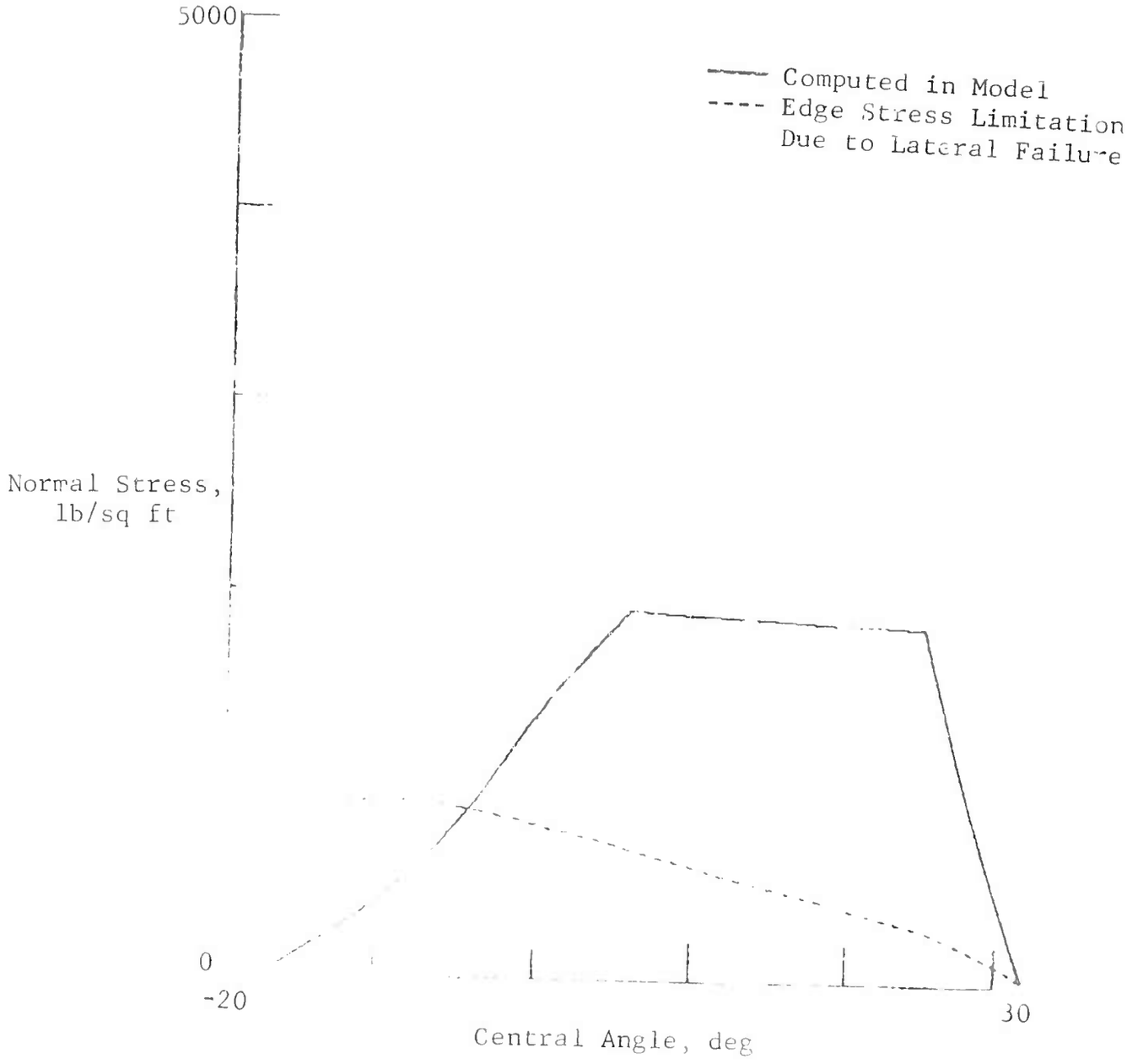

Fig. 66 Limitation of Interface Normal Stresses Imposed by Lateral Failure Conditions - Test 5, 13% Slip, Sinkage = 0.2 in.

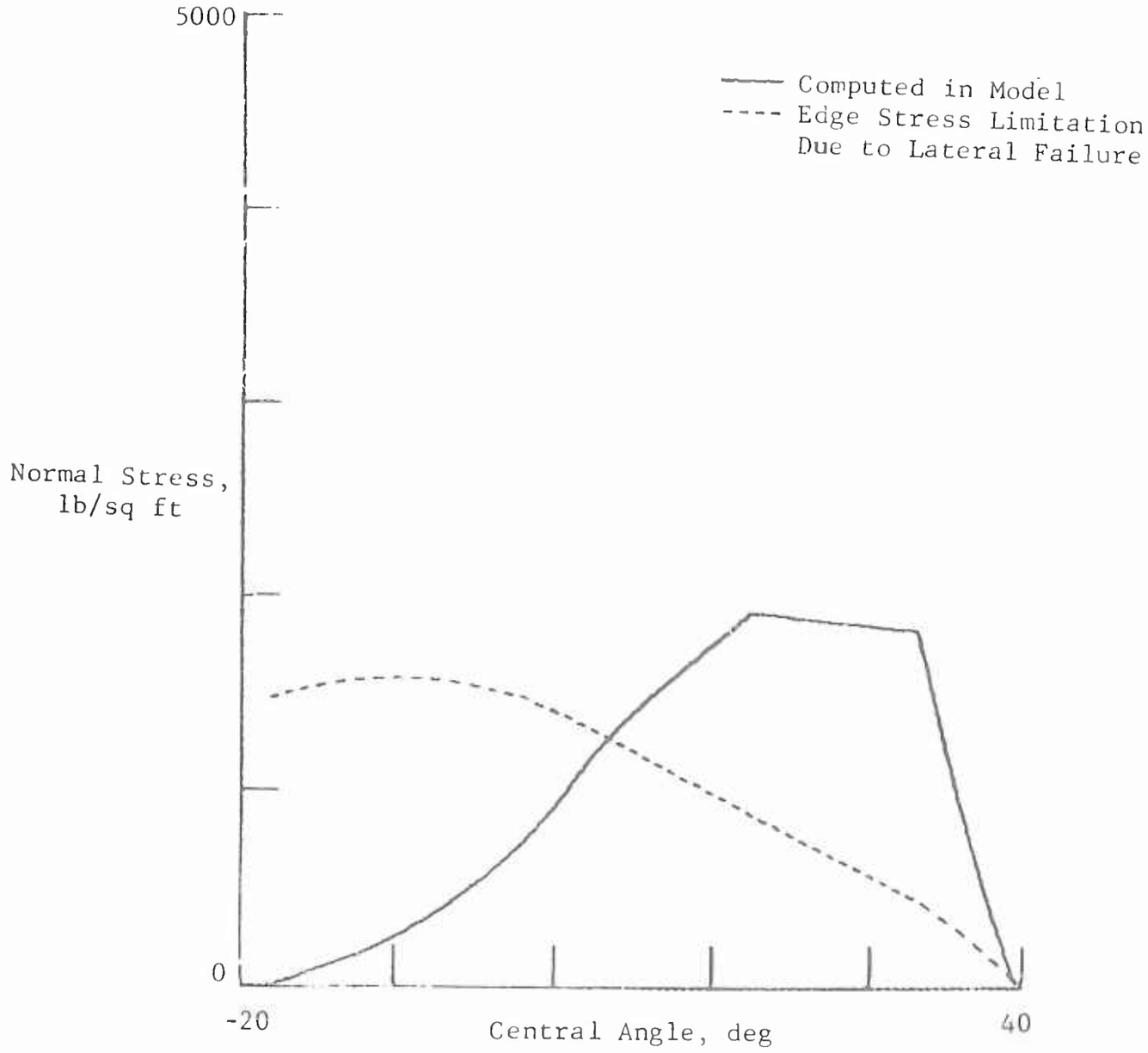

Fig. 67 Limitation of Interface Normal Stresses Imposed by Lateral Failure Conditions - Test 5, 21% Slip, Sinkage = 0.8 in.

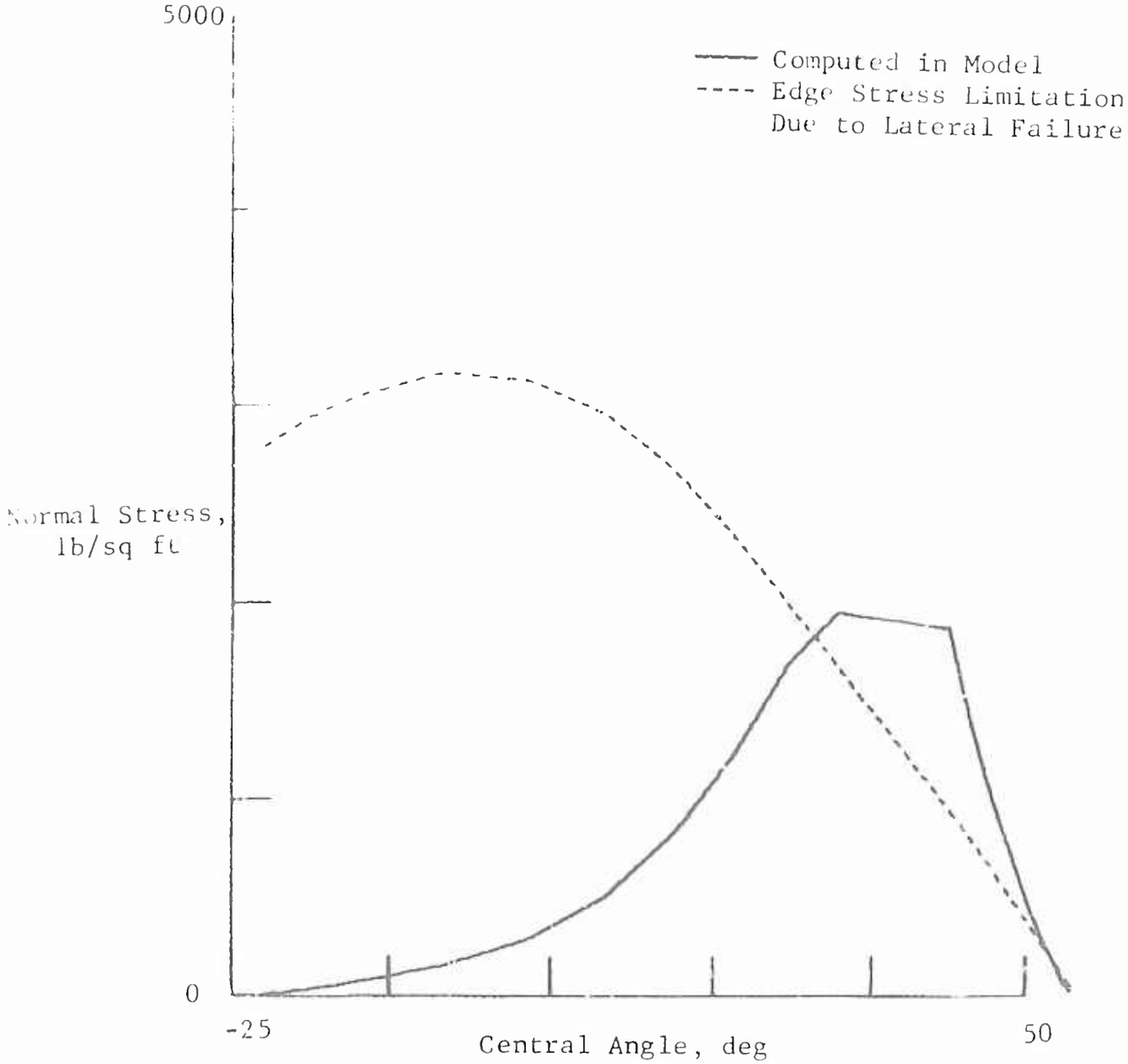

Fig. 68 Limitation of Interface Normal Stresses Imposed by Lateral Failure Conditions - Test 5, 36% Slip, Sinkage = 1.9 in.

sinkage, the more pronounced the effect of lateral failure conditions. In the case of small sinkage, the pull-coefficient is not influenced by the average inclination of the contact area and is essentially determined by the α/σ_n ratio. In such a case the tire-soil model predicts the pull-coefficient accurately even though the computed arc length of the front field is shorter than it would be had the lateral effect been considered. With increasing sinkage, the limitation on the normal stresses due to lateral failure becomes less significant and prediction is acceptable. In cohesive soils, the effect of lateral failure is less significant. Even though this fortuitous situation allows a satisfactory performance prediction by the two dimensional model, consideration of the three dimensional effect would result in the following advantages:

- In the present two dimensional model the relationships established for the estimate of ϵ are different for the various tire types. It is believed that a similar model, expanded to take the limitations on the interface normal stresses due to lateral failure into consideration, would probably result in a uniform relation for ϵ for all tire sizes.
- Consideration of lateral failure in the model would allow performance simulation of dual and multiple tire arrangements with proper consideration of their spacing.
- The development of a technique to consider lateral failure would be directly applicable to tracks and track elements and could be the basis of tracked vehicle modeling.

As regards the bow wave effect, the following considerations apply: The tire-soil interaction, as was shown previously can be

satisfactorily simulated by the model in which the soil is represented by its strength properties. Sinkage as well as stresses in the soil beneath the tire are determined without consideration of the volumetric changes in the soil. However, the total volume change of the soil due to the stress system generated by the tire load should be in balance with the total volume change represented by the size of the rut. If there is an unbalance, bow waves form. In the experiments performed at WES with densely packed wooden rollers (a two dimensional soil model), tire-soil interaction required a certain sinkage and volume change that could not be balanced by further densification of the wooden rollers. Consequently, sizable bow waves developed in these tests even at high slip rates. Since the volume change of the soil model was practically nil, and no lateral displacement occurred in the two dimensional model, no volume balance could be achieved and the size of the bow wave did not stabilize during the test. In actuality the conditions are never rigorously two dimensional and significant bow waves occur only with towed and relatively wide tires.

The effect of bow waves on tire-soil interaction may be analyzed by the model by assuming that the geometry of the free surface in the front of the tire is that of the bow wave. Preliminary studies indicated that it is feasible to account for the bow wave geometry in the computation of the front slip line field. Figure 69 shows the slip line field geometry for an assumed bow wave. Preliminary analyses indicate that the effect of a bow wave on interface stresses and tire performance is not as great as the physical appearance of the bow wave would suggest.

While it would be desirable to take the effect of bow waves into account in tire-soil interaction, this would necessarily involve the determination of at least another parameter that expresses

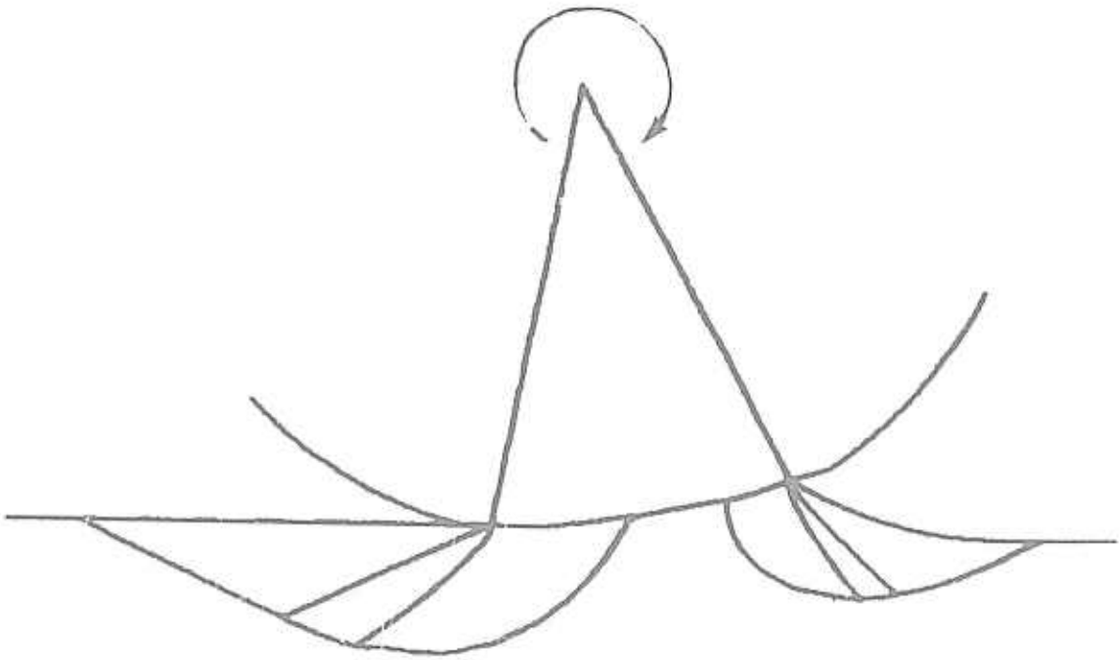

Detail

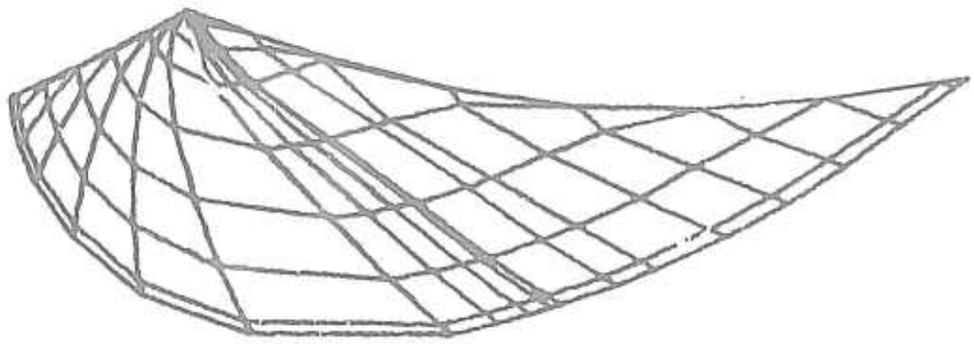

Fig. 69 Geometry of Centerline of Tire and Slip Line Fields in the Case of a Bow Wave. Size of the bow wave is assumed. In the slip line field only selected slip lines are shown. Tire: 9.00-14, Yuma Sand, CGR = 11.4, Load: 830 lb, Drag: 6 lb

the volume change properties of soil. (This is discussed in more detail in Appendix A.) Fortunately, as our preliminary analyses indicate, the bow wave effect does not influence significantly the pull-coefficient determination for driven tires. However, for towed and very wide tires the bow wave effect may not be negligible. The tire-soil model may be expanded to include the consideration of bow wave effects, but further research is needed to develop methods for the estimate of soil volume changes, volume change balance, and bow wave size.

XIII. USE OF THE TIRE-SOIL MODEL AS AN ANALYTICAL TOOL

The simulation of soft soil tire performance by mathematical models is advantageous not only for performance predictions as discussed in Sections IX through XII, but also for the analysis and understanding of tire-soil interaction phenomena. In Section X some examples of the use of the tire-soil model for the analysis of tire-soil interaction phenomena have already been presented. For example, it was shown that a drop in the pull-coefficient experienced at high slip rates occurs in frictional soils even if the developed shear stress increases monotonically with slip. Another analysis in Section X showed the significance of surface layer strength.

The tire-soil model is preeminently suited for the analysis of the effect of changes in any one input variable on tire performance. For example, the maximum drawbar pull that a tire can exert in sand can be analyzed and the maximum drawbar pull at various tire loads determined. Figure 70 shows the results of such an analysis for a 9.00-14 tire inflated to 16.4 psi. The soil is Yuma sand with a cone index gradient of 13.8. It can be seen that there is a maximum drawbar pull that cannot be exceeded by increasing the tire load even if the available torque is unlimited.

Another way of presenting the effect of tire load on pull performance is shown in Fig. 71, which shows the decrease of the pull-coefficient as the tire load increases.

Parametric analysis of design variables can be easily performed by the mathematical tire-soil model. In Fig. 72 the pull-coefficients for various tire diameters are shown, all other variables being constant. The fact that larger diameter tires work better in sand than smaller ones is, of course, well known. The mathematical model confirms this fact in quantitative terms over the whole range of slip.

The respective torque and sinkage values are also available from the computer program. Performing tire performance computations for soil conditions representative of a mission, the design can be optimized and trade-off studies can be made for military decisions.

The effect of inflation pressure on pull performance is shown in Fig. 73. The inflation pressures correspond to 15, 25, and 35 percent deflection (in WES terminology), respectively. The analysis confirms the well-known beneficial effect of lowering the inflation pressure on traction.

The effect of soil properties on tire performance may also be easily analyzed. An example of such an analysis is shown in Fig. 74 where pull performances for the conditions of test 9 are compared for various values of the unit weight .; all other conditions are unchanged. It is seen that a slight increase in . improves tire performance by some three percent in the pull-coefficient. Such a difference may remain obscured in an experimental program where data scatter occurs for many reasons and a detailed statistical analysis would be necessary to show that such observed differences are statistically significant. In an analysis by a mathematical model all other variables (including friction angle) are exactly the same, and the obtained results clearly show the influence of changes in the selected variable, the unit weight. The effect of unit weight is more pronounced under other circumstances. In Fig. 74 computed pull-coefficients are also shown for the case of = 65 lb/cu ft that corresponds to the submerged unit weight of soil. It is seen that the submergence affects tire performance appreciably even if only its effect on unit weight is considered. In this analysis pore water pressures were assumed to be neutral;

the effect of pore water pressures that, depending on the density of soil, decreases or increases the strength of soil may override the effect of unit weight.

Although the comparison of predicted and measured pull performance presented in Section IX includes a wide range of soil strength, it is of interest to show the variation of pull performance when only the strength is varied, all other conditions being equal. Such a comparison is shown in Fig. 75. Soil strength, as Fig. 75 and the other performance analyses indicate, is the most crucial single factor in vehicle mobility.

Figure 76 shows the effect of a small cohesion on the pull performance curve. A cohesion of 10 lb/sq ft, which is indeed very small and could be the result of a slight dampness in frictional soils, improves the pull performance appreciably. The effect of cohesion on pull performance, if it acts in conjunction with a high friction angle, is great.

As these examples indicate, the model is well suited for parametric analysis of various design features. These analyses can be performed at a fraction of the cost of experiments and in a matter of minutes. The availability of such a model is expected to spur interest in optimizing the design of off-road vehicles.

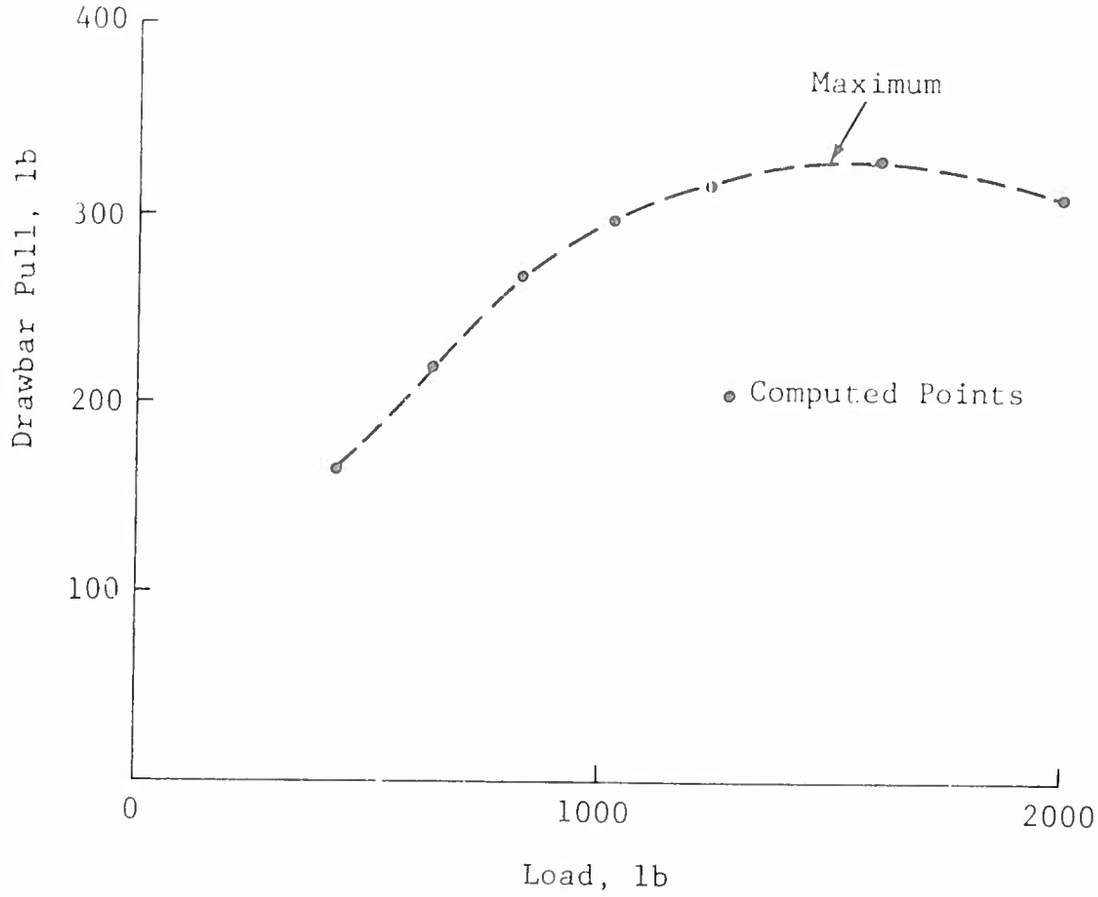

Fig. 70 Maximum Drawbar Pull at Various Tire Loads.
Tire: 9.00-14, Infl Pressure: 16.4 psi
Yuma Sand, CGR = 13.8

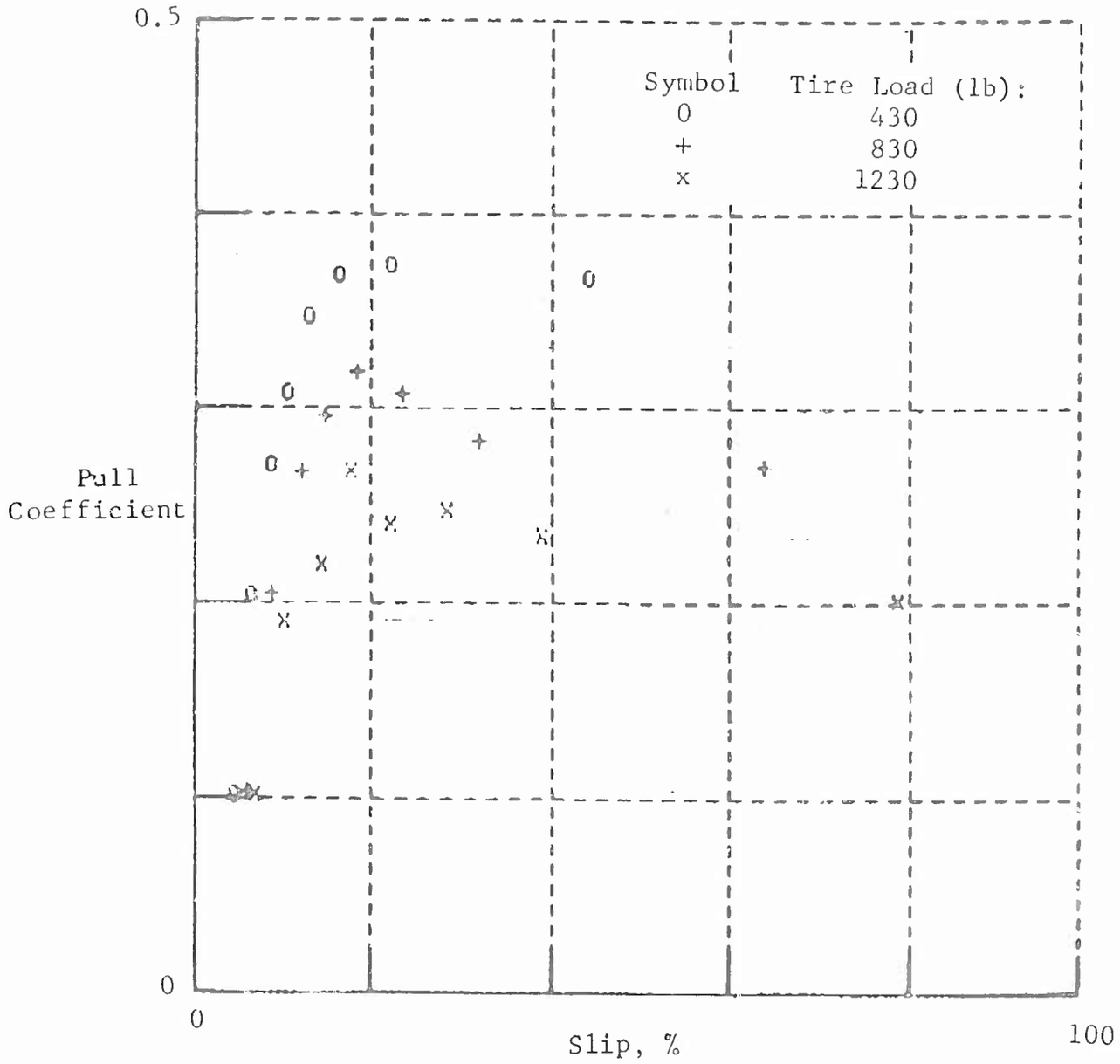

Fig. 71 Effect of Tire Load on Pull Performance
Yuma Sand, CGR = 13.8
Tire: 9.00-14, Infl. Pressure: 16.4 psi

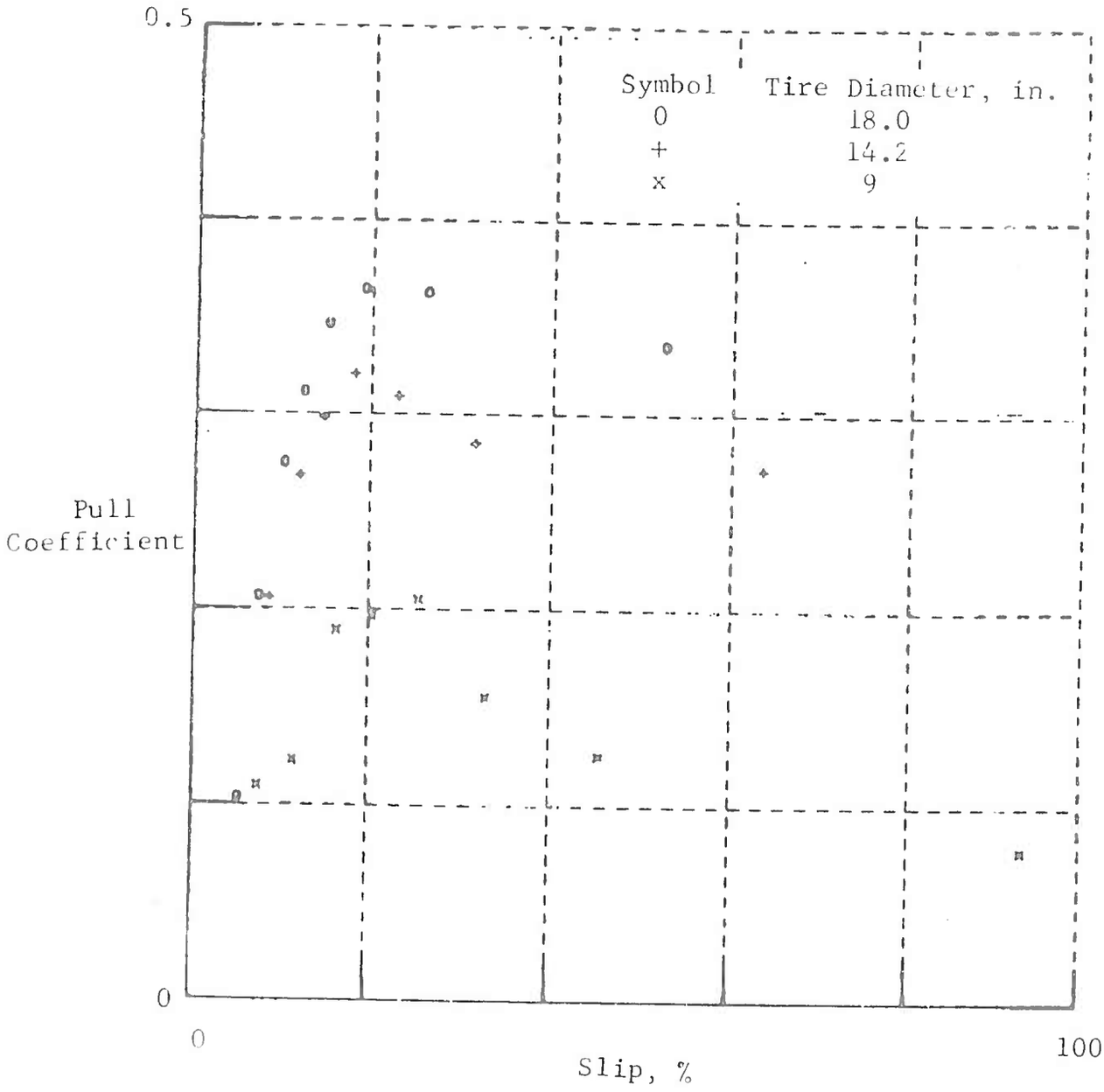

Fig. 72 Effect of Tire Diameter on Pull Performance
Yuma Sand, CGR = 13.8, Load: 830 lb
Tire Width: 8 in., Infl. Pressure: 16.4 psi

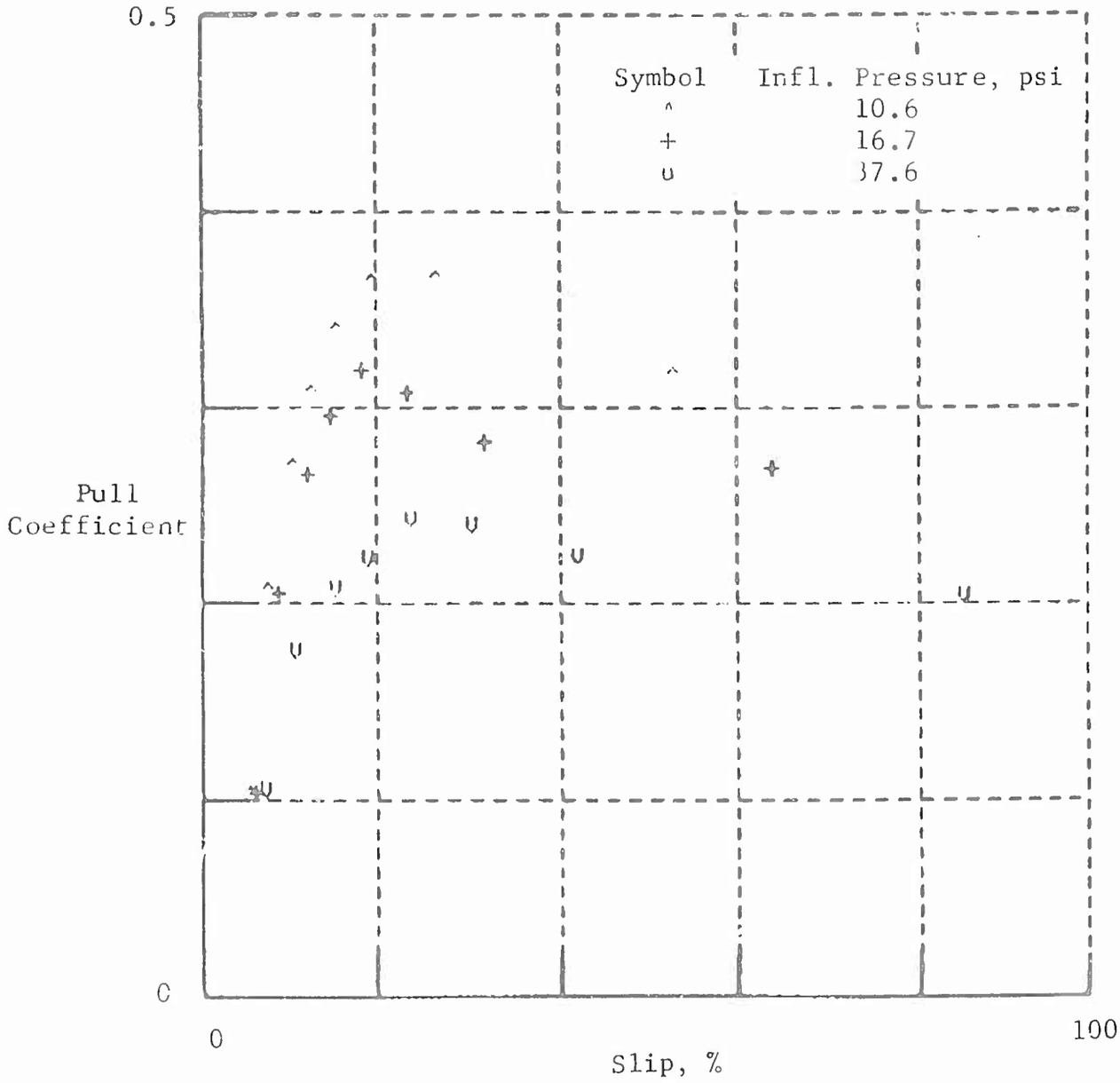

Fig. 73 Effect of Inflation Pressure on Pull Performance
Yuma Sand, CGR = 13.8
Tire: 9.00-14, Load: 830 lb

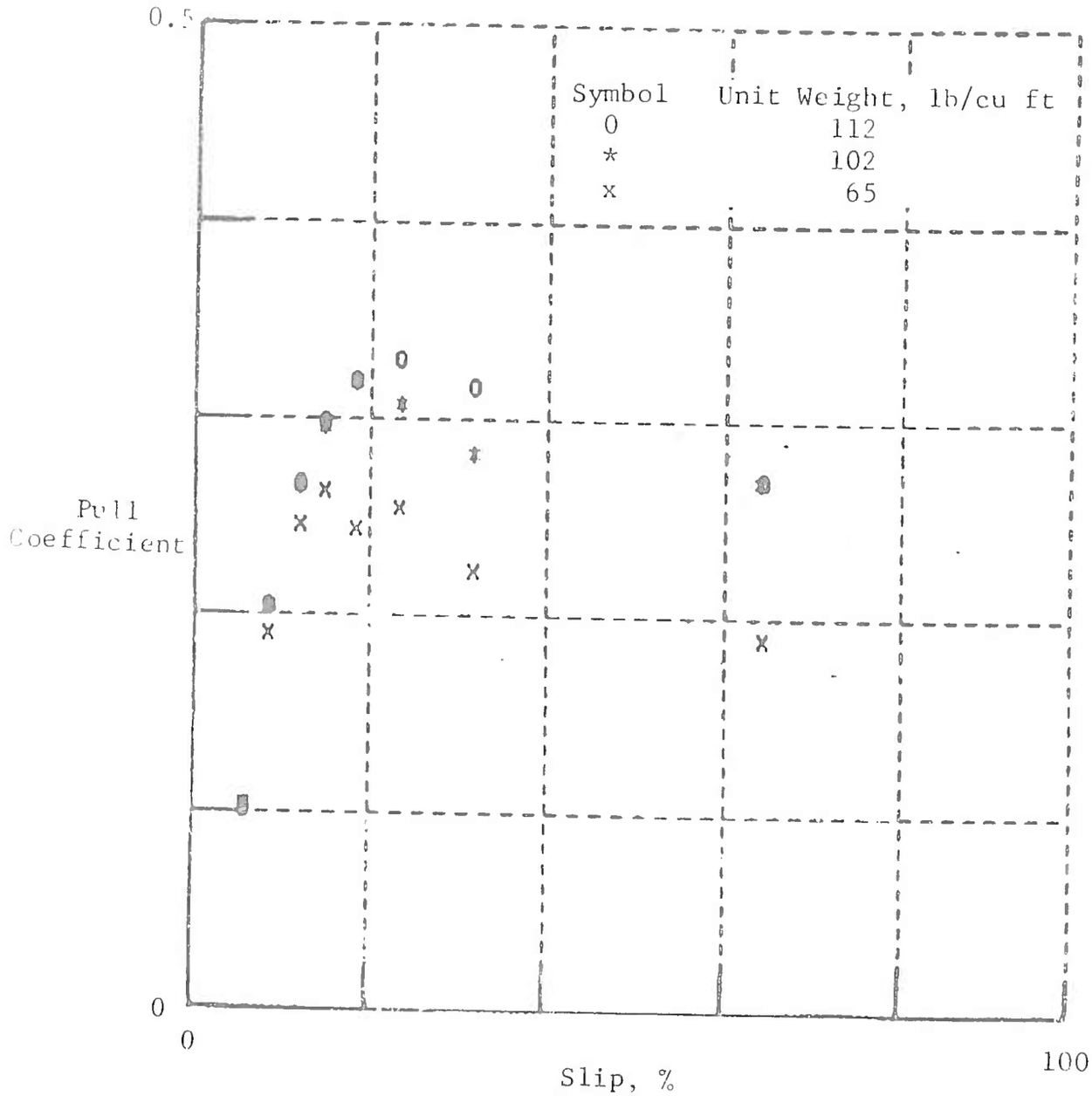

Fig. 74 Effect of Soil Unit Weight on Pull Performance
Yuma Sand, CGR = 13.8, Load: 830 lb
Tire: 9.00-14, Infl. Pressure: 16.4 psi

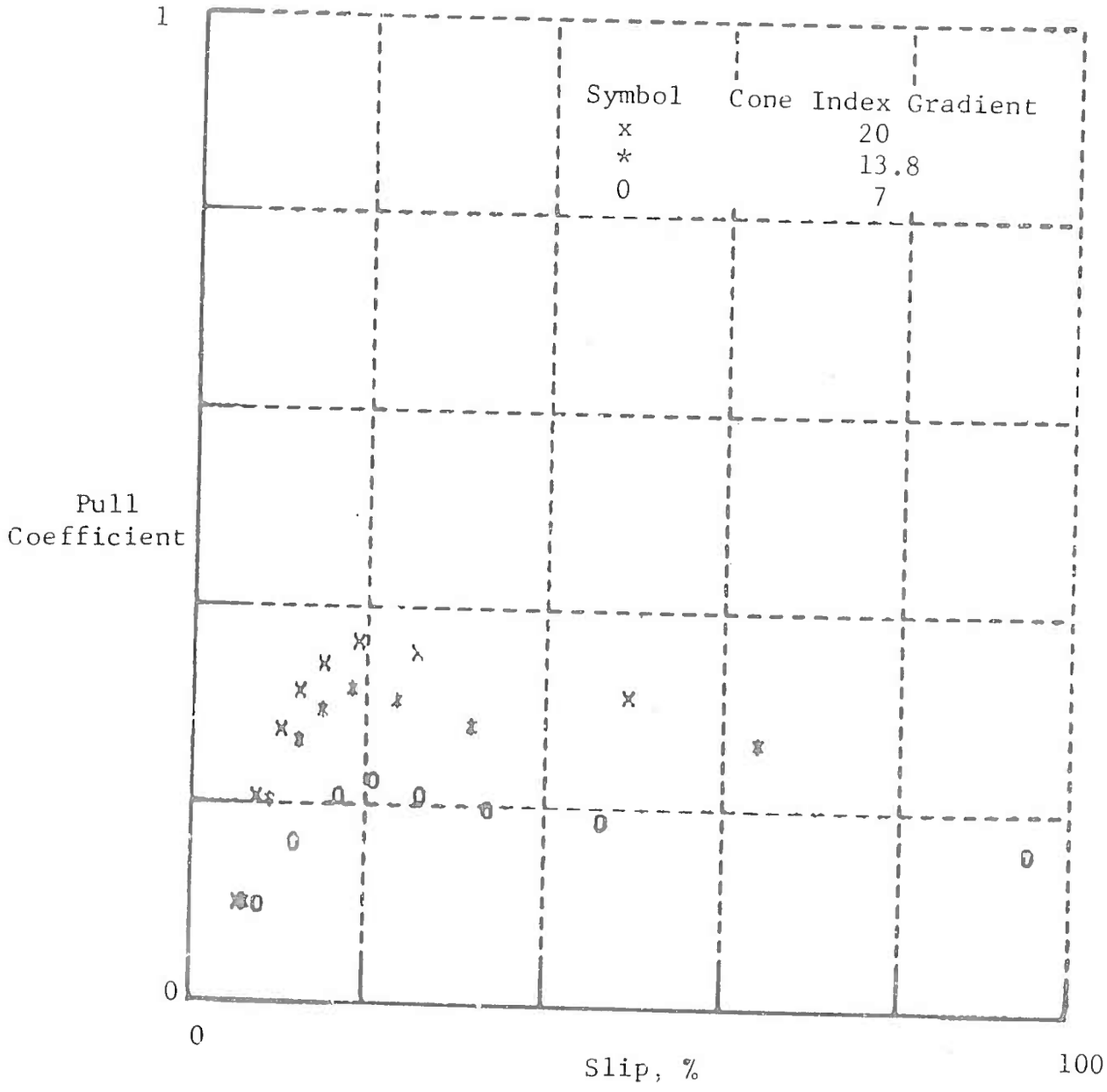

Fig. 75 Effect of Soil Strength on Pull Performance
Yuma Sand, Load: 830 lb
Tire: 9.00-14, Infl. Pressure: 16.4 psi

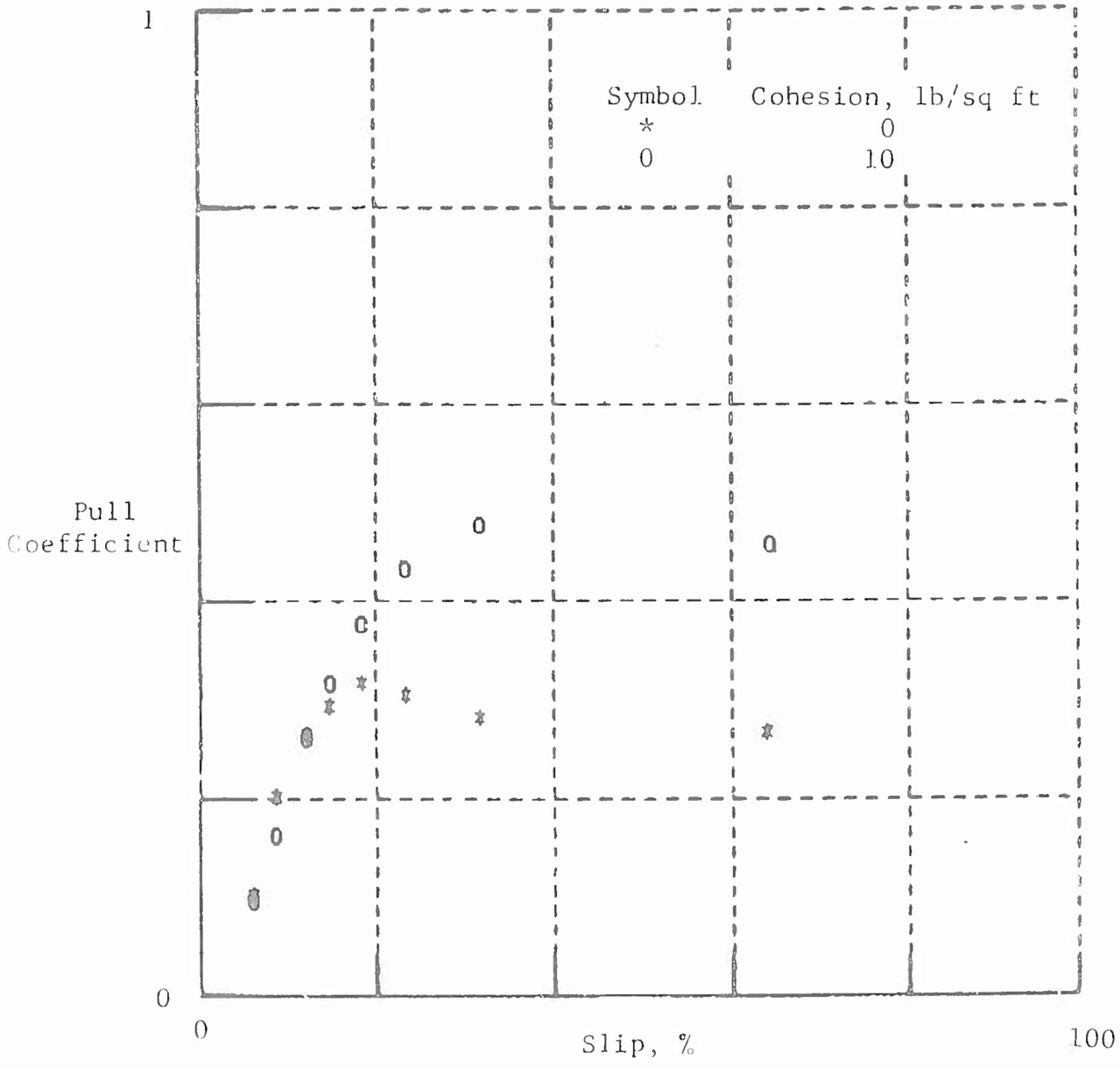

Fig. 76 Effect of a Small Cohesion on Pull Performance in Sand, Yuma Sand, Load: 830 lb
Tire: 9.00-14, Infl. Pressure: 16.4 psi

XIV. CONCLUSIONS AND RECOMMENDATIONS

A mathematical tire-soil model has been developed that reflects the role of tire deflection and soil strength in tire-soil interaction with sufficient fidelity so that prediction of tire performance by the mathematical model is within the range of the accuracy of experiments. On the basis of the mathematical model a computer program was prepared for the prediction and analysis of tire performance. The computer program requires a 9K core on a PDP 10 computer; average running time is 30-60 seconds. The computer program can also be accommodated to minicomputers; considerable savings in running cost can be thereby achieved.

Model input parameters are of three kinds: tire, soil, and slip parameters. For the determination of these parameters from conventionally obtained data theoretical studies and correlation analyses have been made with the following results:

- For the tire input parameter, p_1, a generally valid relationship with p_i, the inflation pressure, has been established. The input tire deflection parameter, ϵ, has been related to the deflection on rigid surface by various relationships, each valid for a particular tire type. For the establishment of a generally valid relationship, three dimensional effects would have to be considered in the model. It is recommended that the tire-soil model be expanded to account for this three dimensional effect. Such an expansion would also allow the meaningful analysis of performance of dual and multiple tire arrangements with respect to tire spacing.

- For the laboratory determination of soil input parameters a triaxial testing technique has been tentatively developed that varies the chamber pressure with strain and simulates thereby the strain and stress paths in the soil under tire loads better than conventional techniques. It is recommended that further research be conducted for the establishment of strain and stress path criteria in triaxial testing for mobility purposes and appropriate chamber pressure control devices be developed.

- For the determination of soil input parameters from cone penetration data, appropriate relationships have been developed and incorporated with the computer program. These relationships are valid for either frictional or cohesive soils. For frictional-cohesive soils it is recommended that evaluation methods for the determination of soil strength properties from field tests be developed, the suitability of the various techniques for soil strength determination be investigated, and appropriate modifications in these techniques undertaken.

- For the input slip parameters correlations with the sand or clay numeric have been established for the Yuma sand and Buckshot clay, respectively, the two soils for which tire performance data were available. It is recommended that a theoretical research on the interface shear stress development with slip be initiated, and methods for the determination of these two parameters in the laboratory and in the field be developed.

The analysis of tire performance tests in clay showed that surface conditions may affect the pull coefficient appreciably, not

only if the surface is wetter, but also when it is drier than the soil beneath the surface layer. Wet surface conditions have been of concern because of the resulting slipperiness. Dry surface conditions improve traction and, therefore, little attention has been paid to their effect. Nevertheless, evaporation from moist soils almost invariably results in a surface layer that is significantly drier than the soil at depth. In order to assess the effect of dry and wet surface conditions on mobility, it is recommended that the present tire-soil model be expanded to include layered soil conditions as well as soil conditions with a gradual increase of strength with depth. Such a model would allow the analysis of slipperiness as well as of dry surfaces and could be used to develop criteria for the evaluation of field tests.

The development and validation of tire-soil model presented in this report is based on experiments performed in either purely frictional or purely cohesive soils. Theoretically, the tire-soil model does not differentiate between purely frictional and purely cohesive soils since the soil is modeled therein by its strength properties that include both friction and cohesion. Nevertheless, it is desirable to compare performance predictions by the model with experiments and make modifications in the model, if necessary. It is recommended that tire performance tests in a variety of cohesive-frictional soils be conducted, the strength properties of these soils be determined and the data made available for analysis and further validation of the model.

XV. REFERENCES

1. "Deflection of Moving Tires - A Pilot Study on a 12 x 22.5 Tubeless Tire," U.S. Army Corps of Engineers, Waterways Experiment Station, Technical Report No. 3-516, Report No. 1, July 1959.

2. "Deflection of Moving Tires - Tests with a 12.00-22.5 Tubeless Tire on Asphaltic Concrete, Sand, and Silt, 1959-1960," U.S. Army Corps of Engineers, Waterways Experiment Station, Technical Report No. 3-516, Report No. 2, August 1961.

3. Smith, M. E. and Freitag, D. R., "Deflection of Moving Tires - Centerline Deflection Studies through July 1963," U.S. Army Corps of Engineers, Waterways Experiment Station, Technical Report No. 3-516, Report No. 3, May 1965.

4. Freitag, D. R., Green, A. J., and Murphy, N. R. Jr., "Normal Stresses at the Tire-Soil Interface in Yielding Soils," Highway Research Record No. 74, 1965.

5. Murphy, N. R. Jr. and Green, A. J. Jr., "Stresses Under Moving Vehicles - Distribution of Stresses beneath a Towed Pneumatic Tire in Air-Dry Sand," U.S. Army Corps of Engineers, Waterways Experiment Station, Technical Report No. 3-545, Report No. 5, July 1965.

6. Freitag, D. R. and Smith, M. E., "Centerline Deflection of Pneumatic Tires Moving in Dry Sand," Journal of Terramechanics, Vol. 3, No. 1, 1966.

7. Trabbie, G., Lask, K., and Buchele, W., "Measurement of Soil-Tire Interface Pressures," Agricultural Engineering, November 1959.

8. VandenBerg, G. and Gill, W., "Pressure Distribution between a Smooth Tire and Soil," Transactions of ASAE, Paper No. 59-108, 1962.

9. Krick, G., "Radial and Shear Stress Distribution under Rigid Wheels and Pneumatic Tires Operating on Yielding Soils with Consideration of Tire Deformation," Journal of Terramechanics, Vol. 6, No. 3, 1969.

10. Krick, G., Die Wechselbeziehungen Zwischen Starren Rad, Luftreifen und Nachgiebigem Boden, Dissertation, Technische Universitat Munchen, 1971.

11. Private communications from C. J. Nuttal, Jr.

12. Turnage, G. W., "Performance of Soils under Tire Loads," U.S. Army Corps of Engineers, Waterways Experiment Station, Technical Report No. 3-666, Report No. 8, September 1972.

13. Karafiath, L. L., Nowatzki, E. A., Ehrlich, I. R., and Capin, J., "An Application of Plasticity Theory to the Solution of the Rigid Wheel-Soil Interaction Problem," U.S. Army Tank-Automotive Command Technical Report No. 11758 (LL141), March 1973.

14. Bekker, M. G. and Janosi, Z., "Analysis of Towed Pneumatic Tires Moving on Soft Ground," U.S. Army Ordnance Tank-Automotive Command, Land Locomotion Laboratory Report No. RR-6, March 1960.

15. Kottler, F. C. Jr. and McGill, R., "Using Minicomputers to Reduce Problem Solving Costs," Instruments and Controls Systems, April 1973.

16. Janosi, Z. and Hanamoto, B., "The Analytical Determination of Drawbar Pull As a Function of Slip for Tracking Vehicles in Deformable Soils," Paper No. 44, Proceedings of the First International Conference on Terrain - Vehicle Systems, Edizion Minerva Technica, Torino, Italy, 1961.

17. Simon, M., "Les Compacteurs a Pneus en Construction Routiers," Annales de l'Institut Technique du Batiment et des Travaux Public, No. 193, January 1964.

18. Freitag, D., "A Dimensional Analysis of the Performance of Pneumatic Tires on Soft Soils," U.S. Army Corps of Engineers, Waterways Experiment Station, Technical Report No. 3-688, August 1965.

19. Wismer, R. D., "Performance of Soils Under Tire Loads - Tests in Clay through November 1962," U.S. Army Corps of Engineers, Waterways Experiment Station, Technical Report No. 3-666, Report 3, February 1966.

20. Taylor, J. H., "Lug Angle Effect on Traction Performance of Pneumatic Tractor Tires," Trans. ASAE, Vol. 16, No. 1, 1973.

APPENDIX A

DETERMINATION OF SOIL STRENGTH PARAMETERS FOR THE PURPOSE OF MOBILITY EVALUATION

Introduction

Soil strength has been recognized as the soil property that controls the behavior of soil-running gear systems in off-road locomotion. Consequently, in the tire-soil model presented in this report the soil is modeled by its strength properties. For both the use of the strength properties in the model and the characterization of soil for mobility purposes in general it is essential that the strength properties of soil and the conditions that apply to the laboratory and field determination of these strength properties for the purpose of mobility evaluation be defined.

Definition of Soil Strength

Soil strength is defined as the maximum shear stress that can be developed on a failure surface. If this shear strength is a linear function of the normal stress acting on the failure surface, then the following equation holds

$$s = c + \sigma_n \tan \varphi \qquad \text{(A-1)}$$

where c and φ are the Coulombian shear strength parameters.

The linear dependence of the shear strength on the normal stress is an approximation. In some cases it may be necessary to consider nonlinear strength relationships; the use of nonlinear relationship in wheel-soil interaction problems is discussed in Ref. A.1. For the purpose of the following discussions

it is assumed that, within the range of normal stresses of interest, the soil strength can be satisfactorily approximated by the linear relationship represented by Eq. (A-1).

The Coulombian soil strength parameters are not material characteristics inasmuch as their value depends on the time rate of loading and the drainage of the soil during loading. Also, the Coulomb parameters refer to normal and shear stresses that act in a plane perpendicular to the failure surface and are, therefore, essentially two dimensional in nature. The stress and strain conditions that obtain perpendicular to that plane may affect the value of the Coulomb parameters. In experiments for the determination of the Coulomb strength parameters for mobility purposes, the transverse stress and strain conditions should duplicate those that exist in the field in the tire-soil interaction.

The following discussion is intended to define the various conditions in tire-soil interaction that have a bearing on the Coulomb strength parameters:

- Drainage conditions in the soil are generally very close to the hypothetical undrained condition during the passage of a tire. Exceptionally, the degree of drainage during the application of wheel load to the soil may be important in the case of submerged, relatively well draining soils, such as fine sand. For the purpose of general mobility evaluation, undrained conditions may be assumed and the above submerged condition treated as an exception.

- The loading rate of soil in tire-soil interaction is directly proportional to the translational velocity of the tire. Very roughly, the soil loading rate may be estimated by assuming that the stresses on a soil element

rise from their initial state to peak during a time interval it takes the tire to pass half of the length of the contact area. For example, a tire traveling at the low speed of 3 ft/sec and having a 1 ft long contact area would impart full loading to the soil in 1/6th of a second. Loading rates encountered in mobility problems generally fall in the category of quick or rapid loading. While the strength of quickly loaded soils may be considerably different from that obtained with slow loading rates, it is generally not too sensitive to changes in the loading rate within the range of translational velocities of interest. Thus, in strength testing, loading rates that are approximately in the range of the rate anticipated in the field are acceptable.

- Strain conditions in tire-soil interaction are generally three dimensional since the compaction of the soil beneath the tire is generally accompanied by lateral displacement. Thus, even though a two dimensional model is used for the computation of stresses, the strength parameters of the soil in that model should be determined by testing methods that allow for strains in the third dimension.

The development of soil strength is always accompanied by volumetric strain. If the displacement constraints in a particular problem involving failure of the soil are such that the volumetric strain associated with the soil strength cannot be attained, the soil strength cannot be developed and the use of a so-called partially mobilized soil strength is in order. In soil mechanics this case is known as local shear failure, as contrasted with the

case of general shear failure when the shear strength is fully mobilized. The situation in tire-soil interaction problems is different from that encountered in conventional bearing capacity problems in that with the advancement of the tire the soil is progressively compacted and the volumetric strain associated with the passage of the tire is, in the case of interest, generally sufficient to mobilize the full strength of soil. Further discussion of strain conditions is presented in connection with the use of triaxial tests for the determination of soil strength properties.

Laboratory Determination of Soil Strength for Mobility Evaluation

Two types of testing technique are used widely in soil mechanics practice for the determination of soil strength: the direct shear type and triaxial type tests. The direct shear tests represent plain strain conditions, whereas in the triaxial test the intermediate principal stress equals the minor principal stress. Strain conditions in the triaxial test correspond to the stress conditions $\sigma_2 = \sigma_3$. This latter strain condition approximates the ones in the field more closely than the plain strain and, therefore, the determination of soil strength properties by triaxial tests is more appropriate for mobility evaluation than direct shear tests. The good agreement between measured interface stresses and those computed on the basis of triaxial shear strength, reported in Ref. 13, and the good simulation of tire performance by the tire-soil model using strength data obtained from triaxial tests give strong support to the preference of triaxial tests for strength determination.

The samples used in triaxial tests are either undisturbed ones obtained in the field or ones prepared in a laboratory mold. In

principle, undisturbed samples should be used since the in situ strength of soil may reflect the grain structure of the soil that cannot be duplicated in laboratory preparation. This is particularly true for residual soils. However, undisturbed sampling of surface soils is difficult and undesirable where field variation in soil properties requires that a large number of samples be taken. Obviously, field testing techniques that test the in situ strength of soil are better suited for the purpose of mobility evaluation. On the other hand, the preparation of soil beds for tire performance tests can be closely duplicated in the preparation of soil samples for triaxial testing. Thus the role of triaxial testing in mobility evaluation is the determination of strength properties for model validation. Triaxial tests are also necessary for the validation of field testing techniques.

In the conventional triaxial testing the chamber pressure (minor principal stress) is kept constant and the vertical load is increased until failure occurs or (in the absence of a clearly defined failure point) a certain strain is reached. In tire-soil interaction the minor principal stress monotonically increases up to its maximum value, then decreases monotonically throughout the passage of the wheel — as can be seen in Fig. A-1, which shows the magnitude and direction of principal stresses in the failure zones beneath a rigid wheel. The stress paths corresponding to those principal stresses in the loading and unloading phase during the passage of the wheel can be constructed in the principal stress space (assuming $\sigma_2 = \sigma_3$) as shown in Figs. A-2a and A-2b for a rigid wheel and in Figs. A-2c and A-2d for a pneumatic tire. Indicated by light lines in these figures are the equivolume contour lines that can also be obtained in triaxial tests. The volumetric strains associated with the stress path of loading increase together

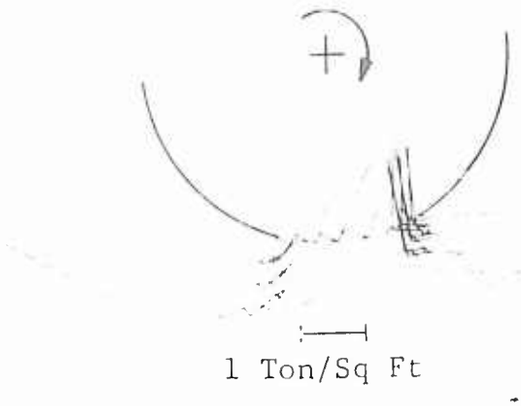

Fig. A-1 Principal Stresses in Soil Beneath a Rigid Wheel

with the increase of minor principal stress. Thus the stress and strain conditions that duplicate those in the field in the triaxial test are such that the minor principal stress (chamber pressure) would have to increase with increasing volumetric strain. Since conventional triaxial testing techniques do not allow a a variation of the chamber pressure during loading, appropriate modifications were made to the triaxial apparatus available at Grumman. Description of the testing apparatus and results obtained with the modified technique are given below.

Triaxial Testing for Mobility Evaluation Purposes

In order to apply loading rates comparable to that in tire-soil interaction, the triaxial chamber was mounted on an Instron TM4 loading frame that allowed a strain controlled application of the vertical load at rates varying from 0.05 to 5 cm/min. Even

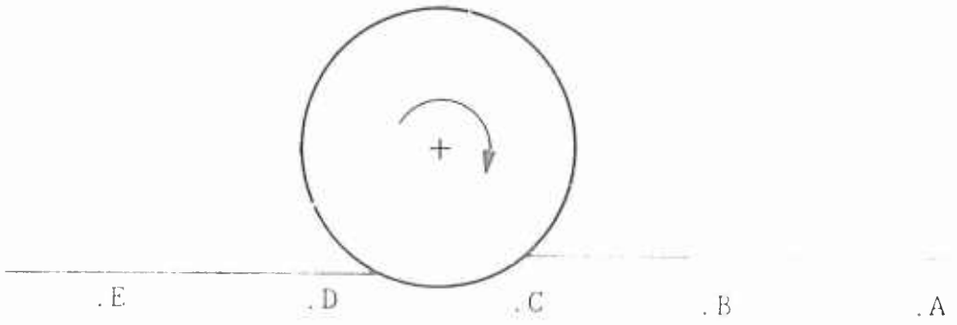

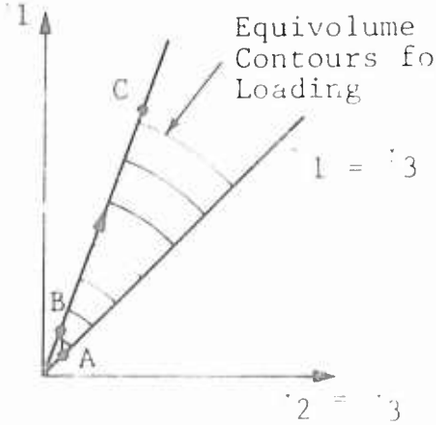

a) Stress Path for Loading Beneath a Rigid Wheel

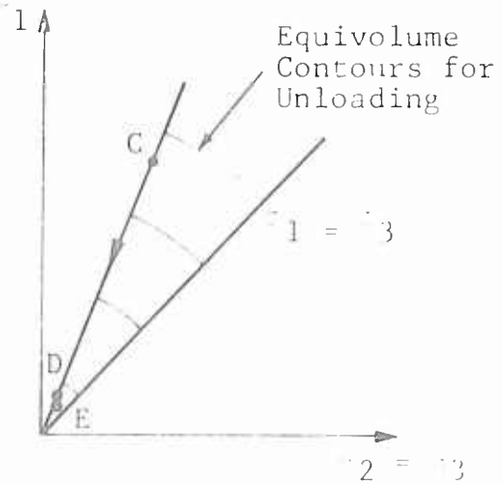

b) Stress Path for Unloading Beneath a Rigid Wheel

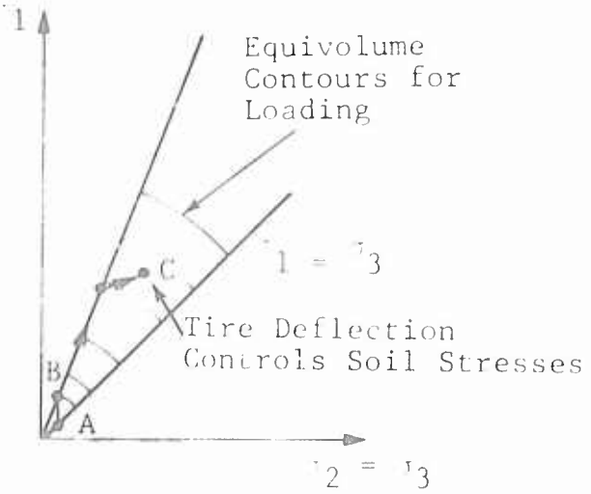

c) Stress Path for Loading Beneath a Tire

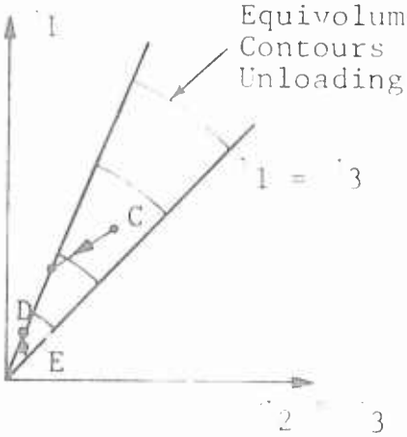

d) Stress Path for Unloading Beneath a Tire

Fig. A-2 Stress and Strain Paths in Soil Under Rigid Wheel and Tire Loading

the highest rate of loading that the loading frame allowed was less than that corresponding to a 3 ft/sec travel velocity; the resources of this program, unfortunately, did not allow for a major modification of the loading frame. Since, in mobility problems, soils are generally less than 100 percent saturated, compression of the sample occurs during loading, and the deformed cross section of the sample cannot be determined without measuring the lateral deformation of the sample. Initially, one circumferential gauge with a centimeter scale, placed at mid-height of the sample, was applied; it was found, however, that at high loading rates the sample deformation was asymmetrical about the mid-height, and it was necessary to apply three circumferential gauges. Since it was not possible to read these gauges even at moderate loading rates, a closed circuit television camera with a video tape recorder was used to record the position of the gauges during the test; readings were made by replaying the video tape and stopping it at appropriate intervals to record the readings. A picture of the setup is shown in Fig. A-3.

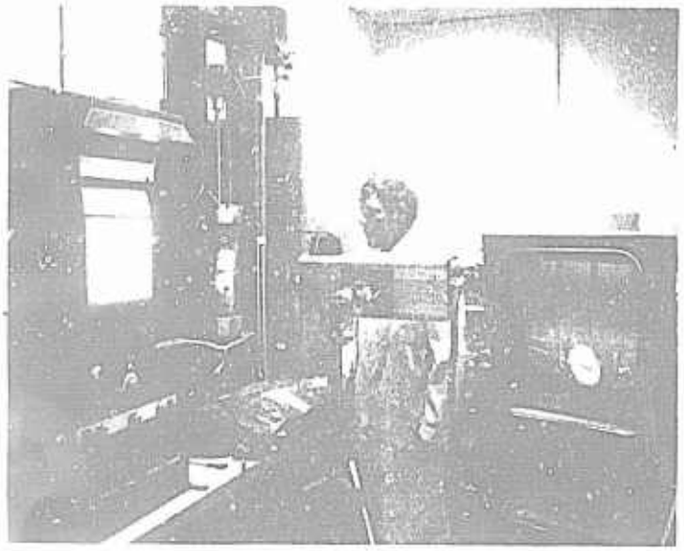

Fig. A-3 Variable Chamber Pressure Triaxial Testing with Video Tape Recording of the Circumferertial Gauges

Triaxial tests with the above technique were performed on samples of Buckshot clay received from WES. Figures A-4 and A-5 show the Mohr circles obtained by this method for tests on 2.9 x 7 in samples of Buckshot clay prepared at 34 percent moisture content and tested at a loading rate of 5 and 0.5 cm/min, respectively. The Mohr circles indicate almost identical strength properties for these two loading rates; differences between the two tests are within the range of accuracy of this type of test. Thus at the loading rates applied in the tests strength properties of the Buckshot clay are not significantly affected by the magnitude of the loading rate.

Unfortunately, even at the highest loading rate that can be employed with the loading frame, about 20 seconds elapse before the maximum load or about 10 percent vertical strain is reached. Investigations performed with a dynamic loading machine (Ref. A.2) showed that at higher loading rates the effect of loading rate becomes more pronounced and a gain in strength with the increase of loading rate can be conclusively observed.

Mohr circles for another typical test on Buckshot clay are shown in Fig. A-6. The moisture content and the loading rate of the sample in this test was the same as in test B1, but the maximum lateral pressure of about 0.5 kg/sq cm was reached at 5 percent strain instead of at 10 percent, as in test B1. The cohesion intercept in the two tests are about the same, but the friction angle is higher in test B7 then in B1.

The measurement of the lateral deformation by the circumferential gauges allows the evaluation of the void ratio during the test. Figure A-7 shows the changes in void ratio as a function of lateral

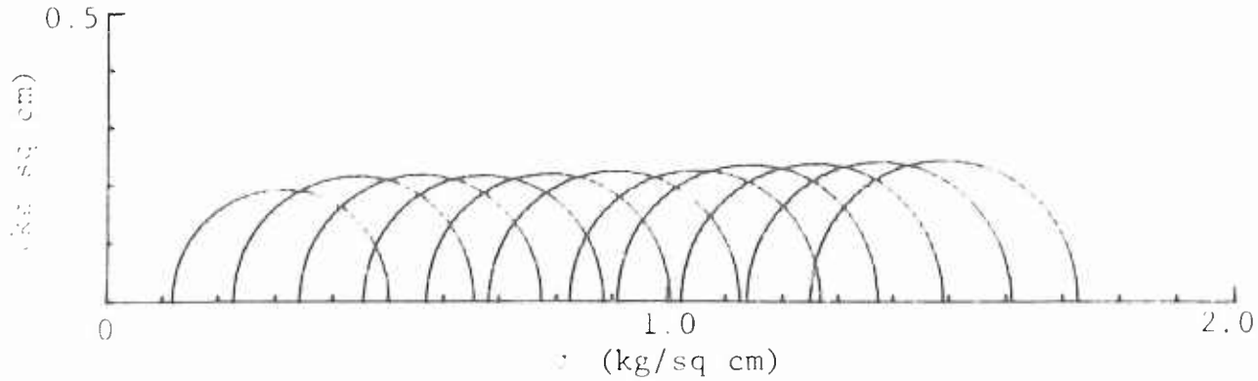

Fig. A-4 Mohr Circles for Variable Chamber Pressure Triaxial Test B-1 - Buckshot Clay. Moisture Content = 34%, Loading Rate: 5 cm/min

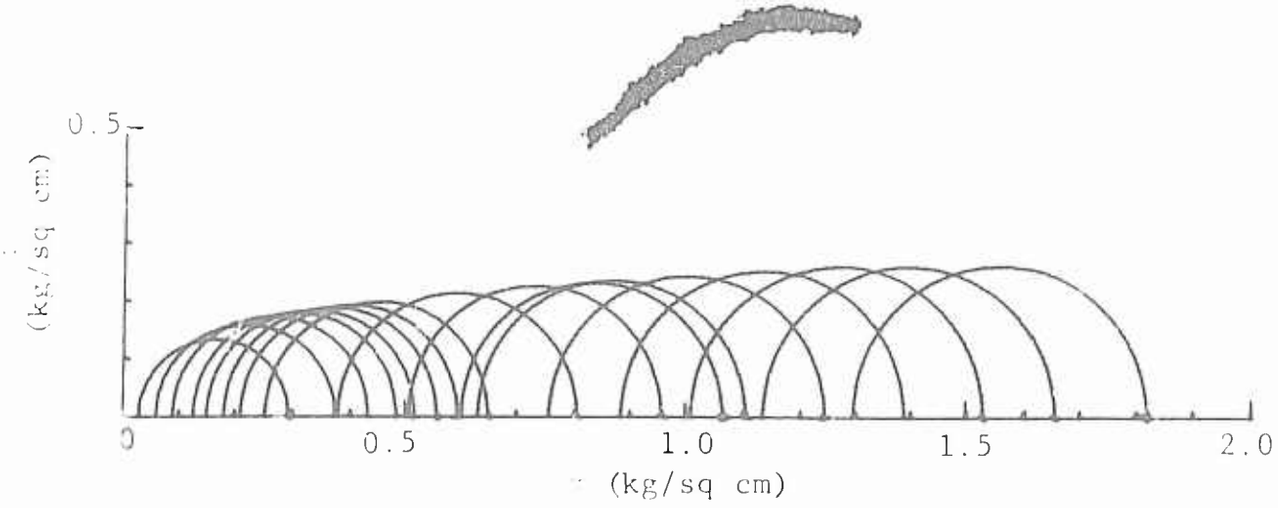

Fig. A-5 Mohr Circles for Variable Chamber Pressure Triaxial Test B-4 - Buckshot Clay. Moisture Content = 34%, Loading Rate: 0.5 cm/min

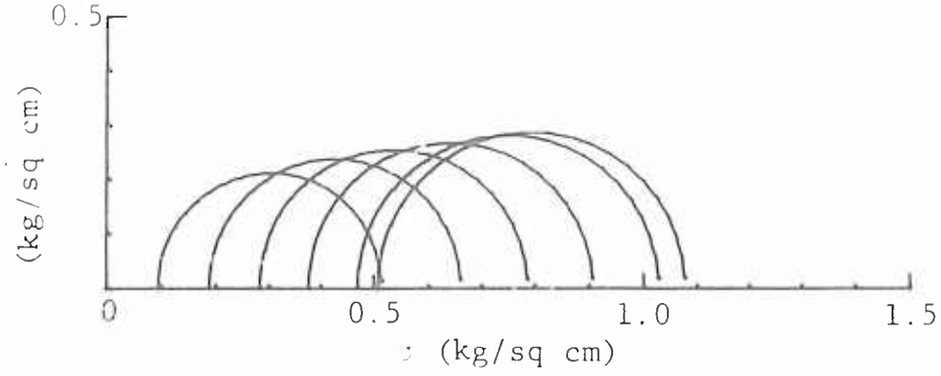

Fig. A-6 Mohr Circles for Variable Chamber Pressure Triaxial Test BS-7 - Buckshot Clay. Moisture Content = 34%, Loading Rate = 0.5 cm/min

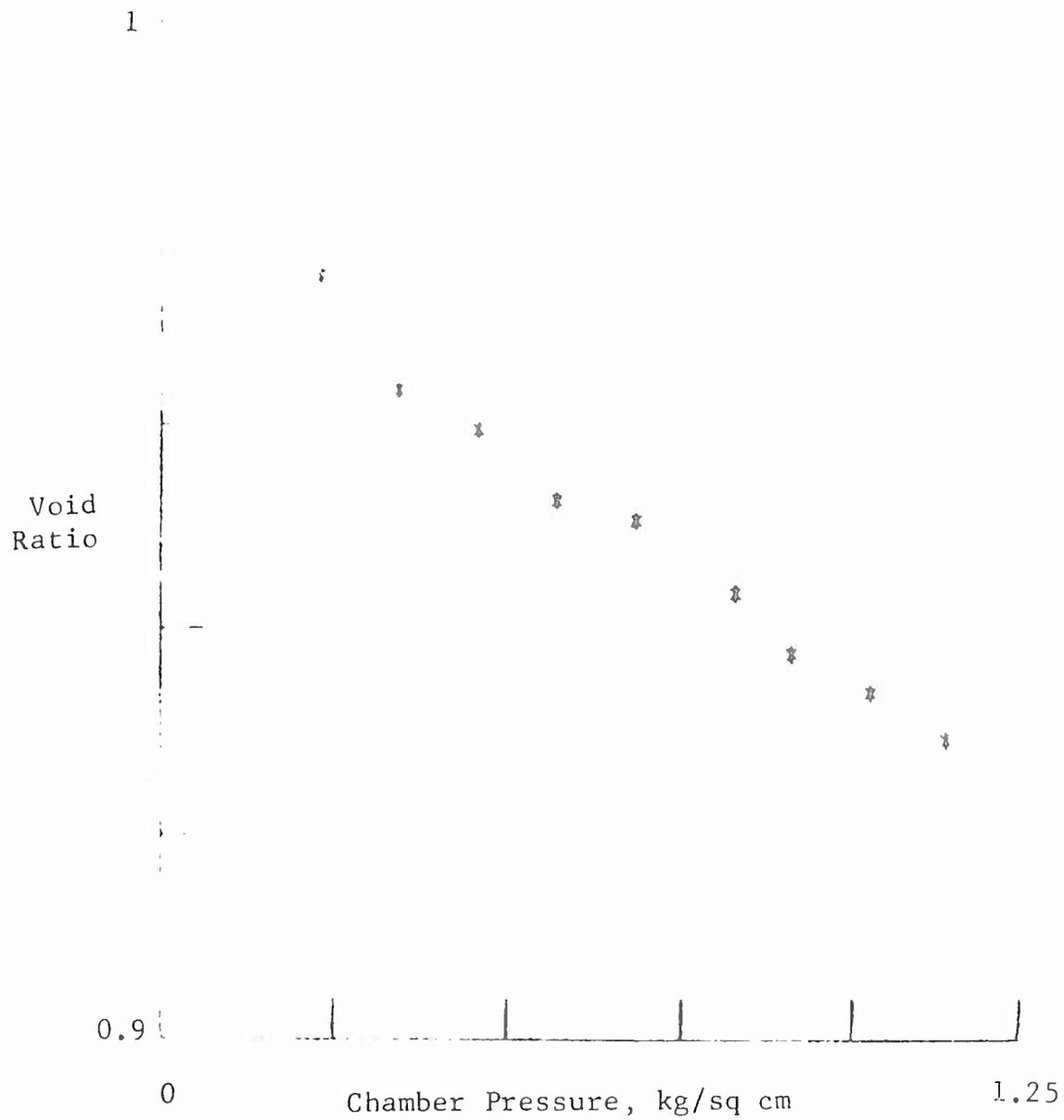

Fig. A-7 Void Ratio Changes in Test B1

pressure in test B1. A relationship between void ratio and stress states in the slip line field may be established by these measurements, and total volume change associated with the development of the slip line field may be computed.

Triaxial tests with the above technique were also performed on materials received from the National Tillage Machinery Laboratory. Figure A-8 shows the Mohr circles for the Decatur silty loam. Moisture contact of the sample was 8.7 percent and bulk density 1.2 g/cu cm, which approximately corresponded to that of the upper 2.5 in. in the tire performance test. From this test the Coulomb parameters are $c = 130$ lb/sq ft and $\varphi = 21°$. Figure A-9 shows the Mohr circles for the Vaiden clay. Moisture contact of the sample was 25 percent and the bulk density 1.08 g/cu cm, approximately corresponding to that of the upper 2.5 in. in the tire performance tests. The Coulomb parameters for this condition were found to be $c = 300$ lb/sq ft, $\varphi = 12°$.

In the above tests an attempt was made to duplicate loading rates, stress paths, and strain conditions as they occur in the field. Since the resources of this program did not allow for major modifications of the equipment, loading rates and variation of chamber pressure had to be compromised. It is believed, nevertheless, that even with the restrictions imposed by the capabilities of the apparatus, the test results are acceptable for most practical purposes. An advantage of the proposed testing technique is that a friction angle is obtained in a single test, whereas several tests are required for the determination of friction angle with the conventional method.

For further development of the testing technique additional information on stress-strain conditions in tire-soil interaction

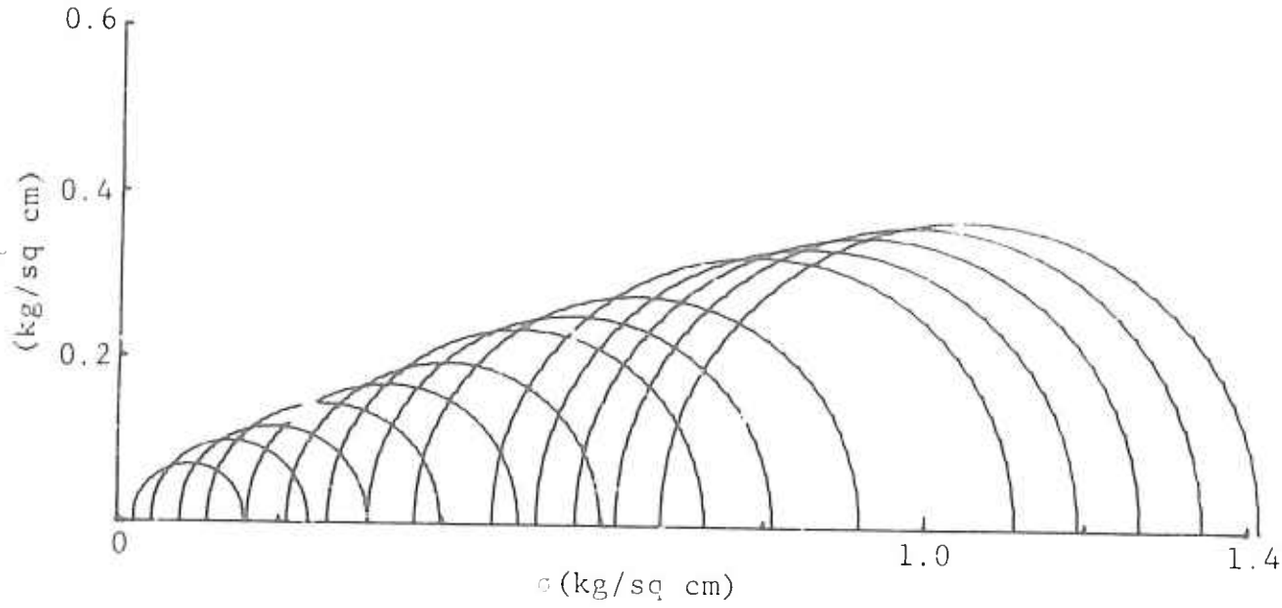

Fig. A-8 Mohr Circles for Variable Chamber Pressure Triaxial Test D1 - Decatur Silty Loam. Moisture Content = 8.7%, Bulk Density: 1.29 cu cm

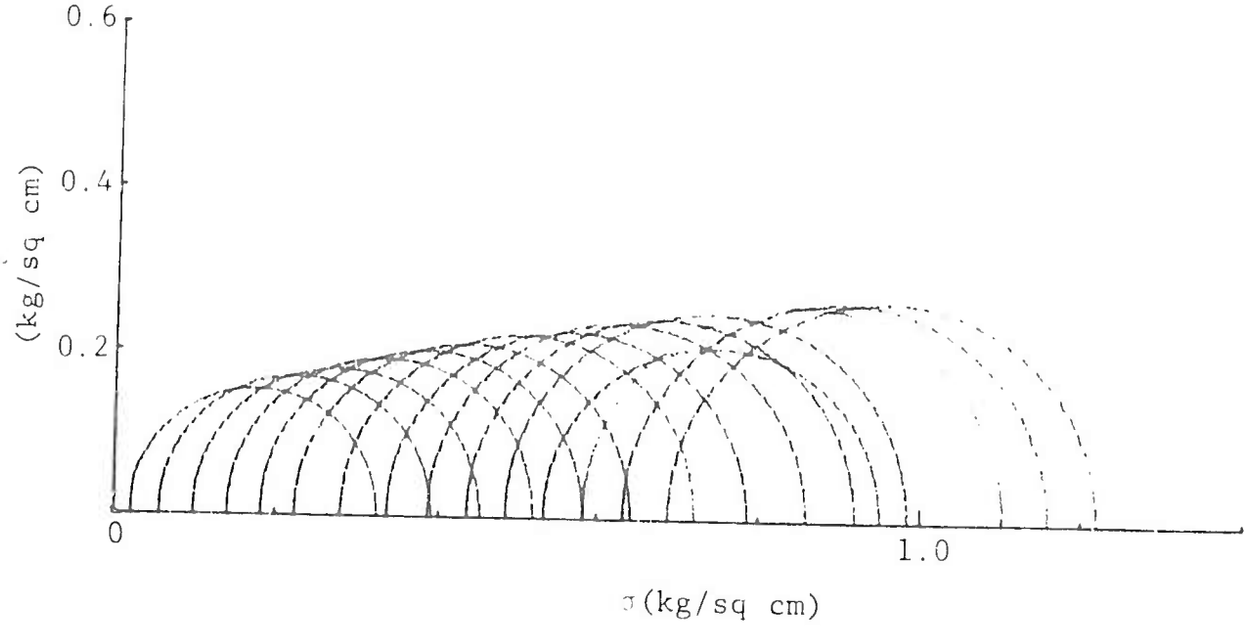

Fig. A-9 Mohr Circles for Variable Chamber Pressure Triaxial Test V1 - Vaiden Clay. Moisture Content = 25%, Bulk Density: 1.089 cu cm

is required. Such information will be forthcoming in connection with the research project aimed at the determination of the effect of speed on tire performance where velocity fields associated with the slip line fields will be determined and strain fields from the velocity field may be derived.

Concerning the testing facility, a loading frame that allows for faster loading rates is necessary. Chamber pressure regulation that would allow for any desired variation of the chamber pressure with vertical strain preferably by computerized control is another necessity for the development of a triaxial testing technique geared toward the needs of mobility evaluation.

Determination of Soil Strength Properties by Field Tests

Many types of field tests have been designed, and several of them are regularly used in off-road mobility research and engineering for the characterization of soil properties. Some of these are intended to measure the strength properties of soils; others are used to obtain some measure of soil strength that is then related to running gear performance. Every field instrument that is forced into the ground and records a displacement-force relationship yields some information on soil properties; if the instrument displaces the soil in such a way that failure zones develop, then, at least theoretically, it is possible to evaluate the soil strength parameters from the results of the field test. In the following the suitability of present field techniques for the determination of soil-strength properties is discussed, and methods for the evaluation of these field tests are proposed.

The Role of Volumetric Strain in Field Tests

As mentioned before, the prerequisite for the use of soil shear strength in the determination of stress states in soil by plasticity theory is that volume changes associated with the shear strength may take place in the loading process. In tire-soil interaction problems of interest this requirement is generally satisfied since the volume of soil displaced by the tire is large compared to the volume of soil affected, as shown in Fig. A-10a. In contrast, in a cone penetrometer test the soil volume displaced by the cone is small compared to that volume of soil affected by the failure mechanism, as shown quantitatively in Fig. A-10b. It should be noted that the areas shown in Fig. A-10b are cross sections of bodies of revolution; to obtain volumetric proportions the areas have to be multiplied by the respective distances of their center of gravity from the axis.

Figure A-10c shows quantitatively the soil volume affected by a plate sinkage test. The proportion of the volume of soil displaced by the plate to that affected by the failure mechanism is greater than in the case of cone penetration and, in most cases, is sufficient to balance the volume changes associated with the development of failure mechanism. In the case of ring shear tests, the volume change requirements associated with the failure mechanism assumed in conventional evaluation procedures are satisfied, but in many cases that failure mechanism is not valid. A more detailed discussion of the failure mechanism of ring shear tests is given later in this appendix.

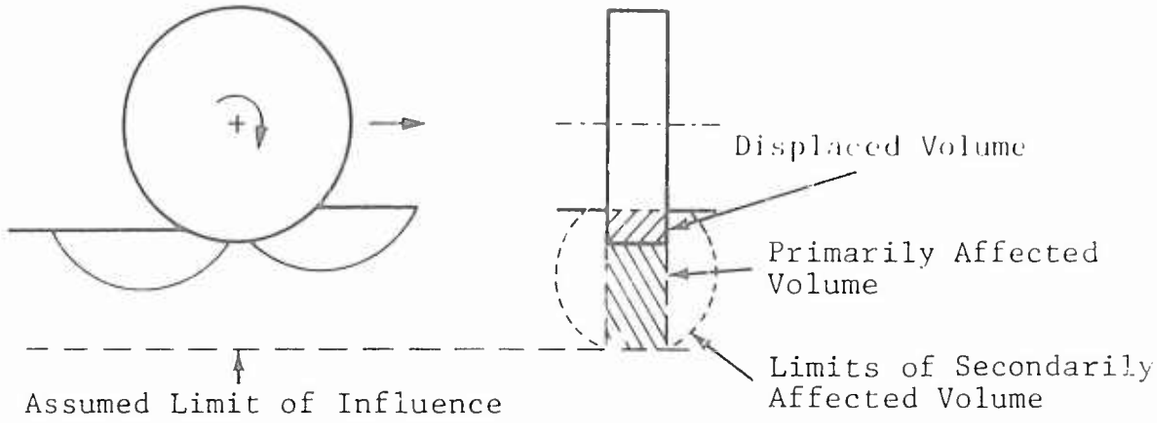

a) Wheel-Soil Interaction

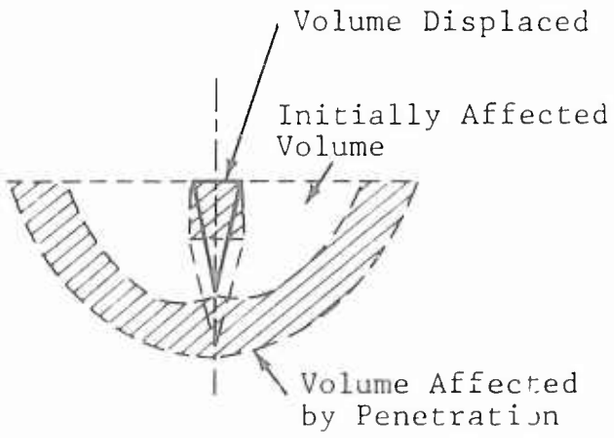

b) Field Determination of Soil Strength By Cone Penetrometer

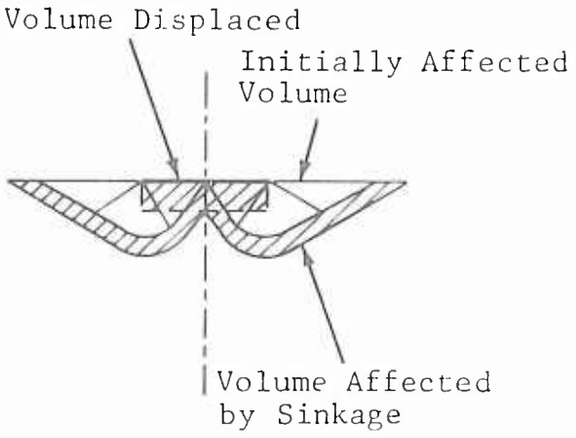

c) Field Determination of Soil Strength By Plate Sinkage Tests

Fig. A-10 Comparison of Soil Volumes Displaced and Affected by Failure Mechanisms in a, b, and c

Determination of Soil Shear Strength Parameters from Cone Penetration Tests

In the tire performance tests performed at WES, cone penetration tests were used for the characterization of soil properties. To simulate the tire performance tests by the proposed tire-soil model it was necessary to establish the Coulomb soil strength parameters on the basis of cone penetration test data. To this end the results of theoretical analyses as well as triaxial tests were used.

For the theoretical analysis of cone penetration tests a computer program was available at Grumman that computes the slip line field and associated stresses as well as the volume changes in the slip line field for various cone angles assuming shear zones up to the level of the base of the cone and a surcharge above this level for the consideration of depth effect. The theoretical basis of this program and other details are described in Ref. A.3. A slip line field generated by this program assuming strength properties of the Buckshot clay is shown in Fig. A-11. Volume change computations using void ratio [minor principal stress relationships determined by triaxial tests (Fig. A-7) performed for the case when the base of the cone is level with the surface] showed that the volume displaced by the cone was generally sufficient to produce the volume changes necessary for the full mobilization of soil shear strength. Thus for the soil conditions in the WES tire performance tests the cone penetration tests may be regarded as a measure of soil strergth. It should be noted, however, that in the WES tests the lowest relative density of the Yuma sand was about 50 percent and the degree of saturation of the Buckshot clay about 95 percent. At that relative density of sand and degree of saturation of clay both soils exhibit relatively small volume changes, and the finding that for

the soil conditions used in these tests cone penetration resistance is representative of soil strength does not necessarily mean that this would be the case for soils exhibiting larger volume changes.

The strength properties of the Yuma sand were established on the basis of relative density. An experimental relationship between the relative density of Yuma sand and cone index gradient was developed at WES (Fig. A-12). Triaxial tests performed at WES on Yuma sand were also related to its relative density (Ref. A.4). On the basis of these data the following linear relationship between cot ϕ and relative density was established

$$\cot \phi = 1.64 - 0.68 \times D_r \quad . \tag{A-2}$$

This relationship is valid for $D_r > 50$ percent. Figure A-13 shows Eq. (A-2) and the values of ϕ determined by various triaxial tests. The friction angles represented by Eq. (A-2) were close to those obtained in variable chamber pressure tests and by theoretical analysis of the cone penetration test (Ref. A.3).

For the Buckshot clay, empirical relationships between the average cone index and strength parameters have been developed at WES (Ref. A.5). These relationships have been compared with results of variable chamber pressure triaxial tests and theoretical analyses. These comparisons showed good agreement with the value of cohesion intercept established by WES but indicated a somewhat higher friction angle. Accordingly, the following relationship was used in tire performance simulation:

$$\begin{aligned} c(\text{psi}) &= CI/12.5 \\ \phi(\text{degrees}) &= CI/4 \quad . \end{aligned} \tag{A-3}$$

Regarding the evaluation of soil strength from cone penetration test data the following comments are pertinent.

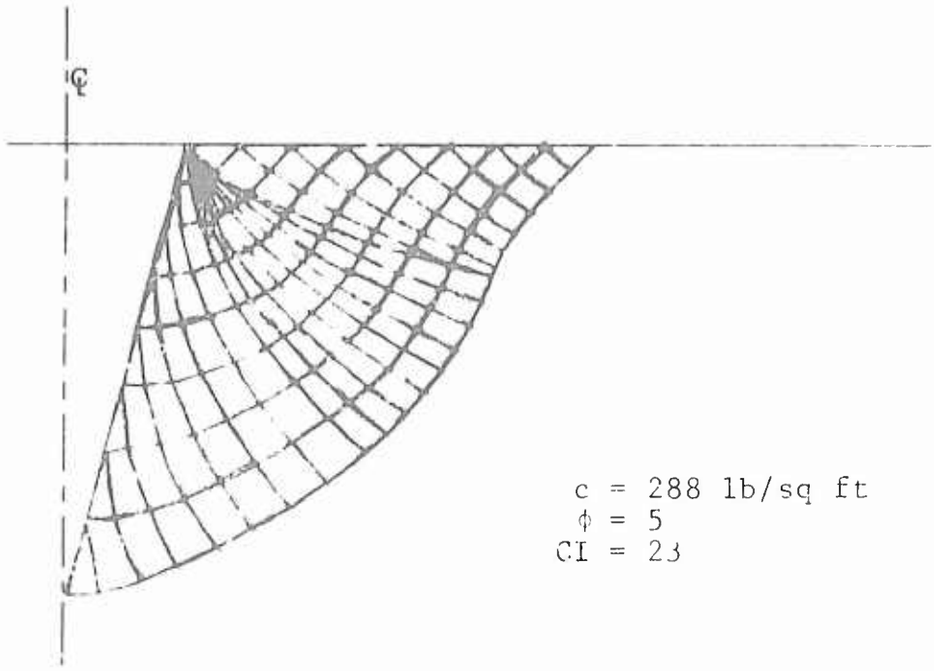

Fig. A-11 Slip Line Field for Cone Penetration

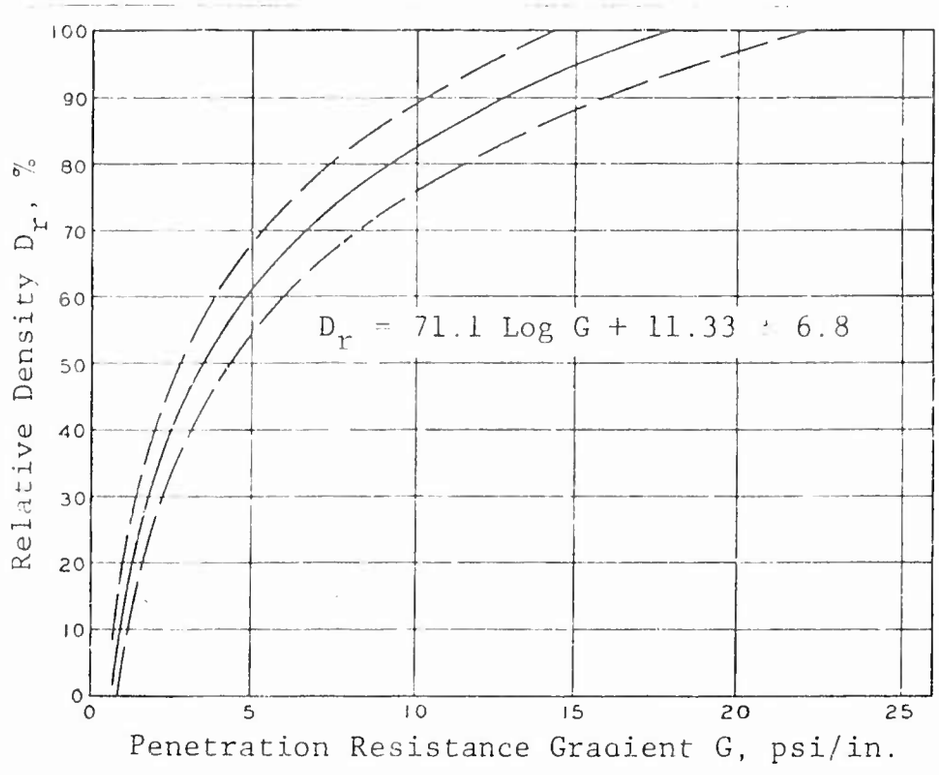

Fig. A-12 Relationship between Relative Density of Yuma Sand and Cone Penetration Resistance (from Ref. 12)

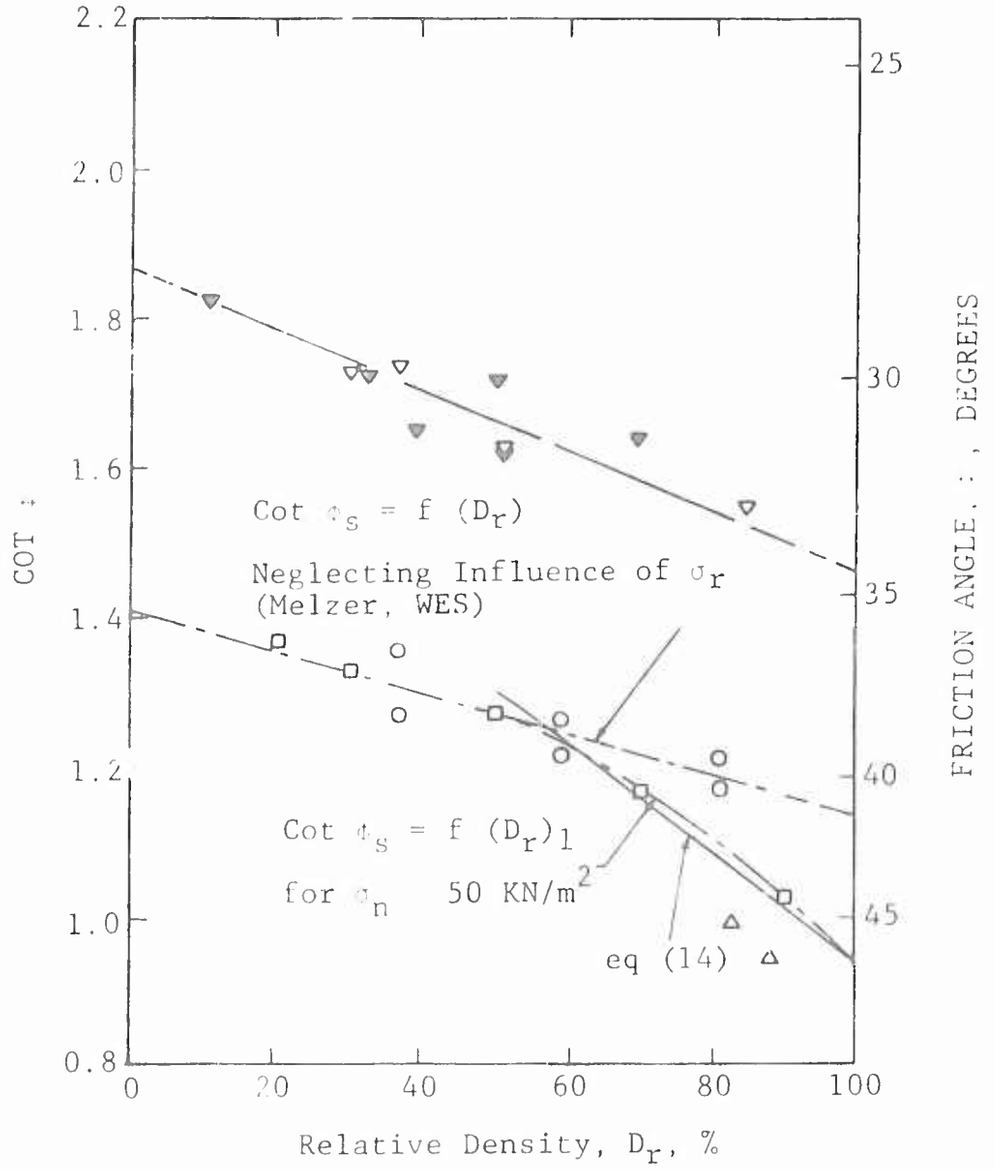

Fig. A-13 Relation between Relative Density and Friction Angle of Yuma Sand (From Ref A-4)

The relationship established between friction angle and cone index gradient for Yuma sand is only approximately valid for other cohesionless materials. Theoretical analyses reported in Ref. A.3 show that in cohesionless materials the cone penetration resistance depends not only on the friction angle but also on the unit weight of material and the interface friction that develops on the surface of the cone. For a particular material, as the Yuma sand, there is a relationship between friction angle and unit weight (expressed by relative density) and, therefore, the cone index gradient is a measure of strength. For another cohesionless material this relationship may be different and the cone index gradient exhibits a different relationship with the friction angle of that material. This theoretical conclusion is supported by tire performance tests performed in mortar sand (Ref. 12) that showed a pull-coefficient relationship different from that for the Yuma sand, although the mortar sand is in many respects very similar to the Yuma sand. For an angular sand, or a sand composed of grains that have a much different specific gravity, the difference would be even greater. In addition, in very loose sands the cone penetration cannot mobilize the full frictional strength and, therefore, it is not a unique measure of strength in loose materials.

The relationship established between Coulomb strength parameters and cone index for the Buckshot clay is probably an acceptable approximation for other clays that are saturated close to 100 percent, but may not be valid even for the Buckshot clay at a different degree of saturation. Theoretical analyses show that the unit weight has but little influence on the cone penetration resistance in cohesive soils whose friction angle is very low. Also, there is little uncertainty about the interface adhesion and friction

that in cohesive soils appears to be fully mobilized in cone penetration tests. Thus the cone index is a fair measure of soil strength in cohesive soils with a high degree of saturation.

Partially saturated cohesive or cohesive-frictional soils may exhibit a high degree of compressibility. In such soils cone penetration cannot mobilize the full soil strength and, therefore, is not a good measure of it. A relatively large proportion of the cone resistance is due to the adhesion on the surface of the cone and the effect of friction angle becomes suppressed. Thus cone penetration tests are not best suited for the determination of the strength properties of such soils.

Even though the above problems raise serious questions about the suitability of cone penetration tests for the determination of the strength properties of frictional cohesive soils, the convenience of field testing by penetrometers makes their use for that purpose very desirable. It is evident that for the determination of the two strength parameters, φ and c, at least two parameters of the field test are needed even if the unit weight is estimated or obtained by other means. The penetration resistance at the surface (CI at $z = 0$) and the rate of increase of this resistance (gradient) would yield two parameters, but the insensitivity of the 30° apex angle cone to the friction angle and the insufficient displacement to mobilize the shear strength in loose soils render these two parameters unsuitable for strength evaluation. Theoretical considerations indicate that the same problems probably would not arise (or would occur only in a much lesser degree) with 90 or 120° apex angle cones. These could be used either in conjunction with the present 30° cone or separately. A theoretical analysis should be made to establish criteria for the penetration resistance measurements and evaluation methods for such cones.

Determination of Soil Shear Strength Parameters from Plate Sinkage Tests

The volume of soil displaced by the plate in plate sinkage tests is generally sufficient to mobilize the full shear strength of soil in the failure zones. Thus, in principle, a plate sinkage tests is better suited for the evaluation of soil strength parameters then the cone penetration test. For the evaluation of soil strength parameters from plate sinkage tests it is necessary to establish the point at which failure conditions are reached (bearing capacity failure) and beyond which the pressure-sinkage curve represents plastic equilibrium at the particular sinkage. For a given soil slip line fields may be constructed on the basis of plasticity theory (Ref. A.6) and the bearing capacity determined. For the evaluation of strength parameters from the results of plate sinkage tests the computation procedure would have to be inverted; since various combinations of ϕ and c could yield the same bearing capacity, either two tests with different plate size are necessary or a relationship between the rate of pressure increase beyond bearing capacity and friction angle would have to be established. This latter method is believed to be feasible on the basis of theoretical considerations. In summary, plate sinkage tests are suitable for the evaluation of strength properties but evaluation procedures would yet have to be developed.

Determination of Soil Shear Strength Parameters by Ring Shear Tests

Ring shear tests were originally designed and are being used for the determination of soil strength parameters for mobility purposes. However, the evaluation of these tests are objectionable because the failure mechanism in these tests consists of oblique failure surfaces, as discussed in Ref. A.7, that do not include

the horizontal surface of the ring. Thus shear stresses referred to this horizontal surface are not representative of the shear strength of the soil and are generally less than that. Unfortunately, by coincidence, this feature of the ring shear test resulted in lower apparent strength and yielded more realistic traction values than the true strength because the full shear strength at the running gear-soil interface generally cannot be mobilized. A more detailed discussion of the mobilization of shear strength is given in Ref. 13.

For the ring shear test to yield true soil shear strength parameters the proper failure mechanism would have to be considered in the evaluation procedure. Another alternative would be to use a sleeve that would be pushed into the ground around the ring shear plate to prevent lateral failure along the oblique failure surfaces and force the failure surface to develop at the base of the ring. Further research is needed to develop the proper technique of ring shear tests for soil strength property determination.

References

A.1 Nowatzki, E. and Karafiath, L., "General Yield Conditions in a Plasticity Analysis of Soil-Wheel Interaction," presented at 8th U.S. National Off-Road Mobility Symposium of the ISTVS, Purdue University, October 1972.

A.2 Whitman, R. V., Richardson, A. M., and Nasim, N. M., "The Response of Soils to Dynamic Loadings," Report No. 10, Strength of Saturated Fat Clay, M.I.T., Department of Civil Eng. Res. Pr. R62-22, June 1962.

A.3 Nowatzki, E. A. and Karafiath, L. L., "Effect of Cone Angle on Penetration Resistance," High Research Record No. 405, 1972.

A.4 Hovland, H. J. and Mitchell, J. K., "Mechanics of Rolling Sphere-Soil Slope Interaction," University of California, Space Sciences Laboratory Report, July 1971.

A.5 "Strength-Moisture-Density Relations of Fine Grained Soils in Vehicle Mobility Research," U.S. Army Engineer, Waterways Experiment Station, Technical Report No. 3-639, January 1969.

A.6 Karafiath, L. L., "On the Effect of Base Friction on Bearing Capacity," Journal of Terramechanics, Vol. 9, No. 1, 1972.

A.7 Liston, R. A., "The Combined Normal and Tangential Loading of Soils," Doctoral Dissertation, Michigan Technological University, 1973.

APPENDIX B

COMPUTER PROGRAM FOR THE PREDICTION OF TIRE PERFORMANCE

Description of Computer Program

The computer program listed at the end of this appendix performs all computations necessary to define the geometry of the tire centerline and slip line fields as postulated by the tire-soil model, computes the interface stresses, and, by appropriate integration of these stresses, the load, torque, and drawbar pull values for initially assumed entry and rear angles; and finds the solution for a given load by an iteration procedure in which the entry and rear angles are appropriately changed.

The computer program consists of two parts: the main program ("KTIRE") and the subroutine ("SLFI"). All computations necessary to determine the coordinates of the nodal points and associated stresses for a single slip line field are performed in the subroutine, all others in the main program.

The flow diagram for the main program is shown in Fig. B-1. In the main program input data are read in from a data file. Input soil properties may be either the values of c, γ, and ϕ or cone penetration data, cone index gradient for frictional soils, or average cone index for cohesive soils. The program computes the c, γ, and ϕ values corresponding to the cone penetration data from the relationships established in Appendix A.

From the input data the program computes the interface friction angle δ, the separation angle θ_d, and the hypothetical normal stress q_m, that is the normal stress for an infinitely small forward field. If this hypothetical normal stress is greater

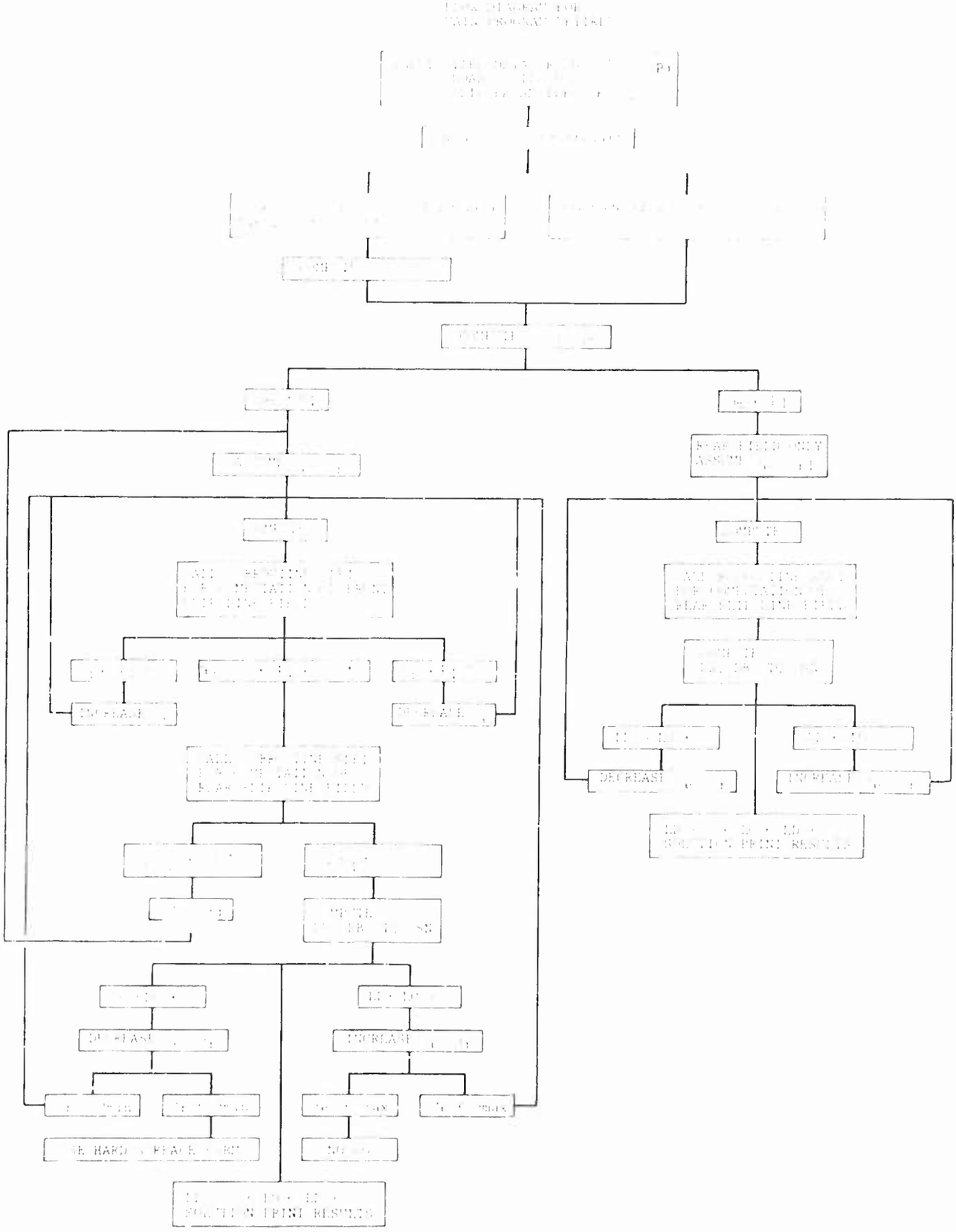

Fig. B-1 Flow Diagram for the Main Computer Program "KTIRE"

than the limiting stress p_1 then there is no forward slip line field. Depending on whether there is a forward field or not the flow diagram separates in two branches (see Fig. B-1).

In the case of both forward and rear slip line fields, the computation starts with the forward field. For an assumed entry angle, the main program computes the coefficient β for the logarithmic spiral and calls subroutine SLFI that computes the normal stress q_d at a θ_d pertaining to the assumed entry angle. The main program iterates on the entry angle until the normal stress q_d at θ_d equals p_1 within the limit of tolerance then calls the subroutine for the computation of the rear slip line field. The extent of the rear slip line field is determined by the condition that it should end at angle θ_d' where the interface normal stress equals p_1. Between angles θ_d' and θ_d the interface normal stress equals p_1 as postulated by the tire-soil model. Should, however, the interface normal stress computations in the rear field show that they are less than p_1 — even if the rear field extends up to the inner end of the forward field (θ_d) — then p_1 is made equal to q_d, the normal stress at θ_d computed from the rear field, and the computation with the new p_1 value is repeated. This situation may occur at high slip values when the relatively large outward directed interface friction angle, δ, reduces the bearing capacity of soil and the resulting normal stresses are lower than p_1. In such cases tire geometry resembles to that of a rigid wheel.

In the last part of the main program load, torque and drawbar pull values are calculated on the basis of the interface stresses obtained from the two slip line fields for the assumed θ_r and θ_d angles. In an iteration procedure these angles are changed until

the load equals the design load within the limits of tolerance. In the case where there is only a rear slip line field the flow diagram shown in the right side of Fig. B-1 holds.

The flow diagram for the subroutine SLFI is shown in Fig. B-2. for the computation of a forward slip line field. Designations and grid are shown in Fig. B-3. The rear field is computed in a similar way except for the condition applied to the determination of the inner end of the slip line held. In the forward field the slip line field ends at σ_d while the rear field ends at the angle where the normal stress equals p_1.

For the computation of the coordinates, principal stresses and their directions, the plasticity theory for soils applies. The differential equations of plasticity are replaced by difference equations and are solved numerically. The solution procedure is described in detail in the previous report on rigid wheel-soil interaction (Ref. 13) and elsewhere (Refs. B.1 through B.3). For brevity, only that part of the solution procedure is discussed here that is different from the rigid wheel problem, the geometric boundary conditions at the interface.

For the rigid wheel the geometric boundary conditions at the interface requires that the coordinate points x and z must lie on a circle with radius R. For the tire these points must lie on a logarithmic spiral. For numerical computations, the logarithmic spiral is approximated by a polygon that is tangential to it. Logarithmic spirals have the property that their tangents make a constant angle (σ_{sp}) with the normal to the radius allowing a simple computational procedure for the determination of the polygon side on which x and z must lie. Accordingly, the following equations apply for the computations of stresses and coordinates at the boundary of the active zone.

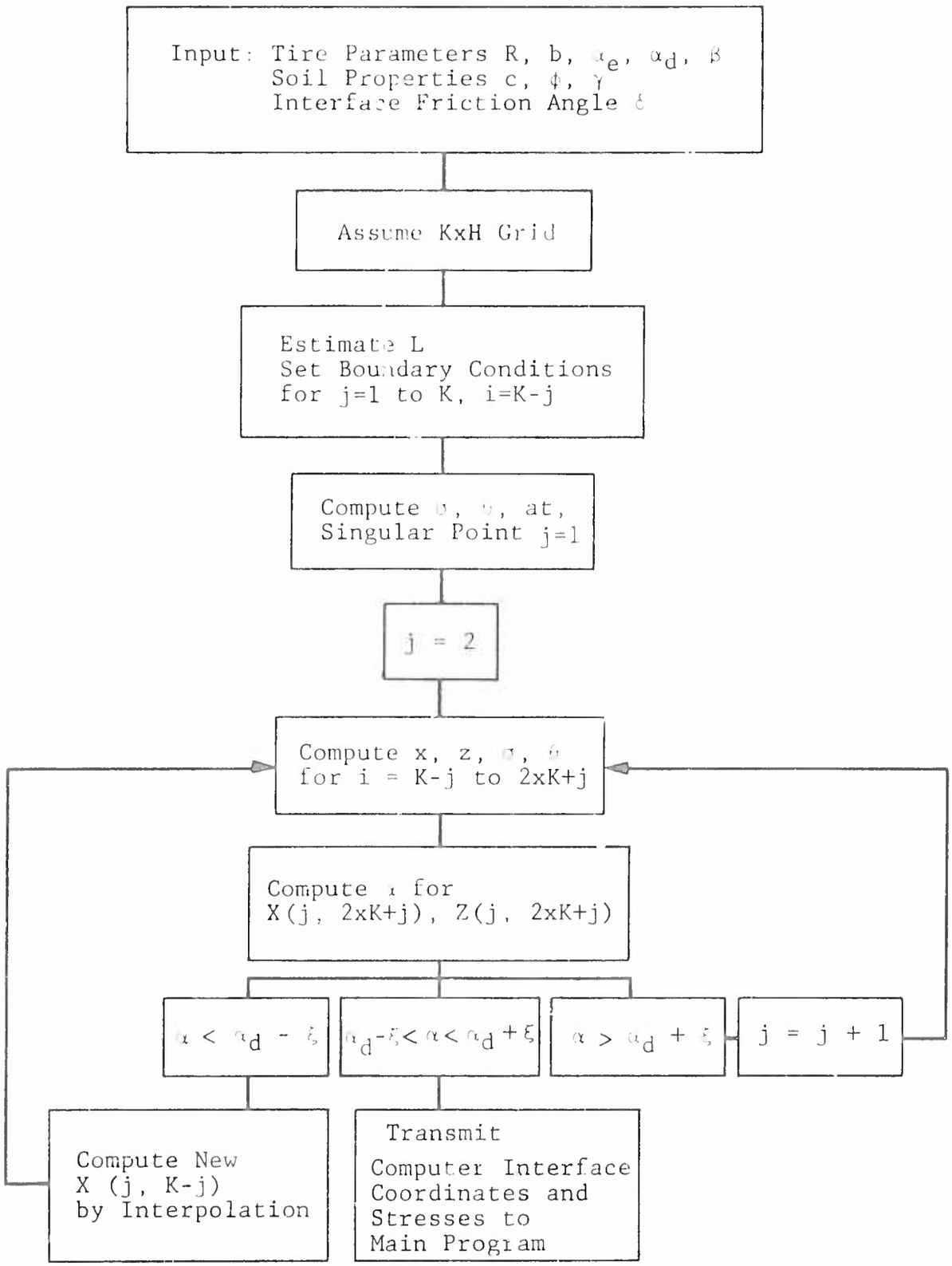

Fig. B-2 Flow Diagram for the Computation of a Forward Slip Line Field by Subroutine SLFI

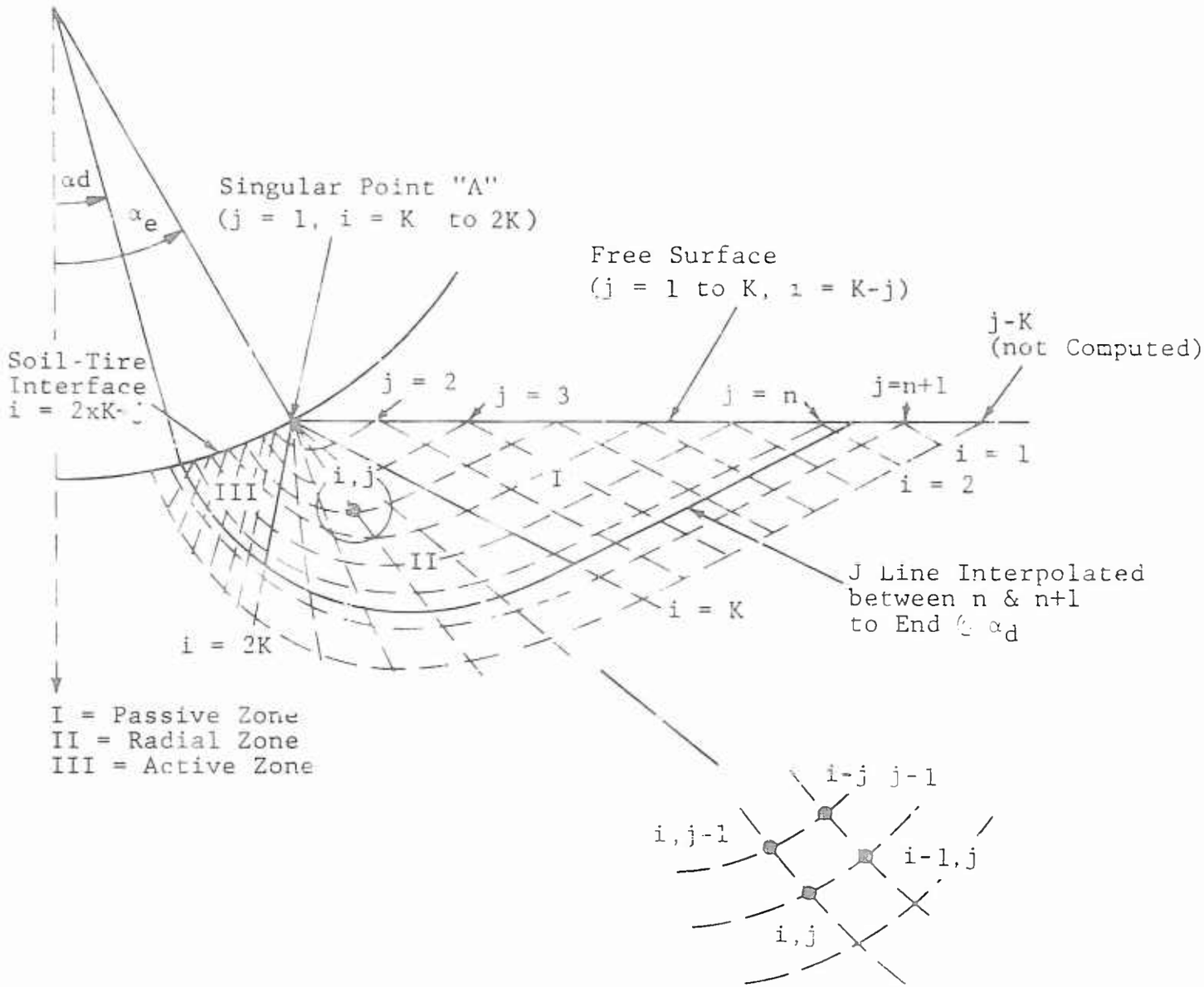

Fig. B-3 Designation of Nodal Points in Slip Line Field and Scheme of Computations

$$x_{i,j} = \frac{1}{1 + \sigma_o F}\, x_{i-1,j} + \sigma_o F x_{i-1,j-1} + \sigma_o (z_{i-1,j-1} - z_{i-1,j})$$

$$z_{i,j} = z_{i-1,j-1} + F(x_{i-1,j-1} - x_{i,j}) \qquad \text{(B-1)}$$

$$\sigma_{i,j} = \sigma_{i-1,j} + 2 \cdot \tan\varphi\, \sigma_{i-1,j} \cdot (\sigma_{i,j} - \sigma_{i-1,j}) + \gamma C$$

where

$$\sigma_o = \operatorname{cotan}\left(\tfrac{1}{2}(\sigma_{i,j-1} + \sigma_{i,j}) - \mu\right)$$

$$C = z_{i,j} - z_{i-1,j} - \tan\varphi \cdot (z_{i,j} - x_{i-1,j})$$

$$F = \tan\sigma_{i-1,j-1} - \gamma_{sp}$$

There are limitations to the curvature of the logarithmic spirals that are incorporated in the program. These limitations are

- In the front field, the σ coefficient is limited to such a value that the z coordinates of the spiral be always positive (below the surface).
- In the rear field, the angle of inclination to the horizontal of the side of the polygon at a particular point is limited to the angle of a straight line from that point to the end point of the forward field (no double curvature in the center portion is allowed).

If both limitations hold the centerline geometry reverts to that of a tire on a rigid surface.

The flow diagrams in Figs. B-1 and B-2 show the general logic of the computations. There are, however, some provisions in the

programs that for clarity have not been included in the flow diagram. These are discussed below.

The finite difference approximations of the differential equations of plasticity become indeterminate if either φ or c equals zero. Instead of providing an alternate and complicated algorithm for these specific cases, a minimum value of $1°$ is assigned for φ and 0.2 lb/sq ft for c. The effect of these assignments on performance calculations is minimal.

In Ref. 13 it was shown that the maximum value of the angle of interface friction is

$$\delta_{max} = \text{arc tan } (\sin \varphi) \quad . \tag{B-2}$$

At this value of the interface friction angle some computational procedures become inaccurate or indefinite. To avoid this computational problem a maximum value of $0.99\ \delta_{max}$ has been assigned to δ.

In the various iteration procedures that are employed to meet certain equality conditions tolerance limits have been assigned to each condition, on the basis of experience gained with running the program for a variety of conditions. These tolerance limits are consistent with the degree of accuracy desired in tire performance predictions. There are inevitable inaccuracies in prediction theories due to the various assumptions, inaccuracies in the determination of soil properties and the approximations inherent in numerical methods. Thus, generally there is no point in setting lower tolerance limits in the equality conditions and performing the ensuing larger number of iterations to achieve an apparent accuracy in the prediction when inaccuracies from other sources would dominate.

Convergence of the various iterations used in the computer program has been generally established in the numerous runs that were required to develop the program and compare predictions with test results. Nevertheless, it is conceivable, that for some unforeseen combination of variables an iteration would not satisfactorily converge. A time limit of 500 seconds has been set for the program; should a solution be not reached within this time limit the originator of the program should be consulted.

Guidance for Users of the Computer Program

Complete listings of the computer programs are given at the end of this appendix.

Designation of variable names, instructions for the preparation of data files and other comments useful for running the program are given below.

Input data are read from input data file "TYR.DAT" in the following order and 2F format.

Cone Index gradient (pci) [CGR]	Cone index (psi) [CI]
Nominal tire radius (ft) [RA]	Tire width (ft) [BØ]
Tire load (lb) [LØ]	Limit pressure (psi) [PØ]
Deflection coefficient [DE]	Slip [SL]
Slip parameter (j_o) [SJ]	Slip parameter K [SKF]
Cohesion in forward field (lb/sq ft) [CF]	Cohesion in rear field [CR]
Friction angle in forward field (degrees) [FF]	Friction angle in rear field [FR]
Unit weight in forward field (lb/cu ft) [GF]	Unit weight in rear field [GR]

Designations of the input variables in the computer program are indicated in brackets.

Cohesion, friction angle, and unit weight are read in as input variables only if both CGR = 0 and CI = 0. If the program is to be used with cone penetration data, the value of either CGR or CI should be entered in the data file, the other value must be zero.

Subscripted Variables and Dimension Statements

Main program KTIRE

J designates a location at the interface

HH(J) = r_j

QQ(J) = q_j

EE(J) = e_j

UU(J) = x_j

VV(J) = z_j

Triple letter subscripted variables are used for storage of double letter arrays.

Subroutine SLFI

X(I,J) = $x_{i,j}$

Z(I,J) = $z_{i,j}$

S(I,J) = $s_{i,j}$

T(I,J) = $\tau_{i,j}$

The dimension statement corresponds to a 48 x 16 grid (I = 1 to 49, J = 1 to 17) for the computation of the geometry of slip line fields. All J locations are not necessarily used in actual computations, as indicated before. Several hundred computations were performed satisfactorily with the above grid size and, therefore, no need for the change of the grid size is anticipated.

Variables with one subscript are as follows:

D(J) = θ_j

H(J) = η_j

Q(J) = q_j

R(J) = r_j

U(J) = x_j

V(J) = z_j

A(J), B(J), C(J) are auxiliary variables.

The dimensions of the variables with one subscript are tied to the J dimensions of the variables with two subscripts.

Limits

In the main program the following limits are set for the entry and rear angles.

$\theta_{e\ max}$(ARE) = 70°

$\theta_{r\ max}$(ARMAX) = 40°

$\theta_{r\ min}$(ARMIN) = 0°

A limit of 20 was set for the number of iterations (ITER) allowed to find the solution for a given load.

A limit for the tire radius at the rear entry angle (RAMIN) was set to correct tire geometries that would have resulted in negative sinkages.

Other Constants

The initial rear angle (AR) is set at 10°.

The δ' angle (AD) is set at 5°.

A constant DF defines a linear variation of δ over the interface. In the present program δ is assumed to be uniform over the interface. For this case a value of DF = 1 is assigned. In the main program XXX, in the subroutine XX, is used to define the conditions for which the slip line field is computed according to the following schedule

XXX = - 1 for forward slip line field

XXX = + 1 for rear slip line field

XXX = + 2 for rear slip line field only

Output

The following results of the computation are printed out.

Pull coefficient (PUN)

Torque coefficient (TON)

Sinkage (SNK) (inches)

Note: The tire-soil model has been developed for driven tires where the applied torque determines the direction of shear stresses

that is the same along the whole interface. In the case of towed tires the direction of shear stresses changes over the interface so that the resultant torque from the shear stresses is zero. Therefore, the tire-soil model, as presented, should not be used for the computation of the drag force of towed tires.

References

B.1 Karafiath, L., "Plasticity Theory and Stress Distribution beneath Wheels," Journal of Terramechanics, Vol. 8, No. 2, 1971.

B.2 Karafiath, L. and Nowatzki, E., "Stability of Slopes Loaded over a Finite Area," Highway Research Board Record No. 323, November 1970.

B.3 Karafiath, L., "On the Effect of Pore Pressures on Soil-Wheel Interaction," Proceedings Fourth International Conference for Terrain Vehicle Systems, Stockholm, April 1972.

COMPUTER PROGRAM LISTING - KTIRE

```
C THIS PROGRAM COMPUTES [illegible] TIRE [illegible] INPUTS
C [illegible] IN DATA FILE'TYP.DAT' IN FORMAT [illegible] IN THE FOLLOWING
C [illegible].
C [illegible] HEIGHT(LBS/[illegible] IN),[illegible](LBS/[illegible] IN)
C TIRE [illegible] (FT) , [illegible] (FT)
C TIRE [illegible] ([illegible]),LIMIT PRESSURE [illegible] (LBS/SQ IN)
C [illegible], [illegible], SLIP (DECIMAL)
C [illegible] SLIP PARAMETER [illegible]
C [illegible] IN [illegible] (LBS/SQ IN), [illegible] IN [illegible].(LBS/
C [illegible]
C [illegible] IN [illegible] F.([illegible]), [illegible] IN [illegible] F.([illegible])
C [illegible] IN [illegible] F.(LBS/[illegible] FT), [illegible] IN [illegible] F.(LBS/ [illegible] FT
C IF THE PROGRAM IS USED WITH SOIL [illegible] VALUES,
C [illegible] SOILS THE [illegible],
C [illegible] SOILS THE [illegible]
C [illegible] WITH THE [illegible] ZERO
C [illegible] FRICTION ANGLE AND UNIT
C [illegible] SHOULD BE [illegible]
C [illegible] PARAMETERS [illegible]
C THE LIMIT PRESSURE [illegible]
C [illegible] (PSI)
C [illegible] SLIP PARAMETER [illegible] REPORT
      DIMENSION [illegible](36),[illegible](36),[illegible](36)
      DIMENSION [illegible](36),[illegible](36)
      DIMENSION [illegible](36),[illegible](36),[illegible](36)
      DIMENSION [illegible](36),[illegible](36)
      [illegible],[illegible],[illegible],[illegible],[illegible],[illegible],[illegible],AI,[illegible],[illegible],[illegible],[illegible],[illegible],
     + [illegible],[illegible](36),[illegible](36),[illegible](36),[illegible](36),[illegible](36)
      [illegible],([illegible],[illegible]),([illegible],[illegible]),
     + ([illegible]),([illegible]),([illegible]),([illegible]),
     + ([illegible]),([illegible]),([illegible]),([illegible]),([illegible]),
     + ([illegible]),([illegible]),([illegible]),([illegible](1),[illegible](1)),
     + ([illegible](1)),([illegible](1),[illegible](1)),([illegible](1),[illegible](1)),([illegible](1),[illegible](1))
      [illegible] REAL (L)
      [illegible]=[illegible]/[illegible]([illegible]))
      [illegible]=[illegible]([illegible])+[illegible]([illegible]**2-[illegible]([illegible])**2)
      [illegible]=[illegible]([illegible])-[illegible]([illegible]**2-[illegible]([illegible])**2)
      [illegible]([illegible],[illegible],[illegible])=[illegible](2*([illegible]-[illegible])*SIN([illegible])/COS([illegible]))
      [illegible]=[illegible]/[illegible]
      [illegible]=[illegible]/[illegible]
      [illegible]=[illegible]([illegible])/([illegible]-[illegible]-[illegible])
      CALL [illegible]
      CALL IFILE([illegible],'TYP')
      CALL [illegible](ITI)
      [illegible] 3,ITI
    3 FORMAT([illegible],'TIME= ',I[illegible])
    4 READ([illegible]) [illegible],[illegible],[illegible],[illegible],[illegible],[illegible],[illegible],[illegible],[illegible],[illegible],[illegible],[illegible],[illegible],
     + [illegible],[illegible]
    6 FORMAT ([illegible])
      IF([illegible].LT.[illegible]) GO TO 7
      GO TO 4
```

```
ITIP1.SRC      11-APR-74  09:35      TAC1 2

      2        IF(CGP.EQ.2) GO TO 5
               [illegible]=(91.1-ALOG10(CGP)+11.33)/1[illegible]
               IF(PILL.GT.1.1) PILL=1.1
               E[illegible]=57.3*ATAN(1/(1.64-.65*PILL))
               C[illegible]=104-17.5*(1-PILL)
               [illegible]=PILL+PO*(1-PILL)/52
               IF(PILLP.GT.1.1) PILLP=1.1
               EOP=57.3*ATAN(1/(1.64-.65*PILLP))
               COP=104-17.5*(1-PILLP)
               GO TO 10
      9        IF(CI.LE.0) GO TO 9
               CO=11.5*CI
               C[illegible]=CO
               IO=.05*CI
               IOP=IO
               C1=100+.1*CI
               C1P=C1
               GO TO 10
      5        CO=CI
               COP=COP
               IO=II
               IOP=IP
               C1=CI
               C1P=CP
      10       EO=EO/57.3
               IF(EOP.LT.EO) EO=EOP/57.3
               EMAX=.95*ATAN(SIN(EO))
               IO=IO*(-(SL+SD)/SEW)
               EMIN=1-IO
               II=ATAN(EMIN*EMAX)
               EO=57.3*II
               PRINT 11,CO,EO,GO
      11       FORMAT(1H ,'COV.=',F5.1,'  DVI=',F5.1,'  GAMMA=',F5.1)
               PRINT 12,DA,PO,LO,DO
      12       FORMAT(1H ,'DAL.=',F5.2,'  WIDTH=' F5.2,'  LOAI=',F5.2,'

     1    DOWNL=',F5.2)
               PRINT 14,SE,IO
      14       FORMAT(1H ,'FINL. COEFF.=',F10.3,'  FILTA=',F[illegible].3)
               PRINT 16,CI,CGP
      16       FORMAT(1H ,'CI=',F10.2,'  COEF DRAI.=',F10.2)
               PRINT 18,EOP,GOP,COP
      18       FORMAT (1H ,'DIAP EP. A.=',F6.2,'  DIAP GAMMA=',F[illegible].2,
     +  '  DIAP COV.=',F7.2)
               PRINT 19,SL,SD,SEW
      19       FORMAT (1H ,'SLIP=',F7.3,'  JZERO=',F5.2,'  F=',F[illegible].3)
               PI=3.141593
               PI=144*PO
               AT=5
               AP=12
               IF(CO.LT.2) GO TO 20
```

```
      GO TO 30
20    CC=.0
      CCR=.0
30    IF(FC.LT.0) GO TO 40
      [illegible]
40    FC=1
      ITIN=0
      [illegible]=40
      [illegible]
      API=[illegible]/57.3
      PSI=CC/TAN(FC)
      [illegible]=ATAN((P1+PSI)*TAN(FC)/P1)
      AAN=[illegible]
41    TEL=T1
      AA2=[illegible]+.1[illegible]
      IF([illegible].LT.[illegible]+.[illegible]1) [illegible]=[illegible]+.[illegible]1
      [illegible]=[illegible](C[illegible],[illegible],AA2,[illegible]/57.3)
      [illegible]=[illegible]1
      [illegible]=ALOG(COS([illegible])/COS([illegible]))
      [illegible]=[illegible]I/([illegible]-AA2)
      IF([illegible]1.LT.[illegible]) [illegible]1=[illegible]
      [illegible]1=[illegible]([illegible]1)
      FI1=F[illegible]/57.[illegible]
      [illegible]1=[illegible]/57.3
      [illegible]=[illegible]
      [illegible]
      [illegible]I=[illegible]/TAN(F[illegible])
      [illegible]=[illegible]([illegible]1,FI1)
      T[illegible]=[illegible]I/[illegible]+.[illegible]([illegible]+[illegible]1)-[illegible]+[illegible]1
      [illegible]1=[illegible]([illegible],[illegible])
      [illegible]=[illegible]I/[illegible]1
      [illegible]1=[illegible]([illegible]1,T[illegible],[illegible])
      [illegible]1=[illegible]*[illegible]1
      [illegible]=[illegible]([illegible]1,FI1)
      [illegible]I[illegible]1-[illegible]*C[illegible]([illegible]1)-C[illegible]1
      [illegible]=-[illegible]([illegible]1*A[illegible]/57.3)
      IF([illegible].[illegible].[illegible]) GO TO 115
      [illegible]=-1
      [illegible]1=1
      [illegible]
      IF([illegible](1).[illegible].[illegible]) [illegible] TO 3[illegible]
      [illegible]=[illegible]-[illegible]
      [illegible]
      IF([illegible].[illegible].[illegible]) GO TO [illegible]
      GO TO [illegible]
      [illegible]
      [illegible]=[illegible]([illegible])
      [illegible]=[illegible]([illegible])
      IF([illegible]) [illegible],[illegible],[illegible]
57    [illegible]
```

```
                    OY=PP(JJ1)
                    HY=HH(JJ1)
                    IF(HY+DY) 50,60,58
 58                 IF(ABS(DY-AY)-0.001) 50,59,60
 59                 QQ(JJ1)=PPL
                    HH(JJ1)=HY*PPL/DY
                    HH(JJ1)=17.3*ALOG(
                    GO TO 65
 60                 AA2=(DY+AY)/2
                    IF(ABS(QQ(I1)-0.05*PPL) 80,80,54
 54                 IF(ABS(QQ(I1)-0.05*PPL) 80,62,79
 62                 IF(QQ(I1).LE.0.001) GO TO 79
                    DQ1=AA2-QQ(I1
                    DH=(PPL+QQ(I1))/2
                    AA1=AH1*DH/QQ(I1
                    IF(DH.LT.0) AID=-0.33
                    IF(DH.GT.0) AID=0.33
                    IF(AA2*1.E-6.(ABS(AA1+0.001)) GO TO 80
                    AA2=AA2+AID+AI
                    IF(ABS(AA2).LT.ABS(AA1)) AA2=AA1+0.001
                    IF(ABS(DQ1).GT.0.1) GO TO 79
                    GO TO 65
 70                 QQ=QQ(I1)
                    GO TO 50
 79                 QQ=QQ(I1)
 65                 HH=HH(JJ1)
                    DH=DH(JJ1)
                    NC=NC+1
                    PQ=PQ+1
                    IF(NC-1) 71,71,72
 71                 WRITE(6,36)
                    DO 73 I=1,NC
                    HH(I)=HH(NC-I)
                    QQ(I)=QQ(NC-I)
                    DH(I)=DH(NC-I)
                    HY(I)=HY(NC-I)
                    PP(I)=PP(NC-I)
 72                 WRITE(6,37)
                    DO 74 I=1,NC
                    WRITE(6,38) I,PP(I),QQ(I),HH(I),DH(I),HY(I)
 74                 CONTINUE
 75                 WRITE(6,39)
                    GO TO 120
 80                 AAM=1.E+6*AD/57.3
                    RI=HIT(II,AAM/2,AAM,II/57.3)
                    IF(RI.GT.RMAX) RI=RMAX
```

```
                      XO=PPC+CIN(AAM)
                      YO=PPC+SIN(AAM)
                      JJ1=0
                      JJ=37
                      XX=0
                      YY=0
                      GO TO 1 1
      120             XXX=1
      121             III=-II/57.3
                      AAC=CD/57.3
                      PPC=-PA*EXP(-II*2*AI/57.3)
                      PAMIN=PP/COS(AA0)
                      IF(PPC.GT.PAMIN) PPC=PAMIN
                      VVV=VC-VS
                      VVV=VC-ZC
                      JJJ=0
                      FFI=IAF/57.3
                      CCC = 3.
                      CCC=CCP
                      AAM=-AAM
                      AA1=ACOS(-1)
                      TTS=PI/2+.5*(I0+FFI)-AAC+AA1
                      SM1=SIN(C,FFI)
                      PPI=CCP/TAN(FFI)
                      PIC=PPI/SM1
                      FF1=FDF(FFI,TI2,')
                      SIG1=SIG*FF1
                      SM2=SIN(LII,FFI)
                      SM3=SIG1*SM2*COS(JJJ)-CCI
                      IF(YY.EQ.0.) GO TO 117
                      IF(SM3.GE.PPL) XXX=0
      117             IFF = 1
                      CALL SUBI
                      IF(XXX.GE.0) GO TO 126
      125             IF(SSS.LT.(.95*PPL)) GO TO 122
                      GO TO 137
      126             IF(SSS.LE.PPL) GO TO 137
                      DO 127 I=1,36
                      IF(SIG(I).GT.PPL) SIG(I)=PPL
      127             CONTINUE
                      GO TO 122
      122             DO 1 I=1,36
                      XP(I)=0
                      YP(I)=0
                      ZP(I)=0
                      VP(I)=0
                      WP(I)=0
      124             CONTINUE
```

```
                    UU1=0
                    UU4=0
                    UU5=0
                    DD1=0
                    DD1=DD1
                    AA1=-AA1
                    AA1=0
                    A1=1
                    A1=0
                    DO 100 I=I3,N4
                    UU1(I)=-U1(N-I3+1)
                    DD1(I)=-D1(I-I3+1)
                    AA1(I)=AA1(I-I3+1)
                    UU1(I)=-U1(I-I3+1)+U1A+X5
                    UU1(I)=U1(I-I3+1)-U1A+Z5
 14                 CALL UU1
                    X1=0
                    X2=0
                    X3=0
                    X4=0
                    DO 1 I=(I3+1),36
                    X1=(X1(I-1)+0.5*AA1(I))/(3.*(D1(I)+
                    U1=UU1(I-1)+(UU1(I)-U1(I-1))*U2
                    U1=UU1(I-1)+(U1(I)-UU1(I-1))*U2
                    U1=(U1(I-1)-UU1(I))/(U1(I)-U1(I-1))
                    CALL UU1(U1)
                    X3=U1-Z1
                    X4=U1-X1
                    X5=0.5*(X3*X3+X4*X4)
                    U2=.5*(D1(I)+D1(I-1))
                    U4=.5*(U1(I)+U1(I-1))
                    U5=(UU1(I)-UU1(I-1))*Z
                    U6=(UU1(I)-UU1(I-1))*Z
                    U7=0.5*(X3*X4+X5)
                    U1=U1+U4
                    U1=U1+U5
                    U1=U1+U6
                    U1=U1+U7
 1                  CALL UU1
                    U1=U1*X1
                    U1=U1*X
                    U1=U1*X1
                    IF(ABS(U1-1.0)-0.1*L2) 30,360,1
```

```
                IF(L0.LT.RUF) ADY=AD
                IF(L0.LT.RUF) AMY=-AAM
                IF(L0.GT.RUF) ADY=AD
                IF(L0.GT.RUF) AMY=-AAM
                IF(AD.LE.ADMAX) GO TO 335
                IF(AD.LE.ADMIN) GO TO 340
                IF(ADY.LE.0.) GO TO 335
                IF (AMY.LE.0.) GO TO 335
                AD=.5*(ADY+ADY)
                AAM=.5*(AMY+AMY)
                ADY=0
                AMY=0
                GO TO 345
                IF(L0.LT.RUF) GO TO 295
                FS=1
                IF(L0.LT..5*RUF) FS=2
                ADY=ADY-AAM*1
                AMY=-((AMY+.07*FS)
                IF(AD.LT.ADMIN) AD=ADMIN
                ADY=
                AMY=0
                GO TO 340
                FS=1
                IF(L0.LT.*RUF) FS=2
                AMY+AAM*1
                AMY=-(AMY-.07*FS)
                IF(AD.LT.RUMX) AD=ADMAX
                ADY=
                AMY=0
                GO TO 335
                ITIS=ITIS+1
                IF(ITIS.GT.5) GO TO 320
                IF(ITIS.LE.5) GO TO 110
                ITIS=0
                WRITE (11,' QUICK INPUT')
                GO TO 335
                ITIS=0
                WRITE (11,'DO DO')
                GO TO 335
                ITIS=0
                WRITE (11,'WRONG VARIABLE FORMULA')
                GO TO 335
                PRINT 345,ITIS
                FORMAT (11,'NORMAL EXIT=',I10.5)
                PRINT 370,ITIS
                FORMAT(11,'TAKE. EXIT=',I10.5)
                PRINT 335,ITIS
                FORMAT (11,' ERROR=',I10.5)
                STOP'END'(13+1)
```

```
 TIPI.SRC       11-APR-74   08:35        PAGE 8

                DO 380 N=N3+1,36
                IF(UUU(N).GT.SNK) GO TO 385
                GO TO 380
      385       SNK=UUU(N)
                COUTINUE
                SNK=12*SNK
                PRINT 390,SNK
      390       FORMAT(1H ,'SINKAGE=',F10.3,'  IN')
                RUN=RTF/RNF
                TON=TTF/(DA*RNF)
                PRINT 395,RUN,TON
      395       FORMAT(1H ,'RULLCOEFF=',F10.4,'  TONNCOEFF=',F10.4)
      380       END
```

COMPUTER PROGRAM LISTING - SUBROUTINE SLF1

```
      SUBROUTINE SLFI
      COMMON RC,GC,CC,FI,DI,AC,AM,A1,VK,UK,PL,DF,XX,
     +  CF,AF,VA,UA,J1,H(36),Q(36),E(36),U(36),V(36)
      DIMENSION X(49,17),Z(49,17),S(49,17),T(49,17),
     +  A(36),B(36),C(36),D(36)
      IMPLICIT REAL (L)
      DEL(F9,E9)=ASIN(SIN(D9)/SIN(F9))
      SUA(L9,F9)=COS(D9)+SQRT(COS(D9)**2-COS(F9)**2)
      SUB(D9,F9)=COS(D9)-SQRT(COS(D9)**2-COS(F9)**2)
      EPC(F9,T9,T8)=EXP(2*(T9-T8)*SIN(F9)/COS(F9))
      TAN(F9)=SIN(F9)/COS(F9)
      EIC(A9,D9,T9,T8,F9)=B0*(A9-D9)*EXP((T9-T8)*
     +  SIN(F9)/COS(F9))
      DO 3 I=1,49
      DO 4 J=1,17
      X(I,J)=0
      Z(I,J)=0
      S(I,J)=0
      T(I,J)=0
    4 CONTINUE
    3 CONTINUE
      DO 6 J=1,36
      A(J)=0
      B(J)=0
      C(J)=0
      D(J)=0
      U(J)=0
      V(J)=0
      W(J)=0
      Q(J)=0
      E(J)=0
    6 CONTINUE
      M=49
      N=17
      INTP=0
      PI=3.14159
      APP=30/57.3
      TF=TAN(FI)
      DIF=TAN(DI)
      II=2*N-1
      C1=C0/TF
      U1=PI/4-FI/2
      F3=1-SIN(FI)
      V3=-TAN(FI)
      V4=1
      V5=TAN(FI)
      V6=1
      D2=0
      D3=DEL(D2,FI)
      T1=(D3-D2)/2
```

```
00510           D5=D1*(1+EF)/2
00520           D4=DEL(D5,F1)
00530           T2=PI/2-.5*(D4+D1)-A0+A1
00540           W1=C1
00550           W2=SUB(E2F1)
00560           S1=W1/W2
00570           T3=.75*PI+.5*F1-T2+T1-A0+A1
00580           L1=FIS(A0,AN,T2,T1,F1)
00590           EMAX=ATAN(SIN(F1))
00600           FAC=2+.5*D1/EMAX
00610           L2=FAC*L1*COS(U1)*COS(T3-F1)/COS(I1)
00620           L=-L2
00630   10      INTP=0
00640           DO 40 J=1,N
00650           I=N+1-J
00660           AJ=J
00670           AI=I
00680           Z(I,J)=0
00690           C(I,J)=S1
00700           T(I,J)=T1
00710           X(I,J)=(AJ-2)*L/(AN-2)
00720           X(N,1)=0
00730           X(I-1,2)=.5*L/(AN-2)
00740   40      CONTINUE
00750   50      DO 70 I=1,(2*N-1)
00760           J=1
00770           AI=FLOAT(I)
00780           AN=FLOAT(N)
00790           X(I,J)=0
00800           Z(I,J)=0
00810           T(I,J)=T1+(T2-T1)*(AI-AN)/(AN-1)
00820           CONIP(F1,T(I,J),T1)
00830           S(I,J)=P0W*S(N,1)
00840   70      CONTINUE
00850           C2=COS(E1,F1)
00860           C(1)=C2*S(2*J-2,1)*COS(D1)-C1
00870           S(1)=(C(1)+C1)*DAF
00880           I(1)=57.3*A0
00890           DO 200 J=2,N
00900   80      DO 120 I=(J+2-J),(J+2*(N-1))
00910           IF (I.EQ.(J+2*(N-1))) GO TO 126
00920           K=0
00930           TU1=T(I,J-1)+U1
00940           TU2=T(I-1,J)-U1
00950           S11=S(I,J-1)
00960           S12=S(I-1,J)
00970           V7=2*S(I-1,J)*S(I,J-1)
00980           V8=S(I-1,J)+S(I,J-1)
00990           V8=(T(I,J-1)-T(I-1,J))*TF
01000           V9=2*S(I-1,J)*S(I,J-1)*V8
```

```
C1010           U6=2*TF*(S(I,J-1)*T(I,J-1)+S(I-1,J)*T(I-1,J))
C1020    85     V1=TAN(TH1)
C1030           V2=TAN(TH2)
C1040           YI=V1*Y(I,J-1)
C1050           YJ=V2*Y(I-1,J)
C1060           V12=1./(V1-V2)
C1070           Y(I,J)=V12*(Z(I-1,J)-Z(I,J-1)+YI-YJ)
C1080           Z(I,J)=Z(I-1,J)+(Y(I,J)-Y(I-1,J))*V2
C1090           AA=V3*(Y(I,J)-Y(I-1,J))+V4*(Z(I,J)-Z(I-1,J))
C1100           BB=V5*(Y(I,J)-Y(I,J-1))-V6*(Z(I,J)-Z(I,J-1))
C1110           V9=S(I,J-1)-S(I-1,J)
C1120           IF (V9.LT.0) GO TO 110
C1130           GO TO 115
C1140    110    PRINT 111
C1150    111    FORMAT(1H-,'CANT COMPUTE CASE : CHECK INPUT')
C1160           GO TO 950
C1170    115    S(I,J)=(V7+V9+G0*(S11*AA+S12*BB))/V9
C1180           T(I,J)=(V5+V6+G0*(BB-AA))/(2*TF*V9)
C1190           IF (N.EQ.1) GO TO 190
C1200           T1=.5*(T(I,J-1)+T(I,J))+V1
C1210           T2=.5*(T(I-1,J)+T(I,J))-V1
C1220           S11=.5*(S(I,J-1)+S(I,J))
C1230           S12=.5*(S(I-1,J)+S(I,J))
C1240           V6=2*TF*(S11*T(I,J-1)+S12*T(I-1,J))
C1250           V7=S11*S(I-1,J)+S12*S(I,J-1)
C1260           V8=2*S11*S12*V8
C1270           V9=S11+S12
C1280           K=1
C1290           GO TO 85
C1300    190    X0=R0*SIN(A0)
C1310           Z0=R0*COS(A0)
C1320           IF(XX.GE.1.0) GO TO 125
C1330           XG=X0
C1340           ZG=Z0
C1350    195    G1=X(J+2*N-3,J-1)-X0
C1360           G2=-Z0+Z(J+2*N-3,J-1)
C1370           IF(XX.EQ.-1.0) GO TO 130
C1380           GA=ATAN(G1/G2)
C1390           IF(Z(J-1+2*(N-1),J-1).LT.(ZK+Z0)) GO TO 131
C1400    130    A(J)=ATAN(G1/G2)-A1
C1410           IF(XX.EQ.-1.0) GO TO 137
C1420           IF(XX.GT.1.0) GO TO 136
C1430    131    K7=1
C1440    136    G5=-ZK+X0-X(J+2*N-3,J-1)
C1450           G6=XK+Z0-Z(J+2*N-3,J-1)
C1460           G7=-ATAN(G6/G5)
C1470           IF(K7.EQ.1) A(J)=G7
C1480           K7=0
C1490           IF(G7.GT.A(J)) A(J)=G7
C1500    137    D(J)=D1*(1-(1-DF)*(A(J)-A(2))/(AN-A(2)))
```

```
                DAJ=TAN(D(J))
                DI=DIL(D(J),FI)
                TC=.5*(D(J)+FI)
                T(I,I-2*(N-1))=PI/2+DI-A(J)
                TM3=.5*(T(I,I-2*(N-1))+T(I-1,I-2*(N-1)))
                TM4=TM3-FI
                TM5=TAN(TM4)
                TAJ=TAN(A(J))
                Z1=1/TM5
                Z2=Z1*TAJ
                Z3=1/(1+Z2)
                Z4=Z1*(Z(I-1,J-1)-Z(I-1,J))
                X(I,J)=Z3*(X(I-1,J)+Z2*X(I-1,J-1)+Z4)
                Z(I,J)=Z(I-1,J-1)+TAJ*(X(I-1 J-1)-X(I,J))
                AA=V3*(X(I,J)-X(I-1,J))+V4*(Z(I,J)-Z(I-1,J))
                U3=R*S(I-1,J)*TF*(T(I,J)-T(I-1,J))
                S(I,J)=S(I-1,J)+U3+G0*AA
                C1=CUA(D(J),FI)
                C(J)=C1*S(I,J)*COS(D(J))-C1
                F(J)=(C(J)+C1)*DAJ
                X(J)=X(J+2*(N-1),J)
                Z(J)=Z(J+2*(N-1),J)
                G3=X(J+2*(N-1),J)-XC
                G4=-ZC+Z(J+2*(N-1),J)
                CM3=ATAN(G3/G4)
                T(J)=57.3*CM3
  130           IF(XX.GE.1) GO TO 138
  145           GO TO 150
  138           IF(CM3 .GT. (AM+.035))GO TO 140
                IF(CM3.LT.AM) GO TO 150
                IF(XX.GT.2) GO TO 220
                IF(ABS(C(J)-PL)-.05*PL) 220,220,145
  140           IF(C(J).LT.PL) GO TO 140
                GO TO 220
  150           IF(J.LT.5) GO TO 165
                IF(INTR.EQ.2) GO TO 220
                AM=57.3*(AM+.017)
                GO TO 170
  140           IF(INTR.EQ.2) GO TO 220
                IF(J.EQ.3) GO TO 170
                IF(XX.GT.1.) GO TO 150
                IF(ABS(C(J)-PL)-.05*PL) 152,152,154
  154           IF(C(J).LT.PL) GO TO 150
  140           CX=C(J)-C(J-1)
                CY=PL-C(J-1)
                R2=CY/CX
                IF(J.LE.5) GO TO 165
                GO TO 170
  150           IF(J.GT.5) GO TO 220
                GO TO 165
```

```
 00010    150      AN=57.3*AM
 00020             IF(CM3.GT.(AN+.001)) GO TO 170
 00030             IF (CM3.LE.(AN-.001)) GO TO 163
 00040             IF(COS(Q(J)-PL)-.05*PL) 162,162,220
 00050    160      IF(J.LE.9) GO TO 165
 00060             GO TO 220
 00070    163      IF( J.GT.9) GO TO 170
 00080    165      L=.6*L
 00090             MS=0
 00100             GO TO 80
 00110    170      P1=P(J)-P(J-1)
 00120             P2=P(N)-P(J-1)
 00130             P3=P2/P1
 00140    175      P4=P3*(Y(N+1-J,J)-Y(N-J+2,J-1))
 00150             Y(N+1-J,J)=Y(N-J+2,J-1)+P4
 00160             IF(MY.EQ.-1) GO TO 80
 00170             INTP=INTP+1
 00180             GO TO 80
 00190    176      IF (J.LT.3) GO TO 190
 00200             L=1.5*L
 00210             MS=0
 00220             GO TO 80
 00230    190      CONTINUE
 00240    200      CONTINUE
 00250    210      J1=J
 00260             QF=Q(J1)
 00270             AF=P(J1)
 00280             IF(MY.GT.1.0) GO TO 230
 00290             MS=0
 00300             MX=MS
 00310             M1=30
 00320             JA=0
 00330             MA=0
 00340             GO TO 1100
 00350    220      MA=MS
 00360             LA=20
 00370             GO TO1200
 00380    250      P(I)=0
 00390    1300     RETURN
 00400             END
```

SYSTEM?..

.